Iminosugars as dengue virus therapeutics: Molecular mechanisms of action of a drug entering clinical trials

Andrew C. Sayce

Pembroke College

University of Oxford

A thesis submitted for the degree of

Doctor of Philosophy

Trinity Term 2014

Acknowledgements

This thesis would not have been possible without the assistance of a number of amazing people. First and foremost, Nicole Zitzmann has been everything I could ask for in a supervisor. I hope if I am ever in a similar position that I can be one tenth the supervisor she has been. Without Raymond Dwek, the Glycobiology Institute wouldn't exist, and I am eternally grateful to have had his encouragement and support for the last five years. Joanna Miller gave me my first exposure to dengue virus and containment level 3 work and has had to put up with my questions ever since – thank you so much for all of your time and advice. I would also like to thank all of the members of the Glycobiology Institute, and in particular the Zitzmann lab, who have been remarkably welcoming and helpful from my time as a summer intern until today. Thanks in particular go to the members of the food office – JL, Steve, and Dina – for being such great officemates and to Ben Oestringer for putting up with me at work and in our shared flat. Fernando Martinez-Estrada provided advice on conducting transcriptomics experiments and analysis as did Dom Alonzi for FOS and GSL assays, for which I am very appreciative. Without a start in science, I would never have made it to Oxford, and for that I must thank David Dalby and Jim Morris. Mr. Dalby's high school chemistry classes have been foundational to everything I have done since then, and I am lucky to have had such a passionate and intelligent teacher so early in my academic career. I somehow managed to convince Jim Morris to take me into his research group as a sophomore in college, and I couldn't have asked for a better mentor. I cut my teeth on real science for the first time in Jim's lab and without his support or the help of Meredith Morris and Heidi Dodson, I would have given up long ago. Thanks also to Marcia Hesser for keeping me on my toes with all manner of questions. The Clarendon Fund, Pembroke College, and the Glycobiology Endowment have provided funding for this work and for the food on my plate for the last four years, for which I am very grateful.

Outside of the lab, there exists an equally large number of people to whom I owe a considerable debt of gratitude. I am not sufficiently eloquent to express my thanks to my mother and father, Mike and Beth Sayce, who have given me every unfair advantage possible in this world. I could fill an entire chapter with my thanks for everything you have done for me and still feel like I had missed something; thank you for being such wonderful parents. Grandma, Papa, Granny, and Jimmy are the grandparents every kid deserves. There is nobody in the world more genetically similar to me than Becky Sayce, and I could not be more proud to call anyone else my sister. Amanda Ring has been keeping me on my toes since 7th grade, and I'm sure the same will be true when I am seventy. To my running friends, Gramz, Kevin, Thomas, Wallace, Arrowsmith, and all of my teammates, thanks for making the trial of miles so much fun. To my rowing friends, Jonny, Maurus, Kris, George, Winters, BJ, Bodo, and all of the guys at PCBC and OUL, thanks for putting up with me in the cold and wet so that we could tear it up in the sun.

Finally, without Lea Carrott I would be lost. This thesis is as much her accomplishment as it is mine as she has made everything I have done in the last two and a half years possible. I again fall short in being able to express my love and appreciation for everything you have done for me and meant to me, and I can't wait to spend the rest of my life with you.

I could use up the entirety of my word limit thanking all of the people that have helped me, but then I wouldn't have much of a thesis. I'd like to close by saying a special thank you to all of my four-legged friends who have taught me about unconditional love and the importance of going for a walk. Diggy Dog, Busbee, Nike, and Molly, this is what I've been up to when I wasn't there to play fetch with you…

Table of Contents

Abstract

Iminosugars as dengue virus therapeutics:
Molecular mechanisms of action of a drug entering clinical trials
Andrew C. Sayce, Pembroke College, Doctor of Philosophy, Trinity Term 2014

Iminosugars are a class of small molecules defined by substitution of a sugar's ring oxygen with nitrogen. Various chemical modifications of these basic structures (*e.g.* alkyl chain addition off of the ring nitrogen) have been developed during the last several decades. These molecules have been considered as therapeutics for a number of pathologies including viral infection, congenital disorders of glycosylation (of both glycoproteins and glycolipids), and diabetes. This thesis focuses on the application of a small subset of iminosugars, known as deoxynojirimycin derivatives, as therapeutics against dengue virus induced pathology. Dengue virus infection predominates in tropical climates, but autochthonous infection has recently emerged in areas of both southern Europe and the southern United States. With 390 million people infected annually, dengue is the most prevalent arthropod-borne viral infection worldwide, and the possibility of severe pathology including haemorrhage, shock, and/or death, necessitates development of effective antiviral therapies. Although the molecular mechanisms responsible for progression to severe dengue disease are not completely understood, there is considerable evidence for the role of both the innate and the adaptive immune responses in development of life-threatening complications. Excessive activation of the innate immune response, a phenomenon known as *cytokine storm*, has been hypothesised to explain development of symptoms related to vascular permeability, whereas the adaptive immune response has been implicated in severe disease through two hypotheses – the *antibody dependent enhancement* and *original antigenic sin* hypotheses. The evidence regarding each of these potential mechanisms of severe pathology is discussed throughout this thesis principally with respect to how iminosugar treatment could alter any detrimental effects of the immune response to dengue virus infection. The principal aim of this thesis is to consider the potential of deoxynojirimycin iminosugars as antiviral therapeutics in dengue infection with a focus on how these molecules exert their antiviral effects in primary human cells. I first consider the contributions of glycoprotein inhibition and glycolipid inhibition on production of infectious dengue virus. These experiments suggest that inhibition of glycoprotein folding is responsible for inhibition of infectious dengue virus production. I next consider the impact of treatment of a promising clinical candidate iminosugar, *N*9-methoxynonyl-deoxynojirimycin (M*O*N-DNJ), on the primary human macrophage transcriptome. In uninfected macrophages as well as macrophages infected with dengue virus or treated with lipopolysaccharide to model bacterial sepsis, iminosugar treatment results in activation of the unfolded protein response and inhibition of several elements of the inflammatory response including signalling by the cytokines IFN-γ and TNF-α, and the inflammatory cascade mediated by NF-κB. Activation of the unfolded protein response as a result of treatment with M*O*N-DNJ can be confirmed by analysis of phosphorylated (activated) NFE2L2, a transcription factor that functions principally to control oxidative stress in response to ER stress signals. Modulation of the inflammatory response of macrophages to dengue infection and bacterial sepsis is confirmed by analysis of secreted cytokines. As predicted by my transcriptomic experiments, levels of TNF-α and IFN-γ produced in response to dengue or lipopolysaccharide are reduced by treatment with M*O*N-DNJ. Finally, I attempted to extend these observations to an animal model of dengue infection with a particular focus on TNF receptor and ligand superfamily members. Unfortunately, heterogeneity of cells types from tissue samples as well as limitations of the animal model complicate interpretation of these findings. Nevertheless, this thesis demonstrates that M*O*N-DNJ is an effective dengue antiviral therapeutic and that this therapeutic activity may be related to both reduction of infectious virus as a consequence of inhibition of glycoprotein processing and as a result of changes to the host's response to the pathogen. These results have been used in part to justify recently initiated clinical trials of M*O*N-DNJ as a dengue antiviral therapy.

Abbreviations

2-AA	2-aminobenzoic acid
A_{xxx}	absorbance at wavelength of xxx nm
Ab	antibody
ADE	antibody dependent enhancement
AFRIMS	United States Armed Forces Research Institute of Medical Sciences, Thailand
ALT	alanine aminotransferase
ANOVA	analysis of variance
APC	antigen presenting cell
Asn	asparagine
AST	aspartate aminotransferase
Atg	autophagy-related gene
BHK-21	hamster kidney cell line
b.i.d	*bis in die* (twice daily)
BuCAST	butylated CAST; celgosivir; 6-*O*-butanoyl-CAST
BVDV	bovine viral diarrhoea virus
C	capsid
C#	complement protein number #
C6/36	*Aedes albopictus* larval cell line
CALR	calreticulin
CaMKII	calmodulin-dependent protein kinase II
CANX	calnexin
CAST	castanospermine
CCL	chemokine (C-C motif) ligand
CC_{50}	concentration required to reach 50% cytotoxicity
CC_{10}	concentration required to reach 10% cytotoxicity
CD	cluster of differentiation

cDNA	complimentary DNA
CFL1	cofilin 1
CGS	Cambridge Genomic Services
CHAPS	3-[(3-cholamidopropyl)dimethylammonio]-1-propanesulfonate
CI	confidence interval
CLEC5A	C-type lectin domain family 5, member A
conA	concanavalin A
C_V	coefficient of variation
CXCL	CXC-chemokine ligand
DAK	dihydroxyacetone kinase
DALYs	disability-adjusted life years
DAPI	4’,6-diamidino-2-phenylindole
DC	dendritic cell
DC-SIGN	DC-specific intercellular adhesion molecule-3-grabbing nonintegrin
DENV	dengue virus
DF	dengue fever
DGJ	deoxygalactonojirimycin
DHF	dengue haemorrhagic fever
DMSO	dimethyl sulfoxide
DNJ	deoxynojirimycin
DSS	dengue shock syndrome
DTT	dithiothreitol
E	envelope
EBOV	Ebola virus
EDTA	ethylenediaminetetraacetic acid
ELISA	enzyme-linked immunosorbant assay
ER	endoplasmic reticulum

ERAD	ER-associated degradation
EtOH	ethanol
FACS	fluorescence activated cell sorting
FAM	6-fluorescein amidite
Fc	antibody Fragment, crystallisable
FcγR	Fc gamma chain receptor
FOS	free oligosaccharides
GAPDH	glyceraldehyde 3-phosphate dehydrogenase
GCS	glucosylceramide synthase
GI	gastrointestinal
Glc	glucose
GlcNAc	*N*-acetyl-glucosamine
GM-CSF	granulocyte macrophage colony-stimulating factor
GM3	monosialodihexosylganglioside
GSL	glycosphingolipid
G-CSF	granulocyte-colony stimulating factor
HBV	hepatitis B virus
HBSAg	HBV surface antigen
HBSS	Hank's balanced salt solution
HCV	hepatitis C virus
HEPES	4-(2-hydroxyethyl)-1-piperazineethanesulfonic acid
HIV	human immunodeficiency virus
HI-FBS	heat-inactivated foetal bovine serum
HL60	human promyelocytic leukaemia cells
HUVEC	human umbilical vascular endothelial cell
ICAM	intercellular adhesion molecule
IC_{50}	concentration required to reach 50% inhibition

IC_{90}	concentration required to reach 90% inhibition
IFA	immunofluorescence assay
IFN-γ	interferon-gamma
i.g.	intragastric (oral gavage)
IL	interleukin
IL1RL1	IL-1 receptor-like-1 protein
INFV	influenza virus
IP	immunoprecipitation
i.p.	intraperitoneal
IPA	Ingenuity® Pathway Analysis
IRF	interferon regulatory factor
ISG	interferon stimulated gene
i.v.	intravenous
JAK	Janus kinase
JEV	Japanese encephalitis virus
JNK	c-Jun N-terminal kinase
kb	kilobase
LAL	*Limulus* amoebocyte lysate
LFT	liver function test
LFA-1	lymphocyte function-associated antigen 1
LILRB1	leukocyte immunoglobulin-like receptor B1
LLC-MK_2	*Macaca mulatta* kidney cell line
LOD	limit of detection
LPS	lipopolysaccharide
M	membrane
mAb	monoclonal antibody
Man	mannose

MARV	Marburg virus
MDA-5	melanoma differentiation-associated gene 5
MDMΦ	primary human monocyte-derived macrophage
MeOH	methanol
MES	2-(*N*-morpholino)ethanesulfonic acid
MHC	major histocompatibility complex
MIF	macrophage migration inhibitory factor
miR	microRNA
m.o.i.	multiplicity of infection
M*O*N-DNJ	*N*9-methoxynonyl-DNJ
MOPS	3-(*N*-morpholino)propanesulfonic acid
MR	mannose receptor
MTS	3-(4,5-dimethyl-2-yl)-5-(3-carboxymethoxyphenyl)-2-(4-sulfophenyl)-2H-tetrazolium
MyD88	myeloid differentiation primary response gene 88
MΦ	macrophage
*N*AP-DNJ	*N*-(6'[4''-azido-2''-nitrophenylamino]hexyl)-1-DNJ
*N*B-DGJ	*N*-butyl-DGJ
*N*B-DNJ	*N*-butyl-DNJ
NF-κB	nuclear factor kappa-light-chain-enhancer of activated B cells
NFE2L2	nuclear factor (erythroid-derived 2)-like 2; Nrf2
*N*M-DNJ	*N*-methyl-DNJ
*N*N-DNJ	*N*-nonyl-DNJ
NOS2	nitric oxide synthase 2
NPC	Niemann-Pick type C
NP-HPLC	normal phase-HPLC
NS	non-structural
PBMC	peripheral blood mononuclear cell

PBS	phosphate buffered saline
PDB	Protein Data Bank
PDGF	platelet-derived growth factor
PDI	protein disulphide isomerase
pfu	plaque forming units
p.i.	post-infection
prM	precursor membrane
PRNT	plaque reduction neutralisation test
PRR	pattern recognition receptor
qRT-PCR	quantitative real time, reverse transcription polymerase chain reaction
RANTES	regulated on activation, normal T cell expressed and secreted
RBC	red blood cell
rhIL-4	recombinant human interleukin-4
RIG-I	retinoic acid-inducible gene 1
SARM	sterile alpha- and armadillo-motif-containing protein
sCD	soluble cluster of differentiation
Ser	serine
SHP-1	Src homology region 2 domain-containing phosphatase-1
SI	selectivity index
SOCS	suppressor of cytokine signalling
STAT	signal transducer and activator of transcription
sTNFR	soluble TNF-α receptor
sVEGFR	soluble VEGF receptor
Syk	spleen tyrosine kinase
TAMRA	tetramethylrhodamine
TANK	TRAF family member-associated NF-κB activator
TCS	tissue culture supernatant

TGF-β	transforming growth factor beta
Th1	T-helper cell 1
$T_{1/2}$	terminal half-life
Th2	T-helper cell 2
Thr	threonine
t.i.d.	*ter in die* (three times daily)
TLR	toll-like receptor
TMB	3,3',5,5'-tetramethylbenzidine
TNFRSF4	tumor necrosis factor receptor superfamily member 4; OX40; CD134
TNFRSF9	tumor necrosis factor receptor superfamily member 9; 4-1BB; CD137
TNF-α	tumor necrosis factor alpha
TNFSF4	tumor necrosis factor (ligand) superfamily member 4; OX40L; CD252
TNFSF9	tumor necrosis factor (ligand) superfamily member 9; 4-1BBL; CD137L
ToP-DNJ	α-tocopherol conjugated DNJ
TRAIL	TNF-related apoptosis-inducing ligand
UGGT	UDP-glucose glycoprotein:glucosyltransferase
UPR	unfolded protein response
UTR	untranslated region
v/v	volume per unit volume
VIC	proprietary fluorescent reporter dye (Life Technologies)
VEGF	vascular endothelial growth factor
VSV	vesicular stomatitis virus
w/v	percent weight per unit volume
WHV	woodchuck hepatitis virus
X	any amino acid

I

Introduction

I.1. Dengue virus

I.1.A. Composition and morphogenesis

Dengue virus (DENV) is an arthropod-borne virus of the genus *Flavivirus* within the *Flaviviridae* family. [1] Amongst dengue viruses there exists a considerable degree of genetic diversity (63-68% amino acid sequence positional homology), [1] such that four antigenically distinct viral serotypes (DENV-1, -2, -3, and -4) can be differentiated by the plaque reduction neutralisation test (PRNT). [2] All four DENV serotypes possess a genome of approximately 11 kilobases (kb) of single-stranded, positive-sense RNA that includes a single open-reading frame of ~10.2 kb. From this coding region, a single polyprotein is produced and processed by both host and viral proteases to produce three structural proteins and seven non-structural (NS) proteins as presented in *Figure 1.1*. [3]

The structural proteins, capsid (C), membrane (M), and envelope (E), in conjunction with a host cell membrane-derived lipid envelope assemble to form a mature virion of approximately 50 nm diameter. [4] In order to form a mature dengue virion, M protein must be cleaved from the precursor membrane (prM) protein by a host-resident furin protease in the Golgi. [4-7] In the case where prM is incorporated into the viral shell, virions form an icosahedrally symmetric 60 nm "spiked" particle. Each spike is composed of three copies of prM/E dimer with epitopes of both proteins accessible at the viral surface. [6,7] In the case of the mature dengue virion, considerable rearrangement of surface proteins takes place post-cleavage such that 90 E protein dimers form a smooth icosahedral shell that masks 180 copies of M protein. [4,8] Within mature dengue virions, the RNA genome associates with the capsid protein [4,9] and is circularised through interaction of conserved motifs in the 5' and 3' untranslated regions. [10,11] Poor resolution of the genomic core is observed in available structural studies, suggesting considerable disorder. [4]

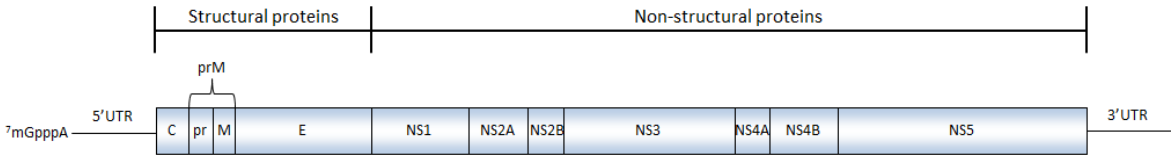

Figure I.1. The dengue genome possesses a 5' cap and untranslated region (UTR) followed by a 10.2 kb single open reading frame and 3' UTR. The RNA lacks a polyadenylated tail, but is circularised by structural motifs in the 5' and 3' UTRs. The three structural proteins are arrayed in tandem followed by the seven non-structural proteins.

DENV morphogenesis depends heavily on host-based pathways – particularly *N*-glycoprotein processing via the calnexin (CANX)/calreticulin (CALR) cycle. [12] Three of the ten proteins encoded by the DENV genome are *N*-linked glycoproteins: E [13-16], prM [13,15,16], and NS1. [13,15-18] The *N*-linked glycans on these proteins are thought to mediate folding of glycoproteins via association of the glycoprotein with endoplasmic reticulum (ER) resident chaperones CANX and/or CALR in order to coordinate interaction with various protein disulphide isomerases (PDIs) and foldases. [19] Indeed, E possesses two such glycans [18] and six intramolecular disulphide bonds, [20] prM possesses one glycan [18] and three intramolecular disulphide bonds, [20] and NS1 possesses two glycans [18] and six intramolecular disulphide bonds. [21] When folded correctly, NS1 monomers can form plasma membrane associated dimers. Alternatively, a hexameric form of NS1 may be secreted as a trimer of dimers with levels of detection in sera of infected patients up to 50 µg/ml. [22-25] The hexameric form of NS1 can also bind to the plasma membrane of cells through an interaction with specific sulphated glycosaminoglycans. [26] Deletion of NS1 glycans, in particular asparagine (Asn) 207, results in decreased monomer and dimer stability although some NS1 is still secreted. [27] Recent crystallographic structures of NS1 monomers and multimers suggest crucial stabilising roles of disulphide bridges in monomer and multimer domain architecture [28] as displayed in *Figure 1.2*. As can be expected, the disulphide bonds of E [20] perform similar roles in stabilising critical epitopes of

protein structure and biological function [29-31] and *N*-linked glycans, particularly Asn67 of E, are crucial for production of infectious virus in mammalian but not insect cells, [32] and differential glycosylation of E produced in different cell types may affect tropism of the mature virion. [33] Intriguingly, the three disulphides and single *N*-glycan of prM are located exclusively in the precursor fragment of the protein cleaved from the mature M protein. [20] Relatively little is known about the structural and physiological contribution of these features in the precursor protein; however, there is speculation that these elements are crucial for interactions between prM and C [34] and/or between prM and E. [7,35] X-ray crystal structures of E as well as prM in complex with E (*Figure 1.3*) demonstrate a herringbone pattern dependent upon disulphides for backbone formation with glycans projected in a single direction towards the exterior of the mature virion.

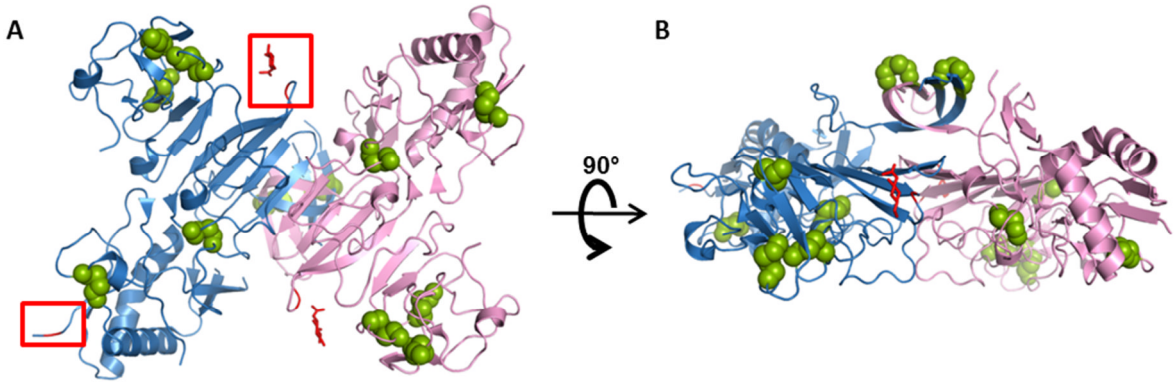

Figure 1.2. Ribbon representation of dengue NS1 dimers (Protein Data Bank (PDB) ID: 406B) demonstrates the considerable structural dependence on disulphide bridges (green spheres). Each monomer (blue, pink) possesses two *N*-linked glycans (red sticks and highlighted red boxes, blue monomer of **A**) one of which is located in the "wing" domain (Asn130, distal lower left in **A**), and the other of which is located along the core β-ladder (diagonal top left to bottom right in **A**). Each monomer possesses six intramolecular bridges whereas interaction between the monomers is non-covalent and centred about a β-roll dimerisation domain composed of β-hairpins intertwined across the dimerisation axis (top central structure of **B**).

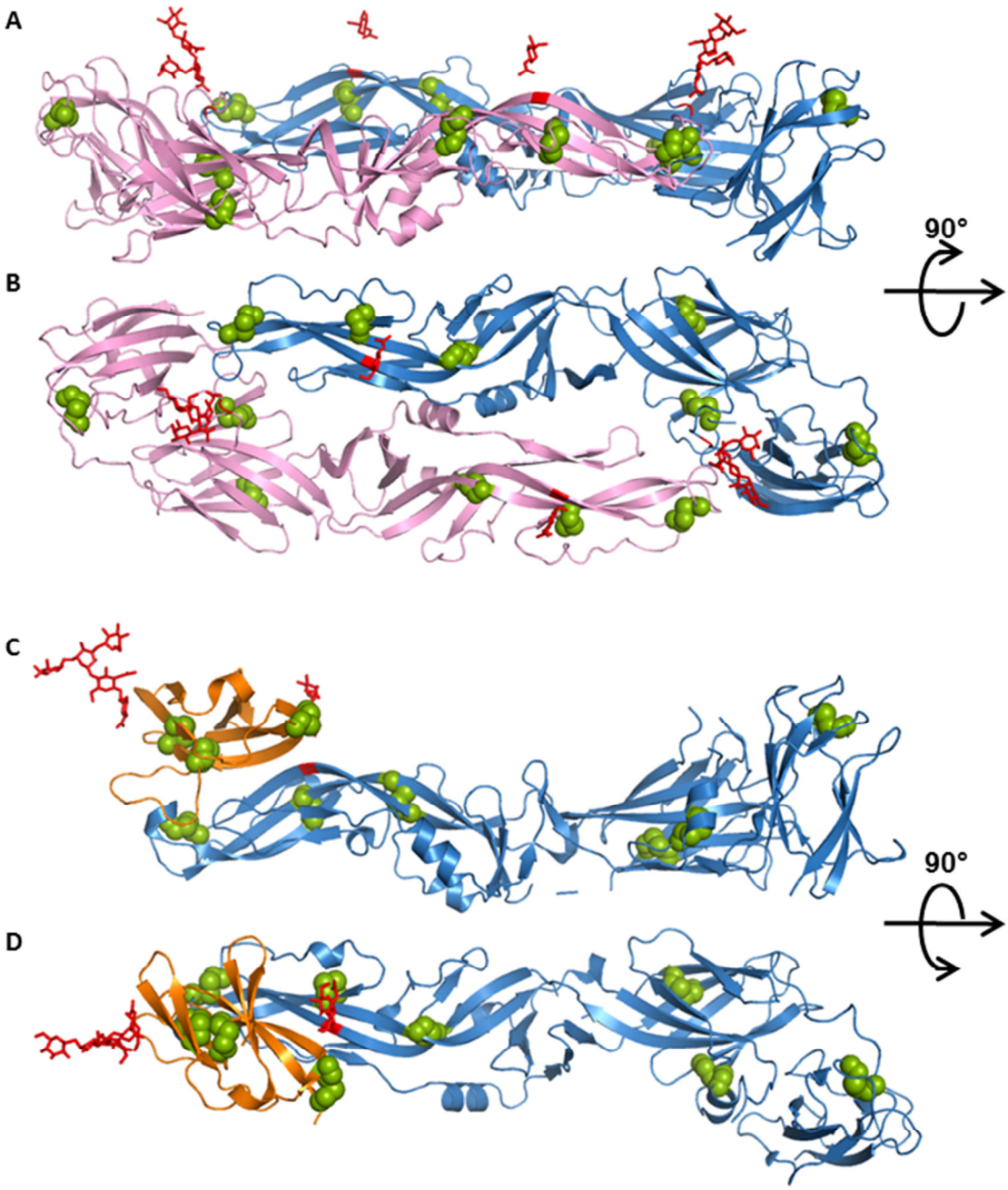

Figure 1.3. Ribbon representation of E dimers (PDB ID: 10AN) (**A**, **B**) and prM/E dimers (PDB ID: 3C5X) (**C**, **D**). The "herringbone" pattern of E dimers depends heavily upon six intramolecular disulphides (green spheres) to form a stable backbone for each monomer (blue and pink). When the dimers are arranged on the surface of the virus, the *N*-linked glycans (red sticks) project outwards as seen in **A**. During production of the virion, prM (orange in **C** and **D**) associates with E (blue) prior to furin-mediated cleavage.

Given the reliance of DENV on glycoprotein processing and subsequent folding, it is not surprising that the ER is highly important in replication of viral RNA, production and processing of the DENV polyprotein, and formation of infectious virions (*viral morphogenesis*). Live cell imaging of subcellular organelles coupled with transmission electron microscopy has facilitated detection of ER derived structures important in nearly all stages of the DENV replication cycle. [36] *Vesicular packets* of approximately 90 nm diameter form via invagination of the ER membrane. The viral RNA polymerase as well as dsRNA can be found within these vesicular packets, suggesting that vesicular packets are the site of DENV RNA replication. Surrounded by these vesicular packets are distinct ER-derived structures termed *convoluted membranes* that are believed to be the site of RNA translation and polyprotein processing due to the singular presence of the DENV NS2B/3 protease complex. Dilated cisternae connect vesicular packets and convoluted membranes to the ER, and within the cisternae, arrays of spiked and presumably immature dengue virions can be identified. Thus, a considerable proportion of functions crucial to the replication of DENV occur within ER-derived compartments. [36] Detection of Golgi-associated virus has been observed, suggesting that the ER-associated virus may not be released into the extracellular environment without further processing in the Golgi to form mature virions. The relative scarcity of Golgi-associated virus suggests that trafficking of virus from the ER to the Golgi and subsequent trimming could be the limiting step in DENV replication; [37] however, it is equally possible that the immature virions observed in the ER are not destined for extracellular secretion due to recognition of misfolding by the cell and/or some alternative mechanism yet to be described. If these immature virions are destined for secretion, the intricacies of protease-mediated cleavage of prM/M, rearrangement of envelope multimers, and further processing of glycans in the Golgi in the context of intact viruses remain to be elucidated. Nevertheless, it is clear that the ER plays a significant role in the infection-cycle of DENV.

I.1.B. Distribution, burden, and intervention

DENV is the most significant arthropod-borne virus (arbovirus) worldwide with approximately 390 million people infected with the virus every year. Of these 390 million individuals, approximately 96 million develop overt clinical or subclinical disease. [38] Prior to 1970, only nine countries had reported severe dengue epidemics, but in the intervening forty years, DENV has become endemic in more than 100 countries. [39] The virus is principally a burden on tropical and sub-tropical regions; however, the expansion of suitable habitats for *Aedes aegypti* and *Ae. albopictus* mosquito vectors has recently resulted in autochthonous DENV infection in southern Europe [40-42] and the southern United States. [43,44] Even with experienced medical care, case fatality rates for severe disease can approach ten percent; [45] however, supportive management of symptoms (*e.g.* fluid management) can typically reduce case fatality rates below one percent. [46,47] Accurate estimates of morbidity (such as disability-adjusted life years (DALYs)) and mortality are difficult to obtain due to severe under-reporting and misclassification, [38] but conservative estimates suggest a toll of 264 DALYs per million population and approximately 20,000 deaths yearly due to DENV infection. [39]

In spite of considerable research efforts over the last decades, there is at present neither a specific antiviral therapeutic nor an effective vaccine against DENV. Lack of clinical efficacy has been reported in the most promising dengue antiviral to date, an iminosugar called Celgosivir that targets host α-glucosidases, although this is possibly a consequence of difficult to achieve clinical endpoints. [48] Similarly, oral prednisolone administration, a glucocorticosteroid intervention aimed at reducing inflammation, has been trialled as a host-based therapeutic but exhibited neither protection nor adverse events. [49] Although the prednisolone study was underpowered to detect enhanced clinical outcomes, a further investigation of the anticipated immunomodulation revealed failure to attenuate the host immune response. [50] Further attempts have been made to modulate the immune response to the virus using both doxycycline and tetracycline. Both drugs demonstrated

effective reduction of several serum cytokines with some success although the study was again underpowered to assess enhanced clinical outcomes. [51] Although chloroquine reduces infectious DENV production *in vitro* [52,53] and is capable of reducing inflammation via several mechanisms (*e.g.* reduced lymphocyte proliferation, inhibition of reactive oxygen species generation, etc. reviewed in [54]), clinical trials of chloroquine failed to demonstrate any efficacy as an effective dengue antiviral or immunomodulator. [55] Finally, balapiravir, a prodrug of a nucleoside analogue, also failed to demonstrate any efficacy as a dengue antiviral. [56] A trial regarding the use of lovastatin with the presumptive use as an inhibitor of viral assembly due to HMG-CoA reductase inhibition and modulation of cellular cholesterol [57] is currently ongoing, [58] but given the recurrent failure of DENV therapeutic strategies to date, continued efforts in antiviral drug development are essential.

Further clinical failure has been observed in vaccine development efforts. A recent phase IIb clinical trial of a tetravalent vaccine candidate by Sanofi-Pasteur provided limited success in Thai schoolchildren. In this trial, variable efficacy against the four dengue serotypes (DENV-1 – 55.6%, DENV-2 – 9.2%; DENV-3 – 75.3%; DENV-4 – 100.0%) was observed. [59] Similar efficacy was observed in the subsequent phase III trial in more than ten thousand children across five countries in the Asia-Pacific region with efficacy against DENV-2 still observed with a 95% confidence interval of -9.2% to 61.0%. Nevertheless, protection against all four serotypes as measured by pooled vaccine efficacy was 56.6% (with a 95% confidence interval of 43.8-66.4%) and breakthrough episodes of DENV infection were milder in individuals administered vaccine in comparison to placebo. [60] A recent press-release by Sanofi-Pasteur suggests more successful protection against all four serotypes in a phase III study in Latin America, [61] but a detailed report has not yet been presented. Given these results, a vaccine strategy to prevent dengue disease is promising; however, lack of protection against DENV-2 is a considerable concern. Although the idea has been presented that efficacy

against three of the four serotypes may be sufficient for long-term success, [62] there is no evidence as yet to support this theory. Further, our relative lack of understanding of the immune events responsible for progression to severe disease (as will be discussed later), suggests a significant cause for concern regarding widespread distribution of a partially efficacious vaccine. The failure of this vaccine raises the additional concern that our current *in vitro* method of predicting *in vivo* protection, the plaque reduction neutralisation test (PRNT) assay, does not accurately predict clinical protection. [59,63,64] Although alternative vaccine candidates such as DENVax [65-68] and TetraVax-DV/TV003 [69] are in varying stages of clinical development, these vaccines like the Sanofi-Pasteur counterpart have been developed based on the PRNT assay (as well as safety measures) and thus may not provide tetravalent clinical protection. Finally, monitoring of safety for a period greater than the currently observed 25 months is essential for partially efficacious vaccines given the potential for antibody-dependent severe disease discussed later in this chapter.

I.1.C. Clinical features of disease

In the effort to develop an efficacious DENV specific antiviral, it is essential to consider the clinical aspects of disease presentation, progression, and pathology in coordination with anticipation of barriers to success. The principal difficulty in treatment of dengue disease is a result of viral kinetics as outlined in *Figure 1.4*. Viral load is thought to remain relatively low following the bite from an infected mosquito until approximate time of onset of febrile symptoms – typically around four (but perhaps as much as twelve) days post-bite. At this point, plasma viral load increases rapidly as symptoms worsen. In dengue endemic areas where awareness of the potential for severe disease is high, infected individuals tend to present between one and three days post-infection; however, even with public awareness, clinical presentation still tends toward later (day three) rather than earlier time frames. Around day four of fever onset, plasma viraemia peaks and afterwards declines rapidly in coordination with the time of defervescence. [70] Thus, the window between presentation to

clinic and natural clearance of plasma viral load is very short – often on the order of twenty-four hours. Following defervescence, the patient enters a *critical period* of twenty-four to forty-eight hours during which severe disease manifestations are most frequent. Previously referred to as dengue haemorrhagic fever (DHF) and dengue shock syndrome (DSS), these severe events have been redefined to *dengue with warning signs* and *severe dengue* and are largely characterised by vascular imbalance as detailed in *Table 1.1*. [71,72] Given the short window between clinical presentation and rapid decline in viral load, any direct acting antiviral must be rapidly and profoundly effective at reduction of viral load to have any reasonable chance at clinical efficacy assuming reduced viral load can improve clinical outcomes. In addition, the onset of severe symptoms following plasma viral clearance has led many investigators to conclude that severe disease is a consequence of the mechanisms of viral clearance rather than a direct result of viral activity. (Reviewed in [70,73]) As will be discussed in the following sections, the molecular mechanisms of this proposed immunopathogenesis remain to be elucidated and are a major area of debate within the dengue research field. Nevertheless, if amelioration of severe disease is our final aim, then consideration must be given to the necessity of treating severe pathology as a result of immune function in addition to, or even rather than, virally-induced pathogenesis.

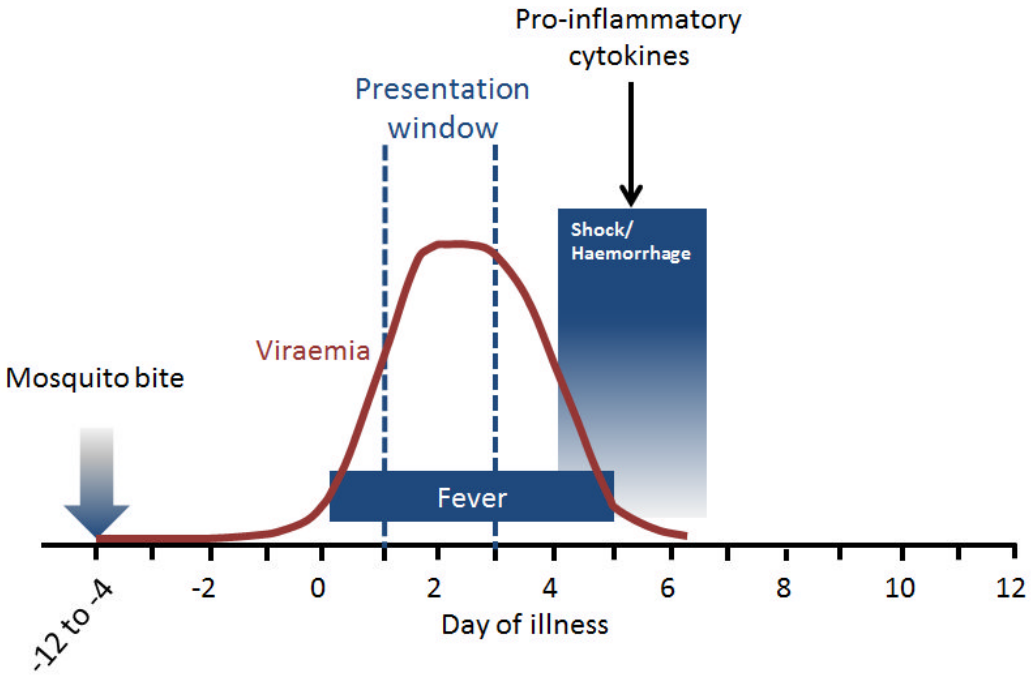

Figure 1.4. The kinetics of dengue virus infection creates complications for clinical intervention. Rapid decline of plasma viral load (red line) occurs shortly after clinical presentation (blue dashed lines). Coordination of severe symptoms (shock/haemorrhage, blue faded box) with immune responses suggests an immunopathogenic mechanism of severe disease progression. Adapted from Halstead.[70]

I.1.D. Immunopathogenesis

Dengue immunopathogenesis is a complicated and highly debated topic. Nevertheless, strong evidence exists for several immune mechanisms as key mediators of development of severe disease. Although severe disease is more frequently noted in secondary (or tertiary, though rarely quaternary) heterologous infection, [74] it is of crucial importance to recall that severe disease may also develop during a primary DENV infection. Thus, while adaptive immune responses may bias the immune environment toward progression of severe disease, innate immune response mechanisms are, at least in some cases, entirely responsible for development of immune-mediated pathology.

Table 1.1. WHO dengue classification guidelines 2009[71]

Dengue without warning signs

Fever and two of the following:

- Nausea, vomiting
- Rash
- Aches and pains
- Leukopenia
- Positive tourniquet test

Dengue with warning signs

Dengue as above with any of the following:

- Abdominal pain or tenderness
- Persistent vomiting
- Clinical fluid accumulation
- Mucosal bleeding
- Lethargy, restlessness
- Liver enlargement >2 cm
- Increase in haematocrit concurrent with rapid decrease in platelet count

Severe dengue

Dengue with at least one of the following:

- Severe plasma leakage leading to:
  - Shock (DSS)
  - Fluid accumulation with respiratory distress
- Severe bleeding as evaluated by clinician
- Severe organ involvement
  - Liver: AST[a] or ALT[b] ≥ 1000
  - Central nervous system: impaired consciousness
  - Heart/other organ failure

[a] ALT (alanine aminotransferase)

[b] AST (aspartate aminotransferase)

I will start by examining the evidence for a role of the innate immune response in observed DENV immunopathology and then consider the role of adaptive immune responses in severe disease.

I.1.D.i. Innate immunity

I.1.D.i.a. Cytokine/chemokine observations

Given the rapid decline in plasma viral load observed prior to the critical phase, many investigators have speculated that immune function/clearance mechanisms are responsible for the severe pathologies noted in DENV infection. Principal among the suspects for such activity are the soluble

mediators of innate immunity: cytokines, chemokines, and their soluble receptors. As a rule, cytokines and chemokines appear to be elevated amongst those individuals that progress to severe disease; however, there is considerable disagreement as to which mediator(s) is/are responsible for progression of immunopathology. Whether a pro-inflammatory T-helper cell 1 (Th1) or anti-inflammatory T-helper cell 2 (Th2) environment is predominant in severe infections remains contentious; [73,75] however, I would suggest that this disagreement is a result of the kinetics of immune surveillance.

The majority of evidence for cytokine/chemokine involvement in severe pathology comes from studies measuring secreted levels of these mediators in the serum/plasma of infected patients; thus, there is considerable potential for variability of viral, host genetic, and other population measurements obtained from one study to another. Amongst the cytokines/chemokines and soluble receptors implicated in the *cytokine storm* are: interferon (IFN)-alpha (IFN-α), IFN-γ, interleukin (IL)-1β, IL-4, IL-6, IL-7, IL-8, IL-10, IL-12, IL-13, IL-17, IL-18, chemokine (C-C motif) ligand 2 (CCL2) (MCP1 or MCAF), CCL3 (MIP-1α), CCL4 (MIP-1β), CXC-chemokine ligand 9 (CXCL9) (MIG), CXCL10 (IP-10), granulocyte-colony stimulating factor (G-CSF), granulocyte macrophage colony stimulating factor (GM-CSF), macrophage migration inhibitory factor (MIF), platelet-derived growth factor (PDGF)-BB, regulated on activation, normal T cell expressed and secreted (RANTES), transforming growth factor-beta (TGF-β), tumour necrosis factor-alpha (TNF-α), TNF-related apoptosis-inducing ligand (TRAIL), vascular endothelial growth factor (VEGF), soluble cluster of differentiation (sCD) 4, sCD8, soluble TNF-α receptor I (sTNFRI), sTNFRII, soluble IL-2 receptor (sIL-2R), IL-1 receptor agonist (IL-1RA), IL-1 receptor-like-1 protein (IL1RL1), soluble VEGF receptor I (sVEGFRI), and sVEGFRII. [73,76-107] In the vast majority of these experiments, measurements are taken at a single time point during severe disease and compared to either a convalescent sample or a similarly timed non-severe disease sample. Perhaps the most illustrative example of why such single time measurements are

problematic can be found in the sequential measurements of IFN-α, IFN-γ, IL-10, sIL-2R, and sTNFRII by Libraty *et al.* wherein a drastic differential expression is noted in daily cytokine measurements. [76] Similar waves of innate response activation are noted in transcriptomics profiles of DHF patients. [108] Furthermore, these measurements are collected for plasma or serum samples and not the tissue sites of capillary leakage. It may be that the molecular mediators of fluid imbalances at the tissue vary greatly from the immune environments of the circulatory system. Nevertheless, the repeated inclusion of several markers, notably TNF-α, IFN-γ, and IL-10, as elevated in severe disease suggests a reliable biological result. Whether these markers are directly responsible for vascular leak or precipitate further signalling cascades that promote vascular imbalances remains to be determined, but the consistent correlation with severe pathology suggests that one of the above scenarios is likely true. For both TNF-α and IFN-γ, these results indicate that a predominately Th1 environment leads to the development of severe pathology as has been observed in other cytokine storm pathologies including avian influenza [109] and bacterial sepsis. [110]

TNF-α is particularly appealing as a causative factor of severe DENV disease. TNF-α is capable of directly increasing endothelial cell permeability, [111] and the TNF-α 308A allele associated with stronger TNF-α responses is more common in DHF patients. [112] Further, antibody (Ab) directed against TNF-α can prevent vascular leak-mediated death in an AG129 mouse model of ADE DENV pathology. [113] However, TNF-α is likely to act in concert with other soluble mediators. Additional work has demonstrated that macrophage (MΦ)-mediated inflammatory responses including production of TNF-α and other inflammatory cytokines but not IFN-α depends upon C-type lectin domain family 5, member A (CLEC5A) recognition of DENV. [114-117] In contrast to the AG129 model, a *STAT1*$^{-/-}$ (signal transducer and activator of transcription 1 knock-out) mouse model was not protected with TNF-α blockade via administration of recombinant TNF receptor fused to Fc, but mice were protected with two independently administered Abs against CLEC5A. This suggests a crucial

immunopathogenic role for CLEC5A-induced TNF-α in concert with other inflammatory cytokines in severe disease of these mouse models. [114] Evidence for the importance of IFN-γ in severe pathology is more controversial; however, induction of downstream inflammatory responses including generation of reactive oxygen species and other reactive free radicals (*e.g.* nitric oxide synthase 2 (NOS2))[118] by MΦs suggests a potential mechanism of pathology. Indeed, reactive nitrogen and oxygen species are important for development of haemorrhage in immune-competent mice challenged with DENV. [119] Both TNF-α and IFN-γ allow increased passage of albumin through endothelial cells in coordination with lowered transendothelial electrical resistance suggesting that both cytokines increase endothelial cell permeability; [120] however, considerable evidence also exists for a protective role for IFN-γ both in animal and human challenge models of DENV infection. [121,122] In contrast to the Th1 cytokines, IL-10 has also been associated with severe pathology. As will be discussed in more detail in the adaptive immune response section of this thesis, IL-10 is considered to be a central regulator of anti-inflammatory response. [123] Therefore, elevation of IL-10 may be a hallmark of existing excessive pro-inflammatory responses that must be controlled by the host with an excessive induction of this anti-inflammatory regulator. In summary, there is considerable evidence for cytokine involvement in severe DENV pathology, but the likelihood that there is one key cytokine is extremely improbable. Rather, the extensive interconnectedness of innate immune regulatory networks means that cytokine involvement is almost certainly multi-factorial.

I.1.D.i.b. Complement cascade interactions

Much like the cytokine response to pathogens, the complement system is capable of mediating immune clearance of pathogens in the absence of previous exposure (*memory*). Ab-mediated recognition of antigen, the classical pathway, initiates cleavage of complement proteins circulating throughout the body as zymogens to their active form. In the absence of memory, activation may be

initiated by lectin binding to pathogen surface or by spontaneous binding of complement protein C3 (complement proteins named in the convention C#) to pathogen surface. As a result, complement proteins initiate inflammatory responses, enhance opsonisation of pathogen by phagocytes, and lyse pathogens or infected cells. [123] Prior to the explosion of interest in cytokine involvement in severe DENV pathology, the complement cascade was suggested as a potential mediator of severe disease. [124,125] This work noted depressed levels of all serum complement proteins (except C1r and C7) in cases of enhanced pathogenesis with C3 exhibiting the most marked reduction. With cleavage of C3, subunits C3a and C3b are produced. The central role of C3 subunits C3a and C3b in complement anaphylatoxin and opsonisation activity, respectively, suggest considerable pathogenic consequences if depressed levels of C3 are a consequence of complement consumption. In particular, C3a (in conjunction with C4a and C5a) drives anaphylatoxin activity which promotes mast cell degranulation and inflammatory cytokine/chemokine production leading to vasodilation and increased vascular permeability with the potential for shock. [126-128]

Recently, interest in complement-mediated pathogenesis has resurfaced following the observation that soluble NS1 can activate complement to completion and that high levels of NS1 and anaphylatoxin C5a were observed in patients experiencing DSS. [22] Somewhat at odds with this observation and the experiments previously mentioned are experiments that demonstrate antagonism of the C4 convertase by NS1. [129,130] This antagonism appears to be mediated by interactions of NS1 glycans with both C4 and C1s. [131] However, complement inhibitory factor clusterin has been immunoprecipitated with NS1 further suggesting induction of the cascade, [132] and endothelial cells infected with DENV induce properdin factor B, an activator that directs C3a and C5a production, by 34-fold. [133] A recent study of C3 structural polymorphisms in a Thai population could not detect any correlation with severe disease. [134] Thus, the net effect of DENV/complement interactions on a population level remains unclear, but as is the case with

cytokine involvement, the net effects of these interactions on an individual basis are likely crucial directors of clinical outcomes.

I.1.D.ii. Adaptive immunity

I.1.D.ii.a. Antibody dependent enhancement (ADE) of infection

Initial speculation for a significant role of the adaptive immune response in development of severe dengue disease stemmed from two clinical observations. As first noted in 1967, the incidence of severe disease amongst individuals experiencing a secondary DENV infection is much greater than the incidence of severe disease in individuals experiencing primary DENV infection. [135,136] In addition, severe dengue disease incidence is elevated amongst children who are born to dengue immune mothers and experience primary dengue infection between two and twelve months of age. [137] It was hypothesised that these enhanced levels of disease could be explained by the presence of non-neutralising antibodies in both instances: in secondary infection, antibodies against the primary infecting serotype predominate but are of relatively low avidity to the epitopes presented on the circulating heterologous virus, and in children younger than one year, waning maternal Ab titres could recognise but not neutralise circulating virus. This hypothesis has come to be known as the ADE hypothesis. In the intervening years, molecular mechanisms related to ADE have been expanded upon in great detail and are summarised in *Figure 1.5* (extrinsic ADE) and *Figure 1.6* (intrinsic ADE). Briefly, non-neutralising antibodies are thought to bind virus and thereby mediate binding to cells bearing Fc (Ab Fragment, crystallisable) γ receptor (FcγR) such as monocytes, MΦs, dendritic cells (DCs), and other leukocytes. [138] In the case of primary infection, DENV is not taken up by FcγR but can be bound by both DC-SIGN (dendritic cell-specific intercellular adhesion molecule-3-grabbing nonintegrin) [139,140] and MR (mannose receptor) [141] amongst other proposed receptors although the mechanism of internalisation remains unclear. As a result of Ab mediated opsonisation, the infected cell mass is thought to increase in secondary infection

(sometimes referred to as *extrinsic ADE*). [142] In addition, immature and partially mature dengue virions (possessing prM) that would not be infectious in primary infections may be rendered infectious by existing antibodies against prM thereby enhancing extrinsic ADE. [143]

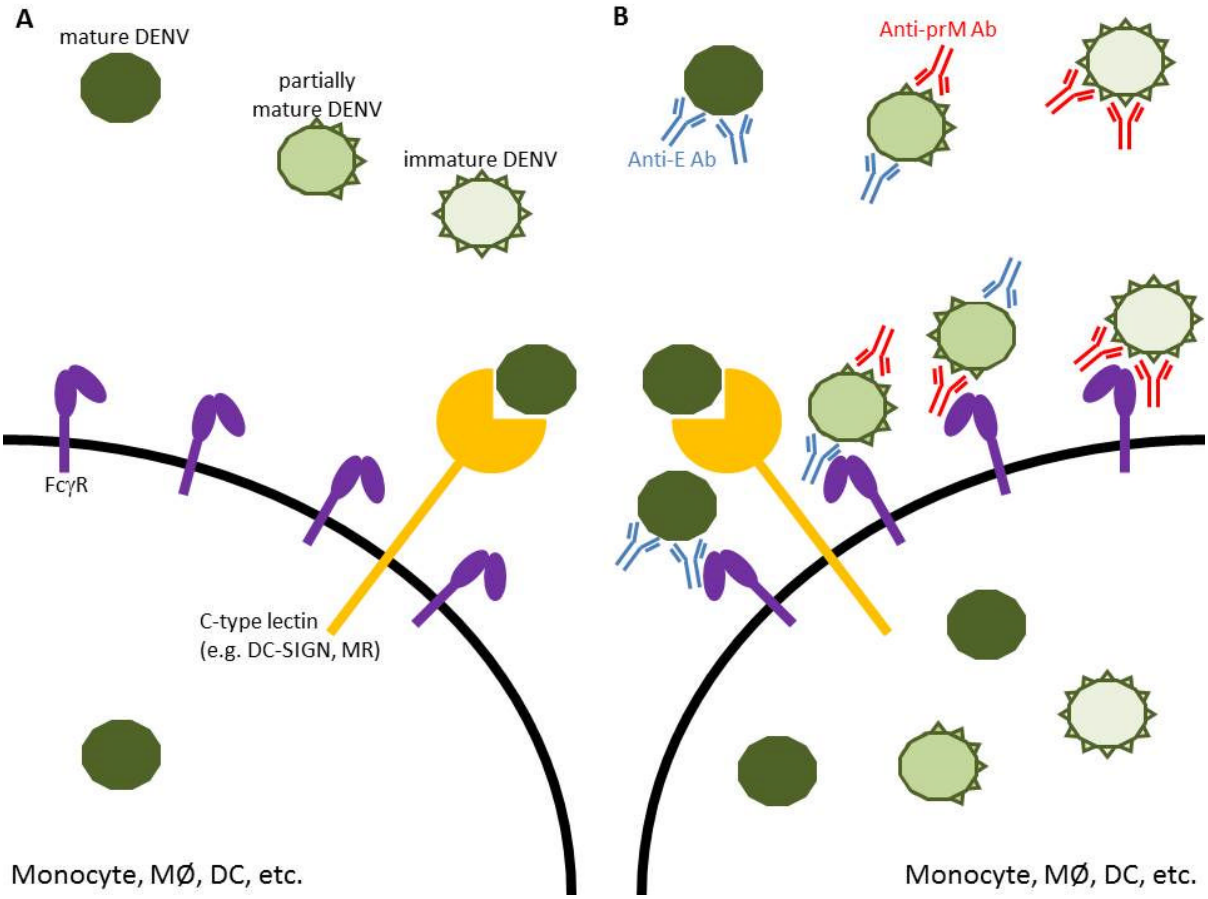

Figure 1.5. The case of primary DENV infection is illustrated in **A** with virus of increasing maturity in darker green. Spikes on immature virus (light green) represent uncleaved prM. Only mature virus can be recognised by lectins such as DC-SIGN (yellow) for eventual uptake due to conformational rearrangement of E following prM cleavage. [144,145] In the case of secondary infection, **B**, where antibody (Ab) against envelope (blue) and prM (red) mediates opsonisation of virus by FcγR (purple), both mature and immature virus can lead to productive infection thereby enhancing viral load. Not to scale.

In addition to extrinsic ADE, signalling mechanisms resulting from FcγR binding leading to enhanced DENV burden and disease have been identified and labelled *intrinsic ADE*. [142,146,147] At present, there remains some debate regarding the molecular signals responsible for intrinsic ADE; however, the field agrees that ligation of Fc to FcγR signals suppression of innate pro-inflammatory mechanisms and that this suppression supports enhanced viral replication. [142,146-149] Following ligation of FcγRI and FcγRIIA, Ubol *et al.* suggest that multiple pathways are activated that result in an anti-inflammatory environment consistent with Th2 responses. First, dihydroxyacetone kinase (DAK) and the Atg5-Atg12 (autophagy-related gene) complex are activated leading to blockade of RIG-I/MDA-5 (retinoic acid-inducible gene 1/melanoma differentiation-associated gene 5) detection of virus. As a consequence, downstream production of type I interferons, IFN-α and IFN-β, and subsequent activation of IFN stimulated genes (ISGs) is attenuated. [146] Concomitant induction of SARM (sterile alpha- and armadillo-motif-containing protein) and TANK (TRAF family member-associated NF-κβ activator) blocks expression of several toll-like receptors (TLRs) – TLR-3, TLR-4, and TLR-7. Thereafter, myeloid differentiation primary response gene 88 (MyD88) signalling is attenuated, and type I IFN response is downregulated in coordination with decreased IFN-γ, TNF-α, and IL-12 pro-inflammatory responses and enhanced anti-inflammatory response as measured (and potentially mediated) by IL-10 production. [149] Finally, IL-10 production stimulates SOCS (suppressor of cytokine signalling) family gene expression which results in suppression of JAK-STAT (Janus kinase-signal transducer and activator of transcription) signalling and a Th2 bias. [146] In contrast, Chan *et al.* suggest that co-ligation of DENV with FcγR and LILRB1 (leukocyte immunoglobulin-like receptor-B1) leads to LILRB1-mediated suppression of ISGs and a Th2 bias through blockade of spleen tyrosine kinase (Syk) signalling by Src homology region 2 domain-containing phosphatase-1 (SHP-1). [148] Irrespective of molecular events, the anti-inflammatory environment created by intrinsic ADE allows for enhanced proliferation of virus within the cell and decreased innate responses to extracellular virus.

I.1.D.ii.b. Biased T cell responses

In addition to (or in place of) Ab-mediated disease severity, T-cell mediated severe DENV disease has been hypothesised. The term *original antigenic sin* was initially used in reference to DENV regarding the ADE hypothesis [150] described above whereby immunological memory of a previous infecting DENV serotype results in expansion of memory B cells and therefore production of antibodies biased towards the original serotype as demonstrated for E domain III. [151] This concept of bias towards the initial DENV serotype has since been extended to memory T cells [152] and original antigenic sin is now more typically associated with memory T cell bias [73,152-156] while ADE is used to describe Ab responses.

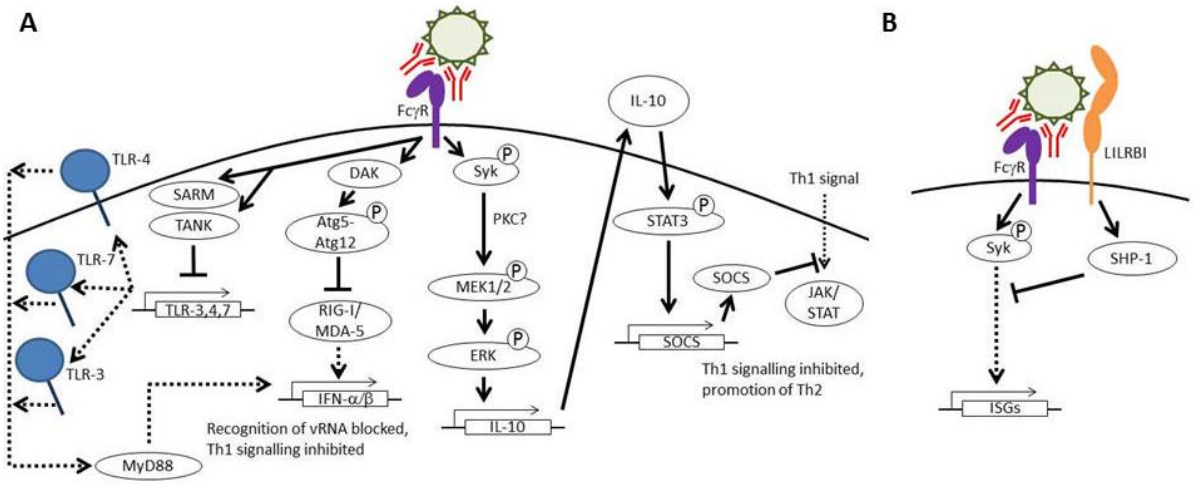

Figure 1.6. Intrinsic ADE results in an anti-inflammatory environment that supports enhanced viral replication. **A** FcγR (purple) binding by antibody (red) opsonised DENV (green) results in several signalling cascades that promote an anti-inflammatory Th2 environment. In particular, eventual induction of IL-10 as a consequence of Syk phosphorylation (encircled P) leads to SOCS-mediated blockade of extracellular Th1 signals. In addition, TLR (blue) induction that would result from primary infection is dampened by inhibition of transcription of the TLRs by SARM and TANK. In concert with RIG-I/MDA-5 blockade by DAK mediated Atg5-Atg12 phosphorylation, these events inhibit recognition of virus by the innate immune system and prevent induction of type I IFNs and downstream ISGs. In **B**, LILRB1 (orange)-mediated co-ligation of DENV induces SHP-1 to block Syk-mediated stimulation of ISGs. This is in contradiction to the signalling cascade described in **A**, but has the same net effect of blockade of an ISG-induced pro-inflammatory environment. Protein products are represented by circles, with genes described by rectangles. Innate signals that would occur in primary DENV infection but are blocked by intrinsic ADE are denoted as dashed lines. Figure **A** based on data from [142,146,147,149] and **B** based on [148].

As might be expected, T cell responses to DENV are complex. Although the virus is translated as a single polyprotein, NS3 [157-160] and NS5 [161] appear to be immunodominant. The reason for such bias remains unclear; however, it has been speculated that the relative conservation of amino acid sequence suggests a functional constraint on immune evasion that allows enhanced T cell recognition. [153] Recently there has been suggestion that NS1, E, and C are predominantly recognised by cluster of differentiation 4 (CD4)+ T cells. [162] Irrespective of peptide recognised, it has been demonstrated that the T cell responses (both CD4+ and CD8+) of patients are highly serotype cross-reactive, and this cross-reactivity has been speculated as a means of inducing the hypercytokinemia correlated with severe pathology. [73,153] In fact, when CD4+ T cells were stimulated *ex vivo* with various DENV-infected cell lysates, relative frequency of TNF-α producing vs. IFN-γ producing T cells demonstrated considerable bias to TNF-α with stimulation by heterologous serotype virus. [163] Further, broadly serotype cross-reactive IFN-γ CD4+ T cell responses were observed frequently in children not requiring hospitalisation compared to those who were hospitalised suggesting that IFN-γ may perform innate antiviral protective roles. In the absence of such a response, low-avidity TNF-α producing cross-reactive CD4+ T cells may compensate, and as a result excessive TNF-α production may promote vascular-leak pathology.

Recent evidence has called into question the veracity of the T cell original antigenic sin hypothesis – mostly on the grounds of lymphocyte kinetics during severe DENV pathology. [164] Indeed, CD8+ T cell responses in acute secondary DENV infection in one cohort of patients were very low to absent during the critical phase of illness and peaked two weeks later. [165] In an additional time course cohort, DENV specific T cells were minimal or absent until one day after progression to the critical phase. [166] As such, the authors suggest that T cell mediated cytokine storm is unlikely to be responsible for the severe pathology noted in these patients. In additional support of these observations is the commonly reported leukopaenia and lymphopaenia associated with severe

disease. [167,168] Some investigators have noted that degree of suppression of CD3+, CD4+, CD5+, and CD8+ cells can discriminate DHF patients from dengue fever (DF) patients during the febrile stage of illness, [169] and in one study, vigorous multifunctional CD8+ T cell response was associated with protection from DENV disease. [154] However, recruitment of T cells from circulation into the tissue sites of viral infection could explain the observed lympopaenia and indicate a crucial role for T cells in antiviral clearance and/or excessive inflammation. Thus, contradictory evidence exists regarding the role of T cell populations in severe DENV pathology, and there is considerable disagreement amongst investigators as to whether T cell involvement is beneficial or detrimental during DENV infection. It is probable that profound T cell responses, particularly of CD8+ T cells, are either protective or develop in response to (and not as a source of) severe disease, but the role of CD4+ T cells in DENV pathology remains less clear.

I.1.E. Summary

DENV disease pathology is a complex event with significant global burden. Much progress has been made in understanding the structural and functional dependencies of the virus, and clinical management of symptoms of severe disease can markedly reduce case fatality. Nevertheless, the risk of dengue infection and disease necessitates significant research investment in development of vaccines, antivirals, and prevention strategies. Although many clinical and molecular markers of severe disease have been elucidated, molecular mechanisms of vascular leak and related symptoms remain unclear. An understanding of these mechanisms could potentiate rational strategies for therapeutic intervention. The enhanced likelihood of severe disease in secondary DENV infection is an intriguing immunological phenomenon, and our understanding of the mechanisms of this process are crucial for development of future anti-DENV pharmaceuticals.

I.2. Iminosugars as antivirals

I.2.A. Iminosugars as a class

In the search for direct-acting dengue antivirals, many classes of compounds have been considered. Promising results for inhibitors of entry (such as sulphated glycosaminoglycans, polyoxotungstates), [170-172] RNA replication (mycophenolic acid, nucleoside analogues), [170,173-175] and viral proteases (quinolone derivatives, peptidomimetics) [174-176] have been reported; however, this work focuses on inhibitors of α-glucosidase enzymatic activity known as iminosugars. [12] As discussed previously, DENV possesses three proteins (prM, E, and NS1) that are glycosylated at specific Asn residues, and iminosugars have been developed as monosaccharide mimetics with the aim of inhibiting host-resident glycan processing enzymes such as the α-glucosidases required for modification of these glycoproteins. Broadly, iminosugars are glycomimetics possessing a nitrogen atom in place of the endocyclic oxygen atom; thus the chemical space of iminosugars as a class is quite broad. In spite of the potential diversity of the class, the iminosugars previously tested in the context of DENV infection can be considered as derivatives or modification of two lead iminosugar structures: deoxynojirimycin (DNJ) and castanospermine (CAST) as displayed in *Figure 1.7*. DNJ-derived iminosugars including *N*-butyl-DNJ (*N*B-DNJ, commercially known as Miglustat and Zavesca®), *N*-nonyl-DNJ (*N*N-DNJ), and *N*9-methoxynonyl-DNJ (M*O*N-DNJ) possess glucose stereochemistry with the exception of an absent hydroxyl group at C1 and are variably modified by decoration of the ring nitrogen with functional groups such as alkyl tails. In contrast, CAST and derivative iminosugars are bicyclic indolizidine alkaloids that cannot be modified at the ring nitrogen but have been otherwise decorated (*e.g.* the pro-drug 6-*O*-butanoyl CAST (BuCAST) also known as Celgosivir) and demonstrated as effective against DENV.

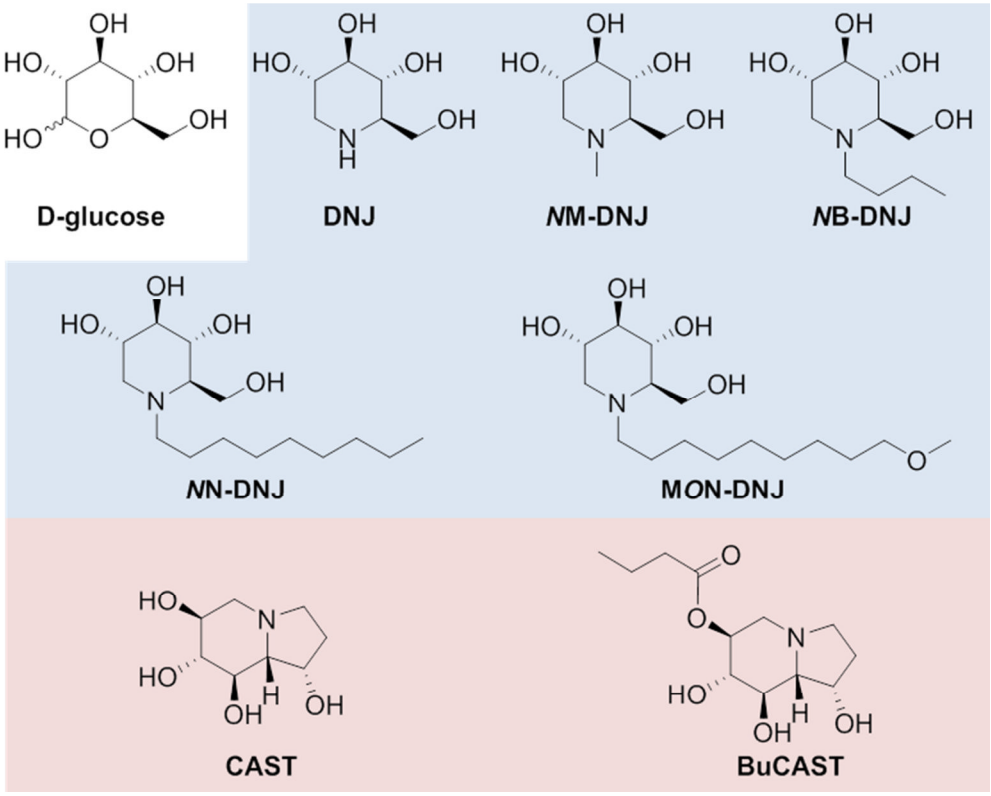

Figure 1.7. Iminosugars that inhibit α-glucosidase enzymes are derivatives of deoxynojirimycin (DNJ) (blue background) or castanospermine (CAST) (pink background). These iminosugars possess an endocyclic nitrogen in place of the oxygen of glucose (white background).

I.2.B. Antiviral mechanisms of action

Iminosugars are thought to be directly antiviral as a function of inhibition of α-glucosidases as described in *Figure 1.8*. [12] During the production of viral glycoproteins (as well as host glycoproteins), a fourteen residue oligosaccharide, $Glc_3Man_9GlcNAc_2$ (Glc, glucose; Man, mannose; GlcNAc, *N*-acetylglucosamine), is cotranslationally transferred to the emerging polypeptide at an Asn residue contained within the signal sequence Asn-X-Ser/Thr (X, any amino acid except proline; Ser, serine; Thr, threonine). The three terminal glucoses of the oligosaccharide are then sequentially trimmed by α-glucosidase enzymes in the ER with the first α1,2-linked glucose removed by α-glucosidase I before α-glucosidase II removes the α1,3-linked glucoses. Prior to the removal of the

second α1,3-linked glucose, the ER chaperones CANX and CALR associate through a lectin-binding activity with the monoglucosylated oligosaccharide intermediate $Glc_1Man_9GlcNAc_2$ to coordinate interaction of the glycoprotein with various PDIs and foldases to sample the protein folding landscape. Removal of the terminal glucose occurs during the folding process, and this event restricts further interaction with chaperones. As folding is completed, the protein is assessed for correct conformation by mechanisms that remain unclear. If this folding checkpoint is successfully passed, the glycoprotein is trafficked to the Golgi apparatus for further glycan processing and eventual release from the cell or incorporation into the relevant cellular membrane; however, if folding sensors detect non-native protein conformation, the glycoprotein is re-glucosylated by UDP-glucose glycoprotein:glycosyltransferase (UGGT) and further folding is attempted. [177] This so-called *calnexin cycle* continues until the protein attains a correct conformation or is deemed terminally misfolded, perhaps through monitoring of the Man residue abundance as a molecular clock, [178] and sent for ER-associated degradation (ERAD). In this cycle, iminosugars are thought to act as glucose-mimetics that prevent glucose trimming by α-glucosidase I and/or α-glucosidase II and thereby prevent interaction with essential foldases and isomerases. As a result, glycoproteins fail to fold correctly and are sent for ERAD or proceed from the ER in non-functional conformations. In the context of viral glycoproteins, this is thought to lead to viral glycoprotein misfolding and result in inhibition or impairment of viral morphogenesis. Poor morphogenesis is thought to interfere with uptake/signalling of extracellular virus with subsequent cells encountered in addition to diminution of virus production. [12]

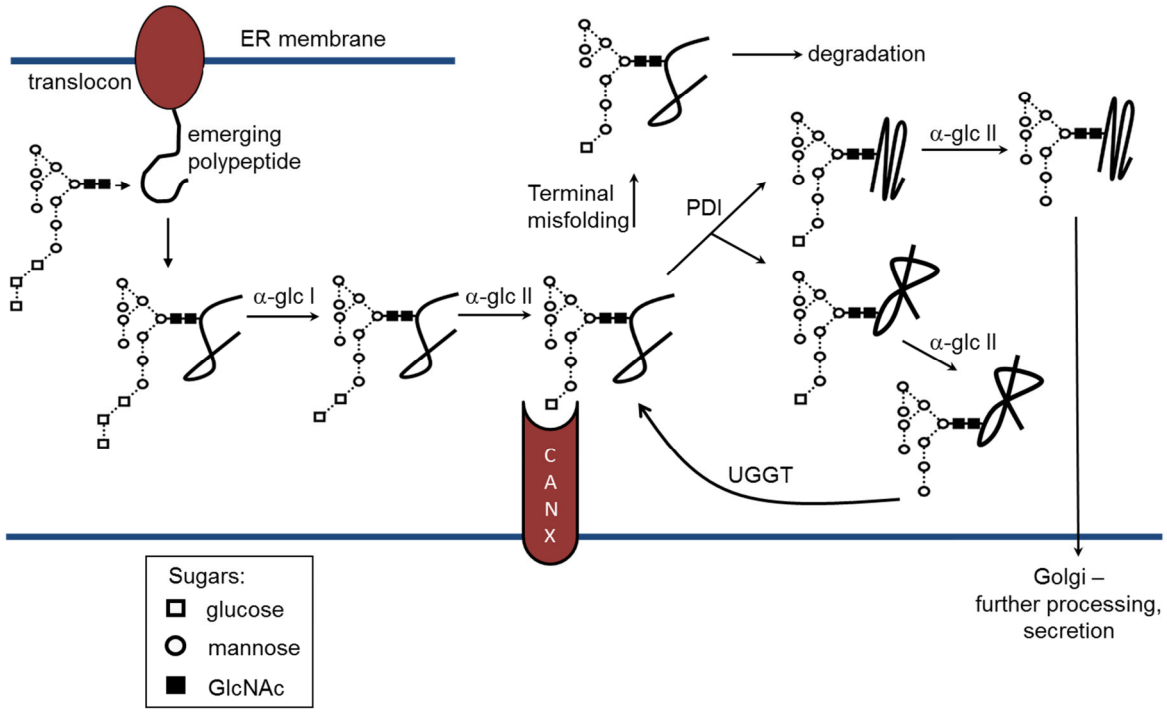

Figure 1.8. The calnexin cycle depends upon α-glucosidases (α-glc) for trimming of terminal glycans to achieve glycoprotein folding. Upon formation of a monoglucosylated species, folding by PDIs may lead to correctly folded glycoprotein (middle) or incorrectly folded glycoprotein. If the glycoprotein folds correctly, egress from the ER to the Golgi follows with subsequent glycan processing and secretion. If the glycoprotein fails to fold correctly, UGGT can reglucosylate the oligosaccharide to prepare the protein for a subsequent round of interactions with CANX (or CRT) and PDIs. Terminally misfolded proteins (recognised by loss of mannose residue(s)) are sent for ER-associated degradation (top).

I.2.C. Broad-spectrum antiviral activity

Observationally, this rationale seems to hold merit. In addition to successful inhibition of DENV production, iminosugars have been demonstrated to effectively interfere with production of many other enveloped viruses. Historically, antiviral activity as a function of inhibition of glycoprotein processing originated with the use of tunicamycin, an inhibitor of the formation of the dolichol phosphate:glycan precursor from which the $Glc_3Man_9GlcNAc_2$ is cotranslationally transferred during glycoprotein synthesis. [179-182] The use of an indolizidine alkaloid iminosugar with structural similarity to CAST called swainsonine was subsequently demonstrated as antiviral against an influenza virus (INFV) family member as a consequence of inhibition of complex glycan formation

due to α-mannosidase inhibition. [183] Inhibition of α-glucosidase mediated trimming of *N*-linked glycans (specifically α-glucosidase II) as a means of anti-INFV activity was demonstrated with bromoconduritol [184] and subsequently with the iminosugar CAST which inhibits both α-glucosidase I and II. [185] Shortly thereafter, *N*-methyl-DNJ (*N*M-DNJ) was demonstrated as an anti-INFV therapeutic as a function of α-glucosidase II inhibition. In these experiments, α-glucosidase I was also inhibited; however, virus possessing $Glc_3Man_7GlcNAc_2$ remained infectious. [186]

Subsequent investigations using *N*M-DNJ suggested mixed antiviral success. The iminosugar alters glycosylation of Rous sarcoma virus glycoproteins, but these virions were shown to remain infectious in chick embryo fibroblasts, [187] and Datema *et al.* raised concerns about non-specific inhibition due to prevention of lipid-linked oligosaccharide synthesis in addition to the previously described protein-linked oligosaccharide inhibition. [188] In contrast to this concern, a strain of vesicular stomatitis virus (VSV) with oligosaccharide structure-dependent temperature sensitivity was shown to be affected by iminosugars (DNJ and CAST) whereas a non-temperature sensitive strain was not affected by drug treatment. [189] This result suggested a glycoprotein-alteration dependence of viral inhibition by iminosugars that was re-capitulated in Sindbis virus. [190] With increasing concern over the human immunodeficiency virus (HIV) pandemic, antiretroviral activity of iminosugars was demonstrated first against Moloney murine leukaemia virus [191] and then against HIV. [192-194] During these investigations, *N*B-DNJ was demonstrated to have profound antiviral effects with minimal cytotoxicity, [194] and as a result, this iminosugar progressed rapidly to clinical trials. [195] Safety concerns related to cataracts in rat toxicology studies (later demonstrated to be transient and animal specific) in addition to gastrointestinal (GI) distress, elevated liver function tests (LFTs), and leukopaenia and neutropaenia in human patients resulted in discontinuation of the trial during phase II testing, but preliminary results suggested trends toward antiviral reduction in combination with zidovudine. [196,197]

Following on from the safety-related clinical failure of *N*B-DNJ against HIV, clinical success was achieved as a therapy for the lysosomal storage disorder termed Gaucher's disease based on the observed "off-target" lipid-linked oligosaccharide inhibition previously described. [198] In the intervening time period during which *N*B-DNJ has been clinically licensed, the iminosugar has been administered at much lower doses than in the antiviral studies due to lower dosage requirements to achieve inhibition of lysosomal glucosylceramide synthase (GCS) enzymatic activity, and minimal side-effects have been reported. [199] Recently, GCS inhibition by *N*B-DNJ has been extended to successful clinical treatment of Niemann-Pick type C (NPC) disease. [200] In the interim, further derivatisation of DNJs has been conducted in an effort to reduce toxicity at doses required for antiviral success. [201-205] These derivatives, including M*O*N-DNJ amongst others, have been shown to be antiviral *in vitro* against DENV, HIV, Japanese encephalitis virus (JEV), hepatitis B virus (HBV), hepatitis C virus (HCV), INFV, Ebola virus (EBOV), Marburg virus (MARV), bovine viral diarrhoea virus (BVDV), arenaviruses, bunyaviruses, poxviruses, and togaviruses, and *in vivo* against DENV, EBOV, INFV, poxviruses, and woodchuck hepatitis virus (WHV). ([201-204,206-214], personal communication U. Ramstedt, M. Duchars, and M. Callahan, and this thesis) Thus, the potential for iminosugars as antivirals remains promising.

I.2.D. Summary

Iminosugars inhibit ER α-glucosidases essential for glycoprotein trafficking and folding and are potent antivirals against a number of glycoprotein-possessing viruses. Although a strategy of iminosugars as direct antivirals has demonstrated mixed clinical potential, the long-term safe administration of *N*B-DNJ to Gaucher's patients alleviates some concerns regarding toxicity. Further optimisation of specificity and safety of DNJ-derived iminosugars suggests that therapeutic administration as an antiviral may be possible based on *in vitro* and *in vivo* data.

I.3. Iminosugars and inflammation

I.3.A. Iminosugars modulate host proteins

Understanding of the folding processes of *N*-linked glycoproteins has been elucidated largely with respect to host-resident proteins (*e.g.* tyrosinase) [215] in addition to viral glycoproteins (*e.g.* VSV G protein and HBV surface antigen (HBSAg)). [189,190,216] As such, the antiviral effects observed for iminosugars must be considered in the context of interference with inhibition of glycoprotein processing of host proteins. In order to do so, it is essential to understand the nature of iminosugar effects on the host. While all *N*-linked glycoproteins rely on α-glucosidase I and II to trim the terminal glucose residues for preparation of the oligosaccharide for interaction with CANX/CALR, the dependence on the CANX cycle is of varying significance for different glycoproteins. [215] That is, inhibition of glycoprotein processing leads to selective inhibition of both folding and functionality of cellular glycoprotein products. For example, treatment with *N*B-DNJ of leukocyte cell lines inhibits expression of transferrin receptor on the cell surface as a consequence of inhibition of glycoprotein processing; however, other surface glycoproteins are expressed normally in the same cells. [217] As well as cell surface molecules, soluble proteins are also differentially affected. Treatment of hepatocytes with iminosugar alters glycosylation patterns of alpha-1-antitrypsin and alpha-1-acid glycoprotein but does not lead to pronounced changes in synthesis or secretion. [218] The above observations extend to soluble and cell-surface mediators of the innate inflammatory response, and are iminosugar specific as will be discussed.

I.3.B. Immunomodulatory functions

I.3.B.i. Cytokines

Cytokines and chemokines are particularly relevant to DENV infection and pathology, and these immunomodulators comprise an interesting class of molecules in their response to treatment by iminosugars. Minimal work with considerable variability of results has been conducted in this area. Significantly, variation in stereochemistry and modification of nitrogen-linked alkyl tails amongst iminosugars appears to have a drastic impact on the resultant immunomodulation. For example, 1,6-dideoxynojirimycin based iminosugars (similar to DNJs) with variable alkyl tails reduce IFN-γ in mouse splenocytes stimulated with concanavalin A (conA) with varying efficacy. In contrast, the Th2 cytokine IL-4 is consistently reduced in the same model independent of ring-nitrogen modification. [219] C1 hydroxylated CAST derivatives are pro-inflammatory as measured by induction of IL-6 and IFN-γ and reduction of IL-4 in a similar mouse splenocyte-conA model. [220] With respect to stereochemistry, altro- and galacto- iminosugars (mimicking altrose and galactose, respectively) demonstrate consistent reduction of IFN-γ and IL-4 to variable degrees in mouse splenocytes [221] although this modulation has not been directly linked with α-glucosidase inhibition, and it is unlikely that α-glucosidase inhibition is linked to such effects in the case of these iminosugars. Of greatest relevance to this thesis are the studies by Kosuge *et al*. [222,223] in which DNJ, *N*M-DNJ, and bromoconduritol were shown to inhibit anti-CD3-stimulated T cell release of IFN-γ, IL-4, and IL-5. In particular, reduced secretion of IFN-γ was linked to retention of cytokine with CALR but not CANX resulting in degradation of newly synthesised IFN-γ. Whether such activity is true in other cell types activated through additional stimuli or can be extended to animal systems remains to be determined.

In fact, immunomodulatory functions of iminosugars are not limited solely to α-glucosidase inhibition mechanisms. Isofagomine derivatives that modulate β-galactosidase activity variably influence lipopolysaccharide (LPS; an endotoxin found in the outer membrane of Gram-negative bacteria) – mediated inflammatory responses in RAW264.7 cells with a tendency toward anti-inflammatory activity as measured by reduced IL-1β and TNF-α production. [224] *In vivo* isofagomine has been used to enhance acid β-glucosidase activity in a mouse model of neuronopathic Gaucher disease. This study demonstrated a reduction in inflammation, particularly of TNF-α, which delayed the onset of neurological disease and extended the life span of treated animals in the absence of changes to glycolipid substrates. [225] Although there was no observable change to glycolipids in this model, the ability of iminosugars to inhibit glycolipid processing may contribute to immunomodulation. In RAW264.7 cells, a mouse macrophage cell line, treatment with an inhibitor of glycosphingolipid and oligosaccharide-protein processing, SR1, was used to induce production of TNF-α amongst other pro-inflammatory cytokines. When *N*B-DNJ was administered, this induction was suppressed at low concentration of iminosugar, but cytokine expression was restored with higher levels of *N*B-DNJ. In contrast, *N*B-DGJ (deoxygalactonojirimycin), a galactose mimic iminosugar that lacks inhibitory activity for α-glucosidases but retains glycolipid inhibitory activity at concentrations tested, was only cytokine suppressive. [226] These data suggest that immunosuppressive effects of iminosugars in SR1 stimulated mouse macrophages are the result of glycolipid processing inhibition whereas pro-inflammatory effects are the result of glycoprotein processing inhibition. Thus, cytokine modulation by iminosugars is likely specific to the different mechanism(s) of action invoked and therefore specific to stimulus, cell type, and cytokine of interest. Effects of the class are difficult to generalise, but there is a propensity for immunosuppression.

I.3.B.ii. Receptors and immune cell function

Soluble mediators of inflammation are not the only immune molecules impacted by iminosugar treatment. In a rat heart allograft model, CAST was shown to be immunosuppressive through subtle downregulation of class I and II major histocompatibility complex (MHC) as well as CD4 and CD8. Further, pronounced reduction of the ligand-receptor adhesion molecule pair LFA-1 (lymphocyte function-associated antigen 1) and α-ICAM1 (alpha-intercellular adhesion molecule 1) suggests disruption of communication between antigen presenting cells (APCs; *e.g.* monocytes, DCs, and MΦs) and T-cells. [227] CAST may further act to inhibit T-cell proliferation. Whereas swainsonine enhanced *ex vivo* proliferation of mouse T-cells in response to antigen and conA, CAST inhibited this proliferative response apparently through reduced signalling capacity of the IL-2 receptor. [228] These observations have been extended to DNJ-derived iminosugars for which late stages of CD2 monocolonal Ab (mAb) stimulated T cell activation are inhibited as a function of α-glucosidase inhibition. [229] As previously mentioned, clinical trials of *N*B-DNJ as an HIV therapeutic revealed leukopaenia in seven patients; however, specific effects on T-cells were not recorded. [197] These results provide significant evidence for 1) reduced T-cell activation (whether by inhibition of interactions with APCs or reduced ability to signal downstream) and 2) suppression of proliferation and/or active killing of T-cell populations. In contrast, expression of scavenger receptor A on RAW264.7 mouse MΦs is increased with *N*B-DNJ treatment and results in greater accumulation of functional receptor with the potential for recognition of low-density lipoproteins and associated pathogens. [230] As with cytokine production, iminosugar immunomodulation of receptors and cell populations is clearly multi-factorial.

I.3.C. Summary

Unfortunately, none of the publications to date assessed drug for endotoxin activity, thus effects may not be solely based on drug mechanisms of action. Nevertheless, interactions of α-glucosidase-inhibiting iminosugars with the immune system are complex. Both pro- and anti-inflammatory cytokines may be reduced as a result of α-glucosidase inhibition, and additional mechanisms must be considered with the potential for opposing or synergistic effects. Inhibition of T-cell effector functions and proliferation is commonly noted *in vitro* and *in vivo*, but the outcome of these effects remains untested in the case of DENV.

I.4. Conclusions

The composition of the dengue virion lends the virus to dependence upon a number of host cell processes, in particular α-glucosidase initiated glycoprotein processing. This dependence permits the use of iminosugars as inhibitors of viral morphogenesis and therefore as direct inhibitors of virus proliferation and infectivity; however, hyperactive immune responses are thought to be major contributors to disease pathology. There is precedent for the use of iminosugars as modulators of immune function *in vitro*, but immunomodulation accomplished by iminosugars has not been considered as a means of clinical treatment of DENV infection as yet. Iminosugar anti-inflammatory properties remain to be investigated and the molecular mechanisms of any such activity remain to be determined.

I.5. Aims of this thesis

This thesis concerns the mechanism of action of iminosugars, in particular M*O*N-DNJ, as a potential dengue virus therapeutic. As such, I will present:

1) Evidence that inhibition of α-glucosidase activity is necessary and sufficient for reduction of infectious DENV production by iminosugars in primary human MDMΦ,
2) An analysis of changes to the host MDMΦ transcriptome in the context of DENV infection as well as LPS treatment as a consequence of iminosugar treatment,
3) Evidence that iminosugars that inhibit α-glucosidase activity can reduce MDMΦ produced inflammatory cytokines in the context of DENV infection as well as other inflammatory stimuli, and
4) *In vivo* evidence for alteration of immune activation in a model of ADE DENV infection as a result of orally administered iminosugar treatment.

II

Materials and Methods

II.1. Viruses and tissue culture

Macaca mulatta kidney cells (LLC-MK_2, a gift from the US Armed Forces Research Institute of Medical Sciences, Thailand (AFRIMS)) were propagated in Medium 199 (Gibco) supplemented with 20% heat-inactivated foetal bovine serum (HI-FBS) (Seralab), 0.1 mg/ml streptomycin (Gibco), and 100 U/ml penicillin (Gibco) at 37°C, 5% CO_2. *Aedes albopictus* C6/36 cells (AFRIMS) were maintained in Leibovitz's L15 medium (Gibco) supplemented with 10% HI-FBS, 2 mM L-glutamine (Gibco), 0.1 mg/ml streptomycin (Gibco), and 100 U/ml penicillin (Gibco) at 28°C in unvented tissue culture flasks in the absence of DENV infection. During DENV infection of C6/36, supplements were diluted 3:20 to final concentrations of 1.5% HI-FBS, 300 μM L-glutamine, 15 μg/ml streptomycin, and 15 U/ml penicillin. For amplification, cells were washed twice with sterile-filtered phosphate buffered saline (PBS; Gibco) before incubation with trypsin-EDTA (EDTA: ethylenediaminetetraacetic acid; Sigma) for 5 minutes at 37°C then collected by PBS wash, centrifuged for 5 minutes at 400 x *g*, and the supernatant was discarded. Cells were resuspended in fresh media either by pipetting or, for LLC-MK_2s, with a 19-gauge needle (Terumo). DENV2 strain 16681 (a gift from E. Gould, Centre for Ecology and Hydrology, Oxford, UK) was propagated in C6/36, collected from supernatant, and concentrated by precipitation with 10% weight per unit volume (w/v) poly(ethyleneglycol) M_r 6,000 (Sigma), 0.6% sodium chloride (Sigma) overnight at 4°C. Following precipitation, virus was centrifuged at 2830 x *g* for 45 minutes at 4°C, resuspended in Leibovitz's L15 + 10% HI-FBS, and stored at -80°C until use.

II.2. Iminosugars and drugs

The iminosugar compounds tested in this thesis include D-DNJ (solubilised in water, JL Kiappes), *N*B-DNJ (solubilised in PBS, gift from United Therapeutics), *N*N-DNJ (solubilised in 83% dimethyl sulfoxide (DMSO), JL Kiappes), M*O*N-DNJ (solubilised in acidified water, gift from United

Therapeutics), *N*-(6'[4''-azido-2''-nitrophenylamino]hexyl)-1-DNJ (*N*AP-DNJ; solubilised in DMSO, gift from United Therapeutics), D-DGJ (solubilised in water, JL Kiappes), *N*B-DGJ (solubilised in 83% DMSO, Toronto Research Chemicals), and *N*N-DGJ (solubilised in 83% DMSO, Toronto Research Chemicals). M*O*N-DNJ and castanospermine (CAST, Toronto Research Chemicals) were administered to mice by oral gavage (i.g.) in aqueous solution three times daily (t.i.d.) at 100 mg/kg/dose and 33 mg/kg/dose, respectively. *N*B-DNJ, M*O*N-DNJ, and *N*B-DGJ were used for immunomodulation experiments and therefore assayed for pyrogen contamination and verified to contain less than 0.05 endotoxin units per ml.

II.3. Endotoxin detection assay

Compounds were subjected to a *Limulus* amoebocyte lysate (LAL) fluorescent assay (Lonza) using recombinant factor C as per manufacturer's instructions. Briefly, samples were prepared in aqueous dilution and plated in triplicate on a 96 well plate. LPS derived from *Escherichia coli* O55:B5 was reconstituted in endotoxin free water and used to produce a standard curve. Recombinant enzyme, buffer, and fluorogenic substrate were prepared separately and then added 1:1 (v:v) of sample and fluorescence was measured for absorption at 380 nm and emission at 440 nm at time 0 and following 1 hour of incubation at 37°C in dark conditions. Log_{10} values of difference in relative fluorescence were plotted against log_{10} values of endotoxin concentration to produce a standard curve.

II.4. Isolation and differentiation of MDMΦ

Human PBMCs (peripheral blood mononuclear cells) were isolated from buffy coats (NHS Blood and Transport, surplus to clinical requirements) by centrifugation over a Ficoll-Paque™ PLUS (Amersham)

gradient. All donors were anonymous and isolations were assigned sequential two character codes for processing and experimentation (*i.e*. donor 1 assigned AA). Autologous plasma was collected, heat inactivated (56°C, 30 minutes), and used to supplement (1%) X-VIVO10 (Lonza) medium to produce monocyte-derived MΦ (MDMΦ) growth medium. Adherent monocytes were isolated from PBMCs by incubation on 2% bovine gelatin (Sigma) coated tissue culture plates (37°C, 5% CO_2, 90 minutes). Non-adherent PBMCs were washed off in RPMI-1640 (Sigma) and remaining monocytes were incubated in MDMΦ growth medium (37°C, 5% CO_2, 18 hours). Supernatants at 18 hours post-seeding containing monocytes were collected and additional monocytes were collected by mechanical removal (vigorous pipetting) following incubation in ice-cold sterile PBS + 5 mM EDTA (Sigma) (4°C, 90 minutes) and combined with monocytes in supernatant. Cells were seeded at 1 x 10^6 cells/ml in 1 ml of MDMΦ growth medium + 25 ng/ml recombinant human IL-4 (rhIL-4, Peprotech) in a 24 well plate and differentiated for 3 days (37°C, 5% CO_2) to generate MDMΦs. For 6 well plates, cells were seeded at 1 x 10^6 cells/ml in 3 ml of MDMΦ growth medium + 25 ng/ml rhIL-4, and for T25 flasks, cells were seeded at 1.5 x 10^6 cells/ml in 5 ml of MDMΦ growth medium + 25 ng/ml rhIL-4. Cells generated in this manner are greater than 95% macrophages phenotypically (CD14+, CD16-, CD86+, HLA-DR+, CD3-) by fluorescence activated cell sorting (FACS) as previously reported. [141] The use of human blood was approved by the NHS National Research Ethics Service (09/H0606/3).

II.5. *In vitro* virus infection and drug treatment

MDMΦ were infected with DENV2 16681 diluted to a multiplicity of infection (m.o.i.) of 1 in X-VIVO10 without supplements for 90 minutes (20°C, with rocking). Upon removal of virus, fresh MDMΦ growth medium without IL-4 but containing serial dilutions of drug or control was placed on the cells and cells were incubated for 48 hours (37°C, 5% CO_2). For collection of infectious virus, supernatant was harvested and centrifuged for 5 minutes (room temperature, 400 x *g*) to pellet any cells/debris and supernatants were aliquoted and stored at -80°C until analysis by plaque assay. In

the case of free oligosaccharides (FOS) assays where MDMΦ were uninfected, treatments were essentially as above except that no virus was added and cells were washed three times with sterile PBS after 24 or 48 hours as per sample time point. On the third wash, cells were removed from tissue culture plastic by mechanical disruption (scraping) and transferred to microcentrifuge tubes for centrifugation (room temperature, 4000 x *g*, 5 minutes). Cells were lysed by three cycles of freeze-thawing (alternating room temperature and -80°C) in deionised H_2O and stored at -80°C for subsequent protein or FOS assay.

II.6. Plaque assays

Virus titres for samples from human and C6/36 infections were obtained by LLC-MK_2 plaque assays as per previous descriptions. [231] Briefly, LLC-MK_2s were seeded in confluent monolayers, allowed to adhere, and washed once with Hank's balanced salt solution (HBSS, Gibco). Log_{10} serial dilution of viral supernatants was conducted in DMEM10 (Gibco), and virus was incubated on cells for 90 minutes (20°C, with rocking). Upon removal of virus, plaque first overlay was added and allowed to dry at 20°C before incubation for 5 days (37°C, 5% CO_2). Plaque second overlay was added and allowed to dry at 20°C before further incubation of 1 day (37°C, 5% CO_2) after which plaques were counted. The limit of detection for this assay is 33 plaque forming units per ml (pfu/ml).

Virus titres of samples isolated from infected mice were obtained by BHK-21 (a hamster kidney cell line) plaque assays in accordance with previous protocols. [232,233] BHK-21 cells were seeded in 12-well plates (3 x 10^5 cells/well) in α-MEM medium containing 10% HI-FBS for 3 hours (37°C, 5% CO_2). Medium was removed, log_{10} serial dilutions of virus in α-MEM with 2% HI-FBS were added, and cells were incubated a further 2 hours (37°C, 5% CO_2). Following incubation, 1.5 ml of α-MEM containing 5% (v/v) HI-FBS and 1% (w/v) low-melting point tissue culture grade agarose (Sigma) was added to

each well and allowed to solidify at room temperature before further incubation (37°C, 5% CO_2) for 5 days. Plaques were visualised after fixation in 10% formaldehyde (1 hour, room temperature) and removal of the agarose plug by staining briefly (approximately 30 seconds) with 1% (w/v) crystal violet (Sigma) in 20% (v/v) ethanol (EtOH, Sigma). Concentrations were normalised to tissue mass (in grams) or serum volume (in ml) as appropriate.

II.7. Protein quantitation

Quantification of proteins in MDMΦ lysates was conducted by a modified Bradford assay as previously described. [234] Briefly, cell lysates were added in a 1:1 volumetric ratio to 1x Bradford Quick Start Reagent (Bio-Rad) and incubated at 20°C for 5 minutes. Absorbance values (A_{xxx}) at 595 nm and 420 nm were measured and the ratio of A_{595} to A_{420} was used to determine protein concentration in comparison to a serially diluted standard of bovine serum albumin.

II.8. Detection of FOS

MDMΦ FOS were detected as previously described by Alonzi *et al*. [235] Cells were cultured in 6 well plates as described above and protein lysates were prepared according to the freeze/thaw protocol. Following cell lysis, samples were subjected to mixed-bed ion exchange and then lyophilised. FOS were labelled with 2-aminobenzoic acid (2-AA) and purified using a DPA-6S column (Sigma). Unconjugated 2-AA was removed by phase splitting with ethyl acetate, and samples were lyophilised and resuspended in water then purified using a con-A column. Glycans were separated by normal phase-high performance liquid chromatography (NP-HPLC) and peak area was used to assess molar quantity in comparison to standards of known identity and quantity. Purification of FOS and NP-HPLC was performed by Dr. D Alonzi; I generated and analysed all samples.

II.9. Detection of glycosphingolipids

MDMΦ glycosphingolipids (GSLs) were detected using NP-HPLC as previously described. [236] Briefly, cells were cultured in TC 25 flasks as described above and treated with appropriate dilutions of iminosugars for 48 hours at 37°C, 5% CO_2. Following incubation, supernatants were removed and cells were washed twice in pre-warmed PBS before mechanical removal by scraping. Flasks were washed once with warm PBS and this wash was combined with the scraped cell fraction and pelleted by centrifugation (room temperature, 4000 x *g*, 5 minutes). The MDMΦ pellet was washed once more in PBS before resuspension in 300 µl of water. Three cycles of freeze/thawing were executed to lyse samples, and an aliquot was removed for modified Bradford protein assay for normalisation. The remaining fraction was used to extract glycolipids by adding 400 µl chloroform and 800 µl methanol (MeOH) to 300 µl of aqueous lysate for lipid extraction by a modified Svennerholm and Fredman method. [237] Extracted GSLs were hydrolysed overnight by incubation with ceramide glycanase (37°C, 50 mM sodium acetate buffer, *p*H 5.0, containing 1 mg/ml sodium taurodeoxycholate). Oligosaccharides released from GSLs were made to 30 µl with water and labelled with 2-AA as described for FOS. These labelled oligosaccharides were analysed by NP-HPLC as described above. I performed all preparation of cell lysates and protein quantitation, and Dr. D Alonzi performed all lipid extraction and HPLC. Peak identification and quantitation was performed by Dr. D Alonzi, and subsequent analysis of results is my work.

II.10. Cytotoxicity assay

Cytotoxicity of compounds was assessed by a cell proliferation assay for metabolic activity using a CellTiter 96® AQ_{ueous} One Solution Cell Proliferation Assay (Promega) as per manufacturer's instructions. Briefly, 20 µl of a solution containing tetrazolium compound [3-(4,5-dimethyl-2-yl)-5-(3-carboxymethoxyphenyl)-2-(4-sulfophenyl)-2H-tetrazolium; MTS] and electron coupling reagent

(phenazine ethosulfate) was added to cells covered or suspended in 100 µl of culture medium in a 96 well plate. Samples were incubated for approximately 4 hours (37°C, 5% CO_2) and the absorbance at 490 nm (A_{490}) was measured on a SpectraMax M5 microplate reader (Molecular Devices). Absorbance was normalised to untreated controls whereby cytotoxicity resulted in decreased A_{490}.

II.11. Immunofluorescence of DENV infection

Human MDMΦ were plated in 24 well tissue culture plates containing sterilised, acid-etched glass coverslips in each well prior to DENV infection for all immunofluorescence assays (IFA). Following infection and drug treatment, supernatants were removed for plaquing and cells were washed once in sterile PBS. A solution of 4% paraformaldehyde in PBS was added to the cells for fixing and samples were incubated at 4°C for 15 minutes. Cells were washed a further four times in PBS and then permeabilised for 15 minutes at room temperature in 0.5% (v/v) Triton X-100 in PBS. Primary antibody against DENV2 E (3H5, mouse IgG1, [238]) was diluted 1:200 to a final concentration of 10 µg/ml in 0.5% (v/v) Triton X-100 in PBS and incubated at room temperature for 50 minutes. Following two further PBS washes, Alexa488-anti-mouse secondary antibody (Molecular Probes) was incubated for 50 minutes at room temperature in 0.5% Triton X-100/PBS. Samples were washed twice in PBS and then mounted with VectaShield mounting medium (Vector Laboratories Inc) containing DAPI (4',6-diamidino-2-phenylindole) for staining of nuclei. After drying overnight in dark conditions at room temperature, slides were imaged on a Nikon Eclipse TE200-U fluorescent microscope such that at least 800 cells were imaged and scored for infection for each technical replicate.

II.12. Curve fitting of high variability data

All data operations, analyses, and curve fits for plaque, IFA, and cytotoxicity data were performed in KaleidaGraph 4.0.3 (Synergy Software). In each instance, raw values (A_{490}, plaque counts, or percent infected cells) of all samples, including untreated controls, were divided by the untreated cell average to yield percent viability, infectious virus, or infectivity, respectively. For each treatment group, averages and standard deviations were calculated for the technical replicates. Drug dilutions were generally carried out in $0.5\log_{10}$ steps (*e.g*. 31.6 mM, 10 mM, 3.16 mM, etc.) and these values were plotted as the independent variable along a $\log_{10}$ x-axis. Dependent variables were plotted as percentages on a linear y-axis with the x-value of untreated cells adjusted to $1.5\log_{10}$ steps lower than the global minimum drug concentration tested (*i.e.* lowest concentration tested of 0.0316 μM, therefore untreated concentration set to 0.001 μM) to allow for plotting along a logarithmic axis ($\log_{10}(0)$=undefined). The coefficient of variation (C_V) for a given data point was calculated to determine precision of the value determined. Relative C_V was subsequently determined by dividing each C_V by the minimum C_V for a given donor/drug experiment. This operation sets the most precise C_V to 1 with all less precise measures set to greater than 1.

Based on plots generated as above for each donor/drug combination, several curve types were fit to the data sets. KaleidaGraph General Curve Fits using an iterative method (the Levenberg-Marquardt algorithm) for $\chi 2$ minimisation were run. Data points were weighted based on the inverse of the square of relative C_V. As such, the most precise measure has a weight equal to $1/1^2=1$ while less precise measures have lower weight (*e.g.* for an estimate with relative $C_V=2$, $1/2^2=0.25$). The following equations were applied to curve fits with initial values defined based on a preliminary dataset:

Modified dose-response standard logarithm:

$$y = A + \frac{B}{1 + \left(x \diagup C\right)^{D}} \Bigg| A = -70; B = 186; C = 5; D = 0.2$$

Standard logarithm sigmoid:

$$y = A + \frac{B - A}{1 + e^{-C(x-D)}} \Bigg| A = 100; B = 0.01; C = 0.05; D = 20$$

Dose-response standard logarithm:

$$y = A + \frac{B - A}{1 + \left(x \diagup C\right)^{D}} \Bigg| A = 95; B = -0.86; C = 0.04; D = -0.95$$

These curve types were additionally fit to summarise biological data for infectious virus production and percent infection following averaging of values and recalculation of standard deviations, C_V, and relative C_V. Standard exponential curve fits were also applied, and the curve that best fit the data as measured by lowest χ^2, was solved for IC_{50}, IC_{90}, CC_{50}, or CC_{10} (concentration required to reach XX% inhibition or cytotoxicity) by calculating intersection with the line y=50, 10, 50, or 90, respectively.

II.13. *In vitro* enzyme inhibition assays

Inhibition of glucosidases and glycosidases was detected *in vitro* by Atsushi Kato (University of Toyama) as part of an ongoing collaboration as previously described. [239] Briefly, assays were performed at the optimum *p*H of each enzyme and appropriate disaccharide was provided as substrate for glucosidase release assays. Release of D-glucose was measured using a Glucose B-test (Wako Diagnostics). Appropriate *p*-nitrophenyl glycoside was added as substrate for additional

glycosidase assays and assays were stopped by adding 400 mM Na_2CO_3. Release of *p*-nitrophenol was measured spectrophotometrically at 400 nm.

II.14. Transcriptomics sample generation and quality control

MDMΦs were isolated and differentiated from four donors as previously described. Cells were seeded at a density of 1 x 10^6 cells/ml in 3 ml of MDMΦ growth medium containing rhIL-4 in a 6 well plate. Samples were mock-infected (media-only), infected with DENV2 16681 (m.o.i of 1), or treated with LPS (200 ng/ml from *Salmonella enterica*, Sigma) for 90 minutes at room-temperature with rocking. Virus and mock-infected supernatants were then removed, and M*O*N-DNJ (25 µM final concentration) or control medium was added to all samples. In the case of LPS treatment, LPS containing medium was not removed and treatment as described above was added such that final LPS concentration of 100 ng/ml was established in the presence or absence of 25 µM M*O*N-DNJ. Samples were incubated at 37°C with 5% CO_2 for a further 4.5 or 22.5 hours to generate time-points post-infection of 6 hours and 24 hours, respectively. Following appropriate incubation, supernatants were removed and stored for plaque assay as described above, and cells were washed once in pre-warmed PBS containing calcium and magnesium (Sigma). Samples were lysed in plate via addition of 1 ml of TRIzol (Life Technologies) with pipetting to mix followed by 5 minute incubation at room temperature. Cellular debris was cleared by centrifugation (12,000 x *g*, 1 minute, room temperature) and RNA containing supernatants were mixed 1:1 with 100% EtOH (Fisher Scientific). Samples prepared as such were applied to a Direct-zol™ RNA Mini-prep column (Zymo Research) and washed in accordance with manufacturer's instructions in buffers containing EtOH and chaotropic salts. RNA was eluted by sequential application of 25 µl of RNase-free water for collection of 50 µl of total sample, and samples were stored on ice prior to analysis of concentration and purity by NanoDrop (Thermo Scientific). Samples were subsequently stored at -80°C prior to aliquoting for shipment to

Cambridge Genomic Services (CGS) and further analysis of RNA integrity using a BioAnalyzer 2100 (Agilent Technologies).

II.15. Transcriptomics

II.15.A. RNA quantitation and normalisation

RNA samples were amplified and biotinylated using the Illumina® TotalPrep™ RNA Amplification Kit (Ambion), directly hybridised to a HumanHT-12v4 BeadChip (Illumina), and scanned using an iScan system (Illumina) by CGS. Illumina GenomeStudio analytical software was used to generate mappings and intensities and perform beadlevel processing by CGS (data available in *Appendix IV*). I performed all subsequent analytical steps. GenomeStudio generated data was imported into R Bioconductor v2.14 using the lumi package. [240-243] Data were normalised via the neqc protocol [244] to account for variation in negative control probes. Inclusion criteria for further analysis required a detection value <0.01 for at least one sample for a given probe; this cut-off allows for "on/off" responses to various stimuli (e.g. DENV, LPS, or M*O*N-DNJ) and reduced the dataset to 21,705 expressed probes. Box-plots of $\log_2$ intensity for each sample following normalisation operations are presented in *Appendix III*. *Appendix VI* contains the list of normalised expression values for all expressed probes.

II.15.B. MDMΦ characterisation by transcriptomics

Uninfected, untreated samples were compared to a list of 490 genes expressed at high levels in macrophages from multiple species and isolated in different fashions [245] to further characterise the model. Gene expression was averaged across all four donors in each case and probes were sorted based on mean expression. Redundant probes were included to capture the genetic variation

of the outbred samples, and probes were considered to be highly expressed if they fell within the top 2500 based on this ordering. Detailed analysis of these 490 genes of interest is presented in *Appendix III*.

II.15.C. Statistical analyses of MDMΦ transcriptomic responses to DENV, LPS, and M*O*N-DNJ

Unsupervised hierarchical clustering was performed using Euclidean distance with complete linkage. Differentially expressed genes were then identified for various treatments using an Analysis of Variance (ANOVA) approach implemented in lumi with an adjusted for multiple comparisons *p*-value less than 0.05 and fold change greater than 20 percent. Genes identified by ANOVA were subjected to Ingenuity® Pathway Analysis (IPA, Qiagen) to identify functionally significant interactions and determine potential upstream regulators of the observed transcriptional responses. Upstream regulators were considered significantly modulated if the *p*-value of enrichment was less than 0.001 or the z-score was greater than 2.000 or less than -2.000.

II.16. MDMΦ protein extraction and Western blotting

MDMΦs were cultured as described above in 6 well tissue culture plates. Cells were washed twice in pre-warmed PBS and then scraped using a cell scraper as described for FOS extraction. Following pelleting, samples were resuspended in 200 µl of ice-cold HSE-CHAPS lysis buffer (see II.21) containing cOmplete ULTRA EDTA-free protease inhibitor (Roche). Samples were kept on ice for one hour with pulse vortexing every 15 minutes for extraction. Proteins extracted from whole-cell lysates were quantitated on a NanoDrop 1000 (Thermo) and diluted to equal concentrations in 4x LDS running buffer (Life Technologies). Samples were run on NuPAGE 4-12% Bis-Tris Gels (Life

Technologies) in MES (2-(*N*-morpholino)ethanesulfonic acid) or MOPS (3-(*N*-morpholino)propanesulfonic acid) running buffer (dependent upon size of protein) in the absence of reducing agent. Proteins were transferred to Immobilon PVDF membranes (Millipore) pre-soaked in MeOH using an XCell II Blot Module (Invitrogen) in Western transfer buffer for 2 hours at 30 V. Membranes were washed briefly in distilled water and blocked in WesternBreeze blocking solution (Life Technologies) with rocking for 30 minutes at 20°C or overnight at 4°C. Membranes were washed once in distilled water then incubated with primary antibody (listed in *Table 2.2*) diluted in WesternBreeze primary antibody solution (Life Technologies) as necessary for 1 hour at 20°C. Following incubation, membranes were washed 3 times in WesternBreeze antibody wash solution (Life Technologies) and then incubated in secondary antibody prepared in WesternBreeze secondary antibody solution (Life Technologies) for 30 minutes at 20°C. Membranes were washed 3 times in WesternBreeze antibody wash solution and twice in distilled water prior to 5 minute incubation with WesternBreeze Chemiluminescent substrate (Life Technologies). Blots were imaged on an Intelligent Dark Box II (Fujifilm) and densitometry measurements were conducted using LiCor Image Studio Lite (LiCor). Where necessary for reprobing, blots were stripped in Western stripping buffer twice (15 minutes, 37°C) and washed three times in PBS/Tween 0.3% v/v prior to incubation with primary antibody.

TABLE 2.2 Antibodies used in western blotting

Target	Species	Clonality[a]	Dilution	Supplier	Cat #
Cofilin (CFL1)	Mouse	Mono, IgG2a, κ	1:1000	Abcam	Ab75510
NFE2L2 (phosphorylated at S-40)	Rabbit	Mono	1:5000 (22 ng/ml)	Abcam	ab76026
OX40 (TNFRSF4)	Rabbit	Mono, TCS	1:500	Abcam	ab76000

[a]Clonality indicates monoclonal (Mono) or polyclonal in addition to isotype information where available. Tissue culture supernatants are denoted by TCS.

II.17. Supernatant cytokine analyses

II.17.A. Luminex-based cytokine quantiation

A pilot experiment measuring the impact on MDMΦ cytokine production of DENV infection and treatment with *N*B-DNJ at concentrations of 10 µM and 100 µM drug was conducted using 6 donors. In this experiment, 20 cytokines/chemokines (IL-1β, IL-2, IL-4, IL-5, IL-6, IL-7, IL-8, IL-10, IL-12(p70), IL-13, IL-17A, G-CSF, GM-CSF, IFN-γ, IP-10, MCAF, MIP-1β, RANTES, and TNF-α) were detected by a multiplex fluorescent bead based assay (Bio-Rad) in supernatants following 3 days of treatment of a standard DENV infection and antiviral treatment assay as described above. Supernatants were collected on day 3, centrifuged (5 minutes, 900 x *g*) to remove cellular debris, aliquoted, and stored at -80°C until analysis. Samples were handled in a 96 well format using a filter bottom plate (Bio-Rad) to allow vacuum manifold washes as per manufacturer's instructions. Briefly, the vacuum plate was equilibrated with assay buffer before addition of labelled fluorescent beads specific for each cytokine of interest (Bio-Rad). Beads were washed with wash buffer (Bio-Rad) and then supernatants/standards were applied and incubated in the dark at 20°C with rocking for 2 hours. Plates were washed three times with wash buffer and detection antibody was added and incubated in the dark at 20°C for 30 minutes with rocking. Plates were washed 3 times in wash buffer and streptavidin-phycoerythrin was added and incubated for 10 minutes with rocking at 20°C in the dark. Plates were washed a further 3 times in wash buffer, fixed in 2% paraformaldehyde, washed a further 3 times in wash buffer, and stored in assay buffer (Bio-Rad). Samples were read on a Luminex 200 (Luminex) fluorescence detector, and concentrations of cytokines were determined based on 5-point linear regression curves in comparison to standards. Values outside of the range of detection based on the standard curve were set to the minimum or maximum value detectable. For the time course experiment including DENV infection and LPS treatment with iminosugars *N*B-DNJ, *N*B-DGJ, and M*O*N-DNJ, four donors were analysed for cytokine/chemokine (IL-6, IL-8, IL-10, IL-17A, G-CSF, IFN-γ, IP-10, MCP-1, MIP-1β, RANTES, and TNF-α) production with supernatants collected at days 1,

3, and 5 post infection (p.i.). Experimental procedures and analyses were identical with the exception of the use of magnetic beads and a magnetic plate holder (Bio-Rad) in place of a vacuum manifold. Figures were generated using Prism 6 (GraphPad Software, Inc.) and statistical analyses were performed using SigmaPlot 12 (Systat Software) using either parametric *t*-tests or ANOVA or, in the case where data compared did not meet necessary assumptions of normality by Shapiro-Wilk test or equality of variance by f-test, non-parametric *t*-tests or ANOVA. Post-hoc testing was conducted by Holm-Šídák method for parametric methods or by Dunnett's test for non-parametric methods.

II.17.B. ELISA-based cytokine analysis

Because IP-10 and MIP-1β cytokine levels exceeded the maximum value of the standard curve generated for Luminex assays in many samples, additional aliquots of cell culture supernatant were diluted 1:100 in Buffer RD5K (R&D Systems) for analysis of these cytokines by enzyme-linked immunosorbant assay (ELISA) using Quantikine kits (R&D Systems). Assays were conducted in accordance with manufacturer's protocols such that samples were conjugated to clear-bottom plates at room temperature in the presence of binding buffer (IP-10: RDI-56 for 2 hours; MIP-1β: RD1X for 1.25 hours). Wells were washed in freshly prepared wash buffer and then appropriate horseradish peroxidase-conjugated antibody was added to each well and incubated at room temperature for the appropriate time (2 hours for IP-10, 1.25 hours for MIP-1β). Wells were again washed and freshly prepared 3,3',5,5'-tetramethylbenzidine (TMB) substrate was added to each well. Plates were incubated at room temperature in the dark for development of reactions and stopped by the addition of 2M sulphuric acid. Plates were read on a SpectraMax M5 microplate reader (Molecular Devices) to determine absorbance at 450 nm with subtractive correction of absorbance at 540 nm. Experimental samples were quantified by linear regression against a standard curve plotted on a $\log_{10}$ vs. $\log_{10}$ graph of standard concentration vs. corrected A_{450}. Samples were

assayed in technical singlicate with biological replicates averaged for statistical analyses. Analysis of significant differences was conducted as for Luminex assays.

II.18. *In vivo* virus infection and drug treatment

All experimental procedures were preapproved by the UC Berkeley Animal Care and Use Committee and were performed according to the guidelines of the UC Berkeley Animal Care and Use Committee, the United States Public Health Service, and the USDA Animal Welfare Act. AG129 mice lacking receptors for interferon-alpha, -beta, and –gamma were infected with DENV in a manner intended to mimic ADE infection as previously described. [201,246] Mice were primed 24 hours prior to infection with a 2 μg intraperitoneal (i.p.) injection of a pan-flavivirus monoclonal antibody against E protein, 4G2. At initiation of infection (t=0), 10^5 pfu of DENV2 D2S10, a mouse adapted strain of DENV2, was injected intravenously. Beginning immediately following infection, mice were treated with M*O*N-DNJ at 100 mg drug per kg bodyweight (mg/kg) t.i.d. i.g. or 33.3 mg/kg CAST t.i.d. i.g. Treatment was continued for 72 hours at which point mice were anaesthetised by isoflurane inhalation and sacrificed by cardiac puncture. Infection, treatment, and tissue harvesting of mice was conducted by Sarah Killingbeck, and I conducted all subsequent isolation protocols and analyses.

II.19. Collection and preparation of mouse tissues for RNA quantitation

Cardiac bleeds (approximately 1 ml) were collected in citrate anti-coagulant tubes (Becton Dickinson) and stored on ice prior to isolation of PBMCs and plasma. To separate plasma, whole blood was centrifuged (18,000 x *g*, 30 minutes, 4°C) and supernatant was collected. Cells were resuspended in 0.14 M ammonium chloride (Sigma), 17 mM Tris (MP Biomedicals), *p*H 7.2 in H_2O and incubated at 37°C for 5 minutes to lyse red blood cells (RBCs). RBC lysis was repeated three

times, and cells were washed in serum free α-MEM (Gibco) prior to resuspension and storage in RNAlater (Qiagen). Spleen, liver, small intestine, kidney, and lymph node tissues were collected into tubes containing zirconia/silica beads (1.0 mm diameter) and protease inhibitor cocktail (Roche) in α-MEM. Tissues were homogenised using a Mini-Beadbeater-8 (BioSpec Products) and stored immediately at -80°C until future use. PBMC and other tissue samples were thawed on ice in the presence of 40 mM dithiothreitol (DTT) and mixed with three volumes of buffer RLT (Qiagen) containing 40 mM DTT prior to isolation of cellular RNAs by RNeasy Mini Kit (Qiagen) as per manufacturer's instructions. Plasma RNA (viral RNA) was isolated by QIAamp Viral RNA Mini Kit (Qiagen) in accordance with the manufacturer's instructions.

II.20. qRT-PCR of endogenous mouse genes

Multiplex quantitative reverse transcription real time polymerase chain reaction (qRT-PCR) was conducted on all tissue isolates and plasma on an Applied Biosystems 7500 real-time PCR system (Life Technologies) using Verso 1-step reverse transcriptase (Thermo Fisher Scientific) in the presence of RT Enhancer (Thermo Fisher Scientific) to remove contaminating DNA. Thermo-Start DNA *Taq* polymerase (Thermo Fisher Scientific) was used to accomplish Taq-mediated release of fluorescently labelled dyes from gene-specific probes. In the case of the rodent glyceraldehyde 3-phosphate dehydrogenase (GAPDH) control (Life Technologies #4308313) a VIC reporter dye was attached to a TAMRA (tetramethylrhodamine) quencher, and experimental gene reporters including mouse and DENV-specific targets were labelled with FAM (6-fluorescein amidite) reporter dyes with a TAMRA quencher. Endogenous mouse experimental probes and primers were obtained from Life Technologies (listed in *Table 2.3*) and used at 1x final concentration while GAPDH primers were used at 10 µM and probe at 20 µM. In the case of DENV qRT-PCR, quantitation using a D2S10-specific primer/probe set for NS5 was conducted using all primers and probe at 10 µM final concentration. Synthesis of complementary DNA (cDNA) was performed for 30 minutes at 50°C followed by a 15

minute activation of Thermo-Start *Taq* polymerase at 95°C. PCR thermocycling with fluorescence detection was executed for 40 cycles of 95°C for 15 seconds followed by 60°C for 60 seconds and a fluorescence read step. Samples were read in technical duplicate and 95% confidence intervals were determined based on biological and technical variation and graphed using Prism 6 (GraphPad Software, Inc.).

TABLE 2.3. *qRT-PCR primers and probes*

Target	Primer	Probe	Label	Quencher	Sequence[a]	Cat #[b]
GAPDH	+	+	VIC	TAMRA		4303212
XBP-1	+	+	FAM	TAMRA	Mm00457360_g1	4351372
OX40 (TNFRSF4)	+	+	FAM	TAMRA	Mm00442037_g1	4331182
OX40L (TNFSF4)	+	+	FAM	TAMRA	Mm00437214_m1	4331182
4-1BB (TNFRSF9)	+	+	FAM	TAMRA	Mm00441899_m1	4331182
4-1BBL (TNFSF9)	+	+	FAM	TAMRA	Mm00437155_m1	4331182
CD28	+	+	FAM	TAMRA	Mm00483137_m1	4331182
D2S10 NS5		+	FAM	TAMRA	TGGGATTTCCTCCCATGATTCCACTGG	Custom
D2S10 NS5	Forward				ACAAGTCGAACAACCTGGTCCAT	Custom
D2S10 NS5	Reverse				GCCGCACCATTGGTCTTCTC	Custom

[a]Sequence indicates Life Technologies accession number or the 5' to 3' sequence of the listed oligonucleotide, as appropriate

[b]Cat # is the catalogue number for the reagent listed with all reagents obtained from Life Technologies

II.21. Laboratory buffers and reagents

Hank's solution A (10x)

NaCl	160 g
KCl	8 g
$MgSO_4 \cdot 7H_2O$	2 g
$MgCl_2 \cdot 6H_2O$	2 g
$CaCl_2 \cdot 2H_2O$	2.8 g
H_2O	to 1000 ml

Sterilise by autoclaving

Hank's solution B (10x)

Na_2HPO_4	1.2 g
KH_2PO_4	1.2 g
D-glucose	20 g
H_2O	to 1000 ml

Filter sterilise

Plaque first overlay

Hank's solution A	1x
Hank's solution B	1x
Vitamin solution (Gibco)	1x
Amino acid solution (Gibco)	2x
HI-FBS (Seralab)	1%
L-glutamine (Gibco)	1.2 mM
Penicillin (Gibco)	100 U/ml
Streptomycin	0.1 mg/ml
$NaHCO_3$	0.15%
H_2O	to volume
Filter sterilise	

Plaque second overlay

Hank's solution A	1x
Hank's solution B	1x
Vitamin solution (Gibco)	1x
Amino acid solution (Gibco)	2x
L-glutamine (Gibco)	1.2 mM
Penicillin (Gibco)	100 U/ml
Streptomycin	0.1 mg/ml
H_2O	to volume
Filter sterilise	

HSE-CHAPS lysis buffer

HEPES; (4-(2-hydroxyethyl)-1-piperazineethanesulfonic acid)	50 mM
NaCl	200 mM
EDTA	2 mM
CHAPS; (3-[(3-cholamidopropyl)dimethylammonio]-1-propanesulfonate)	2% (w/v)

MES running buffer

MES	50 mM
Tris base	50 mM
EDTA	1 mM
SDS	0.1% (w/v)
*p*H to 7.3	

MOPS running buffer

MOPS	50 mM
Tris base	50 mM
EDTA	1 mM
SDS	0.1% (w/v)
*p*H to 7.7	

Western transfer buffer

Bicine	25 mM
Tris base	25 mM
EDTA	1 mM
Methanol	20% v/v
SDS	0.5% w/v
*p*H to 7.2	

Western stripping buffer

Glycine	15% w/v
SDS	1% w/v
Tween 20	1% v/v
*p*H to 2.2	

III

Deoxynojirimycin derivatives inhibit dengue virus as a consequence of α-glucosidase inhibition

III.1. Abstract

Diverse derivatives of deoxynojirimycin iminosugars have been investigated as potential therapeutic agents for dengue virus infection. The prevailing hypothesis within this field of research is that these molecules possess antiviral activity as a function of inhibition of ER-resident α-glucosidases; however, evidence correlating antiviral activity with successful cellular inhibition of glucosidases and/or exclusion of alternative mechanisms of action of iminosugars has not been presented for many of these compounds in the context of dengue virus. In this chapter, I present work that links effective inhibition of cellular ER α-glucosidases with direct reduction of infectious dengue virus production in a primary human macrophage model. These data suggest that α-glucosidase II inhibition is of particular importance to reduction of infectious virus production.

III.2. Introduction

As discussed in *Chapter I*, iminosugars have been considered as broad-spectrum antiviral therapeutic candidates due to their ability to inhibit α-glucosidase processing enzymes. To date, limited work has been done to demonstrate that antiviral properties of iminosugars, specifically in relation to DENV, are a consequence of α-glucosidase inhibition. Wu *et al.* were able to demonstrate interaction of DENV glycoproteins prM, E, and NS1 with CANX by immunoprecipitation (IP) and abrogation of this interaction in the presence of the iminosugar *N*N-DNJ, but direct interactions with either of the ER α-glucosidases were not assessed. [247] Additional work with a diversity of iminosugar derivatives of DNJ and CAST as DENV therapeutics combined with the overlap of presumed capacity for inhibition of ER α-glucosidases by these molecules provides strong circumstantial evidence that α-glucosidase inhibition is responsible for direct reduction of DENV antiviral activity. [201-204,206-209] However, the similarity in structure of DNJ and glucose sugar rings combined with the multitude of interactions of glucose in diverse metabolic processes is cause for concern that one or more

additional mechanisms of inhibition by iminosugars might be of importance for promotion of an effective antiviral state. Indeed, the role of glucose in glycolipid processing, specifically by GCS activity, has been successfully targeted clinically with iminosugars for more than a decade as a treatment against Gaucher disease, [198,199] and more recently against NPC disease. [200] To date, correlation of DENV antiviral activity with efficacy of inhibition of α-glucosidase targets in a cellular context has been conducted in only one instance [206] and the contribution of other potential glucose-dependent pathways to the antiviral activity of these iminosugars has not been ascertained. As such, the aims of this chapter are to:

1) Assess the *in vitro* antiviral efficacy and cytotoxicity of a small panel of DNJ and DGJ iminosugar derivatives in a primary human cell type relevant to DENV infection,
2) Determine the capacity of selected iminosugars for inhibition of a panel of glucosidase and glycosidase enzymes,
3) Measure efficacy of iminosugar inhibition of various glucose-dependent enzymatic activities in primary human MDMΦs, and
4) Correlate enzyme inhibition as assessed in aim 3 with inhibition of production of infectious DENV.

III.3. Results

III.3.A. Cytotoxicity of iminosugars in human MDMΦ

To assess the therapeutic potential of DNJ-derived iminosugars against DENV, primary human MDMΦs were obtained from anonymous donors to provide the closest approximation of the diversity of responses to infection and drug treatment that may occur in a real patient population. Cytotoxicity was first measured in primary human MDMΦs using a commercially available kit to assess metabolic activity (Promega). Considerable donor-to-donor variability was observed as

displayed in *Table 3.1*. In general, shorter alkyl chain modifications demonstrated lower toxicity than longer or bulkier chains (*i.e. N*AP-DNJ) and this trend was observed for both DNJ and DGJ stereochemistries. *N*B-DNJ was the least cytotoxic drug with five of eight donors tested demonstrating no observable cytotoxicity up to concentrations of 32 mM.

III.3.B. DNJ but not DGJ derivatives reduce production of infectious DENV

The ability of *N*B-DNJ, *N*N-DNJ, M*O*N-DNJ, and *N*AP-DNJ to inhibit the release of infectious DENV from primary human MDMΦs was assayed as a measure of antiviral activity. Untreated cells released 10^3 to 10^5 pfu/ml, and antiviral effects of each drug were normalised to untreated cells on a donor-specific basis. Curves of best fit demonstrate considerable variation in potency amongst individual donors as displayed in *Figure 3.1A-D*. The combination of the biological replicates is displayed in *Figure 3.1E*. The concentration of drug required to inhibit 50 percent and 90 percent of infectious virus production (IC_{50} and IC_{90}, respectively) was calculated as in the *Materials and Methods* and these results are summarised in *Table 3.1*. By comparing drug concentrations required to elicit effective reduction of infectious virus with those concentrations required to observe cytotoxic effects, the selectivity of each compound was assessed. Whereas the first selectivity index (SI1; CC_{50}/IC_{50}) predominates in the literature for drug discovery, I believe a more stringent selectivity (SI2; CC_{10}/IC_{90}) better reflects the potential of a drug for clinical consideration. Immunofluorescence assays using an anti-envelope mAb were used to detect successful infection of MDMΦs, and titration of iminosugars (*N*B-DNJ, *N*N-DNJ, and *N*AP-DNJ) were able to reduce the percent of DENV infected cells in a dose-dependent fashion as shown in *Figure 3.2.* Due to lack of clarity regarding the mechanism behind this reduction (*e.g.* reduced viral uptake due to direct effects on receptors vs. reduced MDMΦ-produced infectious virus capable of proliferative infection)

as well as technical concerns regarding variation, the assay was not conducted for M*O*N-DNJ or DGJ-derived iminosugars. Nevertheless, measures of antiviral success correlated well with respect to relative potency across assays.

TABLE 3.1. Anti-DENV activity and cytotoxicity of iminosugars in primary human macrophages[a]

	CC, μM (*n*)[b]		IC, μM (*n*)[c]		SI[d]	
Drug	50%	10%	50%	90%	1	2
*N*B-DNJ	24,903 ± 10,506[e] (3)	837 ± 428	6.00 ± 7.31 (5)	62.1 ± 60.7 (4)	4,151	13.5
*N*N-DNJ	317 (1)	42	0.91 ± 0.40 (4)	8.02 ± 4.14 (3)	348	5.2
M*O*N-DNJ	3,150 ± 1,211 (7)	837 ± 178 (4)	3.09 ± 3.93 (5)	7.74 ± 3.63 (5)	1,019	108.1
*N*AP-DNJ	300 ± 123 (2)	10	0.04 ± 0.01 (3)	0.28 ± 0.14 (3)	7,500	35.7
*N*B-DGJ	1,236 ± 245 (2)	632 ± 512 (2)	ND[f]	ND	ND	ND
*N*N-DGJ	796 ± 113 (2)	298 ± 383 (2)	ND	ND	ND	ND

[a] Throughout, *n* represents the number of monocyte donors tested.

[b] 50% and 10%, CC_{50} and CC_{10}, respectively. Human MDMΦ from multiple donors were incubated for 2 days with serial dilutions of iminosugars, alongside controls containing equivalent medium and DMSO concentrations, as appropriate. Cell viability was measured as described in Materials and Methods and calculated as a percentage of that of the untreated cells. Values were calculated using the line of best fit on graphs of drug concentration versus the percentage of cell viability. Means and standard deviations (or approximations thereof when $n<3$) are shown.

[c] 50% and 90%, IC_{50} and IC_{90}, respectively. Data were calculated for inhibition of release of infectious virus in a similar manner to CC_{50} and CC_{10} values described above.

[d] Selectivity indices (SIs) were calculated as follows: SI1 = CC_{50}/IC_{50}, and the more stringent SI2 = CC_{10}/ IC_{90}.

[e] Cells from 5/8 donors showed no toxicity of *N*B-DNJ when tested at up to 31.6 mM and are not included in the calculation of this value.

[f] Inhibitory and selectivity values for DGJ-derivative iminosugars were not determined (ND) due to a lack of antiviral activity of the drugs against DENV by plaque assay up to 100 μM and 32 μM for *N*B-DGJ and *N*N-DGJ, respectively.

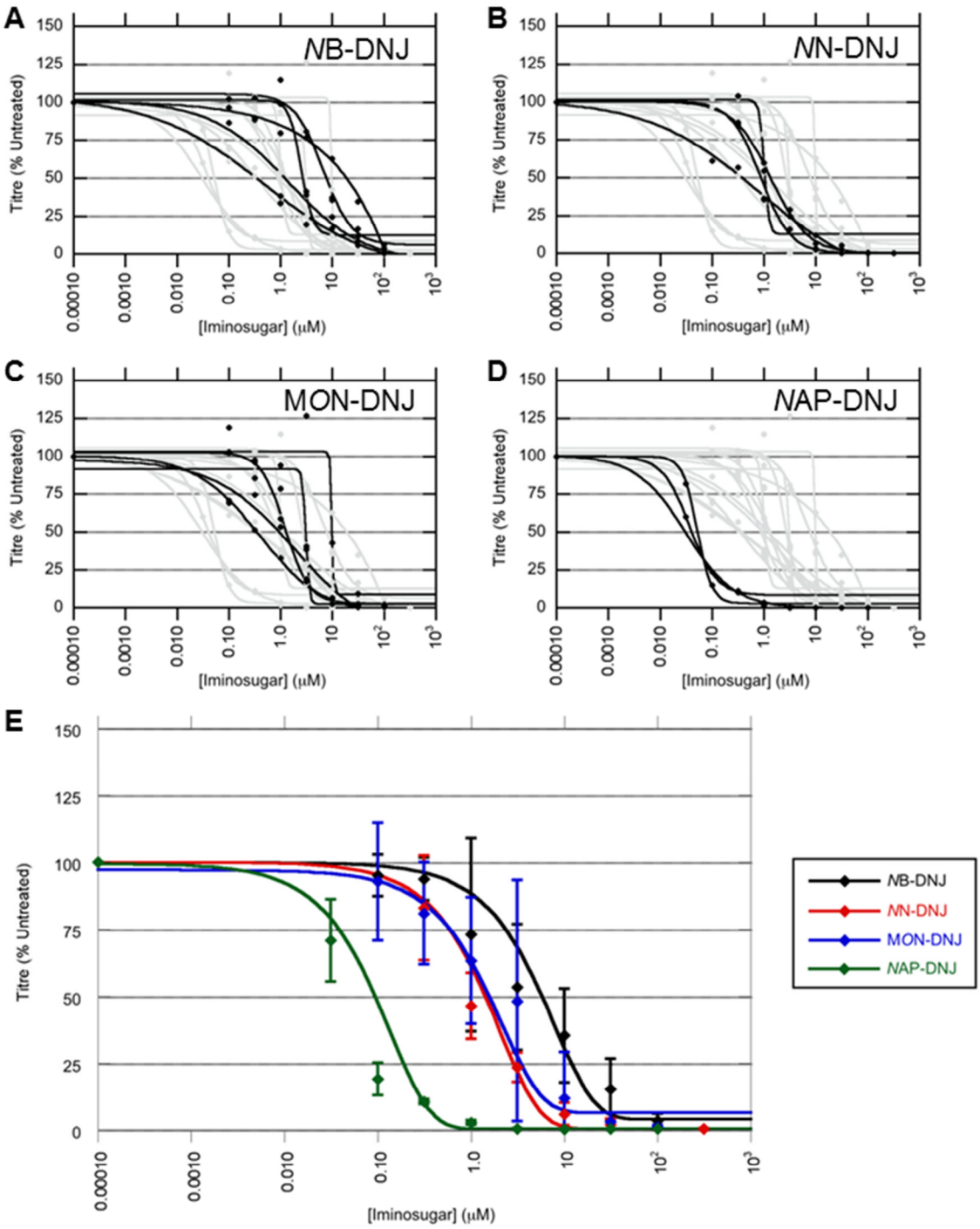

FIGURE 3.1. Iminosugars inhibit release of infectious virus from DENV-infected macrophages. Primary human MDMΦs were infected with DENV and then incubated with medium containing *N*B-DNJ (**A**), *N*N-DNJ (**B**), M*O*N-DNJ (**C**), or *N*AP-DNJ (**D**) for two days in triplicate for each donor. (**A** to **D**) Release of infectious virus was measured by plaquing supernatants of cells treated with drug. Plaques were counted and averaged for each drug concentration, and the percentage of infectious virus released was calculated as a ratio to pfu/ml calculated from untreated cells. Curves of best fit are shown for cells of individual donors (black), with inhibition curves for other iminosugars shown in grey for comparison. (**E**) Iminosugar inhibition of release of infectious virus, with curves representing averages for multiple donors. Error bars represent the standard deviations. Data collected in collaboration with J Williams and Dr. JL Miller.

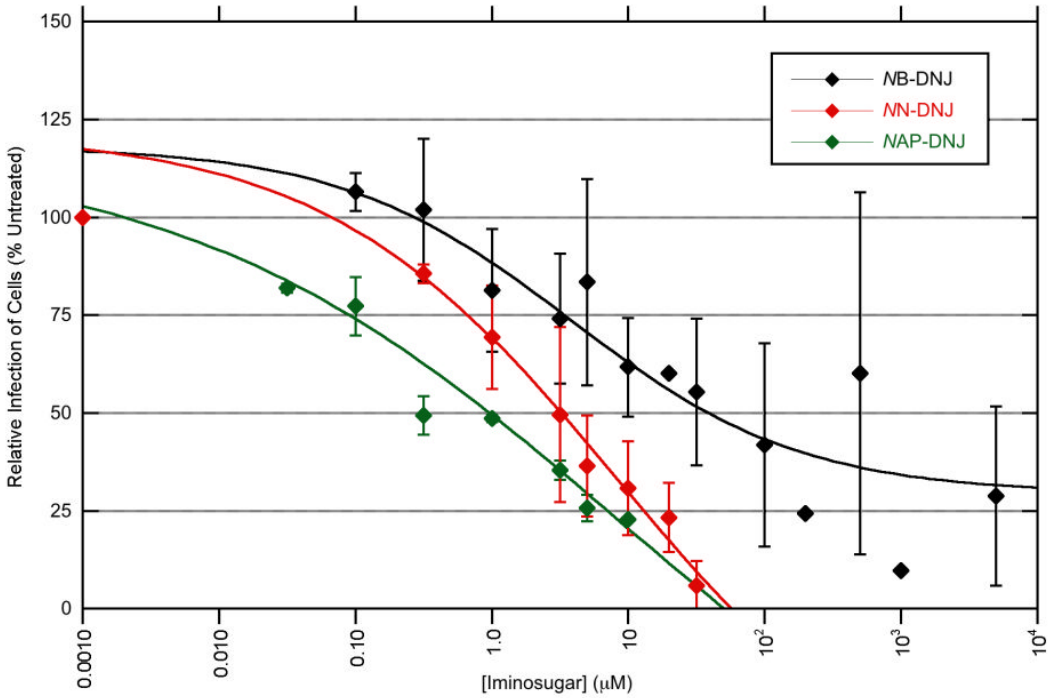

FIGURE 3.2. Iminosugars inhibit infection of DENV-infected macrophages. Primary MDMΦ were infected and treated as in *Figure 3.1*. Following removal of supernatant, cells were stained by DENV E-specific antibody (3H5) which was subsequently detected by immunofluorescence assay (IFA). Calculations and curve fitting relative to controls was performed as described in *Figure 3.1* such that each curve represents an averaged IFA value with respect to control for multiple donors. Error bars represent SDs.

In contrast to the DNJ-derived iminosugars, DGJ derivatives failed to reduce infectious virus production in MDMΦs (*Figure 3.3*). As in *Figure 3.1*, inhibition of production of infectious DENV in MDMΦs was determined by plaque assay. As shown in *Figure 3.3*, *N*B-DNJ and *N*N-DNJ inhibited production of infectious virus with IC_{50}s of 6.00 μM and 0.91 μM, respectively. In contrast, both *N*B-DGJ and *N*N-DGJ failed to reduce production of infectious DENV. These results suggest that glucose stereochemistry confers an antiviral capacity to iminosugars that is not conserved for iminosugars possessing galactostereochemistry.

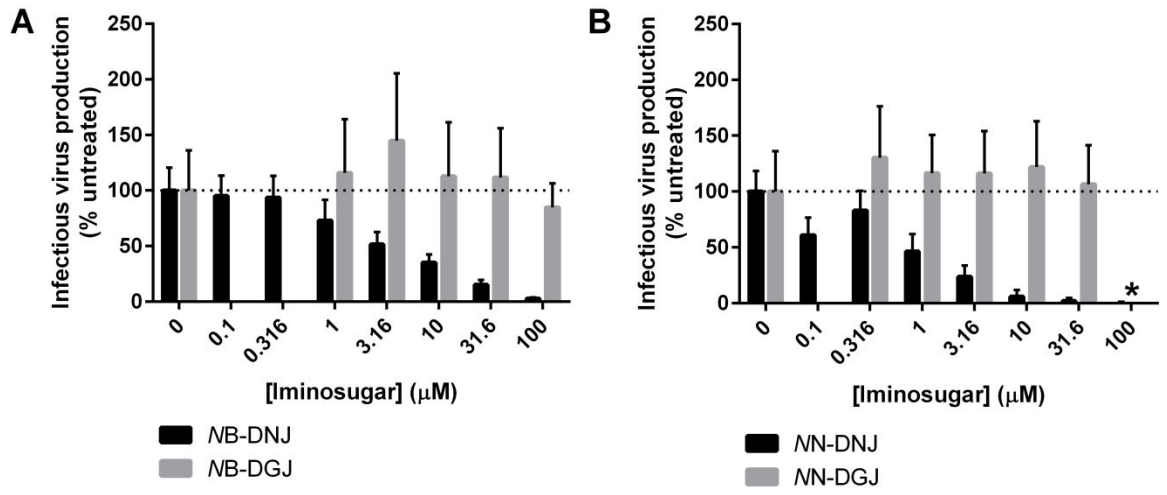

FIGURE 3.3. Galactose analogue iminosugars fail to reduce production of infectious DENV in primary human MDMΦs. (**A)** Primary MDMΦs (n=2 donors assayed in technical triplicate) were treated as previously described with serial dilution of *N*-butylated iminosugar and analysed by plaque assay. Dose dependent inhibition of production of viral plaques was observed for *N*B-DNJ but not *N*B-DGJ (up to 100 μM). **(B)** Primary MDMΦs were similarly treated with *N*-nonylated iminosugar (* indicates treatment up to 100 μM *N*N-DNJ and 31.6 μM *N*N-DGJ due to cytotoxicity of the DGJ compound). Whereas *N*N-DNJ reduced infectious virus production > 90% at 10 μM, *N*N-DGJ failed to reduce production of infectious virus at the maximal dose tested. Error bars represent SDs.

III.3.C. *In vitro* enzyme inhibition of iminosugars

Given the diversity of functions of glycans *in vivo* and the rationale of iminosugar use as monosaccharide mimetics, such drugs might inhibit a considerable number of enzymes involved with glycan processing. Indeed, the differential antiviral effects of gluco- and galactostereochemistry possessing iminosugars indicates that differential inhibition of molecular targets occurs in response to relatively minor changes in stereochemistry. With alteration of one stereocentre, differences in inhibition of glucosidase and glycosidase enzymes specific for various sugar stereochemistries are likely. Such differences were hypothesised to be important in explaining the spectrum of cytotoxicity and antiviral efficacy of the iminosugars tested. As shown in *Table 3.2*, DNJ and derivatives thereof

(*N*B-DNJ and M*O*N-DNJ) demonstrate high nanomolar to low micromolar *in vitro* inhibition of α-glucosidases; whereas, DGJ is only inhibitory of these enzymes at concentrations approaching 1 mM or not at all. Similarly, α-galactosidase is inhibited at low nanomolar concentrations by the iminosugar DGJ with identical stereochemistry to the natural substrate galactose, but absence of or very weak inhibition is detected for glucose-mimetic DNJs. All four iminosugars inhibit α,α-trehalase, an enzyme responsible for digestion of α,α-1,1-glucoside bonds between two α-glucose units. Of particular interest is the trend observed for inhibition of glucosyltransferase isolated from a human promyelocytic leukaemia cell line (HL60) where iminosugars with increasing alkyl chain length, again mimicking the natural substrate of the enzyme glucosylceramide, are more potent inhibitors of the enzyme. A similar trend has previously been described for DGJ derived iminosugars. [248] Inhibition of enzymes responsible for processing of β-linkages and non-glucose, non-galactose containing saccharides was either not detected (up to 1 mM) or only achieved at high micromolar concentrations. Based on these observations, I hypothesise that the most likely mechanism that accounts for antiviral activity of DNJ-derived but not DGJ-derived iminosugars is a function of the difference in inhibition of α-glucosidases; however, the possibility remains that effects on glycolipid processing are responsible for or contribute to iminosugar antiviral characteristics.

TABLE 3.2. *In vitro* inhibition of glucosidases and glycosidases

		IC_{50}, μM[a]			
Class	Enzyme	DNJ	*N*B-DNJ	M*O*N-DNJ	DGJ
α-glucosidase					
	Rat ER α-glucosidase II	16	6.7	0.83	NI
	Rat intestinal maltase	0.2	1.1	0.28	362
	Rat intestinal isomaltase	0.8	2.1	1.4	NI
	Rat intestinal sucrase	0.51	0.44	0.5	340
	Human lysosome	0.37	0.27	0.39	NI
Glucosyltransferase					
	HL60[b]	NI	8.8	0.39	NI
β-glucosidase					
	Bovine liver	NI	NI	NI	NI
	Rat intestinal cellobiase	271	NI	469	123
	Human lysosome	402	NI	55	NI
α-galactosidase					
	Human lysosome	217	NI	NI	0.061
β-galactosidase					
	Bovine liver	NI	NI	634	NI
	Rat intestinal lactase	41	796	139	94
α-mannosidase					
	Jack beans	NI	NI	NI	NI
β-mannosidase					
	Snail	NI	NI	NI	NI
α-L-fucosidase					
	Bovine kidney	NI	NI	NI	876
β-glucuronidase					
	Bovine liver	NI	NI	NI	NI
α,α-trehalase					
	Porcine kidney	64	79	8.9	16
amyloglucosidase					
	Aspergillus niger	781	964	287	NI
α-L-rhamnosidase					
	Penicillium decumbens	NI	429	50	NI

[a] NI: No inhibition (less than 50% inhibition at 1mM). All assays conducted by Prof. A Kato.

[b] HL60: Human promyelocytic leukaemia cells

III.3.D. Iminosugars inhibit glycolipid processing in macrophages

Although differences in glycoprotein processing are perhaps the most logical explanation of antiviral activity of iminosugars, iminosugars possessing glucostereochemistry with *N*-butyl alkylation or longer also inhibit glycolipid processing as shown in *Table 3.2* and demonstrated in previous publications. [198,249] My results further support the hypothesis that the inhibition of glycolipid processing is dependent upon the tail decorating the ring nitrogen rather than the stereochemistry of the iminosugar headgroup (*i.e.* longer, more lipid-like chain decorations demonstrate more potent glycolipid inhibition). In order to determine whether glycolipid processing could contribute to the antiviral efficacy of DNJ iminosugars, whole cell lysates were assayed for monosialodihexosylganglioside (GM3) levels. Gangliosides are reliable markers of iminosugar-mediated alteration of glycolipid processing [248,249] and the relative simplicity of GM3, possessing one β-D-galactose and one β-D-glucose head group, facilitates analysis by NP-HPLC. Three donors were treated for two days with a titration of DNJ derivative iminosugars (*N*B-DNJ and M*O*N-DNJ) and assayed for GM3 levels by NP-HPLC (*Figure 3.4*). Blockade of the glycosyltransferase prevents production of glycolipids and a concomitant drop is observed in GM3 levels. With the lowest concentration of M*O*N-DNJ tested (1 μM), GM3 levels decreased on average by 78 percent, and with 3.1 μM M*O*N-DNJ treatment, GM3 levels were reduced by 90 percent. Reduction of GM3 was weaker with *N*B-DNJ treatment; however, 10 μM *N*B-DNJ treatment still achieved approximately 90 percent reduction. In previous experiments using immortalised cell lines, iminosugar treatment has typically been conducted for a longer duration of three to four days. [248-250] During previously published time-course experiments using *N*B-DNJ in PC12 cells from rat adrenal medulla, maximal concentrations of drug produced only 60% reduction of GSL with two days of treatment whereas three days of drug treatment reduced GSL levels by as much as 90%. [250] Given that the experiments performed herein were conducted with only a two day drug treatment, it appears that primary human macrophages are more susceptible to iminosugar-mediated effects on glycolipids

than other cell types. Inhibition of glycolipid processing by *N*B-DGJ and *N*N-DGJ was assessed at the maximum concentrations tested for antiviral activity of 100 μM and 31.6 μM, respectively, in order to determine whether DGJ-derived iminosugars are equally capable of GSL inhibition in MDMΦs. As anticipated, DGJs also suppressed GM3 levels after two days of treatment by approximately 90 percent (*Table 3.3*). Thus, glycolipid inhibition profiles do not differentiate antiviral properties of iminosugars against DENV in MDMΦs.

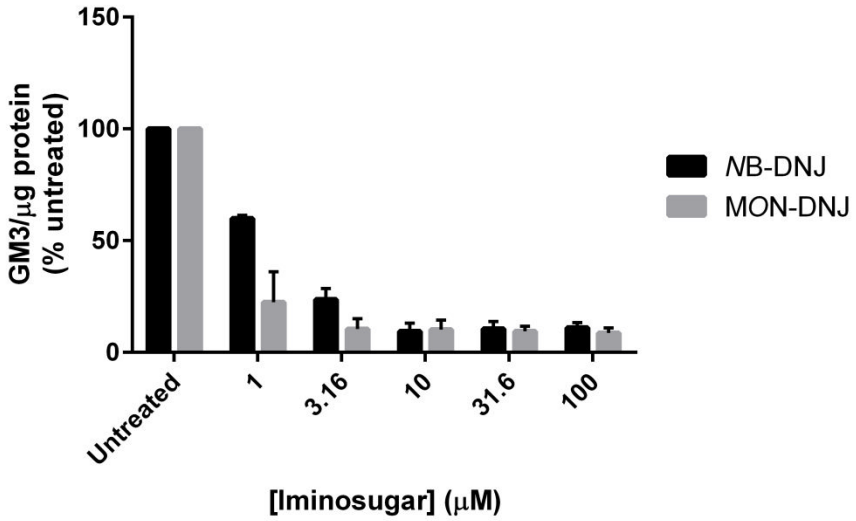

FIGURE 3.4. DNJ derivative iminosugars reduce GM3 levels in MDMΦs after 48 hours of treatment. Three donors were treated with ½ $\log_{10}$ dilutions of *N*B-DNJ (black) or M*O*N-DNJ (grey). GM3 levels were determined by peak area of HPLC elution and normalised to protein concentration. Although levels of GM3 varied quite drastically in untreated samples from each donor (519, 1934, and 2766 area units/μg protein were observed for untreated samples from each of the three donors), the percentage reduction by drug was similar across donors. Quantification of GM3 by HPLC was conducted by Dr. D Alonzi.

TABLE 3.3. GM3 inhibition by treatment with maximal[a] iminosugar concentration

Drug	Concentration (μM)	Peak area GM3/μg protein	GSL production (%)
Untreated	—	2780.4	100.0
DMSO	0.06% (v/v)	2766.1	99.5
*N*B-DNJ	100	264.3	9.5
*N*B-DGJ	100	330.7	11.9
*N*N-DNJ	31.6	233.9	8.4
*N*N-DGJ	31.6	322.9	11.6
M*O*N-DNJ	100	247.3	8.9

[a]Maximal concentrations of iminosugars used are those the highest non-toxic dose of iminosugar for which antiviral data was available (*Figures 3.2 and 3.3*) with the exception of *N*N-DNJ which was used at 31.6 μM instead of 100 μM for direct comparison with *N*N-DGJ. *N*-nonyl compounds were diluted from 100% DMSO stocks, thus an equivalent dilution of DMSO only (0.06% v/v) was assayed to ensure that the solvent did not impact GSL production.

III.3.E. Production of free oligosaccharides (FOS) correlates with antiviral activity

Further to the hypothesis that α-glucosidase inhibition reduces production of infectious DENV in MDMΦs, production of FOS was measured by NP-HPLC in uninfected samples after 24 or 48 hours of drug treatment. As a consequence of inhibition of α-glucosidase II, a monoglucosylated glycoprotein is produced. After trimming of the glycan precursor by mannosidases and recognition of the glycoprotein as terminally misfolded, a $Glc_1Man_4GlcNAc_1$ free oligosaccharide species is cleaved from the peptide during ERAD. In the case of inhibition of α-glucosidase I, a similar process produces a $Glc_3Man_5GlcNAc_1$ species. Thus, presence of each species of FOS can be correlated with successful inhibition of the respective cellular α-glucosidase. [235] Accumulation of FOS possessing two terminal glucose units such as $Glc_2Man_4GlcNAc_1$ and $Glc_2Man_5GlcNAc_1$ is an additional consequence of α-glucosidase II inhibition and was noted following treatment with M*O*N-DNJ as shown in *Figure 3.5*. Increases in FOS species with extended incubation with iminosugar are demonstrated in *Figure 3.6*. Almost all species of FOS were undetectable in the absence of iminosugar treatment as shown

in *Figure 3.5*. In contrast, production of $Glc_1Man_4GlcNAc_1$ was noted for all time points and for all donors at the minimum concentration tested as shown in *Figure 3.7*. For simplicity, $Glc_1Man_4GlcNAc_1$ was used as a measure of α-glucosidase II inhibition and $Glc_3Man_5GlcNAc_1$ was used as a measure of α-glucosidase I inhibition to examine dose-response relationships of M*O*N-DNJ and *N*B-DNJ in MDMΦs. Considerable donor-to-donor variability exists with respect to levels of absolute FOS produced per unit protein in response to iminosugars in these primary human cells; however, relative trends (*e.g.* concentration required to induce a particular glycan species or reach maximal production) are conserved.

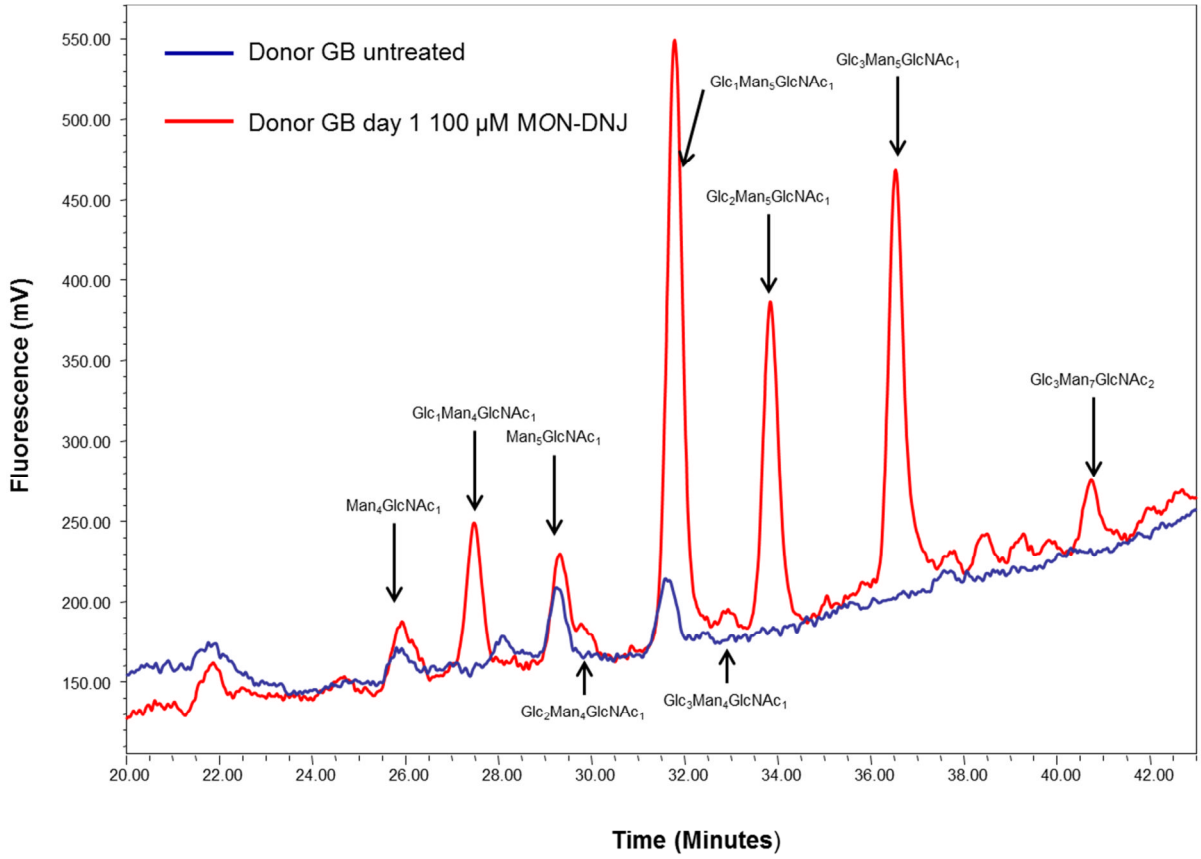

FIGURE 3.5. Generation of FOS in MDMΦs treated with 100 µM M*O*N-DNJ. MDMΦs were treated with 100 µM M*O*N-DNJ for 24 hours and FOS were isolated and measured by HPLC. Although $Man_4GlcNAc_1$, $Man_5GlcNAc_1$, and $Glc_1Man_5GlcNAc_1$ were present in small quantities in untreated samples (blue line, elution times of 26, 29.25, and 31.75 minutes, respectively), most species of FOS were not detectable in the absence of drug treatment. With iminosugar treatment (red line), species indicative of inhibition of α-glucosidase I ($Glc_3Man_4GlcNAc_1$ eluting at 33 minutes and $Glc_3Man_5GlcNAc_1$ at 36.5 minutes) and both steps of α-glucosidase II trimming (first step: $Glc_2Man_4GlcNAc_1$ eluting at 30 minutes and $Glc_2Man_5GlcNAc_1$ at 34 minutes and second step: $Glc_1Man_4GlcNAc_1$ eluting at 27.5 minutes and $Glc_1Man_5GlcNAc_1$ at 31.5 minutes) were detected. Representative data from one of three donors (donor GB) are shown. Quantitation of FOS by HPLC was performed by Dr. D Alonzi.

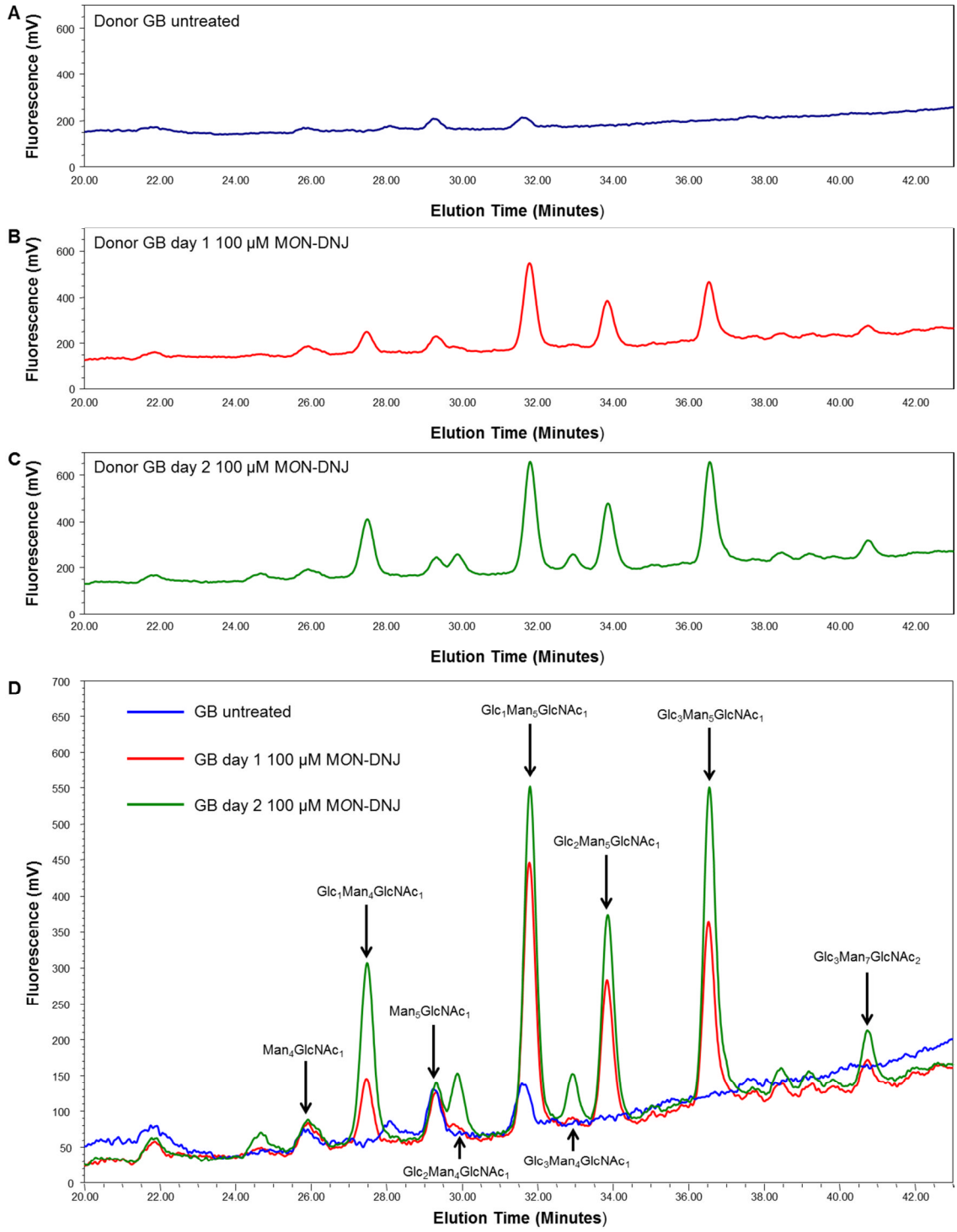

FIGURE 3.6. Generation of FOS by M*O*N-DNJ in donor GB increases with time. MDMΦs were treated with 100 µM M*O*N-DNJ for 24 or 48 hours and FOS were isolated and measured by HPLC. Traces from a single representative sample preparation of FOS generated in response to M*O*N-DNJ treatment in donor GB demonstrates the accumulation of greater quantities of FOS with longer treatment (compare **B** day 1, red line, with **C** day 2, green line). Total quantity of a given oligosaccharide can be calculated by comparing the area under the curve for a sample with a standard of known quantity (data not shown). The only FOS generated in the absence of iminosugar treatment (**A**, blue line) are $Man_5GlcNAc_1$ (29.25 minutes) and $Glc_1Man_5GlcNAc_1$ which is likely the result of normal glycoprotein quality control processing within the ER. Traces are overlaid in **D** to facilitate comparison.

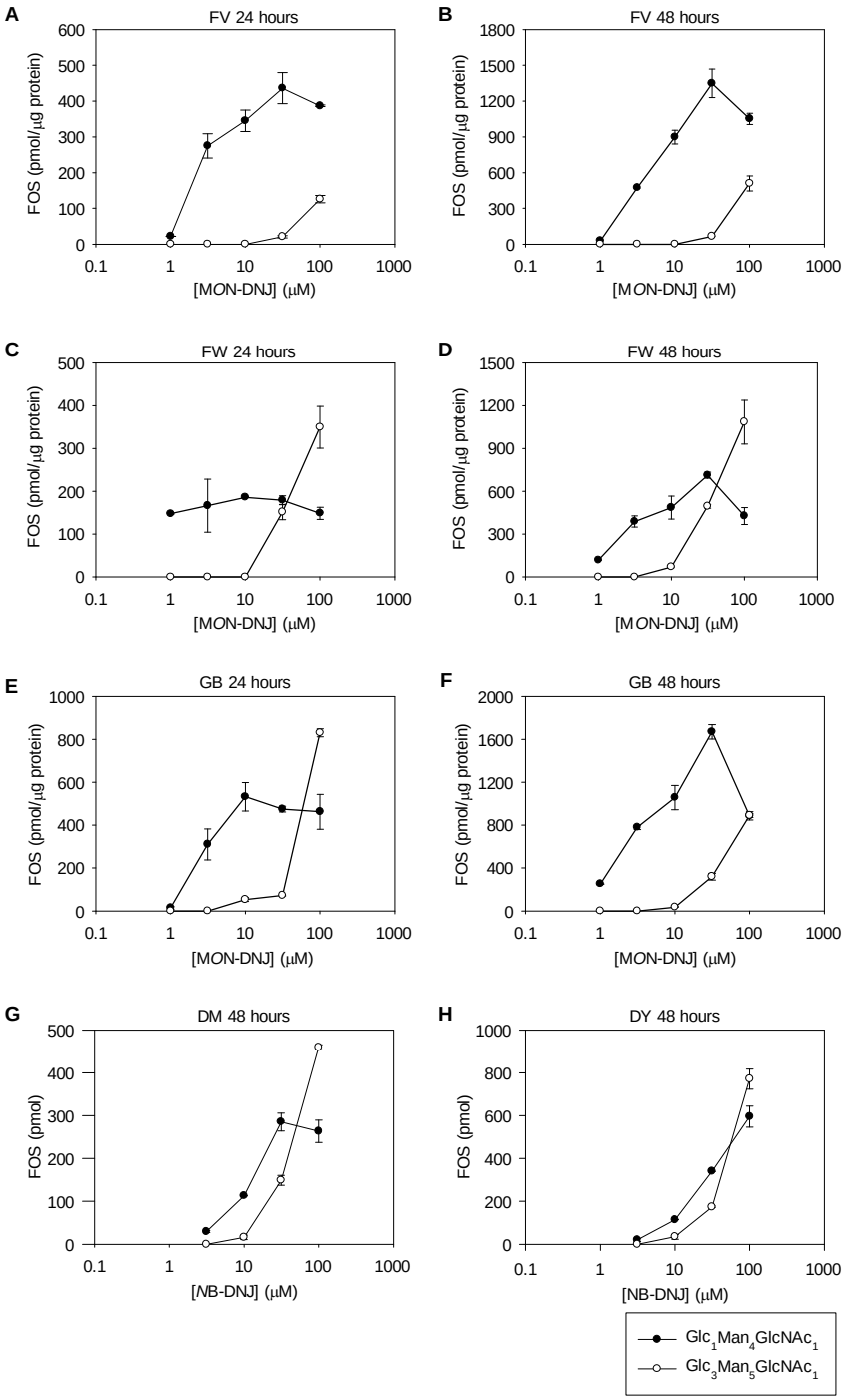

FIGURE 3.7. Initiation of α-glucosidase I inhibition correlates with antiviral activity of iminosugars. Three donors, FV (**A**, **B**), FW (**C**, **D**), and GB (**E**, **F**) were treated in duplicate with a serial dilution of M*O*N-DNJ and another two donors, DM (**G**) and DY (**H**), were treated in duplicate with a serial dilution of *N*B-DNJ. Inhibition of α-glucosidase II and α-glucosidase I activity can be correlated with generation of intracellular $Glc_1Man_4GlcNAc_1$ (black) and $Glc_3Man_5GlcNAc_1$ (white), respectively. Measurements were collected at 24 (**A**, **C**, **E**) and 48 hours (**B**, **D**, **F**, **G**, **H**) post treatment. Donors DM and DY were assayed by Dr JL Miller. Quantitation of FOS by HPLC was conducted in all instances by Dr. D Alonzi.

$Glc_1Man_4GlcNAc_1$, a correlate of α-glucosidase II inhibition, increased markedly in all cases until maximum production was reached at a concentration between 10 and 31.6 μM after which point a slight decrease was observed. Onset of $Glc_3Man_5GlcNAc_1$ accumulation also occurred consistently in samples treated with M*O*N-DNJ at concentrations between 10 and 31.6 μM. Given the sequential nature of glucose trimming in which α-glucosidase II trimming follows α-glucosidase I activity, it is likely that the decrease in $Glc_1Man_4GlcNAc_1$ accumulation at higher drug concentrations is a consequence of limitation of available substrate following effective α-glucosidase I inhibition. With an increase in incubation time in the presence of M*O*N-DNJ from one to two days, a two- to three-fold increase in the absolute levels of both $Glc_1Man_4GlcNAc_1$ and $Glc_3Man_5GlcNAc_1$ is observed. Of note, the concentration at which $Glc_1Man_4GlcNAc_1$ accumulation plateaus and $Glc_3Man_5GlcNAc_1$ accumulation begins correlates well with the concentration at which strong antiviral effects for M*O*N-DNJ are observed in the same cell type (*i.e.* antiviral IC_{90} equal to 7.74 ± 3.63 μM). Given the more pronounced production of FOS following two days of treatment, we verified the trend of overlap of maximal $Glc_1Man_4GlcNAc_1$ production and onset of $Glc_3Man_5GlcNAc_1$ with antiviral efficacy at this time point using *N*B-DNJ as shown in *Figure 3.7* (*G* and *H*). Although one donor, DY, did not demonstrate plateauing of $Glc_1Man_4GlcNAc_1$ at the highest concentration of drug tested, a plateau was observed for donor DM. Similar to the results for M*O*N-DNJ, $Glc_3Man_5GlcNAc_1$ FOS accumulated at or above concentrations of 10 μM NB-DNJ, and this point lies between the antiviral IC_{50} and IC_{90} of *N*B-DNJ.

As for GM3 levels, FOS production by DGJ iminosugars was assayed at the maximal concentrations tested for DENV antiviral activity. In contrast to the capacity for glycolipid inhibition, both *N*B-DGJ and *N*N-DGJ failed to produce appreciable ER-related FOS in three donors (*Figure 3.8*). The major peaks observed in the case of *N*N-DGJ treatment at elution times of 23.3 minutes and 32.6 minutes (*Figure 3.8E*) represent FOS generated by inhibition of lysosomal β-N-acetylhexosaminidases,

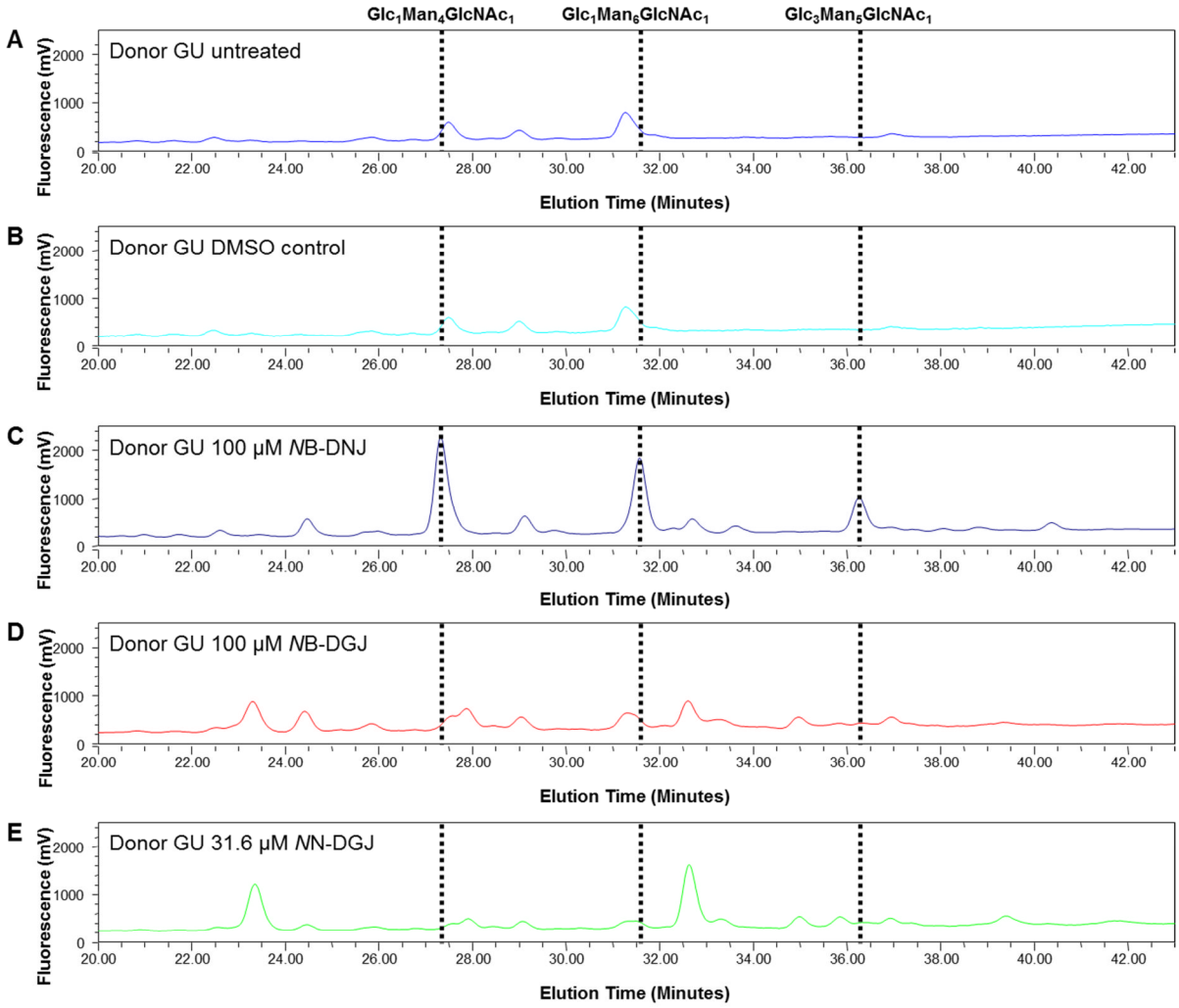

FIGURE 3.8 Iminosugars possessing galactostereochemistry fail to produce ER generated FOS. MDMΦs were isolated and differentiated as per standard protocol then left untreated for 48 hours (**A**) or treated with 0.06% (v/v) DMSO control equivalent to DMSO concentration in *N*N-DNJ and *N*N-DGJ treated cells (**B**), 100 µM *N*B-DNJ (**C**) as for other donors, 100 µM *N*B-DGJ (**D**), or 31.6 µM *N*N-DGJ (**E**). Samples were prepared in technical duplicate from each of three individual donors and generation of FOS was measured by HPLC by Dr. D Alonzi. Peaks characteristic of ER α-glucosidase inhibition are present for *N*B-DNJ treatment (elution time of approximately 27.3 minutes, 31.6 minutes, and 36.3 minutes). In contrast, FOS generated by both *N*B-DGJ (**D**) and *N*N-DGJ (**E**) treatment for $Glc_1Man_XGlcNAc_1$ species and $Glc_3Man_5GlcNAc_1$ species is at or below negative control (**A**, **B**) treatment levels. One representative trace from the same donor (GU) is presented for each drug treatment.

enzymes responsible for trimming terminal glycans from molecules possessing terminal N-acetyl hexosamines (*e.g.* GlcNAc). Such enzymes are frequently implicated in disorders of glycolipid processing such as the lysosomal storage disorders (*e.g.* Tay-Sachs and Sandhoff diseases), thus generation of these species is not suggestive of modulation of glycoprotein processing and further

supports specific inhibition of glycolipid processing by DGJ-derived iminosugars. Therefore, glycolipid inhibition profiles fail to differentiate antiviral from non-antiviral iminosugars. Rather, production of FOS as a marker of glycoprotein processing inhibition correlates well with measures of antiviral activity against DENV.

III.4. Discussion

Previous investigations of iminosugars as dengue antivirals [201,203,206-210,247] suggested promise for development of the class as clinical therapeutics. In the case of *N*B-DNJ, the clinical safety profile as an approved therapy for Gaucher and NPC diseases is advantageous; however, previous failures of *N*B-DNJ in anti-retroviral clinical trials suggested that a more potent inhibitor might be necessary for successful antiviral drug development. Whereas iminosugars had previously been considered as DENV therapeutics, *N*B-DNJ had been overlooked in previous studies *in vitro* and *in vivo*, and iminosugars had never been tested in primary human cells. As such, a panel of DNJ-derived iminosugars including *N*B-DNJ was tested for inhibition of infectious DENV production in primary human MDMΦs. With increasing alkyl-chain length, enhancement of anti-DENV activity was observed. Further modification of the alkyl-chain resulted in drastic enhancement of antiviral efficacy (*i.e. N*AP-DNJ); however, considerable increase in toxicity was concomitantly observed thereby reducing selectivity and precluding further consideration of *N*AP-DNJ as a clinical candidate. Similarly, a poor selectivity index for *N*N-DNJ removed this drug from further consideration as a clinical candidate, and as a result *N*B-DNJ and M*O*N-DNJ were investigated in greater detail.

Given that *N*B-DNJ is used clinically as an inhibitor of GCS in Gaucher and NPC disease therapy in addition to the multi-faceted role of glucose in metabolism, the ability of iminosugars to inhibit

various glucosidases and glycosidases was assayed. For DNJ derivatives, relatively minor fluctuations were noted in inhibition of α-glucosidases in comparison to the parent DNJ; however, the stereoisomer DGJ was a relatively poor inhibitor of α-glucosidase enzymes. The notable exception to this trend was observed for porcine kidney α,α-trehalase. No evidence to date links trehalase activity to DENV fitness; however, this result merits future investigation. As anticipated, the resemblance of longer alkyl-chain iminosugars to glucosylceramide was indicated by more potent inhibition of HL60 glucosyltransferase by M*O*N-DNJ than *N*B-DNJ. Inhibition of other glycosidases by M*O*N-DNJ was either weak or undetectable at the concentrations tested. Thus, although these experiments were not exhaustive (*i.e.* additional untested enzymes may also be inhibited by iminosugars and be responsible for the observed results), the data suggest that iminosugar anti-DENV therapeutic activity is likely the product of either α-glucosidase inhibition or GCS inhibition.

In order to differentiate the two possible mechanisms of iminosugar anti-DENV activity, *N*-butyl and *N*-nonyl derivatives of both DNJ and DGJ were assayed for glycolipid, glycoprotein, and infectious virus production modulatory activity. Whereas all four compounds inhibit GCS activity at similar concentrations, previous work suggests that DGJ-derived iminosugars require much higher concentrations of drug to inhibit α-glucosidases than their DNJ-derived counterparts. [248] At the highest concentrations tested for antiviral activity of DGJ derivatives, FOS generated as markers of α-glucosidase inhibition were undetectable. In contrast, generation of lysosomal FOS associated with inhibition of glycolipid processing was observed in addition to reduction of the specific glycolipid GM3 at these concentrations of both *N*B-DGJ and *N*N-DGJ. These results suggest that DGJs are specific inhibitors of glycolipid processing and not glycoprotein processing. Thus, *N*B-DGJ and *N*N-DGJ can be used as controls where GCS inhibition is present but α-glucosidase inhibition is not. In the MDMΦ system, neither *N*B-DGJ nor *N*N-DGJ exhibited any antiviral activity at concentrations where their DNJ-derived counterparts reliably suppressed infectious virus production by greater

than 90%. This suggests that the reduction of infectious DENV by DNJ-derived iminosugars is a function of α-glucosidase inhibition and not GCS inhibition.

Additionally, the dose-response relationship of M*O*N-DNJ and *N*B-DNJ to GM3, $Glc_1Man_4GlcNAc_1$, and $Glc_3Man_5GlcNAc_1$ was examined. In the case of GM3 inhibition, reduction of the glycolipid occurred at concentrations marginally lower (approximately ½ log_{10}) than the concentrations required for antiviral activity. In contrast, across multiple donors, and at multiple time points for M*O*N-DNJ, the concentration at which pronounced antiviral effects (IC_{50} to IC_{90}) were noted coincided with maximal accumulation of $Glc_1Man_4GlcNAc_1$ and onset of accumulation of $Glc_3Man_5GlcNAc_1$. The linkage of maximal $Glc_1Man_4GlcNAc_1$ FOS with onset of $Glc_3Man_5GlcNAc_1$ is likely a function of the sequential nature of glucose trimming from the nascent *N*-linked glycan precursor. That $Glc_1Man_4GlcNAc_1$ accumulates at lower iminosugar doses than are required for $Glc_3Man_5GlcNAc_1$ indicates that the inhibition of α-glucosidase II in MDMΦs by DNJ iminosugars is of greater relative potency than the inhibition of α-glucosidase I. Disentangling which of these inhibitory mechanisms is involved with antiviral activity is difficult. It is possible that antiviral effects are potentiated by inhibition of α-glucosidase II, but require relatively high levels of this inhibition to realise reduction of infectious virus; however, it is equally possible that such effects are a consequence of any inhibition of α-glucosidase I. Alternatively, the inhibition of glycoprotein processing may facilitate a glycolipid processing-dependent antiviral activity such that both activities must occur in synergy in order to elicit an antiviral response. In each of these scenarios, it is of importance to consider that measurements of FOS are not stringent measures of protein misfolding or even inhibition of the glucosidases within the cell. Rather, generation of FOS is likely to be the result of accumulation of considerable levels of misfolded glycoproteins possessing such glycans. Furthermore, the specific protein source of these glycans cannot be determined with existing methods, and as such impacts to viral glycoproteins and/or specific host glycoproteins of interest

can only be hypothesised. Additional work by colleagues in the Zitzmann lab with a DNJ conjugated to an α-tocopherol tail (ToP-DNJ) has demonstrated anti-DENV activity for this iminosugar at a point where moderate $Glc_1Man_4GlcNAc_1$ FOS accumulate in the absence of $Glc_3Man_5GlcNAc_1$ suggesting that α-glucosidase II inhibition is responsible for the antiviral effects noted; however, additional mechanisms of action cannot be eliminated for ToP-DNJ thereby confounding application of this result to *N*B-DNJ and M*O*N-DNJ. (Personal communication: JL Kiappes, Dr JL Miller, and Dr D Alonzi) In influenza virus systems, α-glucosidase II inhibition alone has been shown to be antiviral [184-186] lending further credibility to the hypothesis that α-glucosidase II inhibition is responsible for anti-DENV activity of iminosugars. In spite of remaining questions, the correlation of presumed misfolding by iminosugar treatment with the ability to inhibit production of infectious virus supports the hypothesis that iminosugar anti-DENV mechanisms of action are a function of disruption of the CANX/CALR cycle via inhibition of ER α-glucosidases.

IV

M*ON*-DNJ modulation of host-responses to diverse pathogens: A transcriptomic approach

IV.1. Abstract

M*O*N-DNJ is a promising candidate for therapeutic treatment of dengue virus infection based on potent reduction of infectious virus and minimal cytotoxicity. Reduction of infectious virus is a function of inhibition of host-based glycoprotein processing, and it is possible that modulation of host proteins by this same mechanism may impact therapeutic effects either detrimentally or synergistically. Therapeutic efficacy of iminosugars such as M*O*N-DNJ may be altered further as a consequence of modulation of other host pathways such as glycolipid processing. Thus, a time course transcriptomics study was undertaken in primary human monocyte-derived macrophages to detect networks of alternatively regulated genes in response to M*O*N-DNJ. I initially characterised the transcriptomic response of MDMΦs to M*O*N-DNJ treatment in the absence of a pathogenic stimulus. Next, I used a transcriptomic approach to generate network-based information regarding the time-dependent macrophage response to dengue infection. The relatively small set of genes responding to DENV infection at the early time point of 6 hours post infection allowed identification of elements of the innate immune response which respond to DENV infection prior to completion of a round of viral replication. Included amongst this set of DENV-response elements are type I and type II interferons as well as transcription factors of the unfolded protein response which may help mediate oxidative stress. A stronger inflammatory response to DENV infection was noted following a round of viral replication at 24 hours post infection. By conducting identical time-course experiments with DENV infected macrophages in the presence of M*O*N-DNJ, I identified transcripts that respond to iminosugar treatment at both time points. Along with induction of the unfolded protein response at both times, a reduction of inflammation mediated in particular by TNF-α and IFN-γ was observed as a result of M*O*N-DNJ treatment at 24 hours p.i. Notably, type I interferon signalling was enhanced in the presence of M*O*N-DNJ suggesting enhancement of some elements of the innate immune response responsible for clearing virus. I next investigated the response of this macrophage model to treatment with LPS to establish a baseline model for bacterial sepsis. With an established sepsis

model in place, the M*O*N-DNJ mediated alteration of the macrophage response to a non-replicating and highly divergent pathogen from DENV virus could be investigated. In particular, LPS-induced signalling by TNF-α was reduced at both time points with M*O*N-DNJ treatment. Induction of the unfolded protein response as a result of iminosugar treatment was also maintained in the context of LPS suggesting that both of these activities occur as a consequence of M*O*N-DNJ treatment in diverse pathogenic contexts and are likely independent of virus replication. Western blotting was conducted to validate TNF receptor and ligand superfamily member response as a class to M*O*N-DNJ treatment. Additionally, the increased signalling of the oxidative stress controlling transcription factor NFE2L2 by administration of M*O*N-DNJ was verified at 24 hours p.i. In summary, these results suggest that M*O*N-DNJ modulates the inflammatory response to diverse pathogenic stimuli in macrophages. This modulation occurs at both a transcription factor signalling level (NFE2L2) and at a protein production level for TNF family proteins. M*O*N-DNJ may therefore be broadly effective at reduction of excess inflammation in diverse pathologies and additional therapeutic applications should be considered.

IV.2. Introduction

The effects of iminosugar treatment on the production and folding of a few individual proteins has been studied as discussed in *Chapter I*; however, a network level approach to understanding the implications of iminosugar treatment on broad host functions has not been conducted. Knowledge of host-pathway modulation by iminosugar treatment may facilitate investigation of the drugs as therapeutics for additional diseases, and an understanding of the interaction of iminosugars with specific pathogens, such as DENV, can provide a more comprehensive knowledge-base for the initiation of clinical trials. As discussed in *Chapter III*, M*O*N-DNJ shows the greatest clinical promise of the iminosugars previously tested as a DENV therapeutic and was therefore selected for these investigations. In order to fully understand how inhibition of α-glucosidase enzyme activity (in

concert with the other activities discussed in *Chapter III*) contributes to an antiviral effect, a genome-wide profile of response is desirable – especially given that the intended target of iminosugar treatment is a host process. Many reports have been presented suggesting that viruses are particularly sensitive to this mode of therapy, but molecular events responsible for sensitivity to inhibition of α-glucosidase enzyme activity remain elusive. How is it possible that viral glycoproteins are so strictly dependent upon α-glucosidase processing but host proteins are not? Or are host proteins equally sensitive to iminosugar treatment, but implications of these perturbations have not been realised because of failure to identify the particularly sensitive host molecules? As discussed in *Chapter I*, limited evidence suggests that iminosugars can elicit changes to the innate immune response, [222,223] but a more thorough characterisation of these effects has not been conducted. As shown in *Figure 4.1*, this study presents a time-course analysis of the transcriptomic responses of MDMΦs to address these questions. First, I examine the impact of M*O*N-DNJ treatment on uninfected macrophage function. Next, the dynamic response of MDMΦs to DENV infection is detailed, and this developing response to DENV is then used as a background to understand how M*O*N-DNJ treatment of DENV infection alters the host cell response. Finally, in order to differentiate the effects of reducing virus from direct impacts to host inflammatory processes, I establish the transcriptomic response of this MDMΦ model to LPS stimulation and then use this response as a background for understanding how M*O*N-DNJ treatment influences the host's response to a potent bacterial stimulus. Whereas M*O*N-DNJ treatment leads to reduction of infectious DENV production, LPS is not a replicating pathogen and the lipid A moiety elicits immune responses via pathways with limited overlap to viral infections. Thus, by understanding the impact of M*O*N-DNJ treatment on uninfected, DENV infected, and LPS treated MDMΦs, a comprehensive picture of the utility of this iminosugar in treatment of diverse cellular contexts is gained.

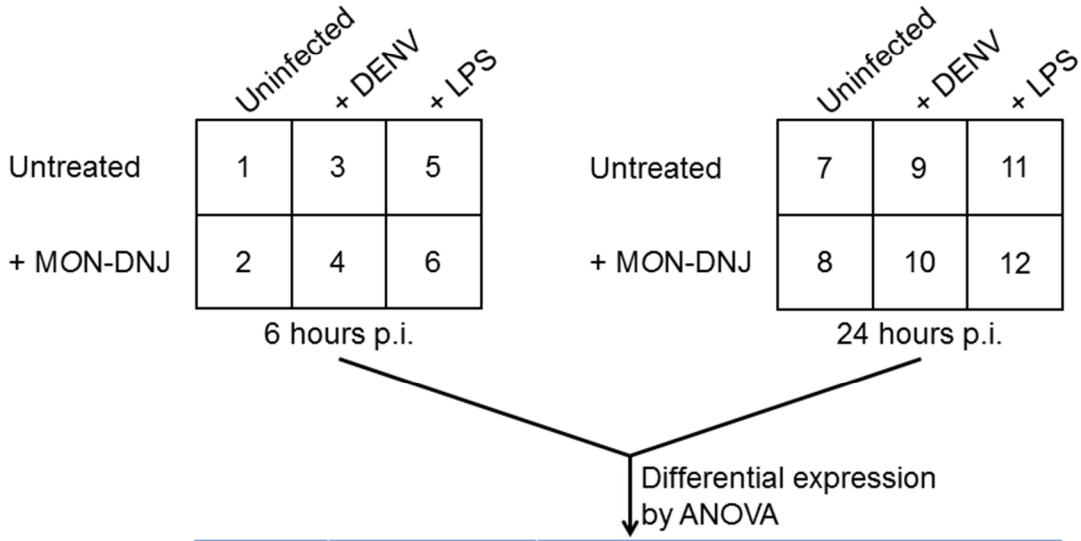

Controls	Experimentals	Result
1,7	2,8	MON-DNJ modulated transcripts
1,7	3,9	DENV modulated transcripts
3,9	4,10	MON-DNJ modulated transcripts in DENV
1,7	5,11	LPS modulated transcripts
5,11	6,12	MON-DNJ modulated transcripts in sepsis

FIGURE 4.1. Experimental design to identify transcriptomic responses of MDMΦs to M*O*N-DNJ treatment in diverse infection environments. PBMCs from four donors were isolated and differentiated to MDMΦs as previously described. Cells were treated according to the plate layout above with media replacement, DENV 2 16681 (m.o.i. of 1) infection, or LPS (*S. enterica* 200 ng/ml) treatment at t=0. After 90 minutes, virus was removed as appropriate and media containing M*O*N-DNJ or media only (Untreated) was added to each well such that final drug concentration was 25 µM and final LPS concentration was 100 ng/ml. RNA was collected at 6 hours and 24 hours from the initiation of infection and submitted for transcriptomic analysis. ANOVA was used as a statistical means for identifying significantly altered transcripts across multiple experimental conditions.

Whereas transcriptomic responses of MDMΦs to LPS have been investigated previously, there is not a clear foundation of understanding of the macrophage response to DENV. The transcriptomic response to DENV infection in cases of human infection has been characterised by several groups in PBMC samples; [50,251-257] however, variability of infecting DENV serotype, diversity of host genetic backgrounds, heterogeneity of cell types within a PBMC isolation, and variability of

responses due to differences in time of sample isolation complicates interpretation of these data. The heterogeneity of responses observed in these studies is likely a reflection of the diversity of responses leading to the spectrum of clinical disease as much as it is due to technical variation. In order to simplify such investigations, transcriptomic analyses of cell lines infected *in vitro* have also been undertaken, [258,259] but the relevance of host responses of immortalised cell lines to development of clinical disease is difficult to resolve. Primary human vascular endothelial cells (HUVECs) have been investigated [133,260] in two instances providing valuable insight into the responses of these cells to DENV infection. To date, the response of the innate immune cells commonly implicated in DENV infection has only been conducted in the context of vaccine strains [261] or in vastly underpowered trials [available in NCBI GEO DataSets GSE16463 and GSE9378]. Thus, this study sought to characterise the response of primary human MDMΦs to *ex vivo* DENV infection in a time-dependent fashion prior to investigation of the interaction of M*O*N-DNJ with the DENV-induced response.

As such, the aims of this chapter are to:

1) Identify transcripts modulated in MDMΦs in response to MON-DNJ treatment in uninfected samples,
2) Determine network regulators responsible for M*O*N-DNJ mediated transcriptomic responses in uninfected samples,
3) Identify transcripts modulated in MDMΦs in response to DENV,
4) Determine the network regulators responsible for transcriptomic response to DENV and consider their significance in the context of DENV pathogenesis,
5) Identify transcripts modulated in MDMΦs in response to M*O*N-DNJ treatment in DENV infected samples and compare to uninfected samples,

6) Determine network regulators responsible for M*O*N-DNJ mediated transcriptomic responses in DENV infected samples,
7) Identify transcripts modulated in MDMΦs in response to M*O*N-DNJ treatment in LPS treated samples and compare to DENV infected and uninfected samples,
8) Determine network regulators responsible for M*O*N-DNJ mediated transcriptomic responses in LPS treated samples.

IV.3. Results

IV.3.A. Transcriptomic response of uninfected MDMΦs to M*O*N-DNJ

M*O*N-DNJ inhibits both glycoprotein and glycolipid processing, and inhibition of glycoprotein processing appears to be the principal factor in inhibition of infectious DENV production. To determine which host transcripts were regulated in the absence of infection, MDMΦs were prepared as described in *Figure 4.1* and treated with M*O*N-DNJ for 6 or 24 hours. By two-way ANOVA, 2137 transcript probes were differentially regulated by M*O*N-DNJ administration of which 1729 could be mapped to unique genes. The ten genes exhibiting the greatest differential expression (both upregulation and downregulation) at 6 hours p.i. are listed in *Table 4.1* with fold change at 24 hours p.i. also given. Of note, the genes with the greatest upregulation are almost exclusively associated with ER-stress and the unfolded protein response (UPR). For example, HSPA5 is more commonly referred to as BiP and is an important member of the ER chaperone family which also includes calnexin and calreticulin. There are three major arms of the UPR – ERN1, EIF2AK3, and ATF6 mediated cascades, [262] and all three cascades are represented by induction of downstream genes in the list of differentially expressed transcripts. Intriguingly, many of the genes strongly upregulated at 6 hours have almost returned to baseline levels by 24 hours (for example DNAJB9, an important element of control of ER-associated degradation and protection of cells from apoptosis) suggesting a

gradual return to a normal ER environment. Because of the conservation of UPR induction following iminosugar treatment, genes in each table that are associated with the UPR are labelled with an asterisk (*). The set of the most strongly downregulated genes does not possess such a strong unifying theme as the upregulated set although the presence of HMGB1, a TLR4 inflammatory cascade inducing cytokine, and PPIG, also known as caspase 10, suggests a level of immunomodulation.

TABLE 4.1. Differentially regulated genes following M*O*N-DNJ treatment (1 vs. 2 and 7 vs.8)

Gene Symbol	Gene Name	Fold Change[a] 6 hrs	Fold Change 24 hrs
CRELD2*	Cysteine-rich with EGF-like domains 2	1.762	1.962
GNL3*	Guanine nucleotide binding protein-like 3 (nucleolar)	1.576	0.306
DNAJB9*	DnaJ (Hsp40) homolog, subfamily B, member 9	1.572	0.647
SDF2L1	Stromal cell-derived factor 2-like 1	1.549	1.899
HERPUD1*	Homocysteine-inducible, endoplasmic reticulum stress-inducible, ubiquitin-like domain member 1	1.381	0.617
ERO1LB*	ERO1-like beta (S. cerevisiae)	1.343	0.382
GMPPB*	GDP-mannose pyrophosphorylase B	1.218	0.712
HSPA5*	Heat shock 70kDa protein 5 (glucose-regulated protein, 78kDa)	1.214	1.324
HYOU1*	Hypoxia up-regulated 1	1.206	1.232
SLC7A5*	Solute carrier family 7 (amino acid transporter light chain, L system), member 5	1.193	0.030
LYPLA1	Lysophospholipase I	-1.450	-0.129
PPP1R15B*	Protein phosphatase 1, regulatory subunit 15B	-1.495	-0.431
RPLP1	Ribosomal protein, large, P1	-1.514	-0.335
SUMO1*	Small ubiquitin-like modifier 1	-1.518	-0.492
HMGB1*	High mobility group box 1	-1.521	-0.562
PTMA	Prothymosin, alpha	-1.538	-0.312
CAPZA1	Capping protein (actin filament) muscle z-line, alpha 1	-1.557	-0.504
PPIG*	Peptidylprolyl isomerase G (cyclophilin G)	-1.568	-0.507
GCLC*	Glutamate-cysteine ligase, catalytic subunit	-1.581	-0.356
CTNNB1	Catenin (cadherin-associated protein), beta 1, 88kDa	-1.662	-0.227

[a]Fold change is the $\log_2$ ratio of treated to untreated samples and therefore indicates the level of induction or reduction of a transcript. A value of 1.000 indicates the transcript is 2-fold more abundant whereas a value of -1.000 indicates a transcript is 2-fold less abundant. Unchanged transcripts have a fold change equal to 0.000.

*Indicates gene ontology association with “unfolded protein response” and/or “endoplasmic reticulum unfolded protein response”

In order to identify the upstream regulators responsible for these gene-level observations, Ingenuity® Pathway Analysis (IPA) was employed. The ERN1 branch of the UPR is principally executed by XBP1 and HAC1, the EIF2AK3 branch of UPR signals principally via NFE2L2, and the ATF6 branch signals principally through ATF6 activity in the Golgi apparatus. As indicated in *Table 4.2*, there is strong evidence for induction of all three arms of the UPR using network analysis at both 6 and 24 hours p.i. It is not surprising that these signalling cascades predominate following iminosugar treatment as administration of these drugs inhibits α-glucosidase mediated glycoprotein trimming leading to an accumulation of unfolded proteins within the ER. As M*O*N-DNJ is a glucose mimic, it is equally logical that signalling by D-glucose is inhibited upon addition of drug. Interestingly, signalling via NF-κB is also inhibited early in the presence of M*O*N-DNJ (z-score = -2.526 at 6 hours p.i.) with prolonged inhibition of signalling by TNF superfamily members such as CD40/CD40LG (z-score = -2.398 at 6 hours p.i. and -2.368 at 24 hours p.i.). The induction of the UPR with concerted attenuation of NF-κB signalling is represented by an upstream regulatory network diagram in *Figure 4.2*. It is possible that a combined antioxidative stress response, principally controlled by NFE2L2, mediates the early suppression of NF-κB and continued immunomodulation is controlled by direct effects of M*O*N-DNJ on TNF family ligands and receptors due to inhibition of folding.

TABLE 4.2. Network analysis reveals UPR regulators as the primary contributors to the M*O*N-DNJ transcriptomic response signature (1 vs. 2 and 7 vs. 8)

Upstream Regulator	*p*-value[a] 6 hours	Evidence[b] 6 hours	*p*-value 24 hours	Evidence 24 hours
XBP1	1.89×10^{-36}	64/64	8.07×10^{-25}	35/39
ATF4	9.47×10^{-6}	16/18	1.98×10^{-3}	9/9
ERN1	4.76×10^{-4}	9/10	8.55×10^{-5}	7/8
NFE2L2	2.24×10^{-3}	23/31	4.89×10^{-7}	22/27
ATF6	2.48×10^{-6}	9/10	4.29×10^{-9}	10/10

[a] *p*-value is the IPA reported value of significance for enrichment of genes under control of the network modulator that change in the anticipated direction if that modulator is responsible for the observed changes.

[b] Evidence is the number of genes that change in support of control by a given network regulator divided by the total number of differentially expressed genes under control of the same regulator. Evidence yields a z-score, a directional measure of confidence of modulation of the upstream regulator.

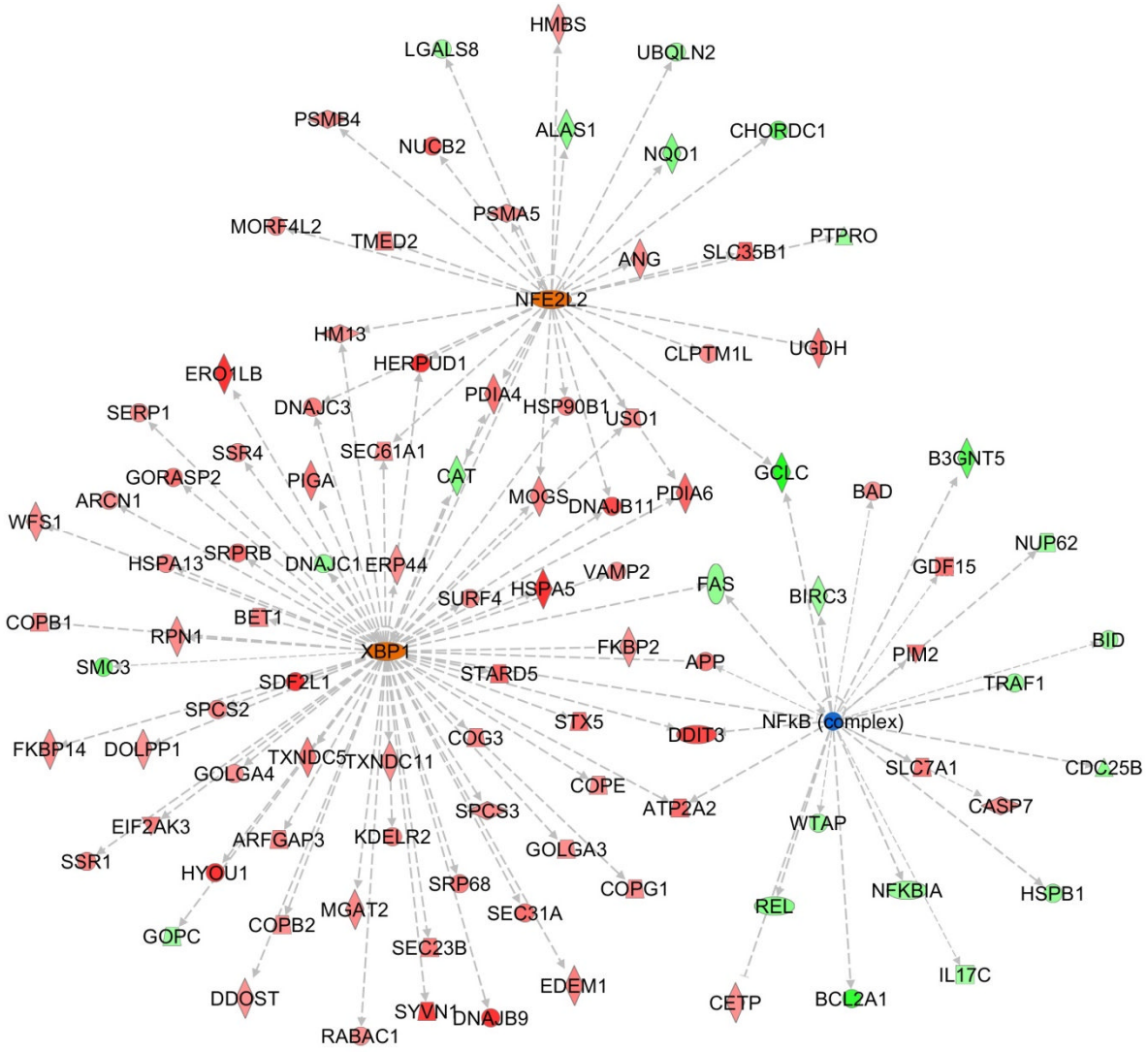

FIGURE 4.2. M*O*N-DNJ treatment of MDMΦs induces the unfolded protein response and downregulates expression of NF-κB controlled transcripts. Changes in transcript levels as a result of treatment with M*O*N-DNJ were used to assemble networks to determine upstream regulators of observed effects using IPA. Upregulated transcripts (red) are strongly associated with induction (orange) of the UPR as indicated by network control by NFE2L2 and XBP1. Downregulated transcripts (green) are generally associated with induction of inflammation and therefore indicate inhibition (blue) of NF-κB signalling.

IV.3.B. The response of MDMΦs to DENV infection

In order to understand how M*O*N-DNJ treatment might impact the transcriptomic response of MDMΦs to DENV infection, it was first necessary to establish the MDMΦ transcriptomic response to DENV. An early time point of 6 hours p.i. was chosen to understand the transcriptomic changes that

occur in response to DENV infection prior to completion of a single viral replication cycle. These results were compared to those obtained at 24 hours p.i. to understand how the immune response develops during the course of infection. Myeloid cells such as circulating monocytes and tissue-resident macrophages and dendritic cells are thought to be important during all times of DENV infection, but particularly during early rounds as demonstrated in both humans [263-267] and mice. [268] Macrophages are one of the cell types that sit at the intersection of the innate and adaptive immune responses, and they play an important role in both productive DENV infection and the host's response to invasion. Thus, an understanding of how these cells respond to viral infection may provide crucial insights into understanding the disease processes associated with DENV.

Surprisingly few transcripts demonstrated differential regulation in response to DENV infection by ANOVA testing at 6 hours post infection. Of 914 probes detected as differentially expressed, 771 could be mapped to unique genes. The ten genes most potently induced by DENV infection at this early time included MERTK, a tyrosine kinase involved in signalling of engulfment and modulation of the innate immune response, and IFIT1, an interferon-induced antiviral protein that specifically targets and inhibits expression of viral RNAs. Thus, virus-specific immune responses are activated. At the same time, downregulation of FAS, a TNF receptor superfamily member that signals apoptosis, and the C-type lectin CLEC2D, a natural killer cell receptor, indicates repression of apoptotic signals which could prove advantageous to viral replication. The ten most strongly upregulated and downregulated genes following DENV infection at 6 hours p.i. (*Table 4.3*) also indicate the cellular stress commensurate with viral replication. This is demonstrated by the induction of CRELD2, an ER stress signal [269], and the RNA polymerase RPAP1. Upstream analysis using IPA further indicates activation of the UPR as exhibited by increased signalling by XBP1 and NFE2L2 and reveals that both type I and type II interferons respond to DENV infection (*Figure 4.3*). The development of an IFN-γ mediated response by macrophages is perhaps controversial, but mounting evidence suggests that

TABLE 4.3. Early response genes of MDMΦs to DENV infection (1 vs. 3)

Gene Symbol	Gene Name	Fold Change
MERTK	c-mer proto-oncogene tyrosine kinase	0.830
IFIT1	Interferon-induced protein with tetratricopeptide repeats 1	0.757
TJP2	Tight junction protein 2	0.689
OLR1*	Oxidized low density lipoprotein (lectin-like) receptor 1	0.674
RPAP1	RNA polymerase II associated protein 1	0.606
CRELD2*	Cysteine-rich with EGF-like domains 2	0.563
FAM57A	Family with sequence similarity 57, member A	0.557
CCNB2	Cyclin b2	0.549
NEK6	NIMA-related kinase 6	0.545
PSMD3*	Proteasone (prosome, macropain) 26S subunit, non-ATPase, 3	0.538
CPED1	Cadherin-like and PC-esterase domain containing 1	-0.482
ZNF254	Zinc finger protein 254	-0.495
CLEC18C	C-type lectin domain family member 18, member c	-0.521
NADK2	NAD kinase 2, mitochondrial	-0.611
RELL1	RELT-like 1	-0.621
COLQ	Collagen-like tail subunit (single strand of homotrimer) of asymmetric acetylcholinesterase	-0.646
FAS	Fas cell surface death receptor	-0.672
CLEC2D	C-type lectin domain family member 2, member D	-0.704
ZFP30	ZFP30 zinc finger protein	-0.719
C4ORF32	Chromosome 4 open reading frame 32	-0.888

*Indicates gene ontology association with “unfolded protein response” and/or “endoplasmic reticulum unfolded protein response”

macrophages are capable of producing IFN-γ [270] and the importance of this molecule in the case of DENV pathogenesis has been highly debated. My results suggest that macrophages as well as lymphoid cells may be contributing to production of IFN-γ in DENV infection.

In contrast to the limited set of genes which meet inclusion criteria for significant differential expression as a result of DENV infection at 6 hours p.i., 6517 transcript probes which map to 5896 unique genes meet the cut-off for significant differential regulation in response to DENV infection at 24 hours post infection. As demonstrated in *Table 4.4*, ER stress related proteins (*e.g.* CRELD2) continue to be strongly induced as do the immune response genes MERTK and IFIT1. Proliferation of inflammation is noted through the induction of specific macrophage produced chemokines such as CCL2 (also known as monocyte chemotactic protein 1, MCP1) and CCL7 (previously known as

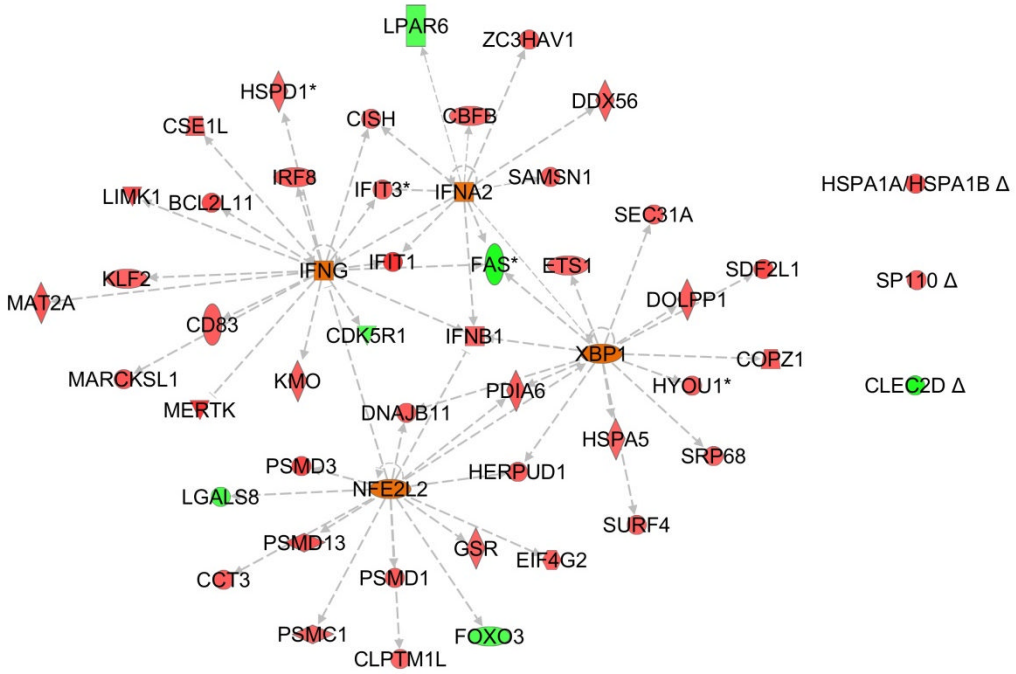

FIGURE 4.3. DENV infection of MDMΦs induces the unfolded protein response and type I and II interferons at 6 hours post infection. Changes in transcript levels as a result of infection with DENV were used to assemble networks to determine upstream regulators of observed effects using IPA. Upregulated transcripts (red) are strongly associated with induction (orange) of the UPR as indicated by network control by NFE2L2 and XBP1. Downregulated transcripts (green). IFN-γ (IFNG) controls transcription of a greater number of induced immune response genes than type I interferon (IFNA2), but both interferon systems are upregulated.

monocyte-specific chemokine 3). Downregulated transcripts are dominated by solute transporters (SLC29A8 and CLIC4) and proteasome associated genes (SUMO1 and PSMC6). Prediction of network regulators at 24 hours highlights the proliferation of inflammation with many inflammatory cytokines predicted to exert control over the transcriptomic response. In addition to the type I and II interferons, several C-C motif cytokines (*e.g.* CCL3 (MIP-1α) and CCL5 (RANTES)) and TNF superfamily members (*e.g.* TNF-α and CD40LG) exert considerable network control. Classical anti-inflammatory pathways controlled by IL-10 and SOCS1 (suppressor of cytokine signalling 1) are inhibited, and oxidative stress is indicated by the induction of hydrogen peroxide. UPR pathways controlled by NFE2L2 and XBP1 are induced indicating that regulatory networks are attempting to control the inflammatory effects of viral infection and replication. A summary of the selected elements of the

proliferating inflammatory response is presented in *Table 4.5* and displayed as a network view in *Figure 4.4*.

TABLE 4.4. Strongest responding genes of MDMΦs to DENV infection at 24 hours p.i. (7 vs. 9)

Gene Symbol	Gene Name	Fold Change
MERTK	c-mer proto-oncogene tyrosine kinase	0.830
IFIT1	Interferon-induced protein with tetratricopeptide repeats 1	0.757
TJP2	Tight junction protein 2	0.689
APP*	Amyloid beta (A4) precursor protein	0.685
OLR1*	Oxidized low density lipoprotein (lectin-like) receptor 1	0.674
TIMP3	TIMP metallopeptidase inhibitor 3	0.591
CCL2	Chemokine (C-C motif) ligand 2	0.576
CCL7	Chemokine (C-C motif) ligand 7	0.575
CRELD2*	Cysteine-rich with EGF-like domains 2	0.563
NAPSB	Napsin B aspartic peptidase, pseudogene	0.559
PSMC6	Proteasome (prosome, macropain) 26S subunit, ATPase, 6	-1.094
DMXL1	Dmx-like 1	-1.104
SUMO1*	Small ubiquitin-like modifier 1	-1.123
SLC39A8	Solute carrier family 39 (zinc transporter), member 8	-1.149
PPIB*	Peptidylprolyl isomerase B (cyclophilin B)	-1.170
CLIC4*	Chloride intracellular channel 4	-1.192
PPP1R15B*	Protein phosphatase 1, regulatory subunit 15B	-1.238
HIAT1	Hippocampus abundant transcript 1	-1.276
DNTTIP2	Deoxynucleotidyltransferase, terminal, interacting protein 2	-1.286
GCLC*	Glutamate-cysteine ligase, catalytic subunit	-1.325

*Indicates gene ontology association with “unfolded protein response” and/or “endoplasmic reticulum unfolded protein response”

TABLE 4.5. Predicted upstream regulators of the MDMΦ response to DENV infection at 24 hours p.i. (7 vs. 9)

Regulator	Direction	Class	Function	p-value	Evidence
CCL3	Activated	Chemokine	Inflammation (recruits leukocytes)	4.29×10^{-4}	6/6
CCL5	Activated	Chemokine	Inflammation (recruits leukocytes)	1.42×10^{-4}	9/11
CD40LG	Activated	Cytokine	Inflammation	5.10×10^{-13}	38/50
IFN-γ	Activated	Cytokine	Inflammation	1.97×10^{-7}	58/88
IFN-α	Activated	Cytokine	Inflammation	6.03×10^{-8}	25/36
TNF-α	Activated	Cytokine	Inflammation	2.86×10^{-6}	58/99
H_2O_2	Activated	Small molecule	Oxidative stress	2.17×10^{-5}	29/36
NFE2L2	Activated	Transcription factor	UPR (oxidative stress)	2.29×10^{-4}	21/31
XBP1	Activated	Transcription factor	UPR (misfolded proteins)	1.41×10^{-7}	17/26
RelA	Activated	Transcription factor	Inflammation	4.43×10^{-6}	26/33
IL-10	Inhibited	Cytokine	Anti-inflammation	1.23×10^{-5}	22/32
SOCS1	Inhibited	STAT inhibitor	Anti-inflammation	1.83×10^{-4}	12/14

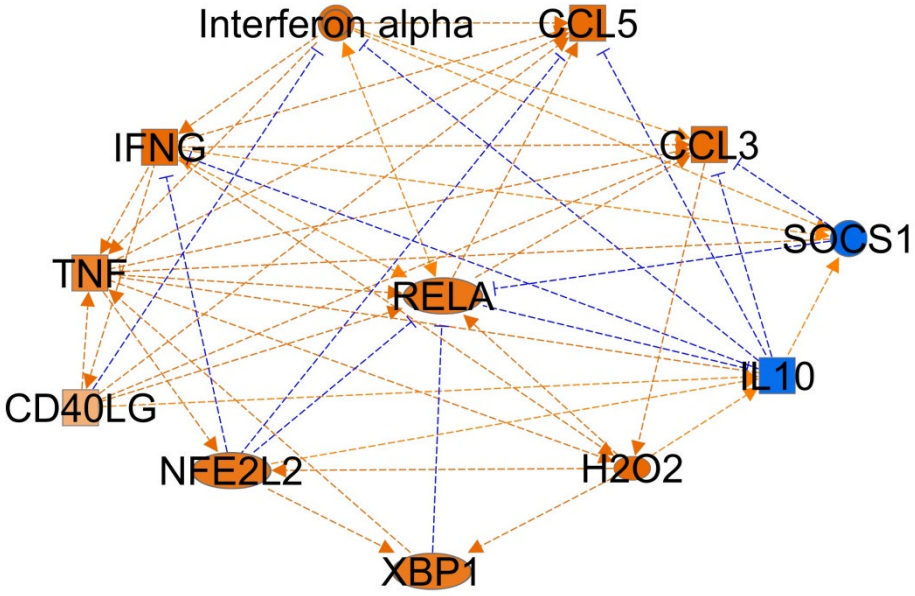

FIGURE 4.4. A network of upstream regulators of DENV infection of MDMΦs at 24 hours p.i. Upstream regulators were identified using IPA as in *Figure 4.2* with activated regulators represented in orange and inhibited network nodes (regulators) represented in blue. The functional interplay between network nodes is represented by dashed lines where blue lines indicate negative feedback and orange lines indicate positive feedback between the identified regulators. Genes that provide evidence for these predictions have been removed to simplify presentation.

IV.3.C. MON-DNJ modulation of the transcriptomic response to DENV infection

Having established the profile of transcriptomic responses to DENV infection in MDMΦs, I next investigated the ability of MON-DNJ to modulate this response. In order to do so, MDMΦ samples infected with DENV at 6 and 24 hours p.i. were used as controls to compare to DENV infected samples treated with 25 µM MON-DNJ at the same time points. As is the case for uninfected samples, DENV infected samples treated with MON-DNJ exhibited robust induction of the UPR. At both time points, the list of most strongly upregulated genes included several genes characteristic of the UPR (*Table 4.6* and *4.7*). At 6 hours p.i., 1765 transcript probes were differentially expressed by

TABLE 4.6. M*O*N-DNJ modulated transcripts in DENV infected MDMΦs 6 hours p.i. (3 vs. 4)

Gene Symbol	Gene Name	Fold Change
MBNL2	Muscleblind-like splicing regulator 2	1.835
GNL3*	Guanine nucleotide binding protein-like 3 (nucleolar)	1.698
TRIB3*	Tribbles pseudokinase 3	1.503
ERO1LB*	ERO1-like beta (S. cerevisiae)	1.396
PSAT1	Phosphoserine aminotransferase 1	1.347
DNAJB9*	DnaJ (hsp40) homolog, subfamily B, member 9	1.339
NUCB2*	Nucleobindin 2	1.337
CRELD2*	Cysteine-rich with EGF-like domains 2	1.254
ARMCX2	Armadillo repeate containing, x-linked 2	1.252
MSTO1	Misato 1, mitochondrial distribution and morphology regulator	1.224
LIMA1	LIM domain and actin binding 1	-0.696
GPR183	G protein-coupled receptor 183	-0.697
ANKRD1	Ankyrin repeat domain 1 (cardiac muscle)	-0.705
HSPH1*	Heat shock 105kDa/110kDa protein 1	-0.739
IER3	Immediate early response 3	-0.757
NFKBIA	Nuclear factor of kappa light polypeptide gene enhancer in B-cells inhibitor, alpha	-0.765
FKBP4	FK506 binding protein 4, 59kDa	-0.774
MERTK	c-mer proto-oncogene tyrosine kinase	-0.789
DNAJA4*	DnaJ (hsp40) homolog, subfamily A, member 4	-0.797
CCL4L2	Chemokine (C-C motif) ligand 4-like 2	-1.065

*Indicates gene ontology association with “unfolded protein response” and/or “endoplasmic reticulum unfolded protein response”

ANOVA and these probes mapped to 1594 unique genes. At 24 hours p.i., 1866 transcript probes mapping to 1578 unique genes were differentially expressed.

As in uninfected samples, the unfolded protein response induced by M*O*N-DNJ is stronger at 6 hours than 24 hours p.i. as indicated by the fold changes of UPR genes at each time point and the relative abundance of such genes (*e.g.* CRELD2 induced 1.254 fold at 6 hours and only 0.826 fold at 24 hours p.i.). In the early transcriptional response to DENV infection, induction of the UPR was noted in response to virus alone, and it appears as though M*O*N-DNJ can enhance this early response. Although the initial inflammatory response to DENV infection is not particularly strong, there are indications that M*O*N-DNJ is capable of modulating this response. Even in the absence of a full round of viral replication, specific elements of the inflammatory response appear to be antagonised by

M*O*N-DNJ treatment. This phenomenon is exemplified by the reduced induction of CCL4L2, a C-C motif cytokine, and can be extended to investigations of upstream regulators (*Figure 4.5*). As demonstrated in *Figure 4.5*, there is an abundance of downregulated (green) transcripts under control of the inflammatory molecules TNF-α, IFN-γ, CD40 ligand, and NF-κB (via RelA). Induction of anti-inflammatory controller SOCS1 is enhanced by M*O*N-DNJ treatment in concordance with induction of the UPR as indicated by the large number of upregulated (red) transcripts under control of XBP-1.

By 24 hours p.i., the effects of M*O*N-DNJ treatment on the transcriptomic profile of DENV-infected macrophages have changed considerably. Although the UPR continues to be induced (activation of XBP1 *p*-value = 9.06×10^{-15}), the abundance of effects of M*O*N-DNJ treatment are centred about the innate immune response. In the limited subset of the most highly differentially expressed genes (*Table 4.7*), there is evidence of bi-directional modulation of the inflammatory response. For example, expression of TNFSF10, a TNF family member also known as TRAIL, is enhanced whereas expression of two TNF receptor superfamily members (TNFRSF4 and 9) is reduced. Recruitment of lymphocyte populations may be enhanced as demonstrated by LY9 induction, whereas EBI3 (also known as IL-27β) downregulation suggests reduction of this cytokine's activity. Prediction of upstream regulators by IPA helps to extend the observation of bi-directional immunomodulation (*Figure 4.6*). In continuation of observations at 6 hours p.i., UPR pathways remain induced with M*O*N-DNJ treatment of DENV infection and TNF-α and NF-κB pathways remain suppressed. Intriguingly, there is considerable evidence (*p*-value = 4.50×10^{-4}) for activation of type-I interferon activity as represented by interferon alpha. These results indicate that M*O*N-DNJ treatment enhances direct antiviral effects while maintaining elements of reduced inflammation following a round of viral replication. Extension of these results to the case of human infection could promote

an environment for effective viral clearance with an absence of the excessive inflammation, or cytokine storm, which has been implicated in dengue pathology.

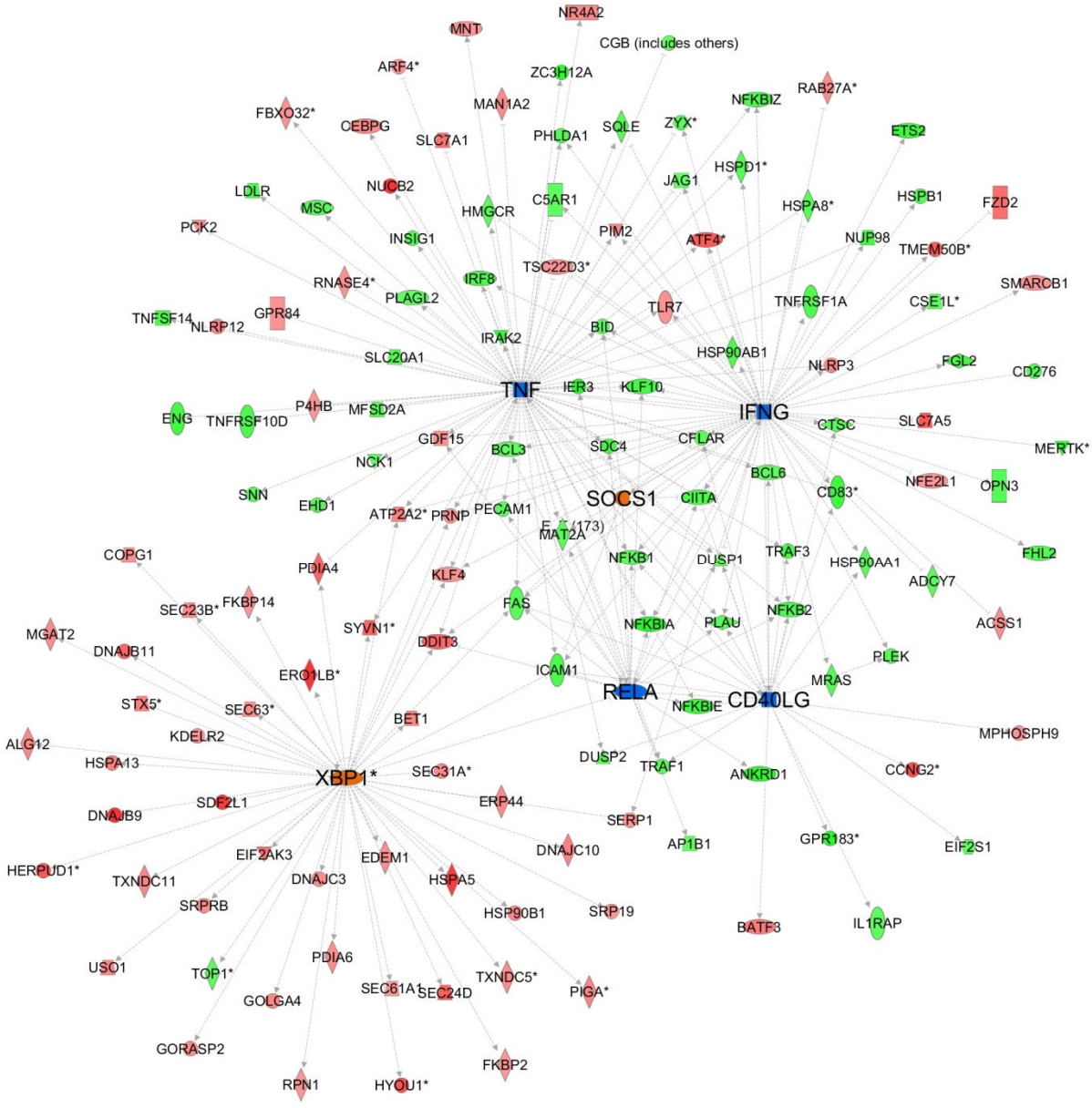

FIGURE 4.5. Treatment of DENV infected macrophages with M*O*N-DNJ induces the UPR and reduces inflammation during the early stages of infection. Comparison of transcripts in DENV-infected MDMΦ and DENV-infected MDMΦs treated with M*O*N-DNJ reveals an abundance of differentially expressed transcripts at 6 hours p.i. that suggest a reduction of specific elements of the inflammatory response. Downregulated transcripts (green) provide support for inhibition (blue) of network regulators TNF-α(TNF), IFN-γ (IFNG), RelA (RELA), and CD40 ligand (CD40LG). Upregulated transcripts (red) suggest activation (orange) of XBP-1 and SOCS1.

TABLE 4.7. M*O*N-DNJ modulated transcripts in DENV infected MDMΦs 24 hours p.i. (9 vs. 10)

Gene Symbol	Gene Name	Fold Change
BEX2	Brain expressed x-linked 2	0.987
TMEM50B	Transmembrane protein 50B	0.931
TUBB3	Tubulin, beta 3 class III	0.903
SPOCD1	SPOC domain containing 1	0.836
CRELD2*	Cysteine-rich with EGF-like domains 2	0.826
SLC3A2	Solute carrier family 3 (amino acid transporter heavy chain), member 2	0.823
TNFSF10	Tumor necrosis factor (ligand) superfamily, member 10	0.820
LY9	Lymphocyte antigen 9	0.803
ID2	Inhibitor of DNA binding 2, dominant negative helix-loop-helix protein	0.793
TRAM2	Translocation associated membrane protein 2	0.780
CHST2*	Carbohydrate (N-acetylglucosamine-6-O) sulfotransferase 2	-0.806
CCDC28B	Coiled-coil domain containing 28B	-0.888
PTGES	Prostaglandin E synthase	-0.899
TNFRSF4	Tumor necrosis factor receptor superfamily, member 4	-0.953
EBI3	Epstein-Barr virus induced 3	-0.963
SLC39A8	Solute carrier family 39 (zinc transporter), member 8	-0.984
SLC9A9	Solute carrier family 9, subfamily A (NHE9, cation proton antiporter 9), member 9	-0.990
CYP27B1	Cytochrome p450, family 27, subfamily B, polypeptide 1	-1.032
TMEM163	Transmembrane protein 163	-1.088
TNFRSF9	Tumor necrosis factor receptor superfamily, member 9	-1.167

*Indicates gene ontology association with “unfolded protein response” and/or “endoplasmic reticulum unfolded protein response”

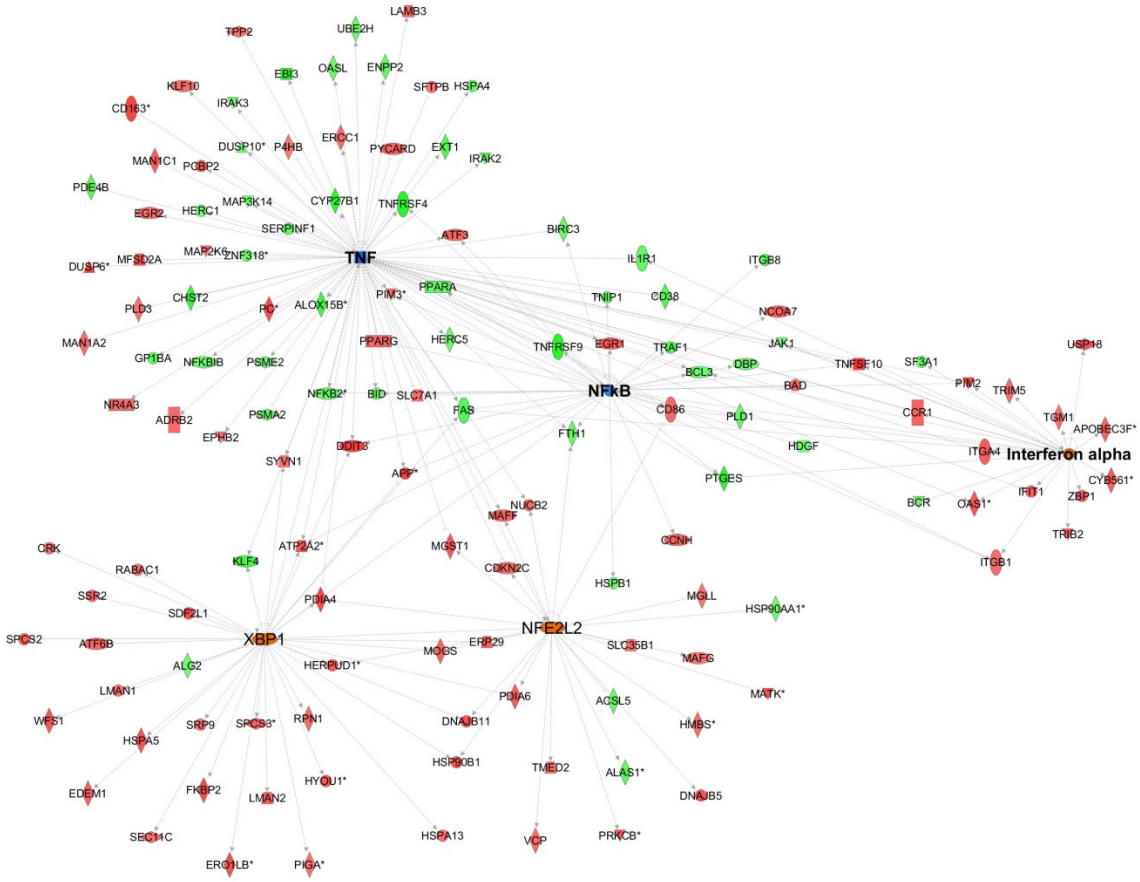

FIGURE 4.6. M*O*N-DNJ treatment of DENV-infected MDMΦs enhances type I interferon production while maintaining suppression of other inflammatory markers. Upregulated transcripts (red) indicate enhanced activity (orange) of XBP1, NFE2L2, and interferon alpha. In contrast, the downregulation (green) of transcripts under the control of TNF-α and NF-κB suggests that MON-DNJ specifically antagonises the activity of these inflammatory mediators.

IV.3.D. M*O*N-DNJ modulation of the transcriptomic response to LPS treatment

In order to address the broad applicability of the immunomodulatory effects of M*O*N-DNJ treatment, an LPS model of bacterial sepsis was assessed for transcriptomic responses to treatment in MDMΦs. Samples were treated with 200 ng/ml of LPS derived from *S. enterica* for 90 minutes and then treated with 25 µM M*O*N-DNJ or left untreated. At the same time as drug administration, LPS concentration was reduced to 100 ng/ml. To establish that this macrophage model behaved as anticipated in response to the LPS stimulus, cells treated with LPS were compared to uninfected,

untreated controls at both time points. This course of treatment led to differential expression of 9188 transcript probes at 6 hours p.i. and 6142 transcript probes at 24 hours p.i. Differentially expressed probes were mapped to 8499 and 5662 unique genes, respectively. At both time points, inflammatory markers characteristic of LPS treatment were strongly induced with IL-6 transcript 7.628-fold higher than uninfected samples at 6 hours p.i. and IL-1β the most strongly induced transcript at 24 hours p.i. with a 7.871-fold induction. Upstream analysis using IPA verified the LPS-signature with LPS being the most significantly identified regulator at both time points (p=1.14 x 10^{-38} for *S. enterica* LPS at 6 hours p.i. and p=6.82 x 10^{-58} for LPS at 24 hours p.i.).

The effects of M*O*N-DNJ treatment on LPS treated cells suggested that even in this strong inflammatory environment the drug is capable of further inducing the UPR and modulating the

TABLE 4.8. M*O*N-DNJ modulated transcripts in LPS treated MDMΦs at 6 hours p.i. (5 vs. 6)

Gene Symbol	Gene Name	Fold Change
MBNL2	Muscleblind-like splicing regulator 2	2.982
CRELD2*	Cysteine-rich with EGF-like domains 2	2.227
ERO1LB*	ERO1-like beta (S. cerevisiae)	2.149
ARMCX2	Armadillo repeate containing, x-linked 2	1.844
NUCB2*	Nucleobindin 2	1.801
ASNS*	Asparagine synthetase (glutamine-hydrolyzing)	1.769
GNL3*	Guanine nucleotide binding protein-like 3 (nucleolar)	1.704
SLFN11	Schlafen family member 11	1.598
RNASE4	Ribonuclease, Rnase A family, 4	1.590
HSPA5*	Heat shock 70kDa protein 5 (glucose-regulated protein, 78kDa)	1.525
BOP1	Block of proliferation 1	-0.614
RPL29	Ribosomal protein L29	-0.615
PDSS1	Prenyl (decaprenyl) diphosphate synthase, subunit 1	-0.623
SFRS12	Serine/arginine-rich splicing factor 12	-0.633
RNASE6	Ribonuclease, Rnase A family, 6	-0.639
CCDC86	Coiled-coil domain containing 86	-0.702
ECE2	Endothelin converting enzyme 2	-0.809
BATF	Basic leucine zipper transcription factor, ATF-like	-0.916
TARP	T cell receptor gamma alternate reading frame protein	-1.016
SLAMF1	Signaling lymphocytic activation molecule family member 1	-1.292

*Indicates gene ontology association with “unfolded protein response” and/or “endoplasmic reticulum unfolded protein response”

inflammatory response. At 6 hours p.i., 2138 probes which mapped to 1889 unique genes were differentially expressed. As shown in *Table 4.8*, upregulated transcripts were heavily associated with the UPR (*e.g.* CRELD2, ERO1LB, HSPA5), and downregulated transcripts were associated with inflammation (e.g. TARP and SLAMF1). Both of these downregulated signalling molecules are receptors commonly associated with inflammatory signalling. Downregulation of SLAMF1 is particularly interesting as it suggests a mechanism for decreased inflammation in the context of LPS and/or IFN-γ stimulated macrophages as well as other myeloid cells and lymphocytes. Upstream analysis using IPA demonstrates activation of UPR response pathways as a result of M*O*N-DNJ treatment as demonstrated by upregulation of transcripts under the control of XBP1, NFE2L2, and EIF2AK3 (*Figure 4.7*). At the same time, downregulation of TNF-α induced transcripts suggests reduced inflammation during the macrophage's response to LPS as a result of M*O*N-DNJ treatment. It is possible that this occurs via the same mechanism as occurs for DENV infection.

At 24 hours p.i., M*O*N-DNJ continues to elicit a strong unfolded protein response in LPS-treated macrophages (*Table 4.9*). In fact, nearly all ten of the transcripts with the greatest differential expression are involved in ER-stress responses including the chaperones CALR (calreticulin) and HSPA5 and protein disulphide isomerases PDIA4 and PDIA6. The tendency toward reduction of inflammation with M*O*N-DNJ treatment is further supported by the downregulation of the complement cascade and TNF-associated protein C1QTNF1 and C-C motif chemokine CCL23. Although not observed in any of the previous experiments, reduction of three members of the metallothionein family (MT1G, MT1H, and MT1M) indicates a potential impact of M*O*N-DNJ on the oxidative stress response. It is alternatively possible that this observation is a by-product of induction of the EIF2AK3/NFE2L2 arm of the UPR observed in all experiments where M*O*N-DNJ is added. Analysis of upstream signalling events as a consequence of M*O*N-DNJ treatment (*Figure 4.8*) indicates that both TNF-α and MyD88 (an activator of the NF-κB pathway) signalling is attenuated.

There was no observable modulation of type I interferon responses, either positive or negative, in this analysis, suggesting that enhancement of type I interferon signalling as a result of M*O*N-DNJ treatment in DENV infection may be a (dengue) virus specific phenomenon.

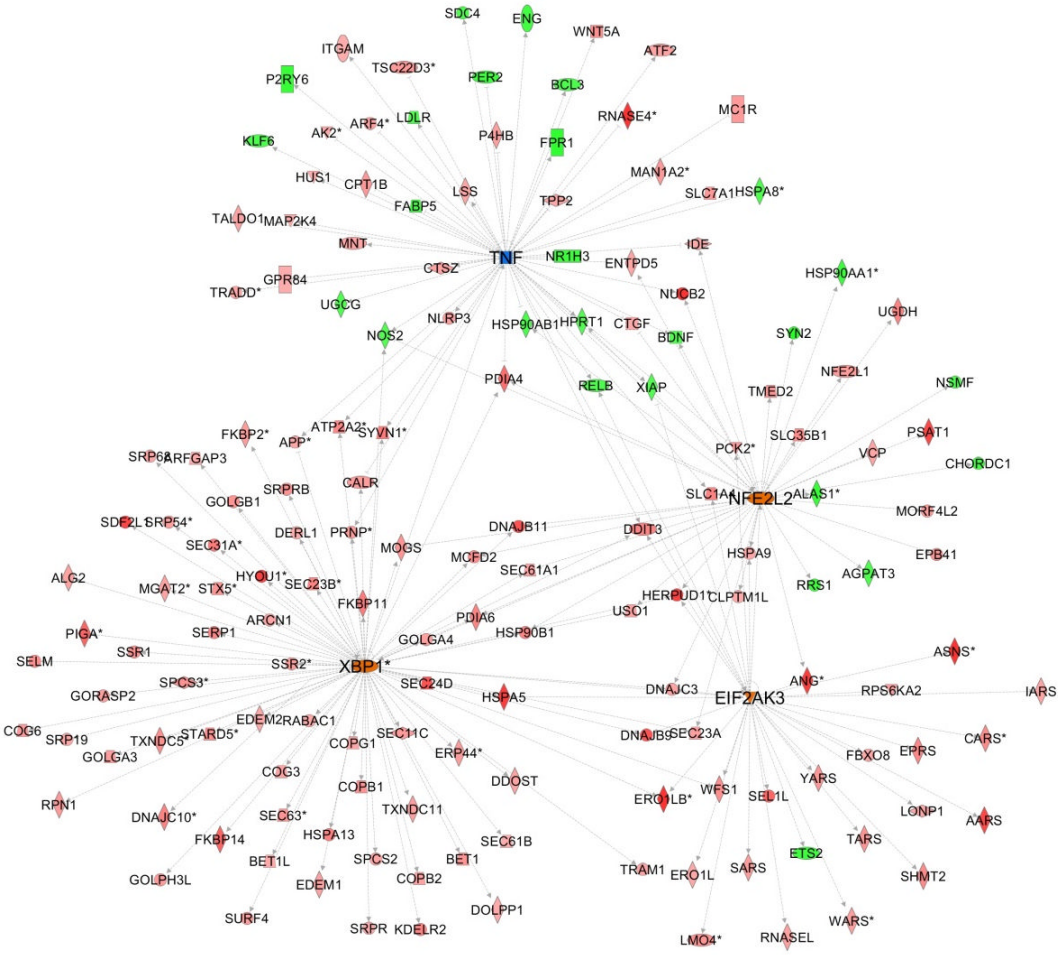

FIGURE 4.7. M*O*N-DNJ treatment of LPS infected MDMΦs induces the UPR and reduces TNF-α signalling at 6 hours p.i. Transcripts under the control of TNF-α are downregulated (green) suggesting inhibition of TNF-α signalling whereas UPR control elements (XBP1, NFE2L2, and EIF2AK3) are activated as demonstrated by upregulation (red) of downstream transcripts.

TABLE 4.9. M*O*N-DNJ modulated transcripts in LPS treated MDMΦs at 24 hours p.i. (11 vs. 12)

Gene Symbol	Gene Name	Fold Change
CRELD2*	Cysteine-rich with EGF-like domains 2	1.584
SDF2L1	Stromal cell-derived factor 2-like 1	1.421
MANF*	Mesencephalic astrocyte-derived neurotrophic factor	1.321
HSPA5*	Heat shock 70kDa protein 5 (glucose-regulated protein, 78kDa)	1.261
ISOC2*	Isochorismatase domain containing 2	1.184
DDIT3*	DNA-damage-inducible transcript 3	1.109
CALR*	Calreticulin	1.108
PDIA6*	Protein disulfide isomerase family A, member 6	1.104
CRELD1*	Cysteine-rich with EGF-like domains 1	1.044
PDIA4*	Protein disulfide isomerase family A, member 4	1.039
FAM63A	Family with sequence similarity 63, member A	-0.647
CCL23	Chemokine (C-C motif) ligand 23	-0.686
LAD1	Ladinin 1	-0.753
RNF19B	Ring finger protein 19B	-0.754
SLC39A8	Solute carrier family 39 (zinc transporter), member 8	-0.876
FPR1	Formyl peptide receptor 1	-0.927
C1QTNF1	C1q and tumor necrosis factor related protein 1	-1.042
MT1G	Metallothionein 1G	-1.301
MT1M	Metallothionein 1M	-1.479
MT1H	Metallothionein 1H	-1.562

*Indicates gene ontology association with “unfolded protein response” and/or “endoplasmic reticulum unfolded protein response”

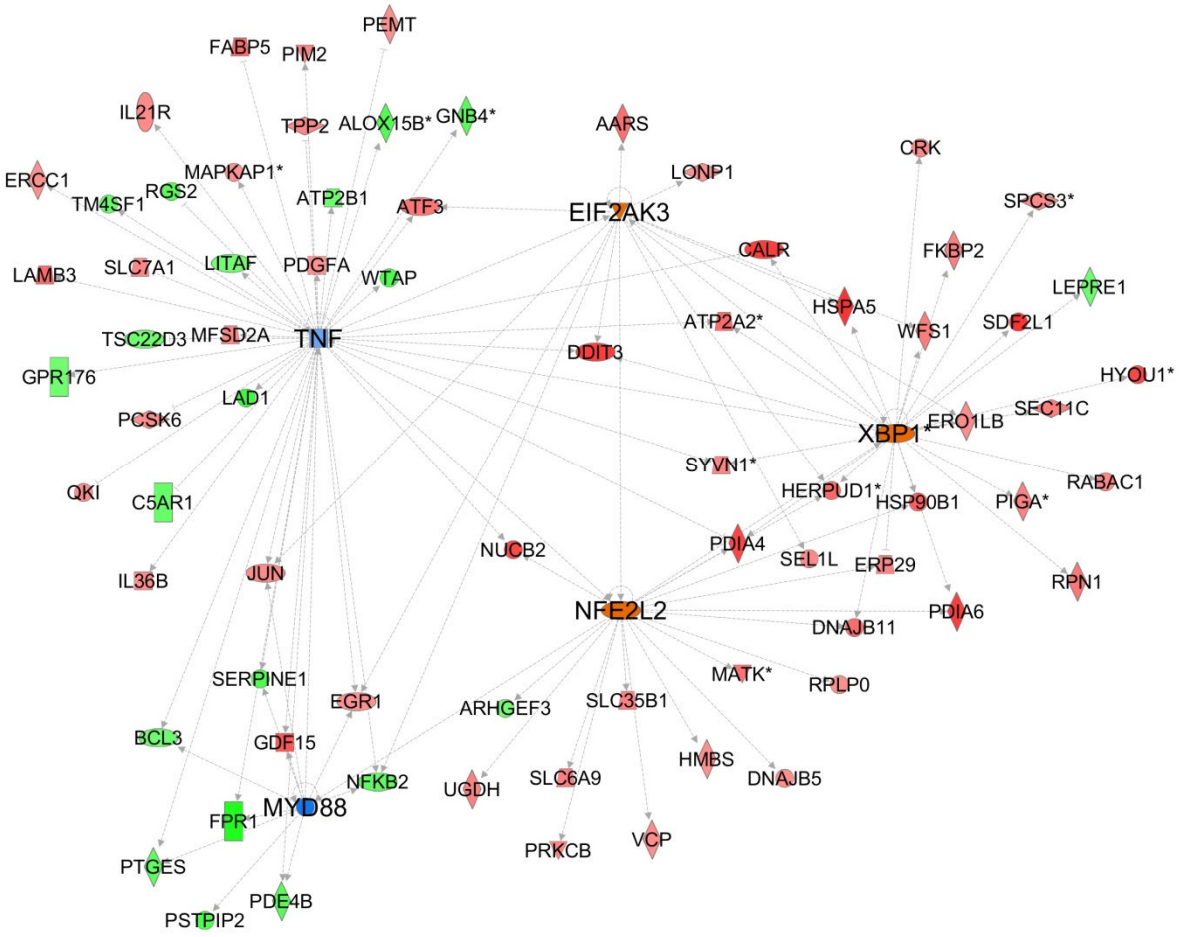

FIGURE 4.8. M*O*N-DNJ treatment of LPS infected MDMΦs induces the UPR and reduces TNF-α and MyD88 signalling at 24 hours p.i. Transcripts under the control of TNF-α and MyD88 are downregulated (green) suggesting inhibition of inflammatory signalling whereas UPR control elements (XBP1, NFE2L2, and EIF2AK3) are activated as demonstrated by upregulation (red) of downstream transcripts.

IV.3.E. Protein level validation of TNF family modulation by M*O*N-DNJ

The transcriptomic results presented above suggest that TNF receptor and ligand superfamily member production that is induced by either DENV infection or LPS treatment can be abrogated with M*O*N-DNJ treatment. In order to address this hypothesis, whole cell lysates were prepared from samples collected under the same treatment conditions and probed for TNFRSF4 (also known as OX40) levels by western blotting. TNFRSF4 was chosen due to the strong transcript response noted in DENV infected samples at 24 hours p.i. As shown in *Figure 4.9*, TNFRSF4 was detected in two of

several glycoforms previously reported. [271] In these experiments, LPS induced TNFRSF4 to a much greater extent than DENV, thus LPS treated samples were exposed for 10 minutes whereas uninfected and DENV infected samples were exposed for 30 minutes. At 6 hours p.i., weak but not statistically significant reduction of TNFRSF4 was detected by western blotting, but by 24 hours p.i. this difference was significant for DENV infected and LPS treated samples. In addition to reduction of overall protein level, a noticeable shift in the lower (~32 kDa) band was detectable with M*O*N-DNJ treatment. This may represent a change in glycosylation (*e.g*. failure to cleave terminal glucoses) resulting in altered gel mobility; however, further analysis using various endo- and exo-glycosidases is required to verify this hypothesis. Nevertheless, these results verify the direct impact of M*O*N-DNJ on TNFRSF4 production.

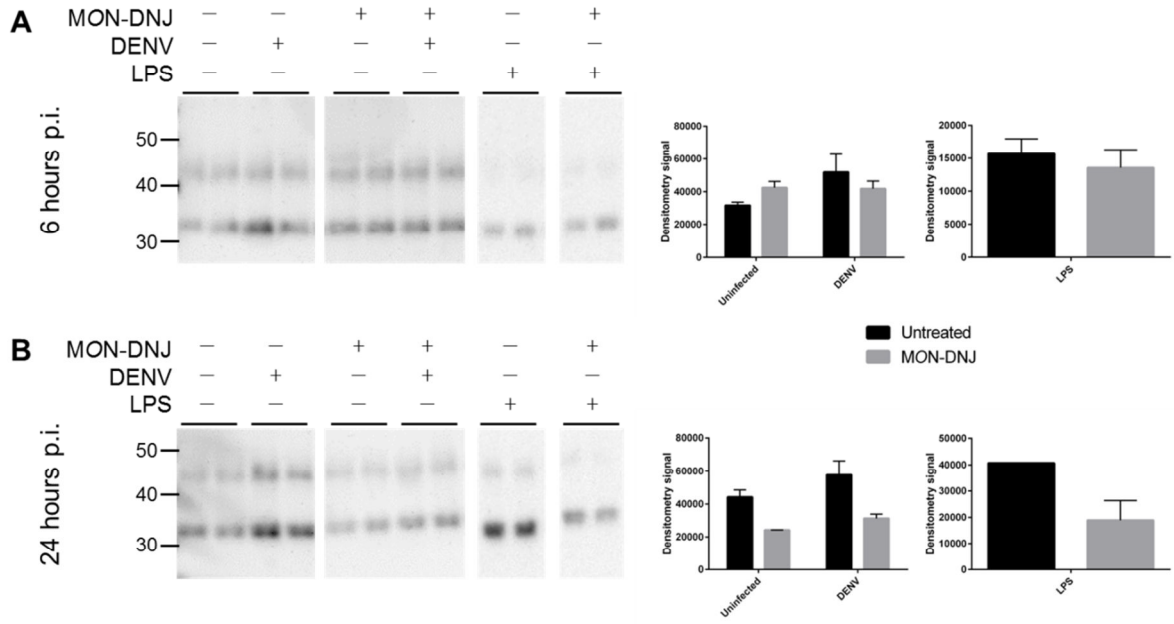

FIGURE 4.9. M*O*N-DNJ treatment of MDMΦs reduces TNFRSF4 (OX40) production independent of mechanism of induction. Production of TNFRSF4 was assayed by western blotting of MDMΦ whole cell lysates treated as presented previously. Samples were prepared in duplicate, assayed for protein content, and 5 µg total protein from each sample was run on a Bis-Tris gel before transfer to a PVDF membrane for western blotting. Protein was detected with a rabbit monoclonal antibody using a chemiluminescent detection method as described in the *Material and Methods*. Blots were exposed for 30 minutes for uninfected and DENV-infected samples and for 10 minutes for LPS treated samples. Densitometry was conducted on the 32 kDa band using LiCor Image Studio. The two bands present at 32 kDa and 44 kDa have been previously described as glycoforms of TNFRSF4. An anti-cofilin mouse monoclonal antibody was used to verify equal loading (data not shown). Representative blot from one of three donors displayed.

IV.3.F. Protein level validation of NFE2L2 modulation by M*O*N-DNJ

Given the importance of the unfolded protein response to the transcriptomic changes observed, induction of NFE2L2 was assayed in a manner similar to TNFRSF4. Because NFE2L2 must be available for rapid response to stress situations, assessment of changes of active transcription factor is of much greater interest than total protein level. Therefore, an antibody specific for phosphorylated (activated) NFE2L2 was employed for these experiments. As shown in *Figure 4.10*, a considerable number of bands which did not react with other rabbit monoclonal antibodies (data not shown) reacted with the NFE2L2 antibody. The nature of the UPR is such that the interaction and heterodimerisation of UPR regulating transcription factors determines the nature of the stress response, and it may be that these bands represent association of NFE2L2 with various other transcription factors. Although NFE2L2 should theoretically migrate at 68 kDa, many investigators have observed bands for the protein which migrate at much larger sizes, for example [272]. Whereas a large number of bands could be detected in all samples generated at 6 hours p.i. (even uninfected, untreated samples), a single large species was dominantly produced in samples collected at 24 hours p.i. Given the ubiquity of bands identified at 6 hours p.i., it may be that the removal of IL-4 from cell media during infection and subsequent drug treatment activates NFE2L2. The band assayed for concentration at 6 hours p.i. was selected as a consequence of reliable detection across samples without considerable variability (for example the predominant band which is slightly larger was overexposed in LPS treated, M*O*N-DNJ treated samples but undetectable in uninfected, untreated samples). Furthermore, it appeared to be relatively indicative of the total NFE2L2 lane profile. The difference in relative intensities between bands supports the hypothesis that each band is a distinct subset of NFE2L2, but resolving which molecules are interacting with the transcription factor requires affinity purification. Nevertheless, analysis of the band chosen verifies induction of this transcription factor as a consequence of M*O*N-DNJ treatment. At 24 hours p.i. the dominant band

produced demonstrated much slower migration through the gel than the band assayed at 6 hours p.i., but induction as a consequence of M*O*N-DNJ treatment was again detectable.

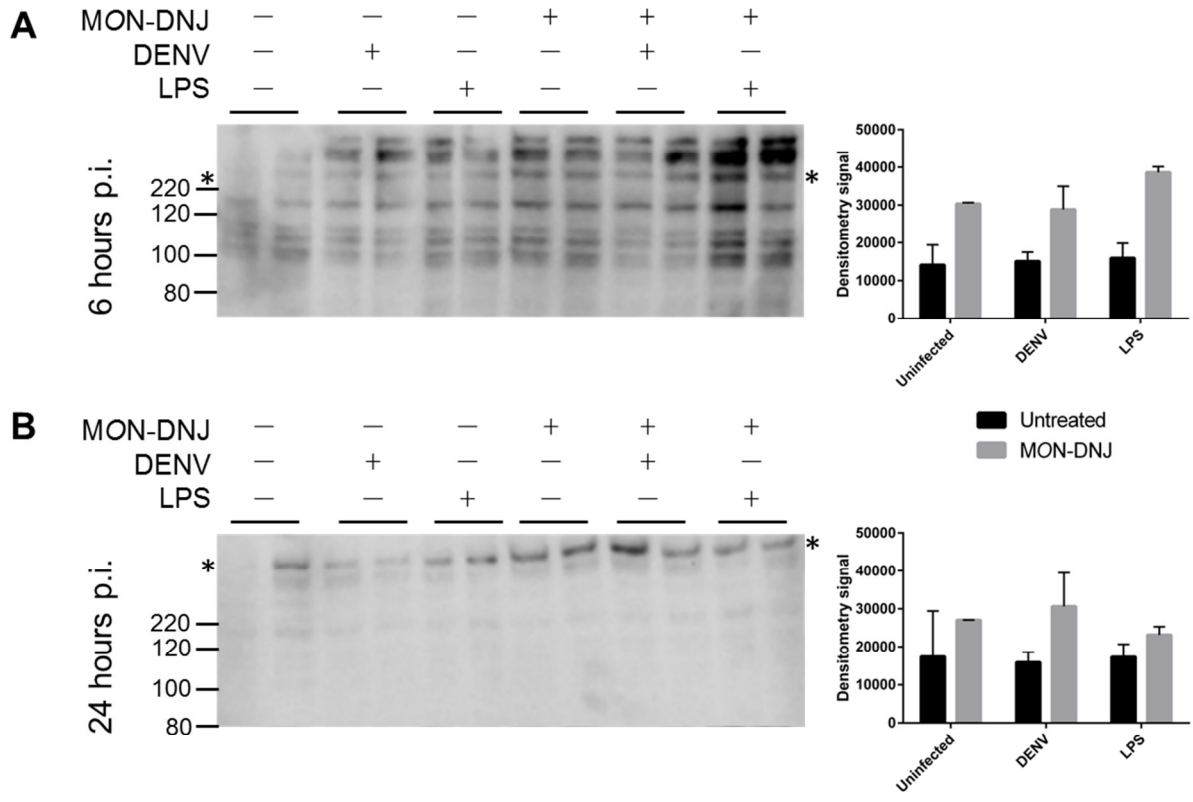

FIGURE 4.10. M*O*N-DNJ treatment of MDMΦs induces NFE2L2 (Nrf2) production. Phosphorylated NFE2L2 was assayed by western blotting of MDMΦ whole cell lysates treated as presented previously. Samples were prepared in duplicate, assayed for protein content, and 5 µg total protein from each sample was run on a Bis-Tris gel before transfer to a PVDF membrane for western blotting. Protein was detected with a rabbit monoclonal antibody using a chemiluminescent detection method as described in the *Material and Methods*. Blots were exposed for 60 minutes. Densitometry was conducted on the 250 kDa band at 6 hours p.i. and the largest molecular weight band at 24 hours p.i. using LiCor Image Studio. An anti-cofilin mouse monoclonal antibody was used to verify equal loading (data not shown). Representative blot from one of two donors.

IV.4. Discussion

Whereas a considerable body of work has accumulated in an effort to unravel the host transcriptional response responsible for progression to severe pathogenesis for many viral infections, relatively limited work has been done to characterise the alteration of host responses as a consequence of treatment with potential antiviral therapeutics. Prior to clinical trials, investigators and/or pharmaceutical companies have rarely, if ever, sought to fully characterise the transcriptional response of primary human cells to a potential therapeutic. This is likely a result of the concern of uncovering previously unnoticed off-target effects of pre-clinical candidates requiring detailed follow-up experiments to validate or reject newly-arisen safety concerns. In the event where off-target effects are confirmed, investigators must then demonstrate to regulatory agencies that these effects will not result in adverse effects in human treatment – a difficult, if not impossible, task – prior to continuation of trials. In the execution of such detailed transcriptomics experiments, a considerable risk of pre-clinical failure is incurred; however, I would argue that failure to engage in such experiments carries a significant cost of lost opportunities. By adding pre-clinical transcriptomics analysis to investigation of new drugs, ensuing clinical trials may be much better informed as to the most likely potential sources of failure which can then be monitored closely in further investigations. Furthermore, such experiments may reveal additional, and potentially more promising, host targets of the therapeutic in question. Thus, pre-clinical transcriptomics could provide better safety monitoring and expand application of therapeutics to investigations of multiple diseases. In contrast, the current work-flow results in clinically-licensed therapeutics being re-appropriated to treatment of secondary diseases following transcriptomics/further experimentation (subsequent to initial clinical approval) to identify additional candidate diseases for therapeutic application or via *compassionate care* by physicians. This results in a limited pool of candidate therapeutics. Through utilisation of pre-clinical transcriptomics, the successful application of therapeutics to secondary diseases or even application to more relevant clinical trials could be

greatly expanded. As such, I have undertaken an investigation of M*O*N-DNJ in primary human MDMΦs in the context of DENV infection and LPS treatment in order to assess the broad clinical potential of this iminosugar.

Initial analyses focused on characterising the MDMΦ response to DENV infection. Although several previous studies have investigated PBMC transcriptomic responses of DENV-infected patients [50,251-257] and various cell culture models [133,258-261,273,274] have been infected with DENV to characterise important transcriptional responses, no work had previously focused on an *ex vivo* primary human infection model of immune cell response, and macrophage-specific response to DENV had not been assessed. My analyses reveal a weak conserved response to DENV infection at an early (6 hour) time frame. This is likely to be a consequence of use of an outbred population with a tendency toward variation in innate immune response; however, this is an attractive feature of this system as robust changes can therefore be differentiated and studied in greater detail. The induced upstream regulators predicted are associated with cellular stress, vascular remodelling, and innate immunity. It is tempting to speculate that the cellular stress observed is the result of increased demands on protein and RNA synthesis co-opted by the virus and that this induces inflammatory responses (notably type I and II interferons) and could lead to vascular remodelling. It is likely that these early responses play a critical role in disease progression and that further investigation of these targets, particularly those involved in directing vascular remodelling, may provide insights into the development of vascular leak and associated severe symptoms of dengue pathogenesis. In particular, the induction of NFE2L2, a primary defence against oxidative stress, [275-278] may play a crucial role in controlling inflammatory processes and limiting cellular damage as a result of oxidative stress following innate immune activation. The results presented in this chapter focus on the most fundamental of responses of this MDMΦ model to DENV infection; however, additional targets can be identified with IPA. For example, only one upstream regulator, WNT5A, is predicted to

be inhibited by these analyses at 6 hours p.i. (data not shown). WNT5A signalling in conjunction with c-Jun N-terminal kinases (JNK) and calmodulin-dependent protein kinase II (CaMKII) has been shown to exert control over expression of IL-1β, IL-6, and TNF-α in response to HIV envelope protein gp120 [279]; however, no association between WNT5A and DENV response has been identified to date. The paucity of predicted inhibited regulators may suggest that the absence of non-structural proteins at this early time point prevents antagonism of cellular response networks and that the activated pathways identified are the primary host response to DENV-infection. Also of note is the predicted activation of miR-122, a microRNA that plays an important role in assisting HCV RNA replication. [280] To date, no association of DENV with miR-122 has been demonstrated; however, these results indicate that the related *Flaviviruses* may both interact with this specific miR.

Following on from these early events, the infected MDMΦ appears to establish a robust inflammatory response by 24 hours p.i. By this time point, a number of innate pattern recognition receptors (PRRs) such as TLR-3 and MAVS, important detectors of double-stranded RNA, are predicted to be activated. At the same time, type I and II interferon responses are predicted to activate downstream signalling of inflammation (via NF-κB, JAK/STAT, and interferon response factors/inducible transcripts) concomitant with blockade of anti-inflammatory signals (SOCS1 and IL-10). As discussed in *Chapter I*, IFN-γ and TNF-α appear to exert considerable control on development of severe pathogenesis. In these studies, IFN-γ in coordination with type I interferons appears to exert considerable control on the development of the inflammatory response. Again, the central role of oxidative stress is highlighted by the predicted activation of hydrogen peroxide, and activation of NFE2L2 controlled transcripts as a likely feedback mechanism to control this stress. Whereas there is a notable bias of transcription factors controlling the stress response at 6 hours p.i., the situation at 24 hours p.i. is dominated by inflammatory molecules. This switch from control of stress to broad

inflammation may explain how the inflammatory environment characteristic of severe DENV-mediated pathology develops.

Conserved effects of M*O*N-DNJ treatment (in uninfected, DENV-infected, and LPS-treated MDMΦs at both 6 and 24 hours p.i.) are limited to activation of ER-stress responding transcription factors such as ATF4, ATF6, EIF2AK3, NFE2L2, and XBP-1 (along with inhibition of D-glucose signalling). Based on the networks assembled for all cases of treatment with M*O*N-DNJ, inhibition of D-glucose and activation of XBP-1 and NFE2L2 appear to be responsible for the majority of changes observed. In relation to M*O*N-DNJ treatment, these interactions can be imagined to be the result of iminosugar acting in competition with glucose. As demonstrated in *Chapter III*, extension of this inhibition to prevention of α-glucosidase trimming of glycoproteins is likely to be the major mechanism of action of iminosugars as antivirals against DENV. In the case of host-based modulation, inhibition of ER-resident glycoprotein processing and subsequent accumulation of misfolded proteins may explain the observed anti-inflammatory tendencies of M*O*N-DNJ. As a consequence of cellular stress, as demonstrated by XBP-1 activation and induction of ERAD-associated processes, induction of inflammation is anticipated; however, reduction of inflammation is observed. In particular, activation of XBP-1 is expected to induce TNF-α. [281] Perhaps crucially, activation of NFE2L2 antagonises inflammation as a result of oxidative stress. [275-278]

Based on the transcriptional response measured, it appears that M*O*N-DNJ mediated induction of NFE2L2 and subsequent anti-inflammatory events dominate inflammation-inducing signals of the UPR. It appears that this NFE2L2-mediated effect, as demonstrated by reduced TNF-α transcript and further identification of many inflammatory molecules as downregulated, dominates the MDMΦ response to M*O*N-DNJ treatment. The observed induction of NFE2L2 by DENV in the absence of

M*O*N-DNJ is likely the result of activation of a robust inflammatory response. Given the further induction of NFE2L2 with M*O*N-DNJ treatment in the presence of inflammatory (infected) cellular environments, it appears that the M*O*N-DNJ mediated activation of NFE2L2 allows the anti-inflammatory effects to predominate. Thereby M*O*N-DNJ treatment may enhance control of excess inflammation but not act as a general anti-inflammatory *per se*. It is tempting to speculate that suppression of TNF-α by this mechanism can reduce excess inflammation in MDMΦs and thereby reduce severe pathology, but validation in an animal model is desirable. Unfortunately, differences in the mouse inflammatory response particularly with respect to *N*-linked glycosylation highlight the difficulties in choosing appropriate animal models for such studies. Alternatively, pre-conditioning of ER stress via activation of XBP-1 blocks inflammation particularly through attenuation of NF-κB and ICAM1 signalling [282] as observed in this experiment. Thus, it may be that rapid ER-stress induction by M*O*N-DNJ prior to the same activity mediated by a pathogen can prevent inflammation rather than induce it. Extension of this mechanism to a clinical therapeutic would be heavily dependent upon viral kinetics in opposition to rapid drug delivery and prophylactic treatment would almost certainly be required. As such, elucidating which of these mechanisms is responsible for reduced inflammation, or the relative contribution of each, is crucial to evaluation of this activity as a therapeutic approach.

In support of the hypothesised reduction of inflammation by M*O*N-DNJ, TNFRSF4 induction was shown to be attenuated at the protein level with M*O*N-DNJ treatment. It is possible that the reduced induction of TNF superfamily members is a consequence of NFE2L2 activation by iminosugars, but it remains possible that iminosugars directly reduce the production of proteins of the TNF superfamily. TNF ligand superfamily members are mostly *N*-glycosylated, with the notable exception of human TNF-α itself. [283] Alternatively, TNF superfamily receptors are heavily *N*-glycosylated and possess 3 to 4 repeats of a motif containing 3 disulphide bonds (described by pfam 00020). In general, heavily

glycosylated proteins possessing multiple disulphide bonds are strong candidates for dependence on CANX-mediated folding although direct evidence has not yet been published of such an interaction for TNF and/or receptor superfamily proteins. Nevertheless, one could envision a mechanism whereby M*O*N-DNJ treatment directly interferes with TNF-family folding via disruption of the CANX interaction, and as a consequence, downstream inflammation is attenuated.

In summary, this chapter presents the first comprehensive time-course transcriptomic response profile of primary human MDMΦs to DENV infection. These experiments allow detection of initial responses to virus and provide an understanding of how the inflammatory response to DENV infection progresses. By investigating the transcriptomic response to M*O*N-DNJ treatment in the context of DENV infection and LPS treatment, I have identified robust effects of the drug that indicate a tendency to reduce inflammation. Reduction of TNF family member signalling has been validated for one superfamily member and in concert with the following evidence in *Chapter V*, these data suggest that M*O*N-DNJ can reduce specific aspects of inflammation which may reduce progression to severe DENV pathology. The implication of excess inflammation, the so-called cytokine storm, in other severe pathologies (*e.g.* avian influenza, Ebola virus infection, and bacterial sepsis) may indicate a much broader potential clinical utility for M*O*N-DNJ – a promising lead for future research.

.

V

M*ON*-DNJ modulation of host-responses to diverse pathogens: A validation of transcriptomic predictions of anti-inflammatory activity

V.1. Abstract

A diverse array of pathologies may develop in response to infection with dengue virus. Whereas an estimated 390 million people are infected with the virus yearly, only approximately 100 million of these individuals develop any overt disease. Amongst this subset, an even smaller percentage of those infected with dengue virus progress beyond the more common febrile illness of dengue fever to develop severe and potentially life-threatening complications such as haemorrhage and shock. The molecular events that control these divergent responses remain unclear; however, early events in response to viral infection are a likely source in determining pathogenic outcomes. Thus, this study aimed to elucidate the time-dependent induction of the innate immune response in primary human monocyte-derived macrophages and compare these results to the findings of the previous transcriptomic studies. Herein, I show that initiation of inflammation is characterised by a strong and robust induction of both IFN-γ and TNF-α from which develops a more broad inflammatory response. As suggested by transcriptomics studies, treatment of infected macrophages with iminosugars possessing glucostereochemistry, and particularly M*O*N-DNJ, attenuated, but did not completely ablate, the induction of both IFN-γ and TNF-α in these experiments. Furthermore, the anti-inflammatory capacity of M*O*N-DNJ extends to diverse pathogenic and non-pathogenic stimuli. In pathology-inducing cases of excessive inflammation, such as cytokine storm, M*O*N-DNJ may prove a viable treatment option via moderation of the inflammatory response.

V.2. Introduction

As with the transcriptomic response to DENV infection, the cytokine response to DENV has been characterised in samples from patients of various states of disease progression, pathology, and immunological history in an attempt to identify which cytokine or cytokines are particularly responsible for severe disease. [73,76-105] In tandem with this work, *in vitro* and *in vivo* animal

studies have examined the role of various cytokines, chemokines, and other soluble mediators of immunity; however, the field of DENV research lacks a conclusive answer to which mediator(s) is/are particularly important for resolution of disease in contrast to development of severe and/or fatal pathology. The cytokine storm hypothesis, whereby excessive pro-inflammatory responses precipitate severe disease, holds considerable momentum at the present time as discussed in *Chapter I*. In particular, evidence has accumulated for TNF-α to play a central role as a *dark lord* of the cytokine storm precipitating downstream inflammation while also possessing the potential to increase endothelial cell permeability, though there is much dispute over whether the results are merely correlative or if they indicate TNF-α as a causative agent of severe disease. Designing an experiment to address the specific factor(s) responsible for severe disease has proved difficult and is beyond the scope of this thesis; however, an understanding of the developing innate immune response to infection in a relevant primary human cell is of crucial importance to understanding how the immune response might develop in an infected individual. Furthermore, limited evidence suggests that iminosugars might modulate the immune response, particularly the production of a few key cytokines, to various pathogens. With the suggestion of an anti-inflammatory propensity of iminosugars indicated by the transcriptomics data presented in *Chapter IV*, validation of these events on a protein level were of particular interest. Thus, the aims of *Chapter V* of this thesis are to:

1) Identify cytokines and chemokines produced by macrophages in response to DENV infection,
2) Determine the long-term kinetics of cytokine induction in response to DENV infection in macrophages,
3) Identify cytokines involved in the early stages of response to DENV infection, and
4) Assess how iminosugars can modulate the developing immune response to DENV infection as well as diverse pathogenic and non-pathogenic stimuli.

V.3. Results

V.3.A. Validation of the MDMΦ inflammatory response to DENV infection

The transcriptomics data discussed in *Chapter IV* present a compelling case for a strong but specific inflammatory response of MDMΦs to DENV infection. The secretion of a panel of 20 cytokines and chemokines (hereafter referred to as cytokines for simplicity) into the supernatant of DENV infected MDMΦs was investigated three days p.i. as an initial screen (*Figure 5.1*). Included amongst the cytokines tested were classical Th1 cytokines and mediators of pro-inflammatory responses such as IL-1β, IL-2, IL-6, IL-8, IL-12(p70), IFN-γ, and TNF-α. Additionally, classical Th2 cytokines IL-4, IL-5, and IL-13 were included along with IL-10 which is often considered to control the Th1/Th2 axis of response. [123] Various chemokines and growth factors responsible for recruitment and/or stimulation of specific leukocyte populations such as G-CSF, GM-CSF, IL-7, MCAF, and MIF were also assayed. Of the six donors tested, one donor, DG, exhibited a strikingly different response to DENV infection from the other five donors. For DG, the response to DENV infection was dominated by a potent IL-7 induction (*Figure 5.1F*) three orders of magnitude greater than the response observed for any of the other donors and a nearly complete absence of any other cytokine response. Both the source and the significance of this difference are unclear, but it is probable that different genetic and/or immunological memory backgrounds for donor DG have driven this response. Unfortunately, the anonymous nature of the blood collection protocol used precludes further investigation of whether this individual's potential clinical response to DENV infection would result in more or less severe pathology. In order to focus on conserved responses to DENV infection, donor DG was excluded from statistical analyses presented in *Table 5.1*. Of the cytokines tested, all of them except for IL-6, IL-8, and G-CSF exhibited statistically significant induction (Bonferroni corrected *p*-value <0.05). Statistical analyses of MIP-1β and IP-10 were not conducted as all infected samples produced a greater concentration of cytokine than could be measured with this assay; however, induction of

these two molecules upon DENV infection is clearly both profound and robust. Whereas many of the cytokine inductions observed with DENV infection were relatively weak (*e.g.* IL-1β increased by 5.0 pg/ml [3.3 to 6.7 pg/ml 95% confidence interval]), the induction of IL-17A, IFN-γ, RANTES, and TNF-α was particularly strong and consistent (*Figure 5.1K, 5.1N, 5.1S, 5.1T*).

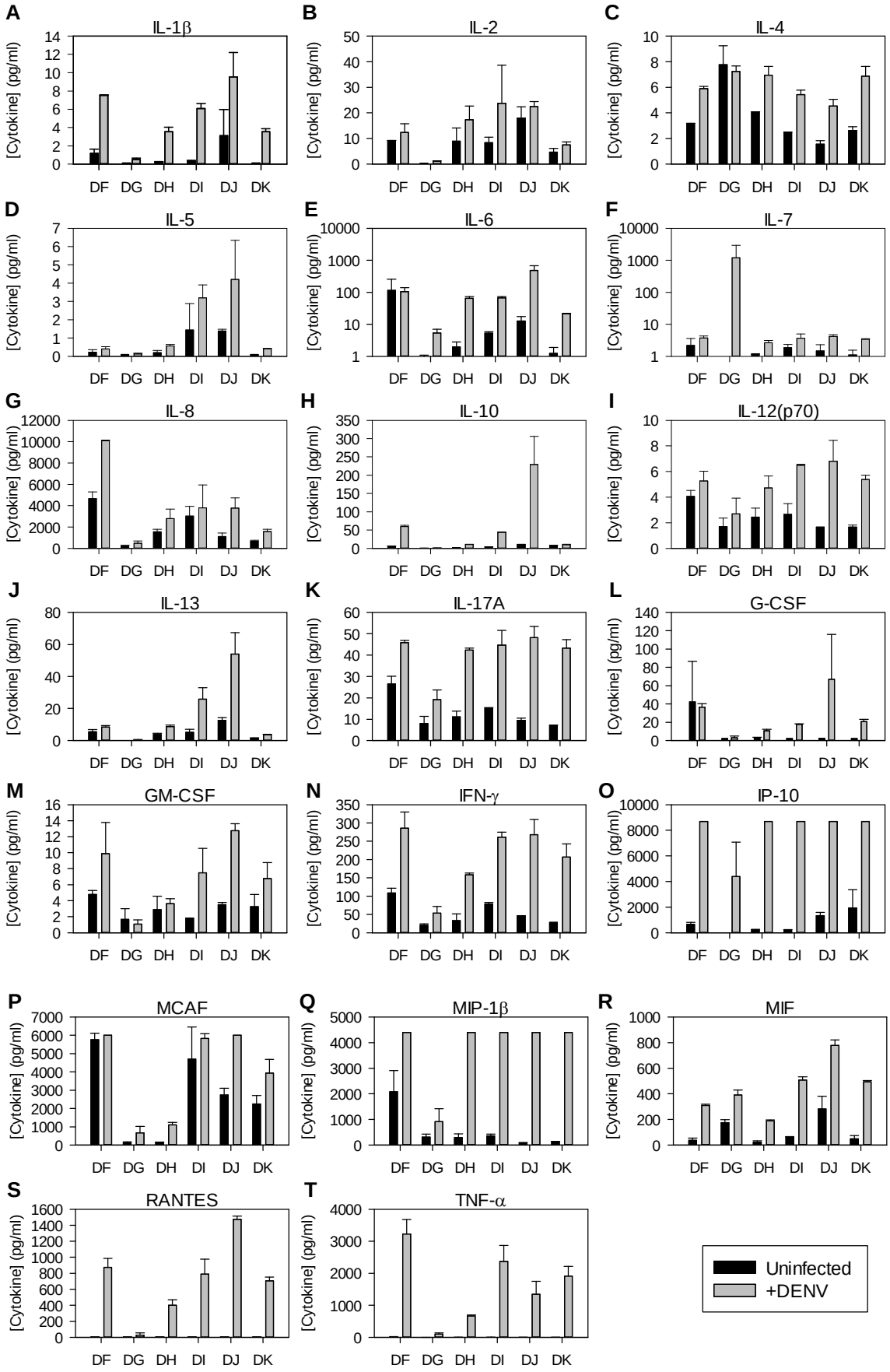

FIGURE 5.1. Cytokine response of MDMΦs to DENV infection. MDMΦs isolated from 6 donors were cultured individually for 3 days in the absence (black bars) or presence of DENV infection (grey bars) and cytokine levels in supernatants were assayed by Luminex multiplex bead assay. Error bars approximate standard deviation of technical replicates (n=2) for each biological replicate. Values beyond the limit of detection were set to the relevant minimum or maximum value.

TABLE 5.1. Summary of cytokine induction by DENV in MDMΦs (day 3 post infection)

	DENV effect (pg/ml)			*p* value	
Cytokine	Mean or median[a]	95% CI[b]	Test	Raw	Adjusted[c]
IL-1β	5.0	(3.3, 6.7)	parametric[d]	<0.001	<0.011
IL-2	4.9	n/a	non-parametric[e]	0.002	0.014
IL-4	3.2	n/a	non-parametric	0.002	0.014
IL-5	0.3	n/a	non-parametric	0.004	0.028
IL-6	65.5	n/a	non-parametric	0.049	0.343
IL-7	2.0	(1.2, 2.8)	parametric	<0.001	<0.011
IL-8	2207.3	(643.7, 3770.9)	parametric	0.011	0.121
IL-10	38.9	n/a	non-parametric	0.002	0.014
IL-12(p70)	3.2	(2.0, 4.4)	parametric	<0.001	<0.011
IL-13	4.8	n/a	non-parametric	0.002	0.014
IL-17A	31.0	(25.4, 36.7)	parametric	<0.001	<0.011
G-CSF	18.5	n/a	non-parametric	0.064	0.448
GM-CSF	4.9	(2.3, 7.4)	parametric	0.002	0.022
IFN-γ	177.4	(146.3, 208.5)	parametric	<0.001	<0.011
MCAF	1464.4	(607.4, 2321.4)	parametric	0.004	0.044
MIF	364.9	(264.5, 465.4)	parametric	<0.001	<0.011
RANTES	841.3	(571.0, 1111.6)	parametric	<0.001	<0.011
TNF-α	1898.5	(1213.8, 2583.2)	parametric	<0.001	<0.011

[a]Mean or median: value presented dependent upon the normality and homogeneity of variance of data used for comparison. Where data are normally distributed and homoscedastic, parametric paired student t-tests were conducted to assess statistically significant differences and mean is presented. Where data violated one or more assumptions of the t-test, a Wilcoxon signed-rank test was applied and median value of effect of DENV infection is presented.

[b]CI: confidence interval. A 95% confidence interval of the estimate of the effect of DENV infection on cytokine production is presented for data amenable to parametric testing.

[c]Adjusted: p-values were adjusted by a simple Bonferroni correction. [284]

[d]parametric: tests were conducted using a paired student t-test given the considerable donor-to-donor variability of baseline cytokine levels.

[e]non-parametric: Wilcoxon signed-rank tests were applied in place of the paired student t-test for data that did not conform to a normal distribution and/or demonstrated heteroscedascity.

V.3.B. Temporal dynamics of inflammation in response to DENV infection of MDMΦs

Given the dynamic environment of immune responses to pathogens, and especially the dynamics of immune responses to DENV discussed in *Chapter I*, twelve of the strongest responding cytokines identified at day three p.i. were investigated in greater detail over a course of five days to understand the dynamics of the MDMΦ-mediated immune response to DENV (*Figure 5.2*). Only two cytokines, IFN-γ and TNF-α, were induced at all three time points measured (*Figure 5.2F* and *5.2L*), although, IP-10 correlated well with IFN-γ induction as anticipated. While IFN-γ was induced at day 5 in comparison to day 1 in uninfected samples (via *media stress*, α=0.008), the level of induction of IFN-γ by DENV was significantly higher. In contrast, the induction of IP-10 at day 5 by media stress saturated the limit of detection of the assay thereby preventing measurement of further induction of the cytokine by DENV infection. Nevertheless, the early and prolonged induction of TNF-α and IFN-γ and the correlated induction of IP-10 validate the central role of these cytokines in the MDMΦ response to DENV as predicted by transcriptomics experiments in *Chapter IV*. Notably, pro-inflammatory cytokines IL-6, IL-17A, MIF, and RANTES were induced at later time points (day 3 and day 5) in coordination with the haemapoietic growth stimulating factor G-CSF. This delayed induction suggests that these cytokines are involved in the proliferation of the immune response but not integral to the establishment of a DENV-specific inflammatory environment. Finally, activation of IL-10 was observed at day 3 p.i. in coordination with the proliferating inflammatory response suggesting that macrophages in the context of DENV infection attempt to control inflammation. Although marginal decreases can be observed for TNF-α and IFN-γ production in comparing day 5 to day 3, this change is relatively weak and not necessarily the result of successful IL-10 mediated control of inflammation. Furthermore, continued induction of other inflammatory cytokines (*e.g.* IL-6 and MIF) indicates unsuccessful control of inflammation via the observed induction of IL-10.

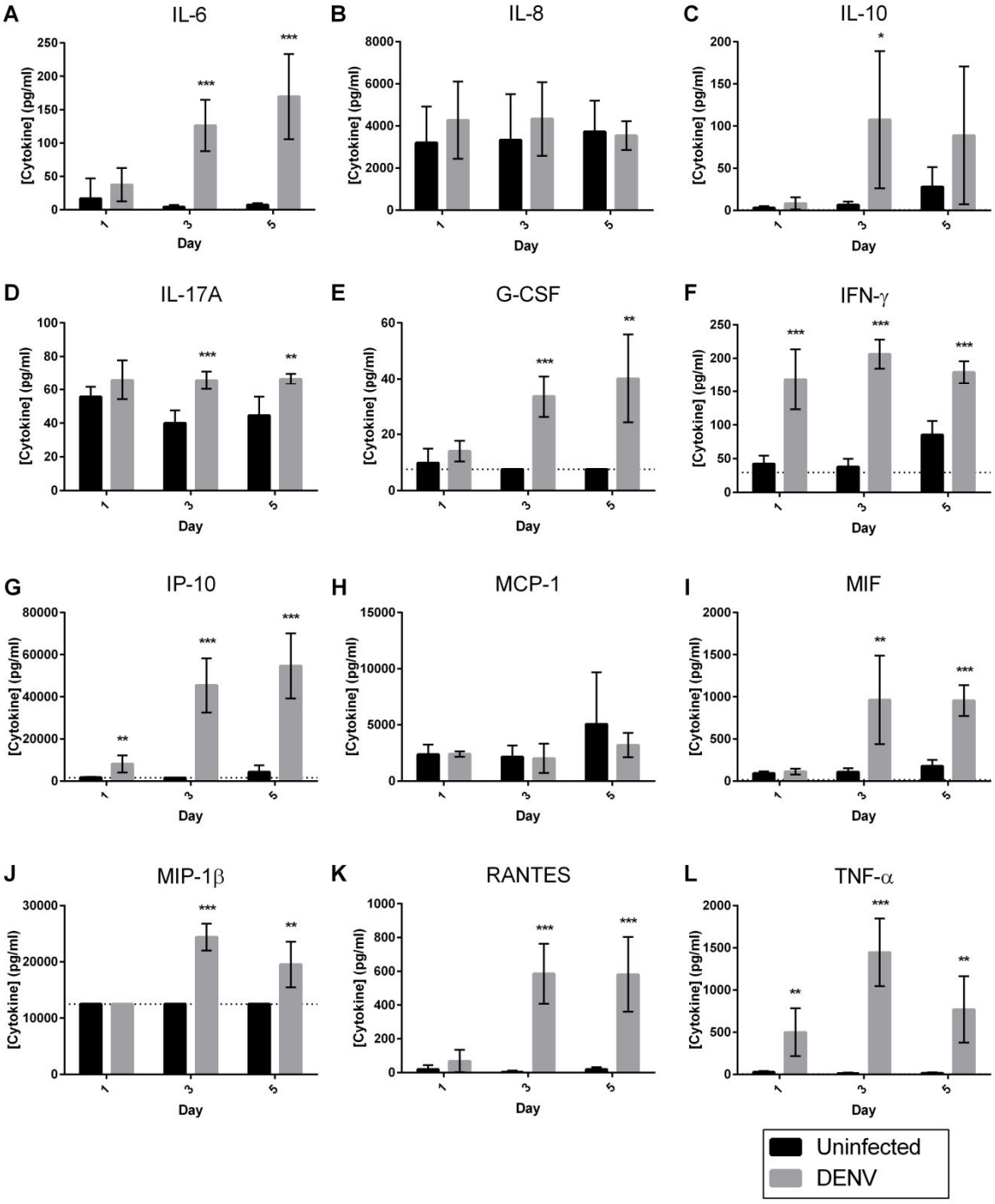

FIGURE 5.2. Temporal dynamics of MDMΦ cytokine response to DENV infection. MDMΦs isolated from 5 donors were individually cultured in the absence (black bars) or presence of DENV infection (grey bars) and cytokine levels in supernatants were assayed by Luminex multiplex bead assay. A 1:100 dilution was required for IP-10 (**G**) and MIP-1β (**J**), and these cytokines were analysed by ELISA. Supernatants were collected at the time post infection as indicated on the x-axis and measured in technical singlicate. Error bars represent standard deviation of biological replicates (n=5). Values beyond the limit of detection (LOD) were set to the relevant minimum or maximum value with minimum LOD indicated by a dashed line. Significant differences ($\alpha<0.05$, $\alpha<0.01$, and $\alpha<0.001$ represented by *, **, and *** respectively) between control and infected cells at a given time-point were determined by parametric *t*-tests and Holm-Šídák correction method for multiple comparisons.

V.3.C. M*O*N-DNJ attenuates the inflammatory response to diverse stimuli

The production of the same twelve cytokines in response to LPS treatment over the same five day time course was assessed as shown in *Figure 5.3*. As with the transcriptomic response described in *Chapter IV*, the rapid and considerable induction of nearly all inflammatory cytokines assayed was in accordance with previously published inflammatory responses to LPS. Whereas only IFN-γ and TNF-α responded to DENV infection at 24 hours p.i., IL-6, IL-10, IL-17A, G-CSF, IFN-γ, IP-10, RANTES, and TNF-α were all induced with LPS treatment. These responses were generally sustained, and only MIF and MIP-1β demonstrated a delayed response to the bacterial stimulus.

Using the divergent stimuli of DENV infection (viral) and LPS treatment (bacterial), the ability of iminosugars to modulate host inflammatory responses elicited through diverse molecular mechanisms was investigated. Responses at 24 hours p.i. were of particular interest to reduce feedback-related obfuscation of results although modulation of all twelve cytokines was assessed at all three time points for uninfected cells as well as those infected with DENV or treated with LPS (*Figures 5.4 - 5.16*). A robust immunomodulatory capacity was noted for M*O*N-DNJ as demonstrated by the drug's ability to reduce production of IFN-γ produced as a consequence of DENV infection, LPS treatment, and media stress and to reduce DENV and LPS induced TNF-α (*Figure 5.4*). *N*B-DNJ, a less potent inhibitor of α-glucosidases as measured previously by FOS (refer to *Figure 3.5*), demonstrated equivalent reduction of media stress-induced IFN-γ and also reduced DENV-induced IFN-γ but to a lesser extent than was observed for M*O*N-DNJ. Reduction of LPS-induced IFN-γ and DENV-induced TNFα was observed with *N*B-DNJ treatment; however, these results were not statistically significant. In contrast, *N*B-DGJ, an iminosugar lacking glucostereochemistry was only weakly able to reduce IFN-γ induced by media stress and did not modulate IFN-γ or TNF-α produced as a consequence of DENV infection or LPS treatment. In addition to the robust reduction of IFN-γ and TNF-α, treatment with

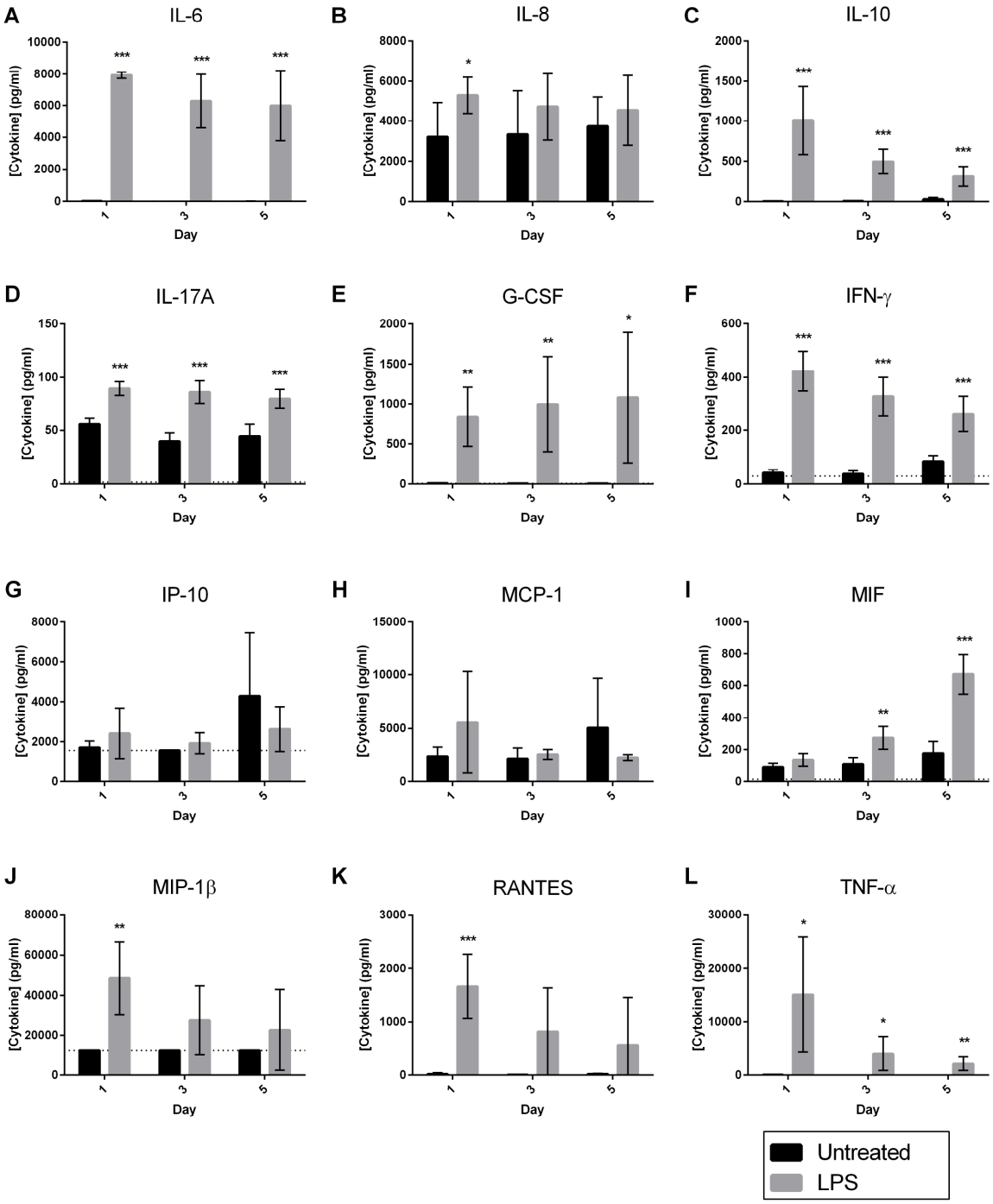

FIGURE 5.3. Temporal dynamics of MDMΦ cytokine response to LPS treatment. MDMΦs isolated from 5 donors were individually cultured in the absence (black bars) or presence of 100 ng/ml of LPS isolated from *Salmonella enterica* (grey bars) and cytokine levels in supernatants were assayed by Luminex multiplex bead assay. A 1:100 dilution was required for IP-10 (**G**) and MIP-1β (**J**), and these cytokines were analysed by ELISA. Supernatants were collected at the time post infection as indicated on the x-axis and measured in technical singlicate. Error bars represent standard deviation of biological replicates (n=5). Values beyond the limit of detection (LOD) were set to the relevant minimum or maximum value with minimum LOD indicated by a dashed line. Significant differences ($\alpha<0.05$, $\alpha<0.01$, and $\alpha<0.001$ represented by *, **, and *** respectively) between control and infected cells at a given time-point were determined by parametric *t*-tests and Holm-Šídák correction method for multiple comparisons.

M*O*N-DNJ reduced production of IL-10 (*Figure 5.7*), G-CSF (*Figure 5.9*), and RANTES (*Figure 5.15*) in the context of various stress situations though to a less robust extent than either IFN-γ or TNF-α (highlighted in *Figure 5.4* and displayed in greater detail in *Figures 5.10* and *5.16*). In concert, these data suggest that iminosugars possessing glucostereochemistry are capable of attenuating the innate immune response to diverse pathogens at early time points during the course of infection and that M*O*N-DNJ is particularly capable of modulating MDMΦ innate immune responses. It is perhaps crucial to consider that the observed reduction in inflammation is not complete (*i.e.* level of inflammatory proteins produced is not reduced to baseline levels) suggesting that inflammatory responses may remain intact but be dampened in the case of human infection.

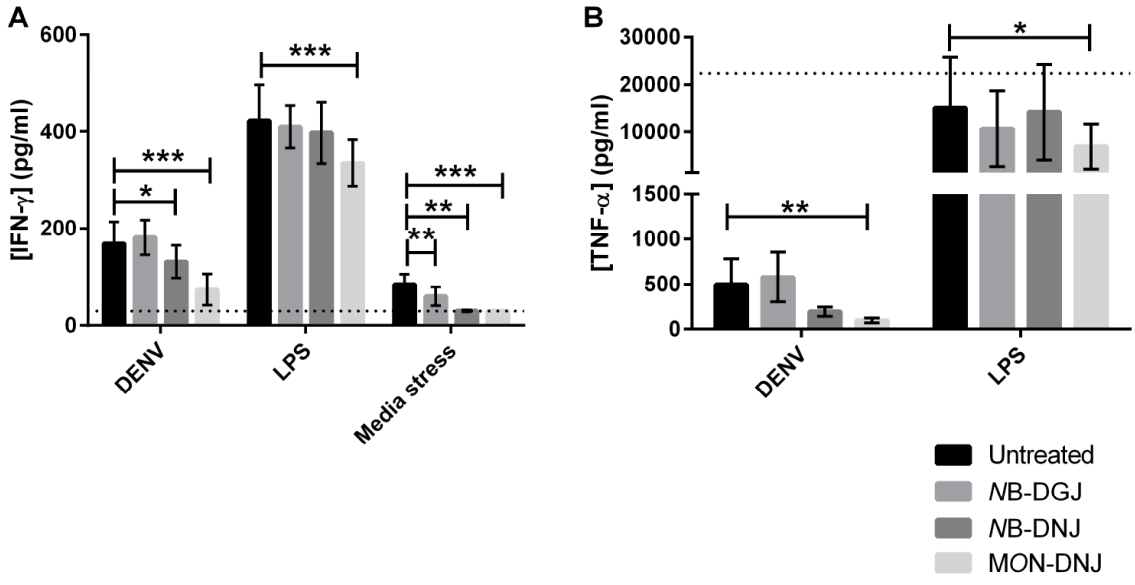

FIGURE 5.4. M*O*N-DNJ treatment of MDMΦs reduces production of IFN-γ and TNF-α. Production of IFN-γ (**A**) and TNF-α (**B**) at 24 hours p.i. is reduced in MDMΦs infected with DENV or treated with LPS through treatment with M*O*N-DNJ (fourth bar). Effects of *N*B-DGJ (second bar) and *N*B-DNJ (third bar) are generally weaker than for M*O*N-DNJ as discussed in the text. Significant differences ($\alpha<0.05$, $\alpha<0.01$, and $\alpha<0.001$ represented by *, **, and *** respectively) between control and drug-treated cells were determined by repeated measures parametric ANOVA and Holm-Šídák post-hoc testing. Uninfected, untreated cells produced 29.54 pg/ml IFN-γ and 1.78 pg/ml TNF-α. Dashed lines represent the limits of detection of the assays.

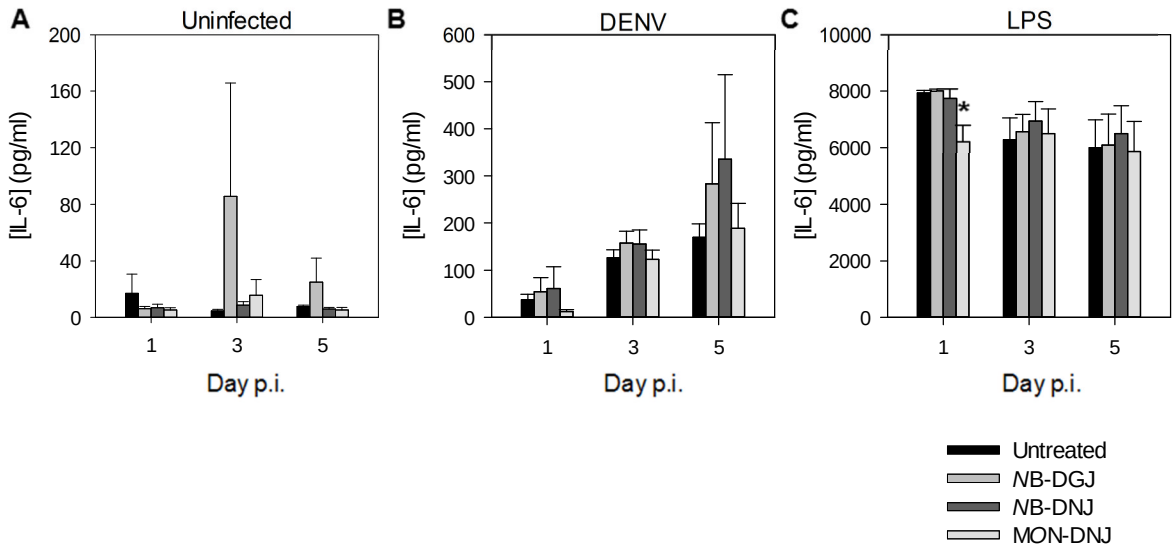

FIGURE 5.5. Modulation of interleukin-6 (IL-6) by iminosugars. MDMΦs were uninfected (**A**), infected with DENV (**B**), or treated with LPS (**C**) and treated with various iminosugars. Cytokines secreted into supernatant were quantified using a Luminex multiplex protocol and significant differences (indicated by an asterisk (*) represent $\alpha<0.05$) were determined with respect to untreated controls by repeated measures ANOVA and Holm-Šidák post-hoc testing.

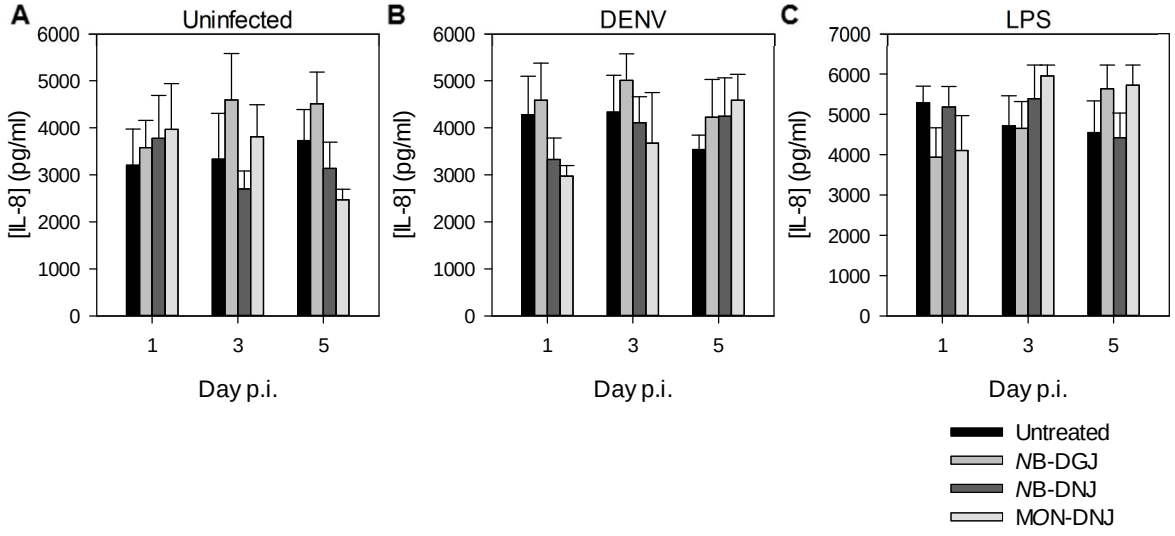

FIGURE 5.6. Modulation of interleukin-8 (IL-8) by iminosugars. MDMΦs were uninfected (**A**), infected with DENV (**B**), or treated with LPS (**C**) and treated with various iminosugars. Cytokines secreted into supernatant were quantified using a Luminex multiplex protocol and significant differences (indicated by an asterisk (*) represent $\alpha<0.05$) were determined with respect to untreated controls by repeated measures ANOVA and Holm-Šidák post-hoc testing.

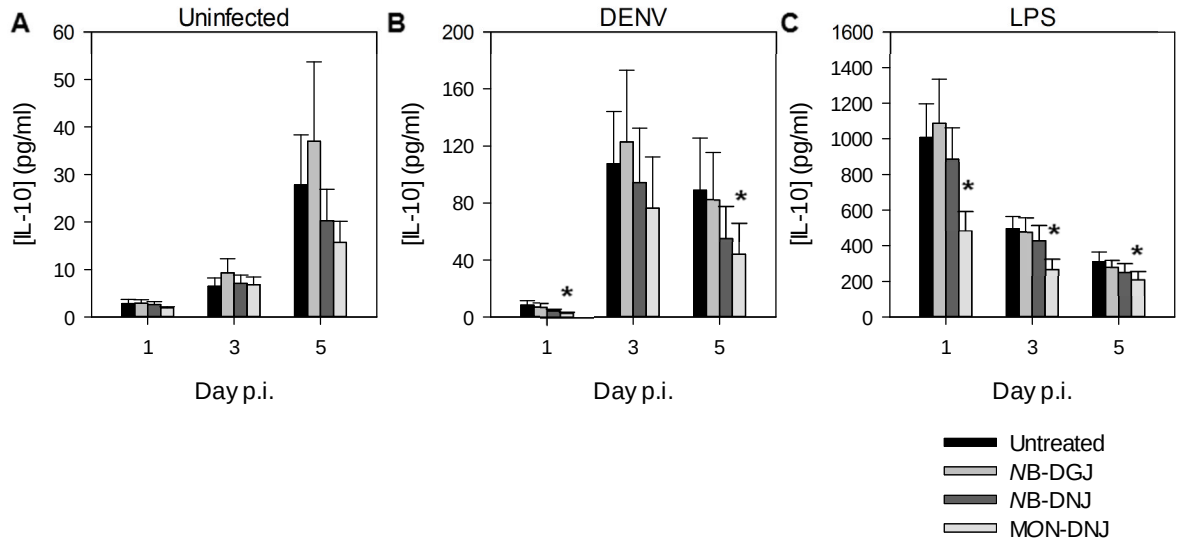

FIGURE 5.7. Modulation of interleukin-10 (IL-10) by iminosugars. MDMΦs were uninfected (**A**), infected with DENV (**B**), or treated with LPS (**C**) and treated with various iminosugars. Cytokines secreted into supernatant were quantified using a Luminex multiplex protocol and significant differences (indicated by an asterisk (*) represent $\alpha<0.05$) were determined with respect to untreated controls by repeated measures ANOVA and Holm-Šidák post-hoc testing.

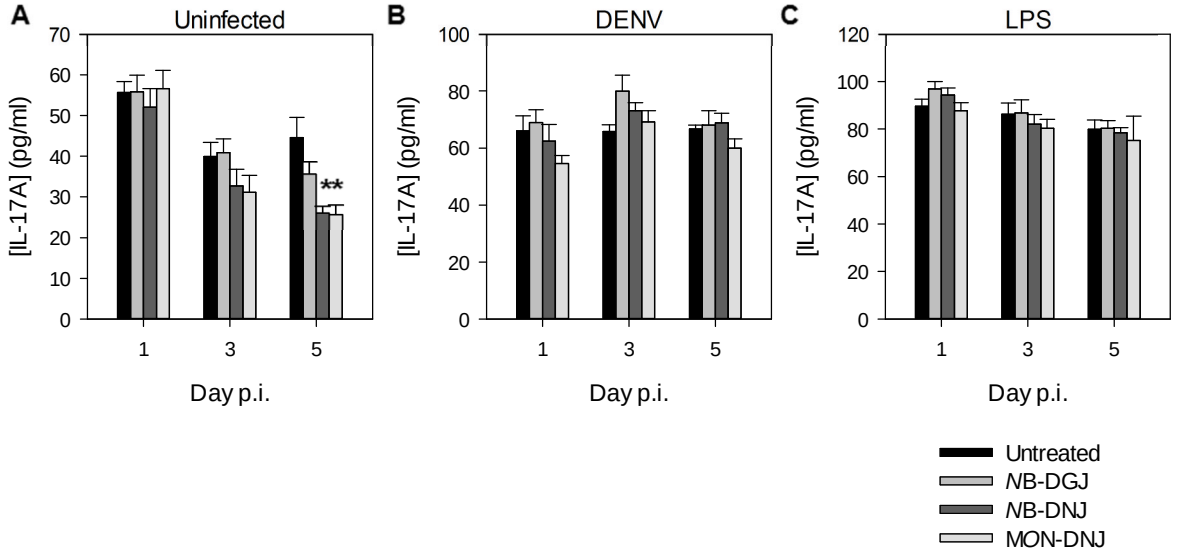

FIGURE 5.8. Modulation of interleukin-17A (IL-17A) by iminosugars. MDMΦs were uninfected (**A**), infected with DENV (**B**), or treated with LPS (**C**) and treated with various iminosugars. Cytokines secreted into supernatant were quantified using a Luminex multiplex protocol and significant differences (indicated by an asterisk (*) represent $\alpha<0.05$) were determined with respect to untreated controls by repeated measures ANOVA and Holm-Šidák post-hoc testing.

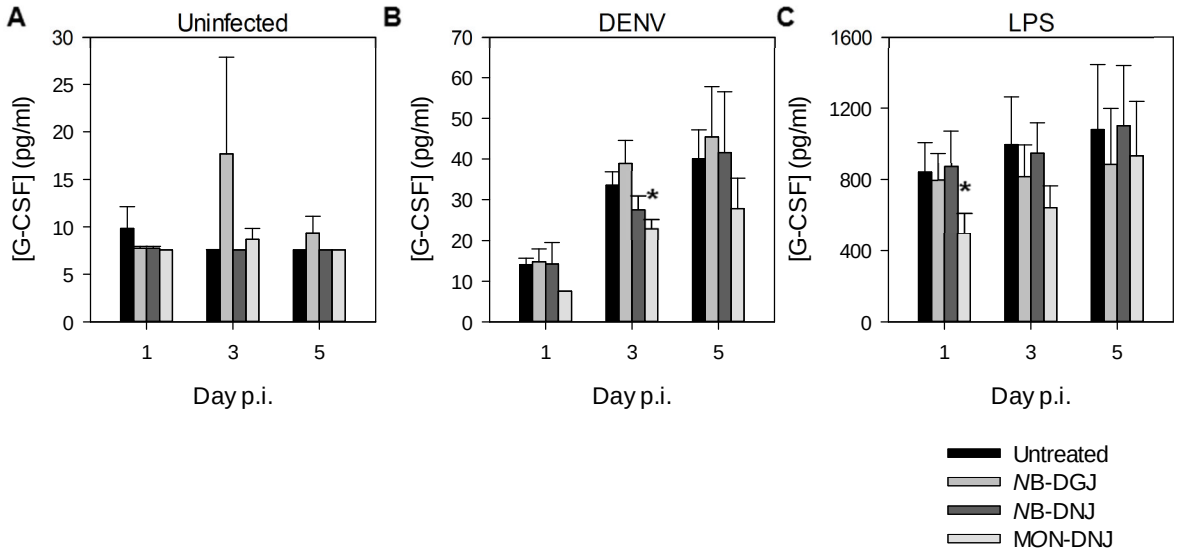

FIGURE 5.9. Modulation of granulocyte colony-stimulating factor (G-CSF) by iminosugars. MDMΦs were uninfected (**A**), infected with DENV (**B**), or treated with LPS (**C**) and treated with various iminosugars. Cytokines secreted into supernatant were quantified using a Luminex multiplex protocol and significant differences (indicated by an asterisk (*) represent $\alpha<0.05$) were determined with respect to untreated controls by repeated measures ANOVA and Holm-Šidák post-hoc testing.

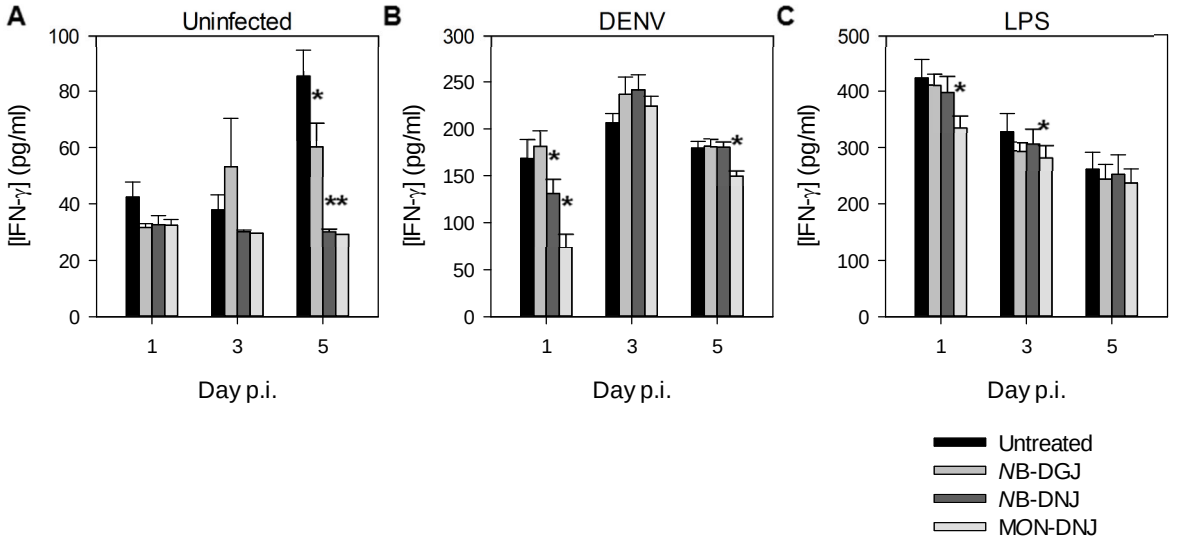

FIGURE 5.10. Modulation of interferon-gamma (IFN-γ) by iminosugars. MDMΦs were uninfected (**A**), infected with DENV (**B**), or treated with LPS (**C**) and treated with various iminosugars. Cytokines secreted into supernatant were quantified using a Luminex multiplex protocol and significant differences (indicated by an asterisk (*) represent $\alpha<0.05$) were determined with respect to untreated controls by repeated measures ANOVA and Holm-Šidák post-hoc testing.

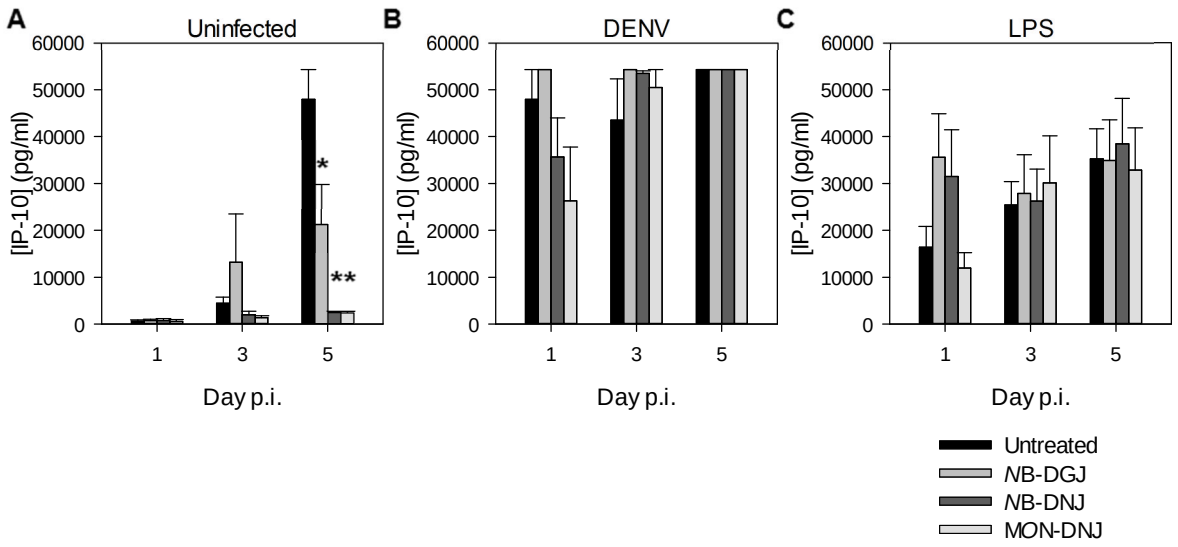

FIGURE 5.11. Modulation of interferon gamma-induced protein 10 (IP-10) by iminosugars. MDMΦs were uninfected (**A**), infected with DENV (**B**), or treated with LPS (**C**) and treated with various iminosugars. Cytokines secreted into supernatant were quantified using a Luminex multiplex protocol and significant differences (indicated by an asterisk (*) represent $\alpha<0.05$) were determined with respect to untreated controls by repeated measures ANOVA and Holm-Šidák post-hoc testing.

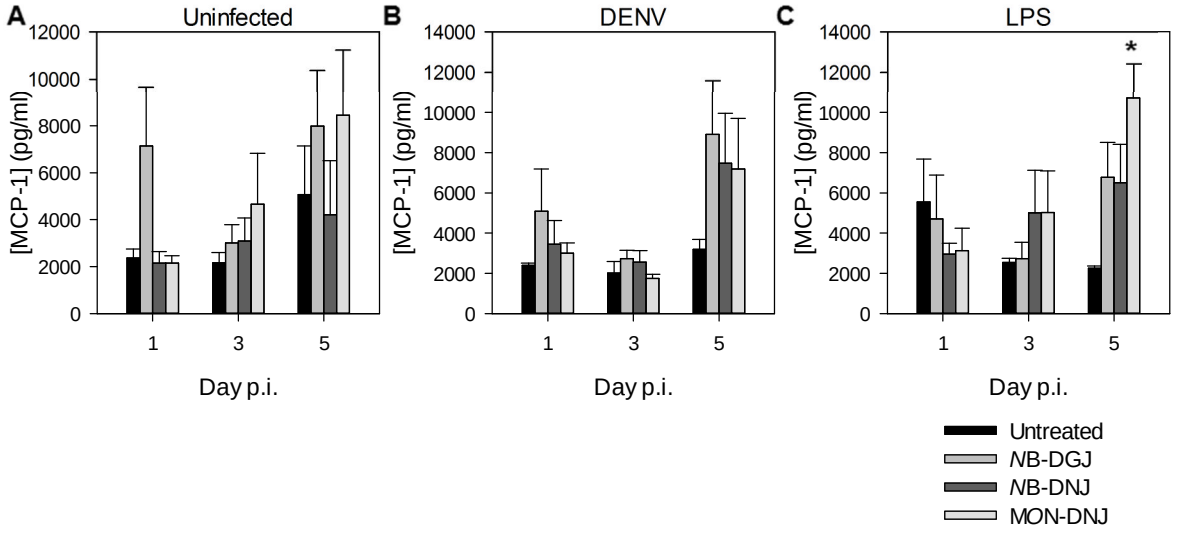

FIGURE 5.12. Modulation of monocyte chemotactic protein 1 (MCP-1/MCAF) by iminosugars. MDMΦs were uninfected (**A**), infected with DENV (**B**), or treated with LPS (**C**) and treated with various iminosugars. Cytokines secreted into supernatant were quantified using a Luminex multiplex protocol and significant differences (indicated by an asterisk (*) represent $\alpha<0.05$) were determined with respect to untreated controls by repeated measures ANOVA and Holm-Šidák post-hoc testing.

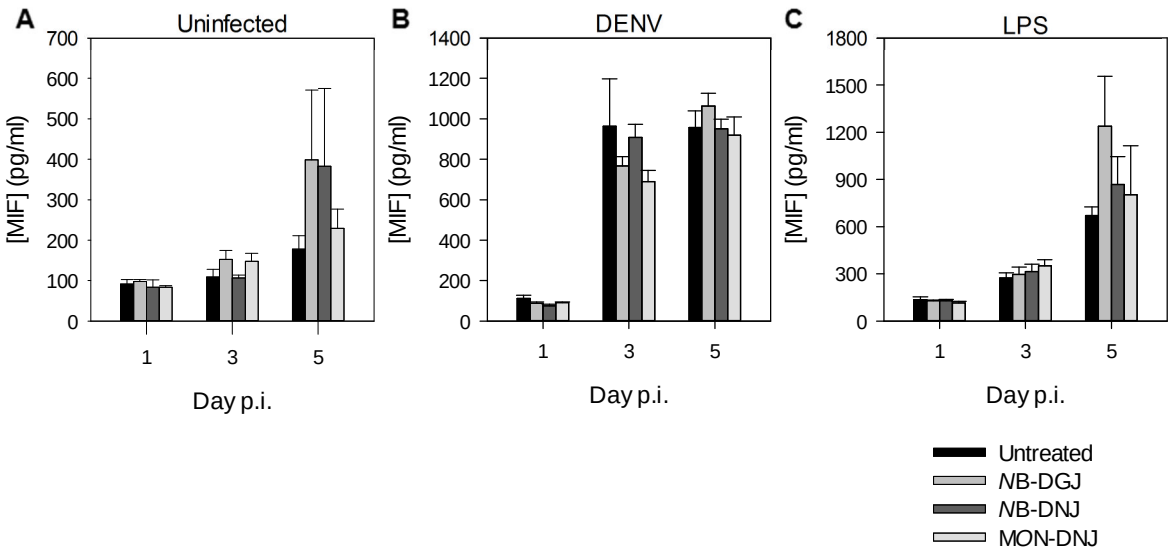

FIGURE 5.13. Modulation of macrophage migration inhibitory factor (MIF) by iminosugars. MDMΦs were uninfected (**A**), infected with DENV (**B**), or treated with LPS (**C**) and treated with various iminosugars. Cytokines secreted into supernatant were quantified using a Luminex multiplex protocol and significant differences (indicated by an asterisk (*) represent $\alpha<0.05$) were determined with respect to untreated controls by repeated measures ANOVA and Holm-Šidák post-hoc testing.

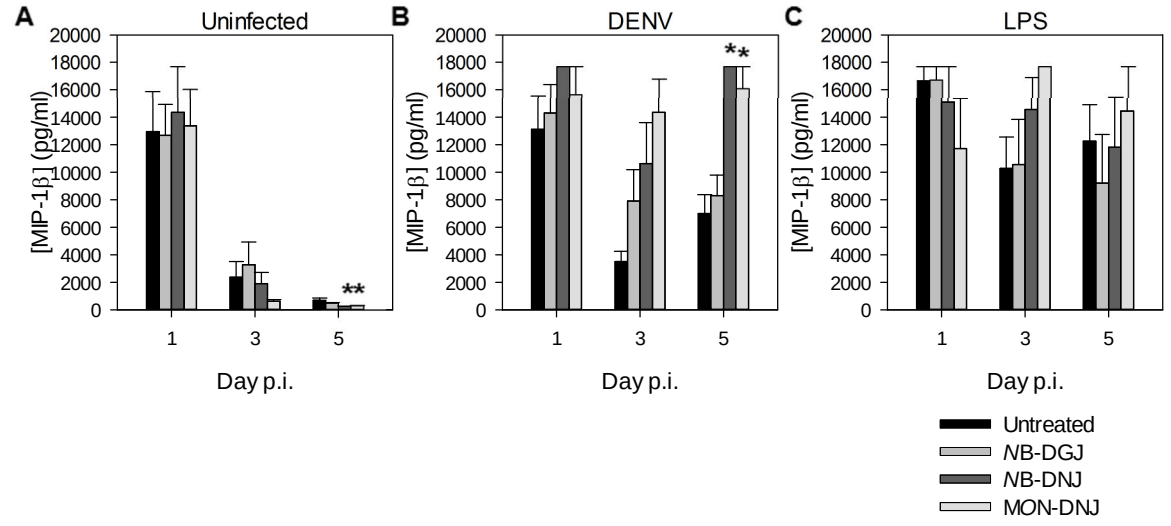

FIGURE 5.14. Modulation of macrophage inflammatory protein-1β (MIP-1β) by iminosugars. MDMΦs were uninfected (**A**), infected with DENV (**B**), or treated with LPS (**C**) and treated with various iminosugars. Cytokines secreted into supernatant were quantified using a Luminex multiplex protocol and significant differences (indicated by an asterisk (*) represent $\alpha<0.05$) were determined with respect to untreated controls by repeated measures ANOVA and Holm-Šidák post-hoc testing.

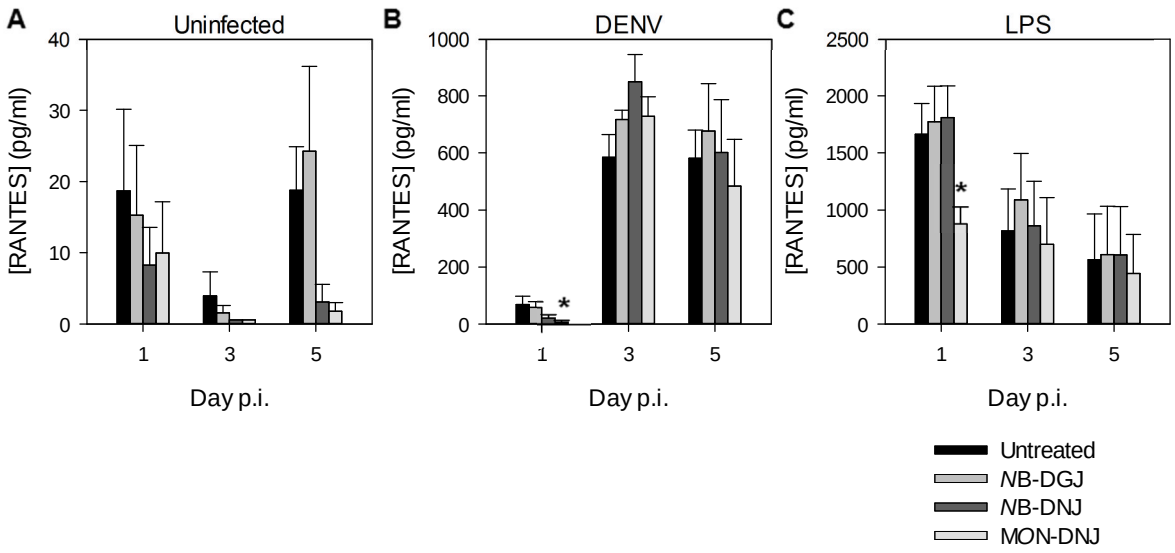

FIGURE 5.15. Modulation of regulated on activation, normal T cell expressed and secreted (RANTES) by iminosugars. MDMΦs were uninfected (**A**), infected with DENV (**B**), or treated with LPS (**C**) and treated with various iminosugars. Cytokines secreted into supernatant were quantified using a Luminex multiplex protocol and significant differences (indicated by an asterisk (*) represent $\alpha<0.05$) were determined with respect to untreated controls by repeated measures ANOVA and Holm-Šidák post-hoc testing.

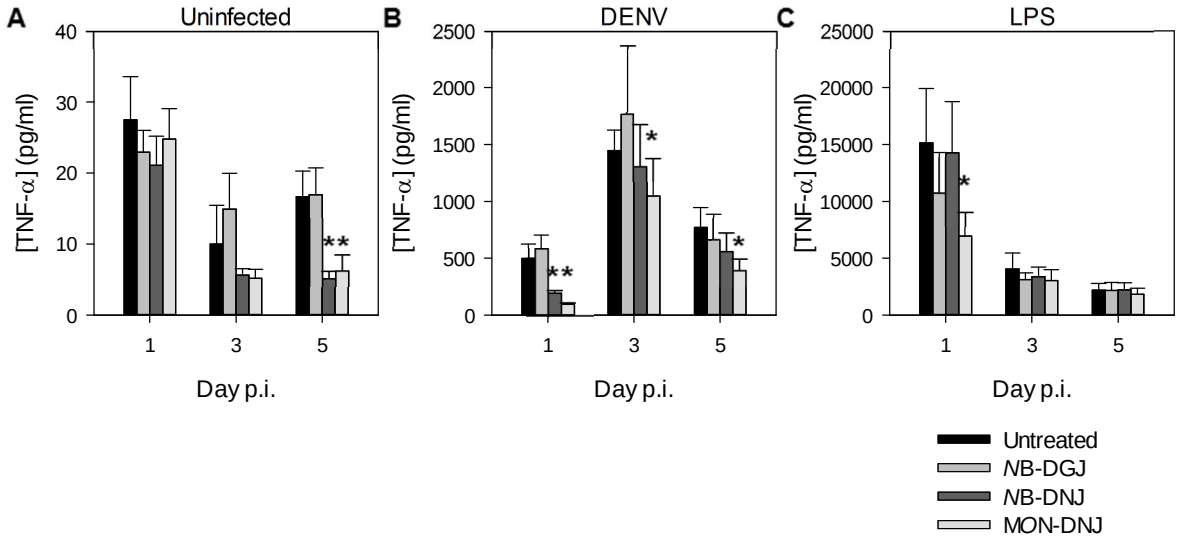

FIGURE 5.16. Modulation of tumour necrosis factor-α (TNF-α) by iminosugars. MDMΦs were uninfected (**A**), infected with DENV (**B**), or treated with LPS (**C**) and treated with various iminosugars. Cytokines secreted into supernatant were quantified using a Luminex multiplex protocol and significant differences (indicated by an asterisk (*) represent $\alpha<0.05$) were determined with respect to untreated controls by repeated measures ANOVA and Holm-Šidák post-hoc testing.

V.4. Discussion

As with the transcriptomics data in *Chapter IV*, a multiplex approach to studying cytokine responses of MDMΦs facilitated a more comprehensive understanding of the implications of using iminosugar treatment as a therapeutic strategy against DENV infection. Initial assays of a considerable number of the cytokines previously implicated in DENV infection and/or severe pathogenic outcomes (see *Chapter I*) demonstrated that MDMΦs produce most of these cytokines in response to DENV infection and that the IFN-γ, TNF-α, and RANTES response at this time point is particularly strong and robust. The aberrant behaviour of one donor, DG, indicates that host genetic background and/or immunological memory may play a crucial role in the cytokine response to infection. It is tempting to speculate that the dominant production of IL-7 by cells from this donor is a product of recognition of the pathogen by the adaptive immune response (donors are cultured in autologous plasma). Given that IL-7 production stimulates production of lymphoid cells [285-287] and is involved in V(D)J rearrangement, [288] previous exposure to DENV and subsequent recognition by the host could promote MDMΦ-driven IL-7 production as a means of amplifying the adaptive immune response to the invading pathogen. Alternatively, genetic pre-disposition to an IL-7 dominant response to DENV infection may be responsible for the observed responses. In the presence of IL-7, CD4+ T cell growth is induced and DENV-specific cytotoxic activity is maintained in the absence of non-specific cytotoxic activity [289] suggesting that this individual may be pre-disposed to effective DENV clearance whether by memory or genetic background. Unfortunately, the anonymous donor protocols used preclude further study of this particular individual's genetic predisposition to cytokine responses and immune status to DENV infection; however, the considerable ability of the IL-7 response to apparently blunt or act in diametric opposition to the conserved inflammatory response to DENV infection warrants future investigation.

The time-course investigation of cytokine induction in response to DENV in MDMΦs was instrumental in validating the predicted importance of IFN-γ and TNF-α in the early stages of the inflammatory response to DENV infection. Whereas many inflammatory (and anti-inflammatory) cytokines could be detected at day three p.i., the cytokine response at day one p.i. was considerably less prolific. Previous investigations of monocytes and monocyte-derived macrophages infected i*n vitro* with DENV have provided a prolific number of cytokines which respond to viral infection [77,87,119,290-299] with a particular focus on the induction of TNF-α and/or MIF promoting the vascular leak phenotype. [87,295,297] Indeed, many of the cytokines previously identified as produced in response to DENV infection of monocytes/macrophages were detected in my analyses. Notably, recent work [116,117] has highlighted the importance of so-called GM-macrophages (differentiated in response to GM-CSF) in contributing to the inflammatory, and potentially detrimental, response of macrophages to DENV via CLEC5A-mediated cytokine signalling. The IL-4 treated MDMΦ system used in my work demonstrates production of IL-1β and IL-17A (markers of GM-macrophage infection with DENV) in response to DENV infection suggesting that at least a proportion of the cells produced are functionally similar to GM-macrophages.

The results of *Chapter IV* indicated that IFN-γ and TNF-α in concert with type I interferons largely drive the inflammatory response to DENV infection observed at a transcriptional level. Indeed, by 24 hours p.i. both IFN-γ and TNF-α are strongly induced in response to DENV infection and these cytokines remain elevated throughout the five day time-course of infection. Consequently, the induction of further inflammatory markers at days three and five p.i. is likely a function of amplification of the initial IFN-γ/TNF-α inflammatory response. These results do not demonstrate any level of control over development of severe pathology for either IFN-γ or TNF-α in isolation or in concert, but the data do suggest a central role of these two cytokines in controlling the development of the innate immune response to DENV infection. The possibility remains that one or both of these

cytokines may be the dark lord cytokine whose excess production in response to DENV infection precipitates the development of severe pathologies, but the complexity of the feedback networks involved in inflammatory responses in conjunction with the difficulty of isolating a single cytokine's molecular mechanism(s) of action and direct (and crucially, independent) effects in a complex system such as the vasculature severely complicate validation of these hypotheses. Nevertheless, significant correlative evidence of severe disease and excess cytokine production coupled with the apparent control of innate inflammatory responses suggests that modulation of IFN-γ and/or TNF-α may alter the progression to severe DENV-induced pathology.

To investigate the hypothesis that iminosugars could influence the innate immune response to DENV, early modulation of both IFN-γ and TNF-α was investigated. Because iminosugars possessing glucostereochemistry reduce production of infectious virus, assessment of modulation of the same cytokines induced in a pathogen-independent context was crucial to establish direct attenuation of cytokine production in contrast to reduced cytokine production as a consequence of reduced viral load (and therefore immune stimulation). In fact, M*O*N-DNJ reduced both IFN-γ and TNF-α produced in response to DENV and the bacterial TLR-4 agonist LPS. In addition, IFN-γ induced by media stress in the absence of any pathogen was reversed to below detectable levels by treatment with M*O*N-DNJ. Treatment with *N*B-DNJ revealed a similar, though less powerful modulation of both IFN-γ and TNF-α, and this immunomodulation was almost entirely absent for *N*B-DGJ. As such, it appears that iminosugars with glucostereochemistry, in particular M*O*N-DNJ, are capable of modulating the innate immune response to both viral and bacterial pathogens. As noted previously, this modulation does not reduce cytokine production to baseline levels suggesting that the inflammatory response remains intact but dampened. Studies of DENV infection in an ADE mouse model have revealed that M*O*N-DNJ can provide full protection in a lethal model down to 10 mg/kg/dose and that this activity is coordinated with a significant reduction of both IFN-γ and TNF-α among other cytokines. [209]

Furthermore in this model, the levels of these cytokines remained above baseline suggesting that the results presented from primary human macrophages translate to survival of a DENV infected living system. It would be of further interest to test if cytokines induced by diverse pathogens (*e.g.* diverse viruses, bacteria, and eukaryotic pathogens) are modulated similarly with M*O*N-DNJ treatment. If such a broad-spectrum immunomodulatory capacity was observed, it could help clarify both the mechanism of action of M*O*N-DNJ cytokine effects and provide a possible treatment strategy for a diverse set of pathogens, and beyond pathogens perhaps also to other inflammatory diseases.

As intriguing as these results may be, the molecular mechanisms responsible for immunomodulation remain to be determined. It is possible that inhibition of *N*-linked glycan trimming is responsible for the reduced inflammation observed. IFN-γ possesses two sites for *N*-linked glycosylation which are occupied [300] suggesting that it may be dependent upon the CANX cycle for proper folding. Indeed, DNJ-derivative iminosugars have been shown to reduce production of IFN-γ in CD3-stimulated T cells [223] via degradation of newly formed IFN-γ due to blockade of interaction with the ER chaperone CALR. [222] Furthermore, significant evidence from diverse pathogen stimulation environments suggests that IFN-γ production enhances TNF-α production, particularly in macrophages. [290,301,302] Thus, if iminosugar inhibition of α-glucosidases is directly capable of reducing IFN-γ production, then the observed inhibition of TNF-α may be a direct consequence of this activity. Alternatively, induction of the UPR may activate transcription factors which activate (oxidative) stress response genes. As such, induction of a cell's stress response by inhibition of glycoprotein folding may account for the reduced inflammation observed. It is additionally possible that inhibition of production/function of a receptor necessary for pathogen identification and/or amplification of the inflammatory immune cascade, such as members of the TNF receptor superfamily which possess many sites for *N*-linked glycosylation and depend heavily upon disulphide bond formation for folding

and function, [303] may be responsible for the reduced pro-inflammatory signals observed. It may also be that an alternative, as yet undefined, activity of M*O*N-DNJ is responsible for the considerable anti-inflammatory capacity described herein or that a combination of the above activities is required for the observed effects.

In any case, the cytokine data presented in this chapter validates the prediction of *Chapter IV* that IFN-γ and TNF-α are central mediators of the early MDMΦ inflammatory response to DENV infection and that M*O*N-DNJ can reduce this inflammation. These observations expand the clinical potential of M*O*N-DNJ as a possible mediator of excess inflammation, generally, in addition to the previously noted antiviral activities. Investigation of M*O*N-DNJ for therapeutic indications defined by excessive inflammation such as cytokine storm in pathologies as diverse as Ebola, avian influenza viruses, and bacterial sepsis may prove successful, and studies to this purpose have been initiated.

VI

M*O*N-DNJ modulation of TNF ligand and receptor superfamily members *in vivo*

VI.1. Abstract

Modulation of the immune response to DENV by M*O*N-DNJ is suggested by *in vitro* work in human macrophages; however, this model lacks the essential interaction of the vast array of immune cells and tissues involved in the developing host response to infection. As such, extension of immunomodulation to a clinical environment needs to be validated first in a living system in which the immune system can function relatively intact. The best available model for DENV at the present time is an ADE model of infection of mice deficient in receptors for type I and II interferons. TNF receptor/ligand pairs were demonstrated in transcriptomics studies to respond to iminosugar treatment, thus these important co-stimulatory molecules were assayed to assess iminosugar immunomodulation *in vivo*. In addition, comparison of M*O*N-DNJ and another clinical candidate for DENV therapeutic use, Celgosivir, was conducted to determine relative antiviral efficacy and tissue effects of the compounds. Gross differences in pathology between uninfected mice and infected mice were observed, particularly in the spleen, lymph node, and liver, and these DENV-induced pathologies appeared to be resolved with treatment with either iminosugar. Visual differences were supported at a molecular level by altered transcript levels of GAPDH – a previously reported *housekeeping* gene. Although molecular mechanisms of iminosugar anti-inflammatory function could not be determined, modulation of TNF receptor/ligand not accounted for by changes in GAPDH were identified following treatment with both M*O*N-DNJ and Celgosivir. Thus, these experiments provide evidence that iminosugars as a class can modulate inflammation, and provide direction for future experiments to determine both tissue-level and molecular events involved in this process.

VI.2. Introduction

Two iminosugars are under consideration as clinical candidates for therapeutic administration in the case of DENV infection. *In vitro* evidence of antiviral activity of castanospermine has facilitated the development of a pro-drug, 6-*O*-butanoyl-castanospermine (Celgosivir). [304] Efficacy of Celgosivir against DENV *in vivo* has been demonstrated, [305,306] and dosing requirements have been established in animal models. [307] Similarly, M*O*N-DNJ has demonstrated *in vitro* antiviral efficacy as discussed in *Chapter III* (and published in [201]), and this activity has recently been extended to an *in vivo* model. [209] In spite of the presumed overlap in mechanism of action of the two drugs (via inhibition of α-glucosidases), the two drugs have not yet been compared either *in vitro* or *in vivo*. Furthermore, biodistribution and pharmacodynamics have not been published with either compound, thus access to and functional activity of iminosugars in tissues relevant to DENV infection remains unexplored. Finally, the previous chapters of this thesis suggest that M*O*N-DNJ, and potentially all iminosugars with glucostereochemistry, can modulate the immune response to diverse pathogens. This hypothesis has been borne-out for M*O*N-DNJ in the context of DENV infection as indicated by reduction of inflammatory cytokines in DENV-infected mice; [209] however, the molecular mechanism of reduced inflammation remains unclear. Is reduced inflammation a product of reduced virus, or is there a direct immunomodulatory effect of M*O*N-DNJ *in vivo*? Thus, the aims of *Chapter VI* of this thesis are to:

1) Compare the antiviral capacity of M*O*N-DNJ and Celgosivir,
2) Assess induction of unfolded protein response in tissues as a consequence of iminosugar treatment, and
3) Determine whether immunomodulatory activities observed *in vitro* can be recapitulated *in vivo*.

VI.3. Results

VI.3.A. Comparison of antiviral efficacy of clinical candidate iminosugars

The two iminosugars that are currently under consideration as clinical candidates for therapeutic treatment of DENV have both demonstrated efficacy in similar mouse models [209,306]; however, a direct comparison of antiviral efficacy has not been conducted. As such, the reduction of viral load as determined by circulating viral RNA and circulating infectious virus was assayed for mice administered either M*O*N-DNJ (100 mg/kg/dose, *t.i.d.,i.g.*) or Celgosivir (33 mg/kg/dose, *t.i.d. i.g.*) as demonstrated in *Figure 6.1*. Based on viral RNA levels, both iminosugars reduced circulating DENV levels of ADE-infected mice ($\alpha<0.05$) at day 3 p.i. and this trend appears to extend to infectious virus although results are not statistically significant due to the considerable variation in the assay ($\alpha=0.115$, power=0.282).

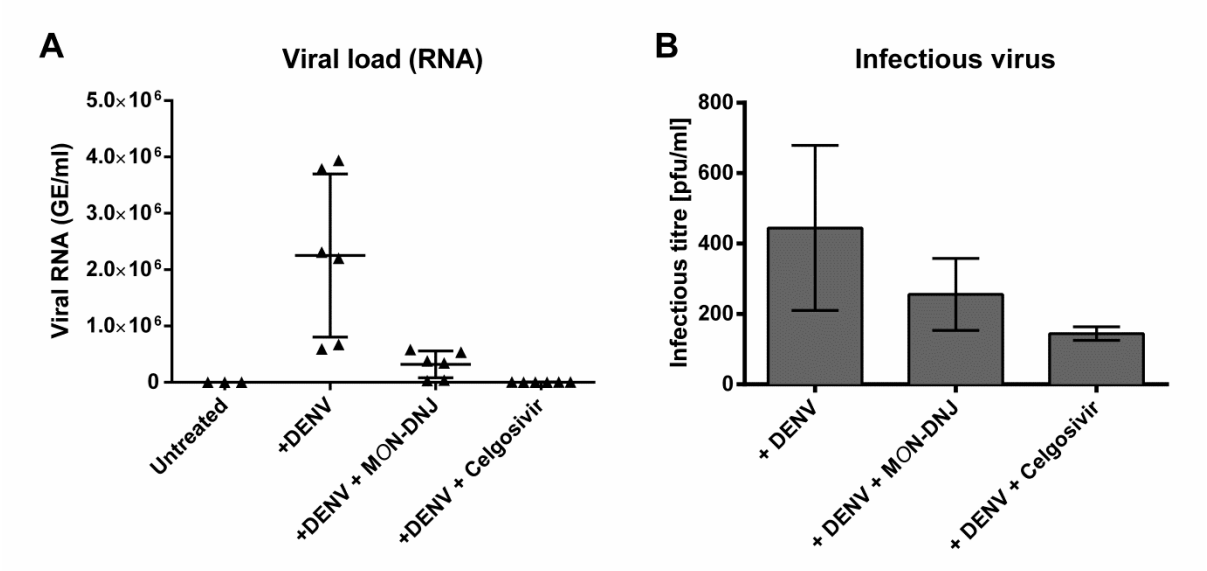

FIGURE 6.1. Antiviral efficacy of M*O*N-DNJ and Celgosivir in plasma of ADE infected mice. An ADE mouse model of DENV disease was infected with a lethal dose of virus and animals were treated with M*O*N-DNJ (100 mg/kg/dose, *t.i.d., i.g.*), Celgosivir (33 mg/kg/dose, *t.i.d., i.g.*), or untreated (n=3 per treatment). Both iminosugars reduced viral load in plasma as determined by viral qRT-PCR assay for NS5 (**A**) and plaque assay (**B**) although the plaque assay lacked sufficient power to conclude that the difference was statistically significant. qRT-PCR assays were conducted in technical duplicate (except for untreated samples for which one mouse was excluded due to sample contamination and one mouse was assayed in singlicate) and plaque assays were conducted in singlicate. In (**A**), large bars represent mean values and small bars represent the standard deviation. Error bars in (**B**) represent standard deviation.

Additionally, the viral load in several tissues was assessed by qRT-PCR for DENV NS5. As shown in *Figure 6.2*, the trend of reduction of viral load in response to iminosugar treatment extended to most tissues examined. The notable exceptions to this rule were the case of M*O*N-DNJ treatment of small intestine and Celgosivir treatment of spleen. Whereas a minor increase in viral load was noted in small intestine, a two fold increase in viral RNA relative to GAPDH controls was noted in spleen samples treated with Celgosivir. In all other cases, a strong reduction of viral load was noted in response to Celgosivir and a similar but generally weaker reduction was observed in response to M*O*N-DNJ.

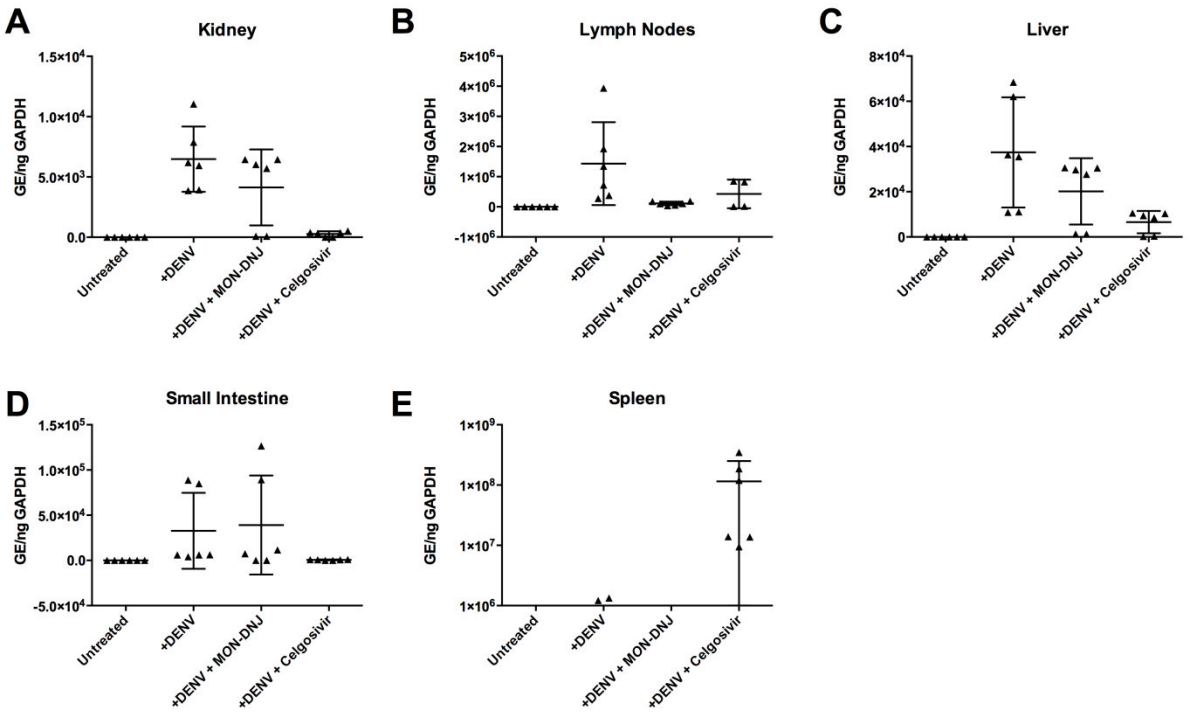

FIGURE 6.2. Antiviral efficacy of M*O*N-DNJ and Celgosivir in tissue of ADE infected mice. Mice were infected with virus and treated with iminosugar as in *Figure 6.1*. Viral load was determined by viral qRT-PCR assay for NS5 with normalisation to GAPDH levels for kidney (**A**), liver (**B**), lymph node (**C**), small intestine (**D**), and spleen (**E**). In all cases except for M*O*N-DNJ treatment in small intestine and Celgosivir treatment in spleen there was a reduction of viral load by iminosugar treatment. All assays were conducted in technical duplicate. Large bars represent mean values and small bars represent standard deviation. Note all y-axes are linear scale except for spleen which is presented in $\log_{10}$ due to $2\log_{10}$ increase in viral load with Celgosivir treatment.

VI.3.B. Modulation of host transcripts by iminosugars

The observed reduction of inflammation by iminosugars on a transcriptional and cytokine production level (described in *Chapters IV* and *V*) begs the question of whether these observations can be realised in a living animal model. In order to test this hypothesis, the modulation of six transcripts was investigated in spleen (*Figure 6.3*), small intestine (*Figure 6.4*), kidney (*Figure 6.5*), liver (*Figure 6.6*), lymph nodes (*Figure 6.7*), and PBMCs (*Figure 6.8*). The modulation of XBP-1 was assayed to assess the induction of the unfolded protein response given the central role of XBP-1 in mediating responses to ER stress induced by unfolded proteins. In order to address the hypothesis that iminosugars as a class can reduce inflammation in response to DENV, TNF receptor/ligand pairs were selected for analyses. In particular, OX40 (TNFRSF4) and the OX40 ligand (OX40L/TNFSF4) demonstrated considerable response to M*O*N-DNJ treatment *in vitro*, thus these transcripts were expected to produce observable responses *in vivo*. Additional network analyses suggested that the 4-1BB receptor/ligand pair, 4-1BB/4-1BBL (also known as TNFRSF9/TNFSF9), might respond to iminosugar treatment (IPA analyses, data not shown). As a control, a non-TNF superfamily receptor with a role in APC/T-cell co-stimulation that was not detected to respond to iminosugar treatment *in vitro* was selected for investigation *in vivo*. The B7 receptor family member CD28 is constitutively expressed on CD4+ T cells [308] and did not respond to M*O*N-DNJ treatment in previous *in vitro* experiments and was therefore assayed *in vivo* to see if lack of response could be extended to a living system.

Tissue specific responses were observed for both M*O*N-DNJ and Celgosivir with every transcript assayed. The spleen of untreated, DENV-infected mice was swollen and bloody (visual observations, myself and Sarah Killingbeck) in comparison to the spleen of uninfected animals. With treatment with either iminosugar, there was no discernible difference between the spleen of treated animals and those that were not infected with DENV suggesting a reversal of pathophysiology. Although

visual pathology was reversed by both iminosugars, reduction of inflammation was only detectable by qRT-PCR for OX40, OX40L, and, unexpectedly CD28 in response to M*O*N-DNJ treatment. Celgosivir treatment did not reduce transcription of any of the immune response genes in spite of the fact that both iminosugars induced UPR to approximately equivalent levels as measured by XBP-1 induction. This contrast of inflammatory modulation suggests that M*O*N-DNJ possesses a(n) mechanism(s) of action that attenuates inflammation in a way not achieved by Celgosivir.

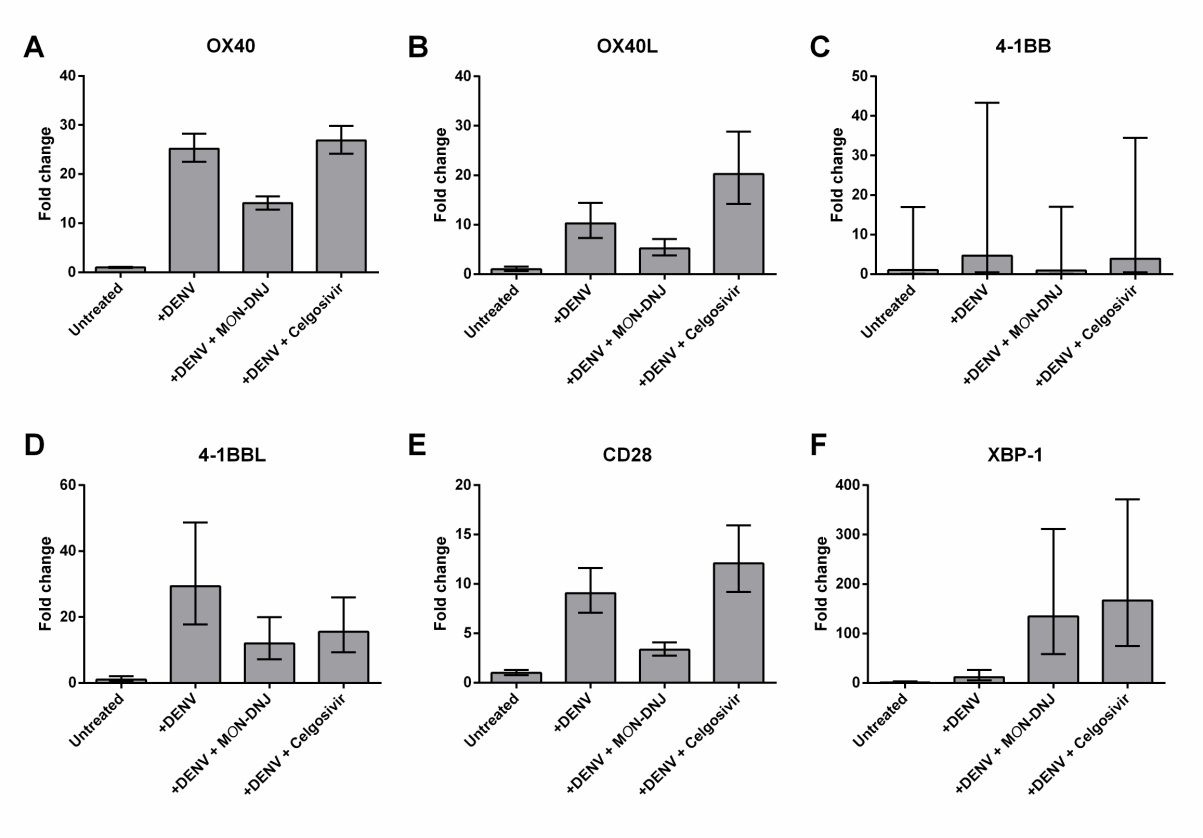

FIGURE 6.3. TNF receptor and ligands respond to iminosugar treatment of ADE model of DENV infection *in vivo* in the spleen. Mice were infected with virus and treated with iminosugar as in *Figure 6.1*. Transcript levels of OX40 (**A**), OX40L (**B**), 4-1BB (**C**), 4-1BBL (**D**), CD28 (**E**), and XBP-1 (**F**) were assayed by qRT-PCR and normalised to GAPDH levels. Fold change (y-axis) was calculated using the $\Delta\Delta C_t$ method [309] relative to untreated samples. Error bars represent 95% CI (confidence intervals).

In diametric opposition to the inflammatory situation observed in the spleen, the only anti-inflammatory activity noted in the small intestine (*Figure 6.4*) was observed for 4-1BBL modulation in response to Celgosivir treatment. Whereas all markers were induced to varying extents by DENV infection, any immunomodulation by iminosugars was weak or non-existent. These results were observed in spite of the fact that strong induction of XBP-1 with both M*O*N-DNJ and Celgosivir treatment suggested functional blockade of *N*-linked glycoprotein folding in small intestine as would be expected with oral drug administration.

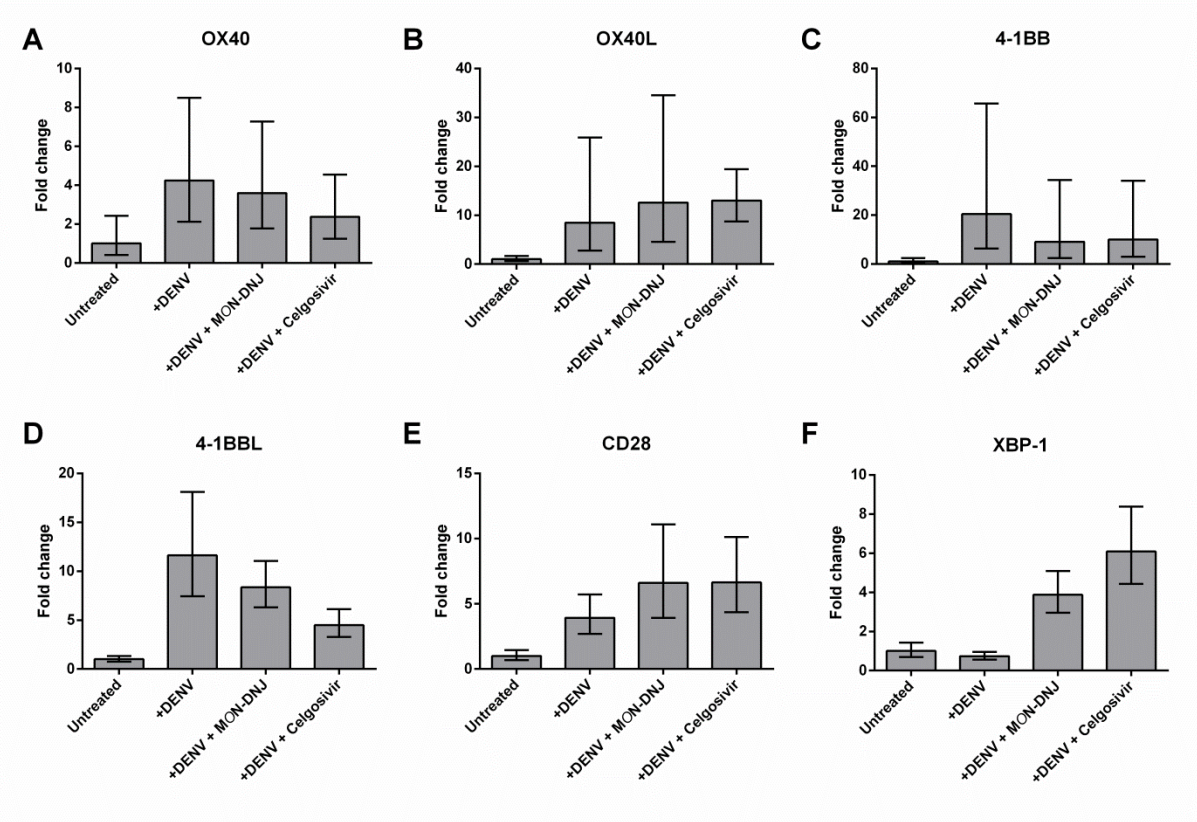

FIGURE 6.4. TNF receptor and ligands respond to iminosugar treatment of ADE model of DENV infection *in vivo* in the small intestine. Mice were infected with virus and treated with iminosugar as in *Figure 6.1*. Transcript levels of OX40 (**A**), OX40L (**B**), 4-1BB (**C**), 4-1BBL (**D**), CD28 (**E**), and XBP-1 (**F**) were assayed by qRT-PCR and normalised to GAPDH levels. Fold change (y-axis) was calculated using the $\Delta\Delta C_t$ method [309] relative to untreated samples. Error bars represent 95% confidence intervals.

In the kidney (*Figure 6.5*) and liver (*Figure 6.6*), anti-inflammatory activities could be observed for both M*O*N-DNJ and Celgosivir. As in the case of the spleen, phenotypic differences in infected and uninfected liver were observable by eye upon examination. Whereas the livers of DENV-infected mice were bloody in comparison to those of uninfected mice, the bloody appearance was absent in mice treated with both iminosugars (data not shown). Unlike in the spleen but similar to the small intestine, the reduction of transcription of TNF receptors and ligands as well as CD28 was stronger for Celgosivir than for M*O*N-DNJ. In both kidney and liver, there was considerable reduction of nearly all transcripts; however, these anti-inflammatory trends occurred in the absence of any increase of UPR as measured by XBP-1 induction. In fact, in the kidney, Celgosivir lowered XBP-1 induction (95%

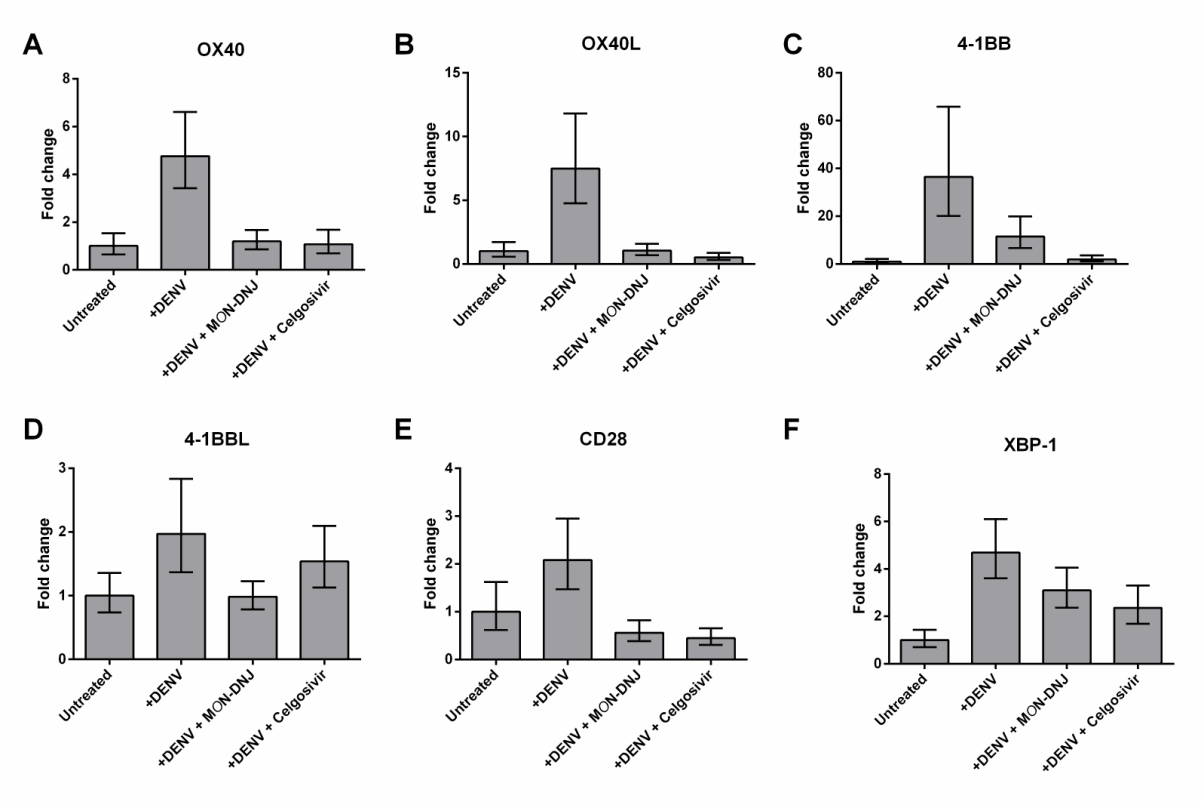

FIGURE 6.5. TNF receptor and ligands respond to iminosugar treatment of ADE model of DENV infection *in vivo* in the kidney. Mice were infected with virus and treated with iminosugar as in *Figure 6.1*. Transcript levels of OX40 (**A**), OX40L (**B**), 4-1BB (**C**), 4-1BBL (**D**), CD28 (**E**), and XBP-1 (**F**) were assayed by qRT-PCR and normalised to GAPDH levels. Fold change (y-axis) was calculated using the $\Delta\Delta C_t$ method [309] relative to untreated samples. Error bars represent 95% confidence intervals.

CI DENV: 3.61 to 6.09 fold vs. 95% CI DENV + Celgosivir: 1.68 to 3.30 fold) and in the liver, M*O*N-DNJ reduced XBP-1 induction (95% CI DENV: 42.23 to 121.52 fold vs. 95% CI DENV + M*O*N-DNJ: 3.86 to 9.28 fold). Reduced XBP-1 may be a consequence of reduced viral load and therefore reduced cellular stress, but such a hypothesis contradicts the effects observed in other tissues of this experiment.

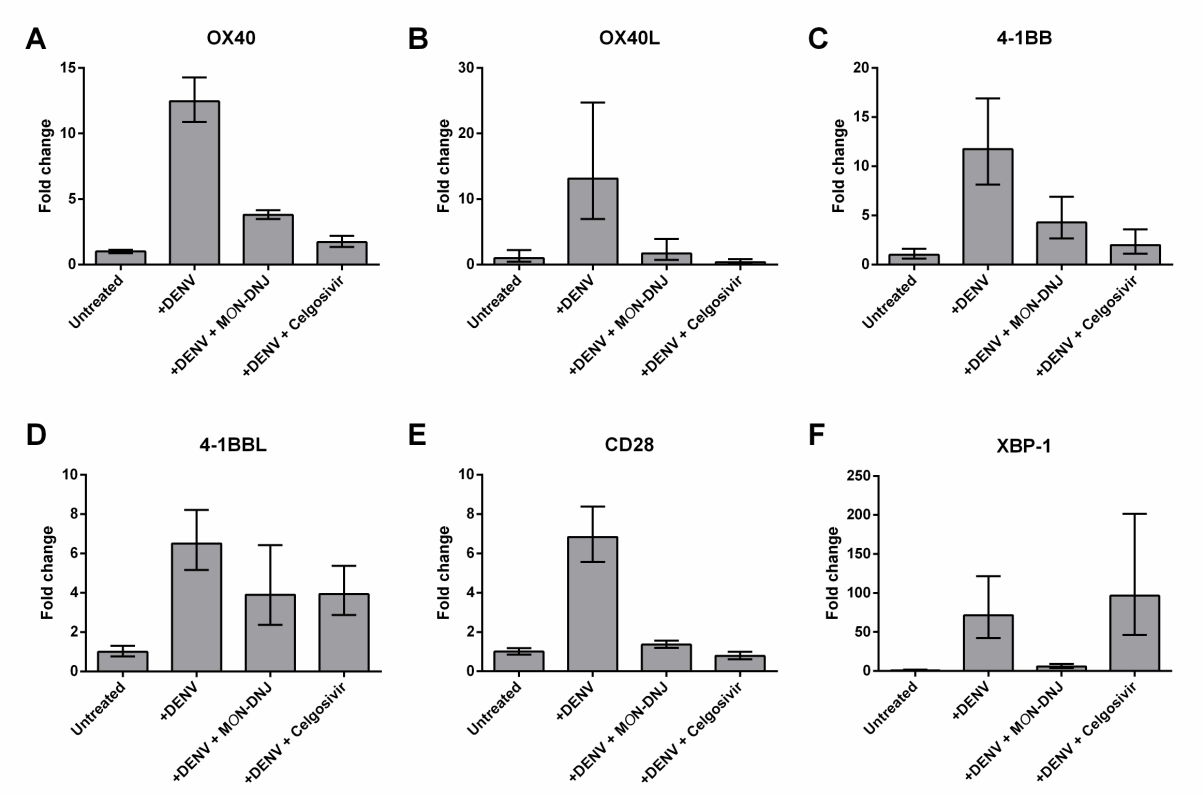

FIGURE 6.6. TNF receptor and ligands respond to iminosugar treatment of ADE model of DENV infection *in vivo* in the liver. Mice were infected with virus and treated with iminosugar as in *Figure 6.1*. Transcript levels of OX40 (**A**), OX40L (**B**), 4-1BB (**C**), 4-1BBL (**D**), CD28 (**E**), and XBP-1 (**F**) were assayed by qRT-PCR and normalised to GAPDH levels. Fold change (y-axis) was calculated using the $\Delta\Delta C_t$ method [309] relative to untreated samples. Error bars represent 95% confidence intervals.

The response of lymph nodes (*Figure 6.7*) and PBMCs (*Figure 6.8*) to DENV infection was particularly surprising in that reduction, rather than induction, of transcript was noted for the majority of TNF receptor and ligand assays with the single exception of 4-1BBL induction in PBMCs. In both lymph nodes and PBMCs, M*O*N-DNJ demonstrated the more potent molecular effect with further reduction of transcript in several cases (*e.g.* OX40 and 4-1BB in lymph nodes). Furthermore, in the singular case of induction (4-1BBL in PBMCs), M*O*N-DNJ treatment restored transcript levels to those of untreated cells. In most assays, Celgosivir had a non-existent or weakly inducing effect on transcript, but this generally was insufficient to restore the transcript level to the relative level observed in uninfected mice. Levels of XBP-1 transcript in lymph nodes were lowered with M*O*N-DNJ treatment in comparison to untreated controls. Only XBP-1 induction by Celgosivir in PBMCs coincided with pre-existing hypotheses. Phenotypic differences were again noted for DENV-infected mice in

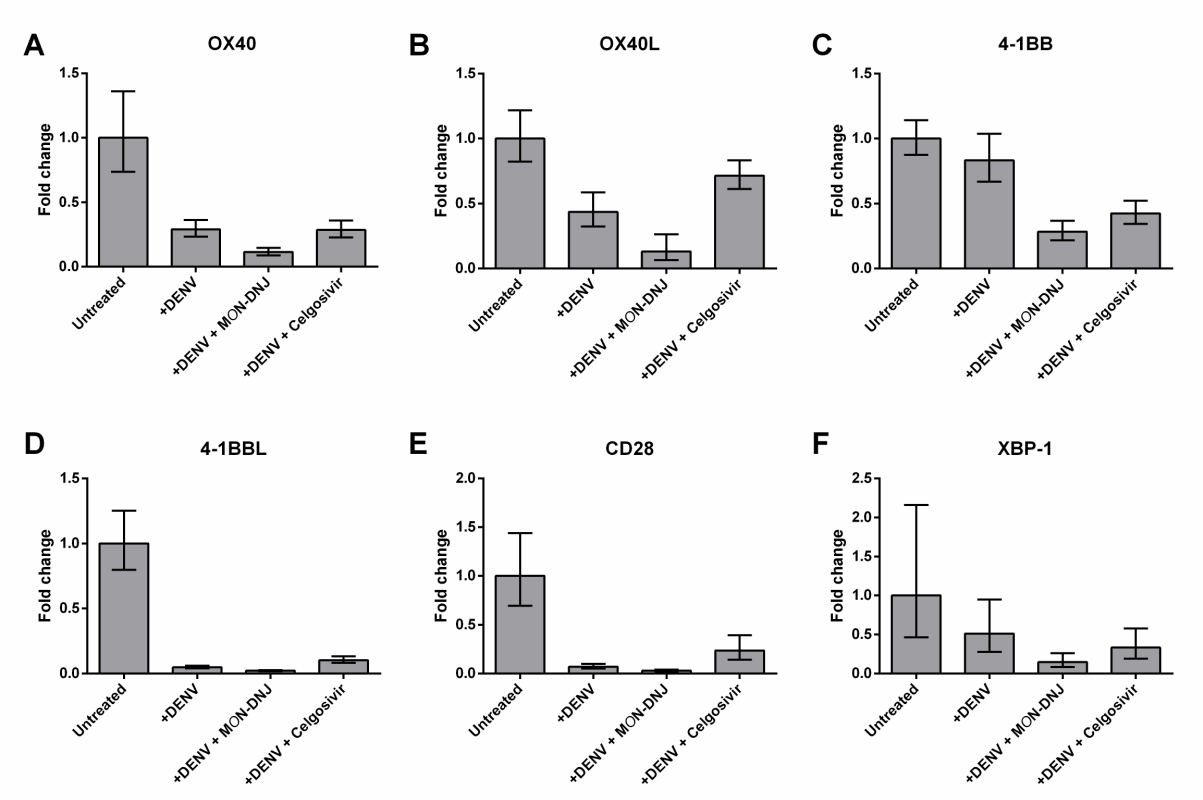

FIGURE 6.7. TNF receptor and ligands respond to iminosugar treatment of ADE model of DENV infection *in vivo* in the lymph nodes. Mice were infected with virus and treated with iminosugar as in *Figure 6.1*. Transcript levels of OX40 (**A**), OX40L (**B**), 4-1BB (**C**), 4-1BBL (**D**), CD28 (**E**), and XBP-1 (**F**) were assayed by qRT-PCR and normalised to GAPDH levels. Fold change (y-axis) was calculated using the $\Delta\Delta C_t$ method [309] relative to untreated samples. Error bars represent 95% confidence intervals.

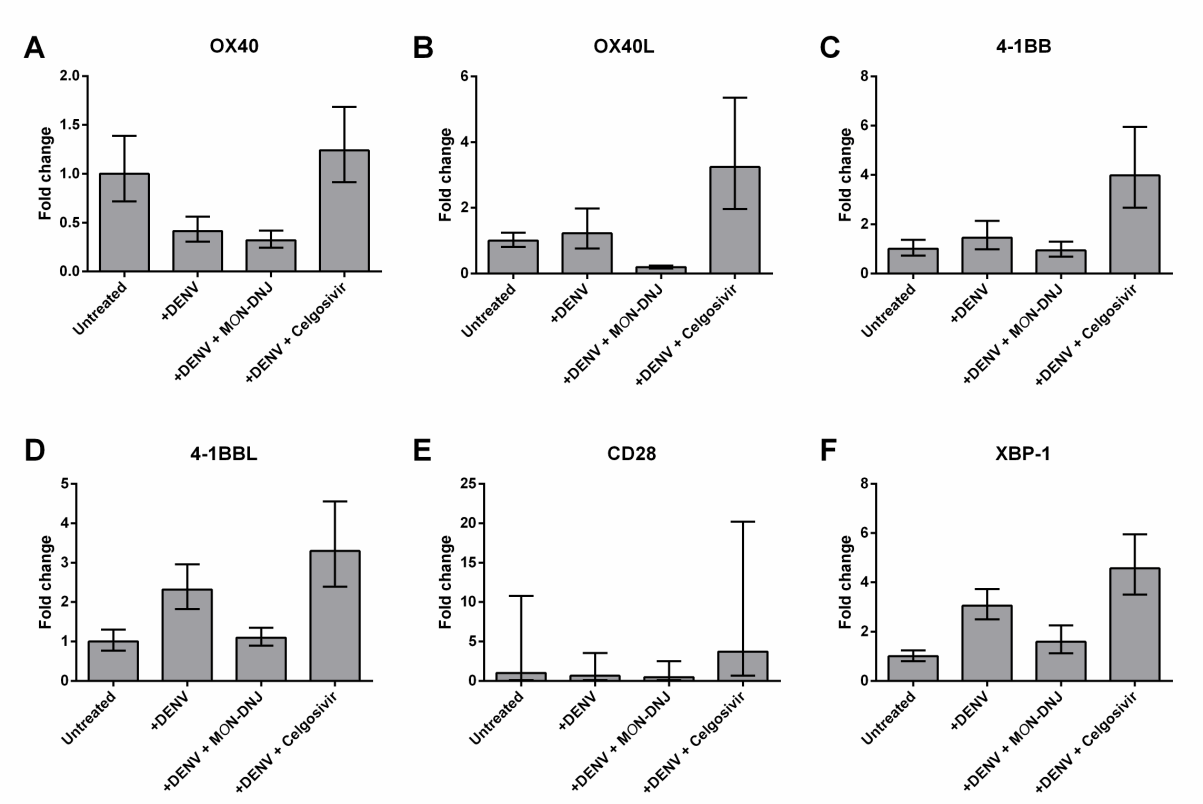

FIGURE 6.8. TNF receptor and ligands respond to iminosugar treatment of ADE model of DENV infection *in vivo* in PBMC. Mice were infected with virus and treated with iminosugar as in *Figure 6.1*. Transcript levels of OX40 (**A**), OX40L (**B**), 4-1BB (**C**), 4-1BBL (**D**), CD28 (**E**), and XBP-1 (**F**) were assayed by qRT-PCR and normalised to GAPDH levels. Fold change (y-axis) was calculated using the $\Delta\Delta C_t$ method [309] relative to untreated samples. Error bars represent 95% confidence intervals.

comparison to uninfected mice as well as those mice infected with virus and treated with either iminosugar in the case of lymph nodes. Whereas mesenteric lymph nodes were very small and difficult to locate in three of the treatment groups, mice infected with DENV but not given any drug had enlarged and easily identifiable lymph nodes.

VI.3.C. Tissue reorganisation in response to DENV infection and iminosugar treatment

The complex, tissue-dependent effects of transcript responses suggest that infiltration, expansion, and/or activation of various cell types in tissues may be at least partially responsible for the observed transcript modulation. Indeed, obvious visual phenotypic differences between uninfected and infected mice described above suggest that expansion of specific cell populations and/or infiltration or proliferation of, particularly, immune cells is likely occurring in response to DENV infection. Furthermore, the similar phenotypic presentation of tissues in iminosugar treated animals to those of uninfected animals suggests that the drug effects may be more large-scale than can be measured or understood by investigating transcript levels of the immune response genes. Although previous investigators have used GAPDH controls for normalisation of endogenous or viral genes [310-312] just as have been used for these experiments, significance testing querying changes in GAPDH levels in these tissues reveals that DENV infection and iminosugar treatment can modulate the level of GAPDH (*Figure 6.9*). Crucially, GAPDH modulation does not appear to be singularly responsible for the changes observed in various tissues; however, changes in GAPDH expression relative to total RNA (*Figure 6.9C*) raise concern over the normalisation procedure. For example, an approximate 10-fold reduction in GAPDH relative to total RNA is observed in lymph nodes infected with DENV and those infected with DENV and treated with Celgosivir. In contrast, M*O*N-DNJ treatment appears to restore GAPDH levels to approximate equivalence with uninfected controls. In comparison to the endogenous genes previously discussed (*Figure 6.7*) differential effects observed in relative expression of experimental genes (*e.g.* OX40 and OX40L) can be explained in part, but not entirely, as a consequence of normalisation with fluctuating GAPDH controls.

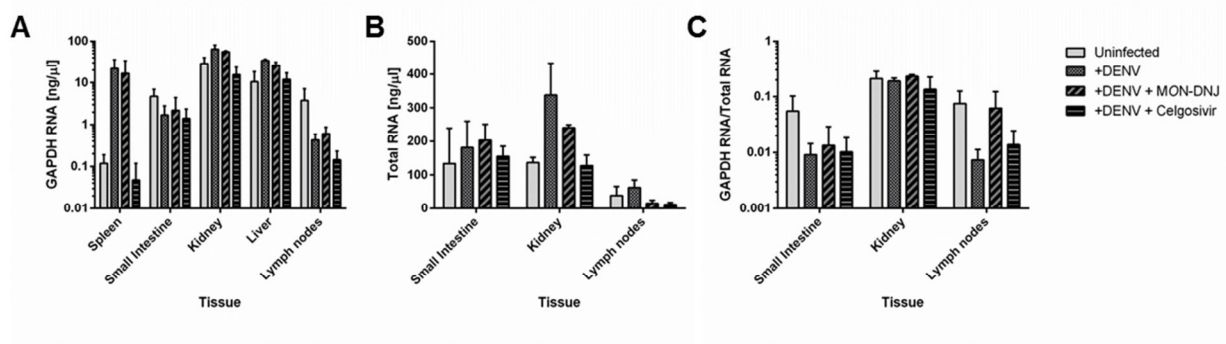

FIGURE 6.9. Mouse GAPDH transcript modulation in response to DENV infection and iminosugar treatment. Mice were infected with virus and treated with iminosugar as in *Figure 6.1*, and mouse GAPDH transcript was used as a normalisation control in all tissue experiments. GAPDH transcript per unit volume (**A**) demonstrated up to $2\log_{10}$ differences in expression with various treatments as determined by qRT-PCR. To ensure that extraction efficiency of RNA was not responsible for this variation, total RNA concentration was measured on a NanoDrop 1000 (**B**) where possible. For tissues with total RNA concentrations determined, total RNA was used to normalise GAPDH RNA concentration (**C**). All error bars represent standard deviation and are based on three biological replicates measured in duplicate (**A**) or singlicate (**B**).

VI.4. Discussion

Two DENV therapeutics are currently poised for the early stages of clinical trials: the primary subject of this thesis, M*O*N-DNJ, and Celgosivir. Both iminosugars are thought to directly reduce DENV production in infected cells via inhibition of α-glucosidase mediated trimming of viral glycoprotein; however, a direct comparison of the two drugs has not previously been conducted. In the AG129 mouse model of ADE DENV infection, Celgosivir appears to be the stronger of the two antivirals. Both iminosugars were dosed orally, three times per day to ensure that mouse handling and stress did not interfere with comparison of the two drugs and daily dosing was kept constant with previously published studies (300 mg/kg/day for M*O*N-DNJ [209] and 100 mg/kg/day for Celgosivir [306]). Previous studies with Celgosivir have utilised a twice daily (*b.i.d.*) intraperitoneal (*i.p.*) dosing schedule yielding a maximal serum concentration of 31.6 µg/ml (122 µM) and a terminal half-life for the drug ($T_{1/2}$) of 5.0 hours. [307] Maintenance of elevated serum concentration of Celgosivir is

essential for survival, thus dosing *b.i.d.* is essential at a minimum. Complicating comparison, the only available pharmacokinetic data for M*O*N-DNJ was conducted with oral and intravenous administration; however terminal half-life for M*O*N-DNJ was similar in both dosing strategies (200 mg/kg *i.g.* vs 5 mg/kg *i.v.*) with oral $T_{1/2}$ equal to 5.14 hours and *i.v.* $T_{1/2}$ equal to 5.65 hours. The maximum serum concentration of M*O*N-DNJ when administered orally was 91.0 µg/ml (285 µM). [209] It is impossible to extrapolate these data to the dosing schedule presented in this work, but the clinical use of either iminosugar as a DENV therapeutic is likely to be identical thus an identical dosing schedule was desirable for comparison of the two drugs. In all tissues except the spleen, Celgosivir appeared to be the more potent antiviral.

Although Celgosivir was generally more potent in reducing viral load, both drugs have demonstrated therapeutic protection in animal models. Additionally, the work of previous chapters of this thesis suggests that M*O*N-DNJ treatment may alter the host response to DENV infection. Whether this property extends to Celgosivir remains to be seen; however, in comparing the two drugs *in vivo*, the possibility of a novel iminosugar-class activity of host immunomodulation was explored. Differential effects for the drugs were observed to be tissue-dependent in modulation of various TNF receptor and ligand transcripts. Although reduction of CD28 was not anticipated, a tissue and drug-dependent response was observed for this marker as well. In concert, these results suggest that there is an immunomodulatory capacity of both iminosugars, but such an activity could not be correlated with the best available marker of tissue access – induction of UPR as measured by XBP-1. Strong induction of XBP-1 with iminosugar treatment was noted in many tissues, but reduction of the transcript in relation to the level observed for DENV-infected, untreated mice was also observed in some tissues for which there was a modulation of the immune-response transcripts. Unfortunately, a clear picture does not emerge to explain the molecular steps involved in iminosugar treatment and modulation of the immune response.

The failure to identify a consistent response of immune system-related transcripts to iminosugar treatment is multi-factorial. Although there is a clear modulation of the transcripts, it is likely that the use of entire tissue samples overcomplicates the intended analysis. Remarkable visible differences in pathology were noted by eye for the spleen, liver, and lymph nodes in the presence of iminosugars, and these visual differences suggest that the composition of tissues is changing in response to DENV infection and that iminosugars can reverse the extent of such changes. For example, the enlargement of the spleen and lymph nodes noted upon DENV infection is reduced with both M*O*N-DNJ and Celgosivir treatment. It is probable that expansion and/or recruitment of immune cells such as monocytes, macrophages, dendritic cells, B-, and T-cells is responsible for the swelling observed, and expansion and recruitment of diverse cell populations makes comprehension of the molecular events measured by transcript responses all but impossible. This difficulty is highlighted by the fact that GAPDH, a supposed endogenous control, demonstrated variable transcript levels in response to both DENV infection and iminosugar treatment. Replication of DENV in tissue resident macrophages (*e.g.* splenic macrophages) has been studied in ADE mouse models, [313] and vascular leakage in tissues including small intestine, large intestine, liver, and spleen has been observed for this infection model. [113] Further complicating interpretation is the lack of an intact immune response in the mouse model utilised. Alternative animal models are available (reviewed in [314]), but each system carries alternative inadequacies. For example, mice with intact immune signalling/response can be infected with DENV by intracranial injection, but pathology and cause of death does not resemble human DENV disease. [232,314] Alternatively, humanised severe combined immunodeficiency (SCID) mice are tractable to DENV infection, but the chimeric immune system would likely produce equally unclear results. Nevertheless, lack of a functional interferon response cascade in the AG129 mice used here presents a serious hurdle in investigation of effects on the immune response. Although an understanding of the molecular events responsible for reduced inflammation remains elusive, it appears as though α-glucosidase inhibiting iminosugars as a class are capable of reducing DENV-induced inflammation in a living system.

Principally, these results highlight the need for a greater understanding of the events that mediate pathology. The complexity of an animal model, especially an animal with a modified innate immune system, makes unravelling complex host responses considerably more difficult than in relevant *ex vivo* systems such as the MDMΦs used elsewhere in this thesis. It is promising to observe that some effects predicted by transcriptomics studies can be recapitulated *in vivo*, but the source of reduced inflammation cannot be determined with these experiments. It is possible that reduced viral load is entirely responsible for the reduced inflammation observed; however, the continued presence of infectious virus and viral RNA observed at this time point supports the hypothesis that the immune response is still actively involved in pathogen clearance. Circulating virus is weakly reduced by iminosugar treatment at the time observed, and the continued presence of infectious virus necessitates a continued activation of the immune system to ensure effective viral clearance and eventually survival of the mouse. Given that successful viral clearance and survival has been observed for both iminosugars with similar treatment schedules, it is likely that the pathological changes observed in concordance with continued but attenuated immune activation may indicate that it is the reversal of pathology rather than viral clearance that is crucial to ensure host survival in a severe dengue infection. These experiments suggest that understanding the changing composition of specific tissues, such as the spleen, in response to DENV infection and iminosugar treatment may better clarify viral pathology and immunomodulation. As such, these experiments provide some support of a novel iminosugar class action and provide insight for future experiments to clarify this hypothesis.

VII

General Discussion

VII.1. Overview

The principal aim of this thesis is to develop an understanding of the consequences of iminosugar-based, host-directed therapeutic intervention for the treatment of dengue virus infection. In my review of the field published at the outset of my research, [12] I focused on the effects of iminosugar inhibition of host α-glucosidases on interference with virion morphogenesis. The field of iminosugar research had largely ignored the potential for manipulation of host proteins principally because of the remarkably minimal toxicity observed with most iminosugar treatment experiments; however, isolated reports of altered responses to stress events (*e.g.* reduced production of IFN-γ following CD3 stimulation of T-cells) indicated that the lack of host protein modulation could be environment dependent. This hypothesis, that iminosugars can modulate the stress response of cells in high flux environments, was principally addressed in *Chapters IV* and *V*, and the transcriptomic and multi-plex cytokine data presented therein suggest that this hypothesis is likely true. In environments of cellular stress including DENV infection, LPS treatment, and media stress, M*O*N-DNJ consistently reduced production of key inflammatory cytokines. Much as is the case for inhibition of infectious virus as demonstrated in *Chapter III*, modulation of host responses to stress, particularly inflammation, appears to be specific for iminosugars possessing glucostereochemistry. In the absence of external stimuli, M*O*N-DNJ treatment elicited a profound induction of the unfolded protein response, but minimal additional network activation or inhibition was observed. In contrast, macrophages infected with DENV or treated with LPS responded to M*O*N-DNJ treatment by reducing inflammation as well as inducing the unfolded protein response. The connection, if any exists, between UPR and modulation of inflammation is difficult to establish, but these data provide direction toward some principal hypotheses that should be further investigated. Whether iminosugar induction of UPR promotes an oxidative stress control response that balances the inflammatory response to pathogens or whether iminosugars directly attenuate folding of key cytokines such as IFN-γ or TNF-α remains to be confirmed. *In vivo* experiments directed at addressing

this question, and whether reduced inflammation could be a mechanism of action of the entire class of iminosugars that inhibit α-glucosidases, failed to provide a clear molecular picture. Although a reduction in markers of antigen presenting cells and markers of the T-cells they stimulate could be detected in many tissues following iminosugar treatment, the most striking result of the experiments in mice was the modulation of GAPDH controls by both DENV and iminosugar treatment and the visual evidence of altered pathophysiology. These tissue-scale effects require further study before a molecular understanding of iminosugar effects on inflammation can be delineated. Although Celgosivir has recently failed to show any antiviral efficacy in a phase Ib trial against DENV due to issues with power and clinical endpoints assessed, the drug also did not worsen outcomes. [48] With the work presented herein, a greater understanding of the molecular events of M*O*N-DNJ activity has been developed which should inform monitoring in impending clinical trials. With the recent description of viral resistance in humans with non-functional α-glucosidase I, [315] hope remains that M*O*N-DNJ could be an effective antiviral against DENV and modulator of the immune response – a multidrug cocktail in a single drug.

VII.2. Future experiments

As is nearly always the case in science, new data begs further questions. It appears to be true that inhibition of α-glucosidase activity is necessary for inhibition of infectious DENV production, but is this activity directly related to misfolding of envelope protein? What happens to each of the three DENV glycoproteins, prM, E, and NS1, when infected cells are treated with α-glucosidase inhibiting iminosugars? In work not presented in this thesis, I attempted to co-immunoprecipitate DENV proteins (as well as host proteins) with the ER chaperones CANX and CALR to address each protein's utilisation and dependence on these pathways. Unfortunately, these efforts were unsuccessful, probably due to problems with sensitivity of detection of co-precipitated proteins; however, optimisation of experimental conditions in concert with more sensitive (and quantitative) detection

methods, such as quantitative mass spectrometry parallel reaction monitoring, should facilitate future efforts. One could hope to identify changes in glycosylation and/or folding of viral glycoproteins as a consequence of iminosugar treatment of infected cells. Identification of changing glycans on proteins requires parallel mass-spectrometry of (viral) glycopeptides with selection for targets of interest and subsequent glycan analysis – a difficult task even with large quantities of glycoprotein. However, such technologies are being developed for recombinant expression systems such as HIV envelope protein gp120 (L. Pritchard, personal communication) and may be available for analysis of less abundant proteins (*e.g.* DENV glycoproteins produced following *in vitro* infection) in the near future. Monitoring protein folding can be accomplished using a panel of conformation dependent and conformation independent antibodies and such investigations are underway for DENV NS1 in our lab (T. Haßler and JL Miller, personal communication). Alternatively or in addition, disulphide bond formation can be monitored by radiolabelling and precipitating proteins of interest and monitoring gel shifts. Such experiments can be executed for both DENV and host proteins in the presence and absence of iminosugars to monitor drug effects.

The data presented in *Chapter IV* provides a starting point for investigations of numerous different hypotheses regarding the macrophage response to DENV infection and iminosugar effects on treatment of human primary cells. The combination of the effects of stress situations such as DENV or bacterial infection with iminosugar treatment presents innumerable additional avenues of research. Predictions based on this transcriptomics data can be validated at the protein level – as in the case of reduction of inflammation presented in *Chapter V*. By gathering comprehensive transcript level data at multiple time points, I hoped to address how the host response to DENV infection develops over time. Identification of dynamic elements of response to infection, with a focus on stress response transcription factors, could help explain the development of severe pathology in select individuals infected with DENV in the natural course of human infection.

Validation of these events, as conducted for NFE2L2 and the cytokines, is the first step in understanding the molecular events of DENV pathology, and these studies should be extended by further delineating the mechanism of induction of these responses. Is NFE2L2 induced by competitive inhibition of the cellular glucose pool? Or does ER stress, as a consequence of accumulation of misfolded proteins, trigger the oxidative stress response? Is this mechanism the same for other transcription factors identified? And do these responses vary in individuals in a manner which can explain the dichotomy of progression to inapparent infection versus potentially life-threatening disease?

The validation of attenuation of the inflammatory response at the protein level is promising for other hypotheses generated by the transcriptomics studies, but even these protein level experiments generate additional questions. How do iminosugars attenuate inflammation? Is direct reduction of properly folded cytokine (such as IFN-γ) solely responsible for this phenomenon? Or is enhanced signalling by stress-controlling transcription factors solely responsible for signalling reduced production of these inflammatory molecules? In these experiments, only twelve cytokines were investigated in detail. What happens to type I interferons? Are the cytokines that are produced, albeit at lower quantities, still functional? Most importantly, what will happen in a living human infected with DENV and treated with iminosugar? These responses will require stringent monitoring during clinical trials, but recapitulation of these events *in vivo* in concert with safety and efficacy of the drug could herald a new broad-spectrum anti-infective treatment.

Finally, what molecular mechanisms are responsible for the gross differences in pathology noted in the presence and absence of iminosugar infection? Is reduction of infectious virus alone responsible for these observations, or does iminosugar treatment specifically alter the pathophysiological

response to infection? Can reversal of tissue pathophysiology with iminosugar treatment observed in mice be recapitulated in the case of human infection, and what would this mean for the drug's therapeutic potential? What are the tissue specific changes that are occurring? Iminosugar treatment could be administered to mice as conducted here and histopathology conducted to identify changing cell populations. Additional monitoring of cell types infiltrating or proliferating in tissues (*e.g.* spleen and lymph node) by FACS for different cell markers could identify specific cells responding to iminosugar treatment by changes in abundance, proliferation, survival, and/or activation. Though the changes that are occurring are as yet unclear, they appear to promote survival in the lethal challenge model of DENV infection. A greater understanding of how and why these events are occurring will facilitate monitoring of clinical trials and inform decisions regarding additional therapeutic applications for iminosugars.

VII.3. Final conclusions

This thesis concerns the mechanism of action of iminosugars, in particular M*O*N-DNJ, as a potential dengue virus therapeutic. To this end, I have presented:

1) Evidence that inhibition of α-glucosidase activity is likely necessary for reduction of infectious DENV production by iminosugars in primary human MDMΦ,
2) An analysis of changes to the host MDMΦ transcriptome in the context of DENV infection as well as LPS treatment as a consequence of iminosugar treatment,
3) Evidence that iminosugars that inhibit α-glucosidase activity can reduce MDMΦ produced inflammatory cytokines in the context of DENV infection as well as other inflammatory stimuli, and
4) *In vivo* evidence for alteration of immune activation in a model of ADE DENV infection as a result of orally administered iminosugar treatment.

VIII

References

1. Gubler DJ, Kuno G, Markoff L (2007) Flaviviruses. In: Knipe DM, Howley PM, editors. Fields Virology. 5th ed. London: Wolters Kluwer Health / Lippincott Williams & Wilkins. pp. 1154-1252.
2. Calisher CH, Karabatsos N, Dalrymple JM, Shope RE, Porterfield JS, et al. (1989) Antigenic relationships between flaviviruses as determined by cross-neutralization tests with polyclonal antisera. J Gen Virol 70 (Pt 1): 37-43.
3. Beasley D, Barrett A (2008) The Infectious Agent. In: Halstead S, editor. Dengue. London: Imperial College Press. pp. 29-73.
4. Kuhn RJ, Zhang W, Rossmann MG, Pletnev SV, Corver J, et al. (2002) Structure of dengue virus: implications for flavivirus organization, maturation, and fusion. Cell 108: 717-725.
5. Stadler K, Allison SL, Schalich J, Heinz FX (1997) Proteolytic activation of tick-borne encephalitis virus by furin. J Virol 71: 8475-8481.
6. Yu IM, Zhang W, Holdaway HA, Li L, Kostyuchenko VA, et al. (2008) Structure of the immature dengue virus at low pH primes proteolytic maturation. Science 319: 1834-1837.
7. Li L, Lok SM, Yu IM, Zhang Y, Kuhn RJ, et al. (2008) The flavivirus precursor membrane-envelope protein complex: structure and maturation. Science 319: 1830-1834.
8. Zhang W, Chipman PR, Corver J, Johnson PR, Zhang Y, et al. (2003) Visualization of membrane protein domains by cryo-electron microscopy of dengue virus. Nat Struct Biol 10: 907-912.
9. Ma L, Jones CT, Groesch TD, Kuhn RJ, Post CB (2004) Solution structure of dengue virus capsid protein reveals another fold. Proc Natl Acad Sci U S A 101: 3414-3419.
10. Alvarez DE, De Lella Ezcurra AL, Fucito S, Gamarnik AV (2005) Role of RNA structures present at the 3'UTR of dengue virus on translation, RNA synthesis, and viral replication. Virology 339: 200-212.
11. Alvarez DE, Lodeiro MF, Luduena SJ, Pietrasanta LI, Gamarnik AV (2005) Long-range RNA-RNA interactions circularize the dengue virus genome. J Virol 79: 6631-6643.
12. Sayce AC, Miller JL, Zitzmann N (2010) Targeting a host process as an antiviral approach against dengue virus. Trends Microbiol 18: 323-330.
13. Shapiro D, Kos KA, Russel PK (1973) Japanese encephalitis virus glycoproteins. Virology 56: 88-94.
14. Stohlman SA, Eylar OR, Wisseman CL, Jr. (1976) Isolation of the dengue virus envelope glycoprotein from membranes of infected cells by concanavalin A affinity chromatography. J Virol 18: 132-140.
15. Shapiro D, Brandt WE, Russell PK (1972) Change involving a viral membrane glycoprotein during morphogenesis of group B arboviruses. Virology 50: 906-911.
16. Rice CM, Lenches EM, Eddy SR, Shin SJ, Sheets RL, et al. (1985) Nucleotide sequence of yellow fever virus: implications for flavivirus gene expression and evolution. Science 229: 726-733.
17. Russell PK, Chiewsilp D, Brandt WE (1970) Immunoprecipitation analysis of soluble complement-fixing antigens of dengue viruses. J Immunol 105: 838-845.
18. Smith GW, Wright PJ (1985) Synthesis of proteins and glycoproteins in dengue type 2 virus-infected vero and Aedes albopictus cells. J Gen Virol 66 (Pt 3): 559-571.
19. Brodsky JL (2012) Cleaning up: ER-associated degradation to the rescue. Cell 151: 1163-1167.
20. Nowak T, Wengler G (1987) Analysis of disulfides present in the membrane proteins of the West Nile flavivirus. Virology 156: 127-137.
21. Wallis TP, Huang CY, Nimkar SB, Young PR, Gorman JJ (2004) Determination of the disulfide bond arrangement of dengue virus NS1 protein. J Biol Chem 279: 20729-20741.
22. Avirutnan P, Punyadee N, Noisakran S, Komoltri C, Thiemmeca S, et al. (2006) Vascular leakage in severe dengue virus infections: a potential role for the nonstructural viral protein NS1 and complement. J Infect Dis 193: 1078-1088.
23. Young PR, Hilditch PA, Bletchly C, Halloran W (2000) An antigen capture enzyme-linked immunosorbent assay reveals high levels of the dengue virus protein NS1 in the sera of infected patients. J Clin Microbiol 38: 1053-1057.

24. Libraty DH, Young PR, Pickering D, Endy TP, Kalayanarooj S, et al. (2002) High circulating levels of the dengue virus nonstructural protein NS1 early in dengue illness correlate with the development of dengue hemorrhagic fever. J Infect Dis 186: 1165-1168.
25. Alcon S, Talarmin A, Debruyne M, Falconar A, Deubel V, et al. (2002) Enzyme-linked immunosorbent assay specific to Dengue virus type 1 nonstructural protein NS1 reveals circulation of the antigen in the blood during the acute phase of disease in patients experiencing primary or secondary infections. J Clin Microbiol 40: 376-381.
26. Avirutnan P, Zhang L, Punyadee N, Manuyakorn A, Puttikhunt C, et al. (2007) Secreted NS1 of dengue virus attaches to the surface of cells via interactions with heparan sulfate and chondroitin sulfate E. PLoS Pathog 3: e183.
27. Pryor MJ, Wright PJ (1994) Glycosylation mutants of dengue virus NS1 protein. J Gen Virol 75 (Pt 5): 1183-1187.
28. Akey DL, Brown WC, Dutta S, Konwerski J, Jose J, et al. (2014) Flavivirus NS1 Structures Reveal Surfaces for Associations with Membranes and the Immune System. Science.
29. Modis Y, Ogata S, Clements D, Harrison SC (2003) A ligand-binding pocket in the dengue virus envelope glycoprotein. Proc Natl Acad Sci U S A 100: 6986-6991.
30. Modis Y, Ogata S, Clements D, Harrison SC (2004) Structure of the dengue virus envelope protein after membrane fusion. Nature 427: 313-319.
31. Roehrig JT, Volpe KE, Squires J, Hunt AR, Davis BS, et al. (2004) Contribution of disulfide bridging to epitope expression of the dengue type 2 virus envelope glycoprotein. J Virol 78: 2648-2652.
32. Mondotte JA, Lozach PY, Amara A, Gamarnik AV (2007) Essential role of dengue virus envelope protein N glycosylation at asparagine-67 during viral propagation. J Virol 81: 7136-7148.
33. Dejnirattisai W, Webb AI, Chan V, Jumnainsong A, Davidson A, et al. (2011) Lectin switching during dengue virus infection. J Infect Dis 203: 1775-1783.
34. Murray JM, Aaskov JG, Wright PJ (1993) Processing of the dengue virus type 2 proteins prM and C-prM. J Gen Virol 74 (Pt 2): 175-182.
35. Keelapang P, Sriburi R, Supasa S, Panyadee N, Songjaeng A, et al. (2004) Alterations of pr-M cleavage and virus export in pr-M junction chimeric dengue viruses. J Virol 78: 2367-2381.
36. Welsch S, Miller S, Romero-Brey I, Merz A, Bleck CKE, et al. (2009) Composition and Three-Dimensional Architecture of the Dengue Virus Replication and Assembly Sites. Cell Host & Microbe 5: 365-375.
37. Chatel-Chaix L, Bartenschlager R (2014) Dengue virus- and hepatitis C virus-induced replication and assembly compartments: the enemy inside--caught in the web. J Virol 88: 5907-5911.
38. Bhatt S, Gething PW, Brady OJ, Messina JP, Farlow AW, et al. (2013) The global distribution and burden of dengue. Nature 496: 504-507.
39. WHO (2014) Dengue and severe dengue.
40. La Ruche G, Souares Y, Armengaud A, Peloux-Petiot F, Delaunay P, et al. (2010) First two autochthonous dengue virus infections in metropolitan France, September 2010. Euro Surveill 15: 19676.
41. Sousa CA, Clairouin M, Seixas G, Viveiros B, Novo MT, et al. (2012) Ongoing outbreak of dengue type 1 in the Autonomous Region of Madeira, Portugal: preliminary report. Euro Surveill 17.
42. Alves MJ, Fernandes PL, Amaro F, Osorio H, Luz T, et al. (2013) Clinical presentation and laboratory findings for the first autochthonous cases of dengue fever in Madeira island, Portugal, October 2012. Euro Surveill 18.
43. Centers for Disease Control and Prevention (CDC) (2010) Locally acquired Dengue--Key West, Florida, 2009-2010. MMWR Morb Mortal Wkly Rep 59: 577-581.
44. Ramos MM, Mohammed H, Zielinski-Gutierrez E, Hayden MH, Lopez JL, et al. (2008) Epidemic dengue and dengue hemorrhagic fever at the Texas-Mexico border: results of a household-based seroepidemiologic survey, December 2005. Am J Trop Med Hyg 78: 364-369.

45. Bunnag T, Kalayanarooj S (2011) Dengue shock syndrome at the emergency room of Queen Sirikit National Institute of Child Health, Bangkok, Thailand. J Med Assoc Thai 94 Suppl 3: S57-63.
46. Arima Y, Edelstein ZR, Han HK, Matsui T (2013) Epidemiologic update on the dengue situation in the Western Pacific Region, 2011. Western Pac Surveill Response J 4: 47-54.
47. Mia MS, Begum RA, Er AC, Abidin RD, Pereira JJ (2013) Trends of dengue infections in Malaysia, 2000-2010. Asian Pac J Trop Med 6: 462-466.
48. Low JG, Sung C, Wijaya L, Wei Y, Rathore AP, et al. (2014) Efficacy and safety of celgosivir in patients with dengue fever (CELADEN): a phase 1b, randomised, double-blind, placebo-controlled, proof-of-concept trial. Lancet Infect Dis.
49. Tam DT, Ngoc TV, Tien NT, Kieu NT, Thuy TT, et al. (2012) Effects of short-course oral corticosteroid therapy in early dengue infection in Vietnamese patients: a randomized, placebo-controlled trial. Clin Infect Dis 55: 1216-1224.
50. Nguyen TH, Vu TT, Farrar J, Hoang TL, Dong TH, et al. (2013) Corticosteroids for dengue - why don't they work? PLoS Negl Trop Dis 7: e2592.
51. Castro JE, Vado-Solis I, Perez-Osorio C, Fredeking TM (2011) Modulation of cytokine and cytokine receptor/antagonist by treatment with doxycycline and tetracycline in patients with dengue fever. Clin Dev Immunol 2011: 370872.
52. Farias KJ, Machado PR, da Fonseca BA (2013) Chloroquine inhibits dengue virus type 2 replication in Vero cells but not in C6/36 cells. ScientificWorldJournal 2013: 282734.
53. Farias KJ, Machado PR, de Almeida Junior RF, de Aquino AA, da Fonseca BA (2014) Chloroquine interferes with dengue-2 virus replication in U937 cells. Microbiol Immunol 58: 318-326.
54. Thome R, Lopes SC, Costa FT, Verinaud L (2013) Chloroquine: modes of action of an undervalued drug. Immunol Lett 153: 50-57.
55. Tricou V, Minh NN, Van TP, Lee SJ, Farrar J, et al. (2010) A randomized controlled trial of chloroquine for the treatment of dengue in Vietnamese adults. PLoS Negl Trop Dis 4: e785.
56. Nguyen NM, Tran CN, Phung LK, Duong KT, Huynh Hle A, et al. (2013) A randomized, double-blind placebo controlled trial of balapiravir, a polymerase inhibitor, in adult dengue patients. J Infect Dis 207: 1442-1450.
57. Martinez-Gutierrez M, Castellanos JE, Gallego-Gomez JC (2011) Statins reduce dengue virus production via decreased virion assembly. Intervirology 54: 202-216.
58. Whitehorn J, Van Vinh Chau N, Truong NT, Tai LT, Van Hao N, et al. (2012) Lovastatin for adult patients with dengue: protocol for a randomised controlled trial. Trials 13: 203.
59. Sabchareon A, Wallace D, Sirivichayakul C, Limkittikul K, Chanthavanich P, et al. (2012) Protective efficacy of the recombinant, live-attenuated, CYD tetravalent dengue vaccine in Thai schoolchildren: a randomised, controlled phase 2b trial. Lancet 380: 1559-1567.
60. Capeding MR, Tran NH, Hadinegoro SR, Ismail HI, Chotpitayasunondh T, et al. (2014) Clinical efficacy and safety of a novel tetravalent dengue vaccine in healthy children in Asia: a phase 3, randomised, observer-masked, placebo-controlled trial. Lancet.
61. Sanofi-Pasteur (2014) Sanofi Pasteur's dengue vaccine candidate successfully completes final landmark phase III clinical efficacy study in Latin America.
62. Halstead SB (2012) Dengue vaccine development: a 75% solution? Lancet 380: 1535-1536.
63. Sabchareon A, Wallace D, Lang J, Bouckenooghe A, Moureau A (2013) Efficacy of tetravalent dengue vaccine in Thai schoolchildren - Authors' reply. Lancet 381: 1094-1095.
64. Moi ML, Takasaki T, Kurane I (2013) Efficacy of tetravalent dengue vaccine in Thai schoolchildren. Lancet 381: 1094.
65. Osorio JE, Huang CY, Kinney RM, Stinchcomb DT (2011) Development of DENVax: a chimeric dengue-2 PDK-53-based tetravalent vaccine for protection against dengue fever. Vaccine 29: 7251-7260.

66. Osorio JE, Brewoo JN, Silengo SJ, Arguello J, Moldovan IR, et al. (2011) Efficacy of a tetravalent chimeric dengue vaccine (DENVax) in Cynomolgus macaques. Am J Trop Med Hyg 84: 978-987.
67. Brewoo JN, Kinney RM, Powell TD, Arguello JJ, Silengo SJ, et al. (2012) Immunogenicity and efficacy of chimeric dengue vaccine (DENVax) formulations in interferon-deficient AG129 mice. Vaccine 30: 1513-1520.
68. Huang CY, Kinney RM, Livengood JA, Bolling B, Arguello JJ, et al. (2013) Genetic and phenotypic characterization of manufacturing seeds for a tetravalent dengue vaccine (DENVax). PLoS Negl Trop Dis 7: e2243.
69. Durbin AP, Kirkpatrick BD, Pierce KK, Elwood D, Larsson CJ, et al. (2013) A single dose of any of four different live attenuated tetravalent dengue vaccines is safe and immunogenic in flavivirus-naive adults: a randomized, double-blind clinical trial. J Infect Dis 207: 957-965.
70. Halstead SB (2007) Dengue. Lancet 370: 1644-1652.
71. WHO (2009) Dengue guidelines for diagnosis, treatment, prevention and control. Geneva: World Health Organization.
72. Yacoub S, Wertheim H, Simmons CP, Screaton G, Wills B (2014) Cardiovascular manifestations of the emerging dengue pandemic. Nat Rev Cardiol 11: 335-345.
73. Rothman AL (2011) Immunity to dengue virus: a tale of original antigenic sin and tropical cytokine storms. Nat Rev Immunol 11: 532-543.
74. Sierra B, Perez AB, Alvarez M, Garcia G, Vogt K, et al. (2012) Variation in inflammatory/regulatory cytokines in secondary, tertiary, and quaternary challenges with dengue virus. Am J Trop Med Hyg 87: 538-547.
75. Tsai TT, Chuang YJ, Lin YS, Wan SW, Chen CL, et al. (2013) An emerging role for the anti-inflammatory cytokine interleukin-10 in dengue virus infection. J Biomed Sci 20: 40.
76. Libraty DH, Endy TP, Houng HS, Green S, Kalayanarooj S, et al. (2002) Differing influences of virus burden and immune activation on disease severity in secondary dengue-3 virus infections. J Infect Dis 185: 1213-1221.
77. Arias J, Valero N, Mosquera J, Montiel M, Reyes E, et al. (2014) Increased expression of cytokines, soluble cytokine receptors, soluble apoptosis ligand and apoptosis in dengue. Virology 452-453: 42-51.
78. Soundravally R, Hoti SL, Patil SA, Cleetus CC, Zachariah B, et al. (2014) Association between proinflammatory cytokines and lipid peroxidation in patients with severe dengue disease around defervescence. Int J Infect Dis 18: 68-72.
79. Sierra B, Perez AB, Garcia G, Aguirre E, Alvarez M, et al. (2014) Role of CC chemokine receptor 1 and two of its ligands in human dengue infection. Three approaches under the Cuban situation. Microbes Infect 16: 40-50.
80. Malavige GN, Gomes L, Alles L, Chang T, Salimi M, et al. (2013) Serum IL-10 as a marker of severe dengue infection. BMC Infect Dis 13: 341.
81. Rathakrishnan A, Wang SM, Hu Y, Khan AM, Ponnampalavanar S, et al. (2012) Cytokine expression profile of dengue patients at different phases of illness. PLoS One 7: e52215.
82. Kumar Y, Liang C, Bo Z, Rajapakse JC, Ooi EE, et al. (2012) Serum proteome and cytokine analysis in a longitudinal cohort of adults with primary dengue infection reveals predictive markers of DHF. PLoS Negl Trop Dis 6: e1887.
83. Malavige GN, Huang LC, Salimi M, Gomes L, Jayaratne SD, et al. (2012) Cellular and cytokine correlates of severe dengue infection. PLoS One 7: e50387.
84. Butthep P, Chunhakan S, Yoksan S, Tangnararatchakit K, Chuansumrit A (2012) Alteration of cytokines and chemokines during febrile episodes associated with endothelial cell damage and plasma leakage in dengue hemorrhagic fever. Pediatr Infect Dis J 31: e232-238.
85. Furuta T, Murao LA, Lan NT, Huy NT, Huong VT, et al. (2012) Association of mast cell-derived VEGF and proteases in Dengue shock syndrome. PLoS Negl Trop Dis 6: e1505.

86. Houghton-Trivino N, Salgado DM, Rodriguez JA, Bosch I, Castellanos JE (2010) Levels of soluble ST2 in serum associated with severity of dengue due to tumour necrosis factor alpha stimulation. J Gen Virol 91: 697-706.
87. Assuncao-Miranda I, Amaral FA, Bozza FA, Fagundes CT, Sousa LP, et al. (2010) Contribution of macrophage migration inhibitory factor to the pathogenesis of dengue virus infection. FASEB J 24: 218-228.
88. Jaiyen Y, Masrinoul P, Kalayanarooj S, Pulmanausahakul R, Ubol S (2009) Characteristics of dengue virus-infected peripheral blood mononuclear cell death that correlates with the severity of illness. Microbiol Immunol 53: 442-450.
89. Bozza FA, Cruz OG, Zagne SM, Azeredo EL, Nogueira RM, et al. (2008) Multiplex cytokine profile from dengue patients: MIP-1beta and IFN-gamma as predictive factors for severity. BMC Infect Dis 8: 86.
90. Chakravarti A, Kumaria R (2006) Circulating levels of tumour necrosis factor-alpha & interferon-gamma in patients with dengue & dengue haemorrhagic fever during an outbreak. Indian Journal of Medical Research 123: 25-30.
91. Chen LC, Lei HY, Liu CC, Shiesh SC, Chen SH, et al. (2006) Correlation of serum levels of macrophage migration inhibitory factor with disease severity and clinical outcome in dengue patients. Am J Trop Med Hyg 74: 142-147.
92. Cardier JE, Marino E, Romano E, Taylor P, Liprandi F, et al. (2005) Proinflammatory factors present in sera from patients with acute dengue infection induce activation and apoptosis of human microvascular endothelial cells: possible role of TNF-alpha in endothelial cell damage in dengue. Cytokine 30: 359-365.
93. Avila-Aguero ML, Avila-Aguero CR, Um SL, Soriano-Fallas A, Canas-Coto A, et al. (2004) Systemic host inflammatory and coagulation response in the Dengue virus primo-infection. Cytokine 27: 173-179.
94. Perez AB, Garcia G, Sierra B, Alvarez M, Vazquez S, et al. (2004) IL-10 levels in Dengue patients: some findings from the exceptional epidemiological conditions in Cuba. J Med Virol 73: 230-234.
95. Suharti C, van Gorp EC, Dolmans WM, Setiati TE, Hack CE, et al. (2003) Cytokine patterns during dengue shock syndrome. Eur Cytokine Netw 14: 172-177.
96. Suharti C, van Gorp EC, Setiati TE, Dolmans WM, Djokomoeljanto RJ, et al. (2002) The role of cytokines in activation of coagulation and fibrinolysis in dengue shock syndrome. Thromb Haemost 87: 42-46.
97. Mustafa AS, Elbishbishi EA, Agarwal R, Chaturvedi UC (2001) Elevated levels of interleukin-13 and IL-18 in patients with dengue hemorrhagic fever. FEMS Immunol Med Microbiol 30: 229-233.
98. Braga EL, Moura P, Pinto LM, Ignacio SR, Oliveira MJ, et al. (2001) Detection of circulant tumor necrosis factor-alpha, soluble tumor necrosis factor p75 and interferon-gamma in Brazilian patients with dengue fever and dengue hemorrhagic fever. Mem Inst Oswaldo Cruz 96: 229-232.
99. Kittigul L, Temprom W, Sujirarat D, Kittigul C (2000) Determination of tumor necrosis factor-alpha levels in dengue virus infected patients by sensitive biotin-streptavidin enzyme-linked immunosorbent assay. J Virol Methods 90: 51-57.
100. Pacsa AS, Agarwal R, Elbishbishi EA, Chaturvedi UC, Nagar R, et al. (2000) Role of interleukin-12 in patients with dengue hemorrhagic fever. FEMS Immunol Med Microbiol 28: 151-155.
101. Avirutnan P, Malasit P, Seliger B, Bhakdi S, Husmann M (1998) Dengue virus infection of human endothelial cells leads to chemokine production, complement activation, and apoptosis. J Immunol 161: 6338-6346.
102. Raghupathy R, Chaturvedi UC, Al-Sayer H, Elbishbishi EA, Agarwal R, et al. (1998) Elevated levels of IL-8 in dengue hemorrhagic fever. J Med Virol 56: 280-285.
103. Bethell DB, Flobbe K, Cao XT, Day NP, Pham TP, et al. (1998) Pathophysiologic and prognostic role of cytokines in dengue hemorrhagic fever. J Infect Dis 177: 778-782.

104. Hober D, Delannoy AS, Benyoucef S, De Groote D, Wattre P (1996) High levels of sTNFR p75 and TNF alpha in dengue-infected patients. Microbiol Immunol 40: 569-573.
105. Kuno G, Bailey RE (1994) Cytokine responses to dengue infection among Puerto Rican patients. Mem Inst Oswaldo Cruz 89: 179-182.
106. Yacoub S, Mongkolsapaya J, Screaton G (2013) The pathogenesis of dengue. Curr Opin Infect Dis 26: 284-289.
107. Dejnirattisai W, Duangchinda T, Lin CL, Vasanawathana S, Jones M, et al. (2008) A complex interplay among virus, dendritic cells, T cells, and cytokines in dengue virus infections. J Immunol 181: 5865-5874.
108. Sun P, Garcia J, Comach G, Vahey MT, Wang Z, et al. (2013) Sequential waves of gene expression in patients with clinically defined dengue illnesses reveal subtle disease phases and predict disease severity. PLoS Negl Trop Dis 7: e2298.
109. Tisoncik JR, Korth MJ, Simmons CP, Farrar J, Martin TR, et al. (2012) Into the eye of the cytokine storm. Microbiol Mol Biol Rev 76: 16-32.
110. Chong DL, Sriskandan S (2011) Pro-inflammatory mechanisms in sepsis. Contrib Microbiol 17: 86-107.
111. Royall JA, Berkow RL, Beckman JS, Cunningham MK, Matalon S, et al. (1989) Tumor necrosis factor and interleukin 1 alpha increase vascular endothelial permeability. Am J Physiol 257: L399-410.
112. Fernandez-Mestre MT, Gendzekhadze K, Rivas-Vetencourt P, Layrisse Z (2004) TNF-alpha-308A allele, a possible severity risk factor of hemorrhagic manifestation in dengue fever patients. Tissue Antigens 64: 469-472.
113. Shresta S, Sharar KL, Prigozhin DM, Beatty PR, Harris E (2006) Murine model for dengue virus-induced lethal disease with increased vascular permeability. J Virol 80: 10208-10217.
114. Chen ST, Lin YL, Huang MT, Wu MF, Cheng SC, et al. (2008) CLEC5A is critical for dengue-virus-induced lethal disease. Nature 453: 672-676.
115. Watson AA, Lebedev AA, Hall BA, Fenton-May AE, Vagin AA, et al. (2011) Structural flexibility of the macrophage dengue virus receptor CLEC5A: implications for ligand binding and signaling. J Biol Chem 286: 24208-24218.
116. Wu MF, Chen ST, Yang AH, Lin WW, Lin YL, et al. (2013) CLEC5A is critical for dengue virus-induced inflammasome activation in human macrophages. Blood 121: 95-106.
117. Wu MF, Chen ST, Hsieh SL (2013) Distinct regulation of dengue virus-induced inflammasome activation in human macrophage subsets. J Biomed Sci 20: 36.
118. Fagundes CT, Costa VV, Cisalpino D, Amaral FA, Souza PR, et al. (2011) IFN-gamma production depends on IL-12 and IL-18 combined action and mediates host resistance to dengue virus infection in a nitric oxide-dependent manner. PLoS Negl Trop Dis 5: e1449.
119. Yen YT, Chen HC, Lin YD, Shieh CC, Wu-Hsieh BA (2008) Enhancement by tumor necrosis factor alpha of dengue virus-induced endothelial cell production of reactive nitrogen and oxygen species is key to hemorrhage development. J Virol 82: 12312-12324.
120. Dewi BE, Takasaki T, Kurane I (2004) In vitro assessment of human endothelial cell permeability: effects of inflammatory cytokines and dengue virus infection. J Virol Methods 121: 171-180.
121. Costa VV, Fagundes CT, Valadao DF, Cisalpino D, Dias AC, et al. (2012) A model of DENV-3 infection that recapitulates severe disease and highlights the importance of IFN-gamma in host resistance to infection. PLoS Negl Trop Dis 6: e1663.
122. Gunther VJ, Putnak R, Eckels KH, Mammen MP, Scherer JM, et al. (2011) A human challenge model for dengue infection reveals a possible protective role for sustained interferon gamma levels during the acute phase of illness. Vaccine 29: 3895-3904.
123. Murphy K, Travers P, Walport M (2008) Janeway's Immunobiology. New York, NY: Garland Science, Taylor & Francis Group, LLC. 887 p.

124. Bokisch VA, Top FH, Jr., Russell PK, Dixon FJ, Muller-Eberhard HJ (1973) The potential pathogenic role of complement in dengue hemorrhagic shock syndrome. N Engl J Med 289: 996-1000.
125. World Health Organisation (1973) Pathogenetic mechanisms in dengue haemorrhagic fever: report of an international collaborative study. Bull World Health Organ 48: 117-133.
126. Bokisch VA, Muller-Eberhard HJ, Cochrane CG (1969) Isolation of a fragment (C3a) of the third component of human complement containing anaphylatoxin and chemotactic activity and description of an anaphylatoxin inactivator of human serum. J Exp Med 129: 1109-1130.
127. Bokisch VA, Muller-Eberhard HJ (1970) Anaphylatoxin inactivator of human plasma: its isolation and characterization as a carboxypeptidase. J Clin Invest 49: 2427-2436.
128. Vallota EH, Muller-Eberhard HJ (1973) Formation of C3a and C5a anaphylatoxins in whole human serum after inhibition of the anaphylatoxin inactivator. J Exp Med 137: 1109-1123.
129. Avirutnan P, Fuchs A, Hauhart RE, Somnuke P, Youn S, et al. (2010) Antagonism of the complement component C4 by flavivirus nonstructural protein NS1. J Exp Med 207: 793-806.
130. Avirutnan P, Hauhart RE, Somnuke P, Blom AM, Diamond MS, et al. (2011) Binding of flavivirus nonstructural protein NS1 to C4b binding protein modulates complement activation. J Immunol 187: 424-433.
131. Somnuke P, Hauhart RE, Atkinson JP, Diamond MS, Avirutnan P (2011) N-linked glycosylation of dengue virus NS1 protein modulates secretion, cell-surface expression, hexamer stability, and interactions with human complement. Virology 413: 253-264.
132. Kurosu T, Chaichana P, Yamate M, Anantapreecha S, Ikuta K (2007) Secreted complement regulatory protein clusterin interacts with dengue virus nonstructural protein 1. Biochem Biophys Res Commun 362: 1051-1056.
133. Dalrymple NA, Mackow ER (2012) Endothelial cells elicit immune-enhancing responses to dengue virus infection. J Virol 86: 6408-6415.
134. Kraivong R, Vasanawathana S, Limpitikul W, Malasit P, Tangthawornchaikul N, et al. (2013) Complement alternative pathway genetic variation and Dengue infection in the Thai population. Clin Exp Immunol 174: 326-334.
135. Halstead SB, Nimmannitya S, Yamarat C, Russell PK (1967) Hemorrhagic fever in Thailand; recent knowledge regarding etiology. Jpn J Med Sci Biol 20 Suppl: 96-103.
136. Russell PK, Udomsakdi S, Halstead SB (1967) Antibody response in dengue and dengue hemorrhagic fever. Jpn J Med Sci Biol 20 Suppl: 103-108.
137. Halstead SB, Nimmannitya S, Cohen SN (1970) Observations related to pathogenesis of dengue hemorrhagic fever. IV. Relation of disease severity to antibody response and virus recovered. Yale J Biol Med 42: 311-328.
138. Halstead SB, O'Rourke EJ (1977) Antibody-enhanced dengue virus infection in primate leukocytes. Nature 265: 739-741.
139. Navarro-Sanchez E, Altmeyer R, Amara A, Schwartz O, Fieschi F, et al. (2003) Dendritic-cell-specific ICAM3-grabbing non-integrin is essential for the productive infection of human dendritic cells by mosquito-cell-derived dengue viruses. EMBO Rep 4: 723-728.
140. Tassaneetrithep B, Burgess TH, Granelli-Piperno A, Trumpfheller C, Finke J, et al. (2003) DC-SIGN (CD209) mediates dengue virus infection of human dendritic cells. J Exp Med 197: 823-829.
141. Miller JL, de Wet BJ, Martinez-Pomares L, Radcliffe CM, Dwek RA, et al. (2008) The mannose receptor mediates dengue virus infection of macrophages. PLoS Pathog 4: e17.
142. Halstead SB, Mahalingam S, Marovich MA, Ubol S, Mosser DM (2010) Intrinsic antibody-dependent enhancement of microbial infection in macrophages: disease regulation by immune complexes. Lancet Infect Dis 10: 712-722.
143. Dejnirattisai W, Jumnainsong A, Onsirisakul N, Fitton P, Vasanawathana S, et al. (2010) Cross-reacting antibodies enhance dengue virus infection in humans. Science 328: 745-748.
144. Zhang Y, Corver J, Chipman PR, Zhang W, Pletnev SV, et al. (2003) Structures of immature flavivirus particles. EMBO J 22: 2604-2613.

145. Pokidysheva E, Zhang Y, Battisti AJ, Bator-Kelly CM, Chipman PR, et al. (2006) Cryo-EM reconstruction of dengue virus in complex with the carbohydrate recognition domain of DC-SIGN. Cell 124: 485-493.
146. Ubol S, Phuklia W, Kalayanarooj S, Modhiran N (2010) Mechanisms of immune evasion induced by a complex of dengue virus and preexisting enhancing antibodies. J Infect Dis 201: 923-935.
147. Ubol S, Halstead SB (2010) How innate immune mechanisms contribute to antibody-enhanced viral infections. Clin Vaccine Immunol 17: 1829-1835.
148. Chan KR, Ong EZ, Tan HC, Zhang SL, Zhang Q, et al. (2014) Leukocyte immunoglobulin-like receptor B1 is critical for antibody-dependent dengue. Proc Natl Acad Sci U S A 111: 2722-2727.
149. Modhiran N, Kalayanarooj S, Ubol S (2010) Subversion of innate defenses by the interplay between DENV and pre-existing enhancing antibodies: TLRs signaling collapse. PLoS Negl Trop Dis 4: e924.
150. Halstead SB, Rojanasuphot S, Sangkawibha N (1983) Original antigenic sin in dengue. Am J Trop Med Hyg 32: 154-156.
151. Midgley CM, Bajwa-Joseph M, Vasanawathana S, Limpitikul W, Wills B, et al. (2011) An in-depth analysis of original antigenic sin in dengue virus infection. J Virol 85: 410-421.
152. Mongkolsapaya J, Dejnirattisai W, Xu XN, Vasanawathana S, Tangthawornchaikul N, et al. (2003) Original antigenic sin and apoptosis in the pathogenesis of dengue hemorrhagic fever. Nat Med 9: 921-927.
153. Mathew A, Rothman AL (2008) Understanding the contribution of cellular immunity to dengue disease pathogenesis. Immunol Rev 225: 300-313.
154. Weiskopf D, Angelo MA, de Azeredo EL, Sidney J, Greenbaum JA, et al. (2013) Comprehensive analysis of dengue virus-specific responses supports an HLA-linked protective role for CD8+ T cells. Proc Natl Acad Sci U S A 110: E2046-2053.
155. Zompi S, Harris E (2013) Original antigenic sin in dengue revisited. Proc Natl Acad Sci U S A 110: 8761-8762.
156. Weiskopf D, Sette A (2014) T-Cell Immunity to Infection with Dengue Virus in Humans. Front Immunol 5: 93.
157. Kurane I, Brinton MA, Samson AL, Ennis FA (1991) Dengue virus-specific, human CD4+ CD8- cytotoxic T-cell clones: multiple patterns of virus cross-reactivity recognized by NS3-specific T-cell clones. J Virol 65: 1823-1828.
158. Lobigs M, Arthur CE, Mullbacher A, Blanden RV (1994) The flavivirus nonstructural protein NS3 is a dominant source of cytotoxic T cell peptide determinants. Virology 202: 195-201.
159. Mathew A, Kurane I, Rothman AL, Zeng LL, Brinton MA, et al. (1996) Dominant recognition by human CD8+ cytotoxic T lymphocytes of dengue virus nonstructural proteins NS3 and NS1.2a. J Clin Invest 98: 1684-1691.
160. Duangchinda T, Dejnirattisai W, Vasanawathana S, Limpitikul W, Tangthawornchaikul N, et al. (2010) Immunodominant T-cell responses to dengue virus NS3 are associated with DHF. Proc Natl Acad Sci U S A 107: 16922-16927.
161. Imrie A, Meeks J, Gurary A, Sukhbataar M, Kitsutani P, et al. (2007) Differential functional avidity of dengue virus-specific T-cell clones for variant peptides representing heterologous and previously encountered serotypes. J Virol 81: 10081-10091.
162. Rivino L, Kumaran EA, Jovanovic V, Nadua K, Teo EW, et al. (2013) Differential targeting of viral components by CD4+ versus CD8+ T lymphocytes in dengue virus infection. J Virol 87: 2693-2706.
163. Mangada MM, Rothman AL (2005) Altered cytokine responses of dengue-specific CD4+ T cells to heterologous serotypes. J Immunol 175: 2676-2683.
164. Malavige GN, Ogg GS (2013) T cell responses in dengue viral infections. J Clin Virol 58: 605-611.

165. Mongkolsapaya J, Duangchinda T, Dejnirattisai W, Vasanawathana S, Avirutnan P, et al. (2006) T cell responses in dengue hemorrhagic fever: are cross-reactive T cells suboptimal? J Immunol 176: 3821-3829.
166. Dung NT, Duyen HT, Thuy NT, Ngoc TV, Chau NV, et al. (2010) Timing of CD8+ T cell responses in relation to commencement of capillary leakage in children with dengue. J Immunol 184: 7281-7287.
167. Sarasombath S, Suvatte V, Homchampa P (1988) Kinetics of lymphocyte subpopulations in dengue hemorrhagic fever/dengue shock syndrome. Southeast Asian J Trop Med Public Health 19: 649-656.
168. Nielsen DG (2009) The relationship of interacting immunological components in dengue pathogenesis. Virol J 6: 211.
169. Fadilah SA, Sahrir S, Raymond AA, Cheong SK, Aziz JA, et al. (1999) Quantitation of T lymphocyte subsets helps to distinguish dengue hemorrhagic fever from classic dengue fever during the acute febrile stage. Southeast Asian J Trop Med Public Health 30: 710-717.
170. Damonte EB, Pujol CA, Coto CE (2004) Prospects for the therapy and prevention of dengue virus infections. Adv Virus Res 63: 239-285.
171. Li Z, Khaliq M, Zhou Z, Post CB, Kuhn RJ, et al. (2008) Design, synthesis, and biological evaluation of antiviral agents targeting flavivirus envelope proteins. J Med Chem 51: 4660-4671.
172. Perera R, Khaliq M, Kuhn RJ (2008) Closing the door on flaviviruses: entry as a target for antiviral drug design. Antiviral Res 80: 11-22.
173. Malet H, Masse N, Selisko B, Romette JL, Alvarez K, et al. (2008) The flavivirus polymerase as a target for drug discovery. Antiviral Res 80: 23-35.
174. Sampath A, Padmanabhan R (2009) Molecular targets for flavivirus drug discovery. Antiviral Res 81: 6-15.
175. Yin Z, Chen YL, Schul W, Wang QY, Gu F, et al. (2009) An adenosine nucleoside inhibitor of dengue virus. Proc Natl Acad Sci U S A 106: 20435-20439.
176. Lescar J, Luo D, Xu T, Sampath A, Lim SP, et al. (2008) Towards the design of antiviral inhibitors against flaviviruses: the case for the multifunctional NS3 protein from Dengue virus as a target. Antiviral Res 80: 94-101.
177. Taylor ME, Drickamer K (2011) Introduction to Glycobiology: Oxford University Press. 320 p.
178. Lederkremer GZ (2009) Glycoprotein folding, quality control and ER-associated degradation. Curr Opin Struct Biol 19: 515-523.
179. Takatsuki A, Tamura G (1971) Effect of tunicamycin on the synthesis of macromolecules in cultures of chick embryo fibroblasts infected with Newcastle disease virus. J Antibiot (Tokyo) 24: 785-794.
180. Takatsuki A, Arima K, Tamura G (1971) Tunicamycin, a new antibiotic. I. Isolation and characterization of tunicamycin. J Antibiot (Tokyo) 24: 215-223.
181. Takatsuki A, Tamura G (1971) Tunicamycin, a new antibiotic. 3. Reversal of the antiviral activity of tunicamycin by aminosugars and their derivatives. J Antibiot (Tokyo) 24: 232-238.
182. Takatsuki A, Tamura G (1971) Tunicamycin, a new antibiotic. II. Some biological properties of the antiviral activity of tunicamycin. J Antibiot (Tokyo) 24: 224-231.
183. Elbein AD, Dorling PR, Vosbeck K, Horisberger M (1982) Swainsonine prevents the processing of the oligosaccharide chains of influenza virus hemagglutinin. J Biol Chem 257: 1573-1576.
184. Datema R, Romero PA, Legler G, Schwarz RT (1982) Inhibition of formation of complex oligosaccharides by the glucosidase inhibitor bromoconduritol. Proc Natl Acad Sci U S A 79: 6787-6791.
185. Pan YT, Hori H, Saul R, Sanford BA, Molyneux RJ, et al. (1983) Castanospermine inhibits the processing of the oligosaccharide portion of the influenza viral hemagglutinin. Biochemistry 22: 3975-3984.

186. Romero PA, Datema R, Schwarz RT (1983) N-methyl-1-deoxynojirimycin, a novel inhibitor of glycoprotein processing, and its effect on fowl plague virus maturation. Virology 130: 238-242.
187. Bosch JV, Schwarz RT (1984) Processing of gPr92env, the precursor to the glycoproteins of Rous sarcoma virus: use of inhibitors of oligosaccharide trimming and glycoprotein transport. Virology 132: 95-109.
188. Datema R, Romero PA, Rott R, Schwarz RT (1984) On the role of oligosaccharide trimming in the maturation of Sindbis and influenza virus. Arch Virol 81: 25-39.
189. Schlesinger S, Malfer C, Schlesinger MJ (1984) The formation of vesicular stomatitis virus (San Juan strain) becomes temperature-sensitive when glucose residues are retained on the oligosaccharides of the glycoprotein. J Biol Chem 259: 7597-7601.
190. Schlesinger S, Koyama AH, Malfer C, Gee SL, Schlesinger MJ (1985) The effects of inhibitors of glucosidase I on the formation of Sindbis virus. Virus Res 2: 139-149.
191. Sunkara PS, Bowlin TL, Liu PS, Sjoerdsma A (1987) Antiretroviral activity of castanospermine and deoxynojirimycin, specific inhibitors of glycoprotein processing. Biochem Biophys Res Commun 148: 206-210.
192. Tyms AS, Berrie EM, Ryder TA, Nash RJ, Hegarty MP, et al. (1987) Castanospermine and other plant alkaloid inhibitors of glucosidase activity block the growth of HIV. Lancet 2: 1025-1026.
193. Gruters RA, Neefjes JJ, Tersmette M, de Goede RE, Tulp A, et al. (1987) Interference with HIV-induced syncytium formation and viral infectivity by inhibitors of trimming glucosidase. Nature 330: 74-77.
194. Fleet GW, Karpas A, Dwek RA, Fellows LE, Tyms AS, et al. (1988) Inhibition of HIV replication by amino-sugar derivatives. FEBS Lett 237: 128-132.
195. Myers MW (1990) New antiretroviral agents in the clinic. Rev Infect Dis 12: 944-950.
196. Fischl MA, Resnick L, Coombs R, Kremer AB, Pottage JC, Jr., et al. (1994) The safety and efficacy of combination N-butyl-deoxynojirimycin (SC-48334) and zidovudine in patients with HIV-1 infection and 200-500 CD4 cells/mm3. J Acquir Immune Defic Syndr 7: 139-147.
197. Tierney M, Pottage J, Kessler H, Fischl M, Richman D, et al. (1995) The tolerability and pharmacokinetics of N-butyl-deoxynojirimycin in patients with advanced HIV disease (ACTG 100). The AIDS Clinical Trials Group (ACTG) of the National Institute of Allergy and Infectious Diseases. J Acquir Immune Defic Syndr Hum Retrovirol 10: 549-553.
198. Cox T, Lachmann R, Hollak C, Aerts J, van Weely S, et al. (2000) Novel oral treatment of Gaucher's disease with N-butyldeoxynojirimycin (OGT 918) to decrease substrate biosynthesis. Lancet 355: 1481-1485.
199. Venier RE, Igdoura SA (2012) Miglustat as a therapeutic agent: prospects and caveats. J Med Genet 49: 591-597.
200. Patterson MC, Vecchio D, Prady H, Abel L, Wraith JE (2007) Miglustat for treatment of Niemann-Pick C disease: a randomised controlled study. Lancet Neurol 6: 765-772.
201. Miller JL, Lachica R, Sayce AC, Williams JP, Bapat M, et al. (2012) Liposome-mediated delivery of iminosugars enhances efficacy against dengue virus in vivo. Antimicrob Agents Chemother 56: 6379-6386.
202. Gu B, Mason P, Wang L, Norton P, Bourne N, et al. (2007) Antiviral profiles of novel iminocyclitol compounds against bovine viral diarrhea virus, West Nile virus, dengue virus and hepatitis B virus. Antivir Chem Chemother 18: 49-59.
203. Chang J, Wang L, Ma D, Qu X, Guo H, et al. (2009) Novel imino sugar derivatives demonstrate potent antiviral activity against flaviviruses. Antimicrob Agents Chemother 53: 1501-1508.
204. Liang PH, Cheng WC, Lee YL, Yu HP, Wu YT, et al. (2006) Novel five-membered iminocyclitol derivatives as selective and potent glycosidase inhibitors: new structures for antivirals and osteoarthritis. Chembiochem 7: 165-173.

205. Courageot MP, Frenkiel MP, Dos Santos CD, Deubel V, Despres P (2000) Alpha-glucosidase inhibitors reduce dengue virus production by affecting the initial steps of virion morphogenesis in the endoplasmic reticulum. J Virol 74: 564-572.
206. Chang J, Schul W, Butters TD, Yip A, Liu B, et al. (2011) Combination of alpha-glucosidase inhibitor and ribavirin for the treatment of dengue virus infection in vitro and in vivo. Antiviral Res 89: 26-34.
207. Chang J, Schul W, Yip A, Xu X, Guo JT, et al. (2011) Competitive inhibitor of cellular alpha-glucosidases protects mice from lethal dengue virus infection. Antiviral Res 92: 369-371.
208. Yu W, Gill T, Wang L, Du Y, Ye H, et al. (2012) Design, synthesis, and biological evaluation of N-alkylated deoxynojirimycin (DNJ) derivatives for the treatment of dengue virus infection. J Med Chem 55: 6061-6075.
209. Perry ST, Buck MD, Plummer EM, Penmasta RA, Batra H, et al. (2013) An iminosugar with potent inhibition of dengue virus infection in vivo. Antiviral Res 98: 35-43.
210. Chang J, Warren TK, Zhao X, Gill T, Guo F, et al. (2013) Small molecule inhibitors of ER alpha-glucosidases are active against multiple hemorrhagic fever viruses. Antiviral Res 98: 432-440.
211. Zitzmann N, Mehta AS, Carrouee S, Butters TD, Platt FM, et al. (1999) Imino sugars inhibit the formation and secretion of bovine viral diarrhea virus, a pestivirus model of hepatitis C virus: implications for the development of broad spectrum anti-hepatitis virus agents. Proc Natl Acad Sci U S A 96: 11878-11882.
212. Mehta A, Ouzounov S, Jordan R, Simsek E, Lu X, et al. (2002) Imino sugars that are less toxic but more potent as antivirals, in vitro, compared with N-n-nonyl DNJ. Antivir Chem Chemother 13: 299-304.
213. Qu X, Pan X, Weidner J, Yu W, Alonzi D, et al. (2011) Inhibitors of endoplasmic reticulum alpha-glucosidases potently suppress hepatitis C virus virion assembly and release. Antimicrob Agents Chemother 55: 1036-1044.
214. Mehta A, Carrouee S, Conyers B, Jordan R, Butters T, et al. (2001) Inhibition of hepatitis B virus DNA replication by imino sugars without the inhibition of the DNA polymerase: therapeutic implications. Hepatology 33: 1488-1495.
215. Petrescu SM, Branza-Nichita N, Negroiu G, Petrescu AJ, Dwek RA (2000) Tyrosinase and glycoprotein folding: roles of chaperones that recognize glycans. Biochemistry 39: 5229-5237.
216. Mehta A, Lu X, Block TM, Blumberg BS, Dwek RA (1997) Hepatitis B virus (HBV) envelope glycoproteins vary drastically in their sensitivity to glycan processing: evidence that alteration of a single N-linked glycosylation site can regulate HBV secretion. Proc Natl Acad Sci U S A 94: 1822-1827.
217. Platt FM, Karlsson GB, Jacob GS (1992) Modulation of cell-surface transferrin receptor by the imino sugar N-butyldeoxynojirimycin. Eur J Biochem 208: 187-193.
218. Ludolph D, Gross V, Katz NR, Giffhorn-Katz S, Kreisel W, et al. (1989) Effect of the alpha-glucosidase inhibitor N-hydroxyethyl-1-deoxynojirimycin (Bay m 1099) on the biosynthesis of liver secretory glycoproteins. Biochem Pharmacol 38: 2479-2486.
219. Zhou J, Zhang Y, Zhou X, Zhang LH, Ye XS, et al. (2008) An expeditious one-pot synthesis of 1,6-dideoxy-N-alkylated nojirimycin derivatives and their inhibitory effects on the secretion of IFN-gamma and IL-4. Bioorg Med Chem 16: 1605-1612.
220. Vyavahare VP, Chakraborty C, Maity B, Chattopadhyay S, Puranik VG, et al. (2007) Synthesis of 1-deoxy-1-hydroxymethyl- and 1-deoxy-1-epi-hydroxymethyl castanospermine as new potential immunomodulating agents. J Med Chem 50: 5519-5523.
221. Ye XS, Sun F, Liu M, Li Q, Wang Y, et al. (2005) Synthetic iminosugar derivatives as new potential immunosuppressive agents. J Med Chem 48: 3688-3691.
222. Kosuge T, Toyoshima S (2000) Increased degradation of newly synthesized interferon-gamma (IFN-gamma) in anti CD3-stimulated lymphocytes treated with glycoprotein processing inhibitors. Biol Pharm Bull 23: 545-548.

223. Kosuge T, Tamura T, Nariuchi H, Toyoshima S (2000) Effect of inhibitors of glycoprotein processing on cytokine secretion and production in anti CD3-stimulated T cells. Biol Pharm Bull 23: 1-5.
224. Kumar KS, Rathee JS, Subramanian M, Chattopadhyay S (2013) Divergent synthesis of 4-epi-fagomine, 3,4-dihydroxypipecolic acid, and a dihydroxyindolizidine and their beta-galactosidase inhibitory and immunomodulatory activities. J Org Chem 78: 7406-7413.
225. Sun Y, Ran H, Liou B, Quinn B, Zamzow M, et al. (2011) Isofagomine in vivo effects in a neuronopathic Gaucher disease mouse. PLoS One 6: e19037.
226. Boomkamp SD, Rountree JS, Neville DC, Dwek RA, Fleet GW, et al. (2010) Lysosomal storage of oligosaccharide and glycosphingolipid in imino sugar treated cells. Glycoconj J 27: 297-308.
227. Grochowicz PM, Hibberd AD, Smart YC, Bowen KM, Clark DA, et al. (1996) Castanospermine, an oligosaccharide processing inhibitor, reduces membrane expression of adhesion molecules and prolongs heart allograft survival in rats. Transpl Immunol 4: 275-285.
228. Wall KA, Pierce JD, Elbein AD (1988) Inhibitors of glycoprotein processing alter T-cell proliferative responses to antigen and to interleukin 2. Proc Natl Acad Sci U S A 85: 5644-5648.
229. van Kemenade FJ, Rotteveel FT, van den Broek LA, Baars PA, van Lier RA, et al. (1994) Glucosidase trimming inhibitors preferentially perturb T cell activation induced by CD2 mAb. J Leukoc Biol 56: 159-165.
230. Tian G, Wilcockson D, Perry VH, Rudd PM, Dwek RA, et al. (2004) Inhibition of alpha-glucosidases I and II increases the cell surface expression of functional class A macrophage scavenger receptor (SR-A) by extending its half-life. J Biol Chem 279: 39303-39309.
231. Russell PK, Nisalak A, Sukhavachana P, Vivona S (1967) A plaque reduction test for dengue virus neutralizing antibodies. J Immunol 99: 285-290.
232. Whitby K, Pierson TC, Geiss B, Lane K, Engle M, et al. (2005) Castanospermine, a potent inhibitor of dengue virus infection in vitro and in vivo. J Virol 79: 8698-8706.
233. Diamond MS, Roberts TG, Edgil D, Lu B, Ernst J, et al. (2000) Modulation of Dengue virus infection in human cells by alpha, beta, and gamma interferons. J Virol 74: 4957-4966.
234. Zor T, Selinger Z (1996) Linearization of the Bradford protein assay increases its sensitivity: theoretical and experimental studies. Anal Biochem 236: 302-308.
235. Alonzi DS, Neville DC, Lachmann RH, Dwek RA, Butters TD (2008) Glucosylated free oligosaccharides are biomarkers of endoplasmic- reticulum alpha-glucosidase inhibition. Biochem J 409: 571-580.
236. Neville DC, Coquard V, Priestman DA, te Vruchte DJ, Sillence DJ, et al. (2004) Analysis of fluorescently labeled glycosphingolipid-derived oligosaccharides following ceramide glycanase digestion and anthranilic acid labeling. Anal Biochem 331: 275-282.
237. Svennerholm L, Fredman P (1980) A procedure for the quantitative isolation of brain gangliosides. Biochim Biophys Acta 617: 97-109.
238. Henchal EA, McCown JM, Burke DS, Seguin MC, Brandt WE (1985) Epitopic analysis of antigenic determinants on the surface of dengue-2 virions using monoclonal antibodies. Am J Trop Med Hyg 34: 162-169.
239. Asano N, Nishida M, Kato A, Kizu H, Matsui K, et al. (1998) Homonojirimycin isomers and N-alkylated homonojirimycins: structural and conformational basis of inhibition of glycosidases. J Med Chem 41: 2565-2571.
240. Du P, Kibbe WA, Lin SM (2007) nuID: a universal naming scheme of oligonucleotides for illumina, affymetrix, and other microarrays. Biol Direct 2: 16.
241. Du P, Kibbe WA, Lin SM (2008) lumi: a pipeline for processing Illumina microarray. Bioinformatics 24: 1547-1548.
242. Lin SM, Du P, Huber W, Kibbe WA (2008) Model-based variance-stabilizing transformation for Illumina microarray data. Nucleic Acids Res 36: e11.

243. Du P, Zhang X, Huang CC, Jafari N, Kibbe WA, et al. (2010) Comparison of Beta-value and M-value methods for quantifying methylation levels by microarray analysis. BMC Bioinformatics 11: 587.
244. Shi W, Oshlack A, Smyth GK (2010) Optimizing the noise versus bias trade-off for Illumina whole genome expression BeadChips. Nucleic Acids Res 38: e204.
245. Martinez FO, Helming L, Milde R, Varin A, Melgert BN, et al. (2013) Genetic programs expressed in resting and IL-4 alternatively activated mouse and human macrophages: similarities and differences. Blood 121: e57-69.
246. Balsitis SJ, Williams KL, Lachica R, Flores D, Kyle JL, et al. (2010) Lethal antibody enhancement of dengue disease in mice is prevented by Fc modification. PLoS Pathog 6: e1000790.
247. Wu SF, Lee CJ, Liao CL, Dwek RA, Zitzmann N, et al. (2002) Antiviral effects of an iminosugar derivative on flavivirus infections. J Virol 76: 3596-3604.
248. Platt FM, Neises GR, Karlsson GB, Dwek RA, Butters TD (1994) N-butyldeoxygalactonojirimycin inhibits glycolipid biosynthesis but does not affect N-linked oligosaccharide processing. J Biol Chem 269: 27108-27114.
249. Platt FM, Neises GR, Dwek RA, Butters TD (1994) N-butyldeoxynojirimycin is a novel inhibitor of glycolipid biosynthesis. J Biol Chem 269: 8362-8365.
250. Townson KH, Speak AO, Greenshields KN, Goodyear CS, Willison HJ, et al. (2008) Glycosphingolipid depletion in PC12 cells using iminosugars protects neuronal membranes from anti-ganglioside antibody mediated injury. J Neuroimmunol 203: 33-38.
251. Simmons CP, Popper S, Dolocek C, Chau TN, Griffiths M, et al. (2007) Patterns of host genome-wide gene transcript abundance in the peripheral blood of patients with acute dengue hemorrhagic fever. J Infect Dis 195: 1097-1107.
252. Long HT, Hibberd ML, Hien TT, Dung NM, Van Ngoc T, et al. (2009) Patterns of gene transcript abundance in the blood of children with severe or uncomplicated dengue highlight differences in disease evolution and host response to dengue virus infection. J Infect Dis 199: 537-546.
253. Hoang LT, Lynn DJ, Henn M, Birren BW, Lennon NJ, et al. (2010) The early whole-blood transcriptional signature of dengue virus and features associated with progression to dengue shock syndrome in Vietnamese children and young adults. J Virol 84: 12982-12994.
254. Loke P, Hammond SN, Leung JM, Kim CC, Batra S, et al. (2010) Gene expression patterns of dengue virus-infected children from nicaragua reveal a distinct signature of increased metabolism. PLoS Negl Trop Dis 4: e710.
255. Devignot S, Sapet C, Duong V, Bergon A, Rihet P, et al. (2010) Genome-wide expression profiling deciphers host responses altered during dengue shock syndrome and reveals the role of innate immunity in severe dengue. PLoS One 5: e11671.
256. Tolfvenstam T, Lindblom A, Schreiber MJ, Ling L, Chow A, et al. (2011) Characterization of early host responses in adults with dengue disease. BMC Infect Dis 11: 209.
257. Popper SJ, Gordon A, Liu M, Balmaseda A, Harris E, et al. (2012) Temporal dynamics of the transcriptional response to dengue virus infection in Nicaraguan children. PLoS Negl Trop Dis 6: e1966.
258. Fink J, Gu F, Ling L, Tolfvenstam T, Olfat F, et al. (2007) Host gene expression profiling of dengue virus infection in cell lines and patients. PLoS Negl Trop Dis 1: e86.
259. Sessions OM, Tan Y, Goh KC, Liu Y, Tan P, et al. (2013) Host cell transcriptome profile during wild-type and attenuated dengue virus infection. PLoS Negl Trop Dis 7: e2107.
260. Long X, Li Y, Qi Y, Xu J, Wang Z, et al. (2013) XAF1 contributes to dengue virus-induced apoptosis in vascular endothelial cells. FASEB J 27: 1062-1073.
261. Balas C, Kennel A, Deauvieau F, Sodoyer R, Arnaud-Barbe N, et al. (2011) Different innate signatures induced in human monocyte-derived dendritic cells by wild-type dengue 3 virus, attenuated but reactogenic dengue 3 vaccine virus, or attenuated nonreactogenic dengue 1-4 vaccine virus strains. J Infect Dis 203: 103-108.

262. Schroder M, Kaufman RJ (2005) The mammalian unfolded protein response. Annu Rev Biochem 74: 739-789.
263. Hall WC, Crowell TP, Watts DM, Barros VL, Kruger H, et al. (1991) Demonstration of yellow fever and dengue antigens in formalin-fixed paraffin-embedded human liver by immunohistochemical analysis. Am J Trop Med Hyg 45: 408-417.
264. Neves-Souza PC, Azeredo EL, Zagne SM, Valls-de-Souza R, Reis SR, et al. (2005) Inducible nitric oxide synthase (iNOS) expression in monocytes during acute Dengue Fever in patients and during in vitro infection. BMC Infect Dis 5: 64.
265. Jessie K, Fong MY, Devi S, Lam SK, Wong KT (2004) Localization of dengue virus in naturally infected human tissues, by immunohistochemistry and in situ hybridization. J Infect Dis 189: 1411-1418.
266. Bhoopat L, Bhamarapravati N, Attasiri C, Yoksarn S, Chaiwun B, et al. (1996) Immunohistochemical characterization of a new monoclonal antibody reactive with dengue virus-infected cells in frozen tissue using immunoperoxidase technique. Asian Pac J Allergy Immunol 14: 107-113.
267. Boonpucknavig S, Boonpucknavig V, Bhamarapravati N, Nimmannitya S (1979) Immunofluorescence study of skin rash in patients with dengue hemorrhagic fever. Arch Pathol Lab Med 103: 463-466.
268. Kyle JL, Beatty PR, Harris E (2007) Dengue virus infects macrophages and dendritic cells in a mouse model of infection. J Infect Dis 195: 1808-1817.
269. Oh-hashi K, Koga H, Ikeda S, Shimada K, Hirata Y, et al. (2009) CRELD2 is a novel endoplasmic reticulum stress-inducible gene. Biochem Biophys Res Commun 387: 504-510.
270. Darwich L, Coma G, Pena R, Bellido R, Blanco EJ, et al. (2009) Secretion of interferon-gamma by human macrophages demonstrated at the single-cell level after costimulation with interleukin (IL)-12 plus IL-18. Immunology 126: 386-393.
271. Byun M, Ma CS, Akcay A, Pedergnana V, Palendira U, et al. (2013) Inherited human OX40 deficiency underlying classic Kaposi sarcoma of childhood. J Exp Med 210: 1743-1759.
272. Stachel I, Geismann C, Aden K, Deisinger F, Rosenstiel P, et al. (2014) Modulation of nuclear factor E2-related factor-2 (Nrf2) activation by the stress response gene immediate early response-3 (IER3) in colonic epithelial cells: a novel mechanism of cellular adaption to inflammatory stress. J Biol Chem 289: 1917-1929.
273. Chen HW, King K, Tu J, Sanchez M, Luster AD, et al. (2013) The roles of IRF-3 and IRF-7 in innate antiviral immunity against dengue virus. J Immunol 191: 4194-4201.
274. Dalrymple NA, Mackow ER (2012) Roles for endothelial cells in dengue virus infection. Adv Virol 2012: 840654.
275. Venugopal R, Jaiswal AK (1998) Nrf2 and Nrf1 in association with Jun proteins regulate antioxidant response element-mediated expression and coordinated induction of genes encoding detoxifying enzymes. Oncogene 17: 3145-3156.
276. Itoh K, Wakabayashi N, Katoh Y, Ishii T, Igarashi K, et al. (1999) Keap1 represses nuclear activation of antioxidant responsive elements by Nrf2 through binding to the amino-terminal Neh2 domain. Genes Dev 13: 76-86.
277. Nguyen T, Huang HC, Pickett CB (2000) Transcriptional regulation of the antioxidant response element. Activation by Nrf2 and repression by MafK. J Biol Chem 275: 15466-15473.
278. Ishii T, Itoh K, Takahashi S, Sato H, Yanagawa T, et al. (2000) Transcription factor Nrf2 coordinately regulates a group of oxidative stress-inducible genes in macrophages. J Biol Chem 275: 16023-16029.
279. Li B, Shi Y, Shu J, Gao J, Wu P, et al. (2013) Wingless-type mammary tumor virus integration site family, member 5A (Wnt5a) regulates human immunodeficiency virus type 1 (HIV-1) envelope glycoprotein 120 (gp120)-induced expression of pro-inflammatory cytokines via the Ca2+/calmodulin-dependent protein kinase II (CaMKII) and c-Jun N-terminal kinase (JNK) signaling pathways. J Biol Chem 288: 13610-13619.

280. Randall G, Panis M, Cooper JD, Tellinghuisen TL, Sukhodolets KE, et al. (2007) Cellular cofactors affecting hepatitis C virus infection and replication. Proc Natl Acad Sci U S A 104: 12884-12889.
281. Martinon F, Chen X, Lee AH, Glimcher LH (2010) TLR activation of the transcription factor XBP1 regulates innate immune responses in macrophages. Nat Immunol 11: 411-418.
282. Li J, Wang JJ, Zhang SX (2011) Preconditioning with endoplasmic reticulum stress mitigates retinal endothelial inflammation via activation of X-box binding protein 1. J Biol Chem 286: 4912-4921.
283. Pennica D, Hayflick JS, Bringman TS, Palladino MA, Goeddel DV (1985) Cloning and expression in Escherichia coli of the cDNA for murine tumor necrosis factor. Proc Natl Acad Sci U S A 82: 6060-6064.
284. Bonferroni CE (1936) Teoria statistica delle classi e calcolo delle probabilita. Pubblicazioni del R Instituto Superiore di Scienze Economiche e Commerciali di Firenze 8: 3-62.
285. Namen AE, Lupton S, Hjerrild K, Wignall J, Mochizuki DY, et al. (1988) Stimulation of B-cell progenitors by cloned murine interleukin-7. Nature 333: 571-573.
286. Goodwin RG, Lupton S, Schmierer A, Hjerrild KJ, Jerzy R, et al. (1989) Human interleukin 7: molecular cloning and growth factor activity on human and murine B-lineage cells. Proc Natl Acad Sci U S A 86: 302-306.
287. Murray R, Suda T, Wrighton N, Lee F, Zlotnik A (1989) IL-7 is a growth and maintenance factor for mature and immature thymocyte subsets. Int Immunol 1: 526-531.
288. Muegge K, Vila MP, Durum SK (1993) Interleukin-7: a cofactor for V(D)J rearrangement of the T cell receptor beta gene. Science 261: 93-95.
289. Berrios V, Kurane I, Ennis FA (1996) Immunomodulatory effects of IL-7 on dengue virus-specific cytotoxic CD4+ T cell clones. Immunol Invest 25: 231-240.
290. Matic M, Simon SR (1992) Effects of gamma interferon on release of tumor necrosis factor alpha from lipopolysaccharide-tolerant human monocyte-derived macrophages. Infect Immun 60: 3756-3762.
291. Mukherjee R, Chaturvedi P, Chaturvedi UC (1993) Binding of the two polypeptide chains of dengue virus-induced suppressor cytokine to its receptor isolated from macrophages. Int J Exp Pathol 74: 259-266.
292. Mukherjee R, Chaturvedi P, Chaturvedi UC (1993) Identification and purification of a receptor on macrophages for the dengue virus-induced suppressor cytokine. Clin Exp Immunol 91: 257-265.
293. Mukherjee R, Chaturvedi P, Chaturvedi UC (1994) Specific receptors for dengue virus-induced suppressor cytokine on macrophages and lymphocytes. Int J Exp Pathol 75: 29-36.
294. Chen YC, Wang SY (2002) Activation of terminally differentiated human monocytes/macrophages by dengue virus: productive infection, hierarchical production of innate cytokines and chemokines, and the synergistic effect of lipopolysaccharide. J Virol 76: 9877-9887.
295. Puerta-Guardo H, Raya-Sandino A, Gonzalez-Mariscal L, Rosales VH, Ayala-Davila J, et al. (2013) The cytokine response of U937-derived macrophages infected through antibody-dependent enhancement of dengue virus disrupts cell apical-junction complexes and increases vascular permeability. J Virol 87: 7486-7501.
296. Valero N, Mosquera J, Levy A, Anez G, Marcucci R, et al. (2014) Differential induction of cytokines by human neonatal, adult, and elderly monocyte/macrophages infected with dengue virus. Viral Immunol 27: 151-159.
297. Chuang YC, Lei HY, Liu HS, Lin YS, Fu TF, et al. (2011) Macrophage migration inhibitory factor induced by dengue virus infection increases vascular permeability. Cytokine 54: 222-231.
298. Lee IK, Hsieh CJ, Chen RF, Yang ZS, Wang L, et al. (2013) Increased production of interleukin-4, interleukin-10, and granulocyte-macrophage colony-stimulating factor by type 2 diabetes'

mononuclear cells infected with dengue virus, but not increased intracellular viral multiplication. Biomed Res Int 2013: 965853.
299. Boonnak K, Dambach KM, Donofrio GC, Tassaneetrithep B, Marovich MA (2011) Cell type specificity and host genetic polymorphisms influence antibody-dependent enhancement of dengue virus infection. J Virol 85: 1671-1683.
300. Rinderknecht E, O'Connor BH, Rodriguez H (1984) Natural human interferon-gamma. Complete amino acid sequence and determination of sites of glycosylation. J Biol Chem 259: 6790-6797.
301. Nedwin GE, Svedersky LP, Bringman TS, Palladino MA, Jr., Goeddel DV (1985) Effect of interleukin 2, interferon-gamma, and mitogens on the production of tumor necrosis factors alpha and beta. J Immunol 135: 2492-2497.
302. Collart MA, Belin D, Vassalli JD, de Kossodo S, Vassalli P (1986) Gamma interferon enhances macrophage transcription of the tumor necrosis factor/cachectin, interleukin 1, and urokinase genes, which are controlled by short-lived repressors. J Exp Med 164: 2113-2118.
303. Jones MD, Hunt J, Liu JL, Patterson SD, Kohno T, et al. (1997) Determination of tumor necrosis factor binding protein disulfide structure: deviation of the fourth domain structure from the TNFR/NGFR family cysteine-rich region signature. Biochemistry 36: 14914-14923.
304. Sunkara PS, Kang MS, Bowlin TL, Liu PS, Tyms AS, et al. (1990) Inhibition of glycoprotein processing and HIV replication by castanospermine analogues. Ann N Y Acad Sci 616: 90-96.
305. Schul W, Liu W, Xu HY, Flamand M, Vasudevan SG (2007) A dengue fever viremia model in mice shows reduction in viral replication and suppression of the inflammatory response after treatment with antiviral drugs. J Infect Dis 195: 665-674.
306. Rathore AP, Paradkar PN, Watanabe S, Tan KH, Sung C, et al. (2011) Celgosivir treatment misfolds dengue virus NS1 protein, induces cellular pro-survival genes and protects against lethal challenge mouse model. Antiviral Res 92: 453-460.
307. Watanabe S, Rathore AP, Sung C, Lu F, Khoo YM, et al. (2012) Dose- and schedule-dependent protective efficacy of celgosivir in a lethal mouse model for dengue virus infection informs dosing regimen for a proof of concept clinical trial. Antiviral Res 96: 32-35.
308. Evans EJ, Esnouf RM, Manso-Sancho R, Gilbert RJ, James JR, et al. (2005) Crystal structure of a soluble CD28-Fab complex. Nat Immunol 6: 271-279.
309. Pfaffl MW (2001) A new mathematical model for relative quantification in real-time RT-PCR. Nucleic Acids Res 29: e45.
310. Shresta S, Kyle JL, Robert Beatty P, Harris E (2004) Early activation of natural killer and B cells in response to primary dengue virus infection in A/J mice. Virology 319: 262-273.
311. Sung JM, Lee CK, Wu-Hsieh BA (2012) Intrahepatic infiltrating NK and CD8 T cells cause liver cell death in different phases of dengue virus infection. PLoS One 7: e46292.
312. Fibriansah G, Tan JL, Smith SA, de Alwis AR, Ng TS, et al. (2014) A potent anti-dengue human antibody preferentially recognizes the conformation of E protein monomers assembled on the virus surface. EMBO Mol Med 6: 358-371.
313. Prestwood TR, May MM, Plummer EM, Morar MM, Yauch LE, et al. (2012) Trafficking and replication patterns reveal splenic macrophages as major targets of dengue virus in mice. J Virol 86: 12138-12147.
314. Zellweger RM, Shresta S (2014) Mouse Models to Study Dengue Virus Immunology and Pathogenesis. Front Immunol 5: 151.
315. Sadat MA, Moir S, Chun TW, Lusso P, Kaplan G, et al. (2014) Glycosylation, hypogammaglobulinemia, and resistance to viral infections. N Engl J Med 370: 1615-1625.

A

Appendices

Appendix I. Accepted publications

The following papers have been accepted for publication and were prepared either in preparation for my thesis research or arose as a direct result of this work. Anticipated publications are not included.

Sayce AC, Miller JL, Zitzmann N (2010) Targeting a host process as an antiviral approach against dengue virus. *Trends Microbiol*. **18**(7):323-30.

Miller JL, Lachica R, **Sayce AC**, Williams JP, Bapat M, Dwek R, Beatty PR, Harris E, Zitzmann N (2012) Liposome-mediated delivery of iminosugars enhances efficacy against dengue virus in vivo. *Antimicrob Agents Chemother*. **56**(12):6379-86.

Sayce AC, Miller JL, Zitzmann N (2013) Glucocorticosteroids as dengue therapeutics: resolving clinical observations with a primary human macrophage model. *Clin Infect Dis*. **56**(6):901-3.

Appendix II. Glucocorticosteroids

The following letter was published in Clinical Infectious Diseases Vol 57, Issue 6, pages 901-903. This work describes the immunomodulatory potential of a glucocorticosteroid in the macrophage model presented in this thesis as a direct comparison for M*O*N-DNJ.

TITLE: Glucocorticosteroids as dengue therapeutics: resolving clinical observations with a primary human macrophage model

AUTHORS: Andrew C. Sayce, Joanna L. Miller, and Nicole Zitzmann

AFFILIATIONS: Oxford Glycobiology Institute, Department of Biochemistry, University of Oxford, South Parks Road, Oxford, OX1 3QU, United Kingdom

CONTACT: Nicole Zitzmann (nicole.zitzmann@bioch.ox.ac.uk)

Ph: +44 (0)1865 275341

Fax: +44 (0)1865 275216

KEYWORDS: dengue, glucocorticosteroid, cytokine, macrophage

RUNNING TITLE: Dengue treatment by glucocorticosteroids

Dear Editor,

A recent trial [1] investigated the use of a glucocorticosteroid, prednisolone, as a therapy for reduction of severe dengue disease. Many pathogens induce accelerated or excessive inflammation resulting in detrimental rather than protective effects [2], and dengue virus is a well-characterized example of this phenomenon. Several soluble mediators of the innate inflammatory response have been linked with severe pathology [3]; however, these studies are largely correlative and have failed to elucidate molecular mechanisms facilitating specific pathologies. Nevertheless, continued observation of excessive inflammation concurrent with a drop in viremia and development of severe symptoms [4, 5] has prompted several previous attempts of immunosuppressive strategies as a means of reducing severe dengue disease [6-9].

Enhancement of disease due to suppression of innate antiviral mechanisms has been a primary concern. The study by Tam *et al.* [1] revealed neither protective effects (as discussed by Prof. Barrett [10]) nor enhancement of disease. These results are surprising as it seems likely that glucocorticosteroid treatment would prove either productive (i.e. reduce excessive inflammation and resultant severe symptoms) or detrimental (i.e. reduce innate mediators of viral clearance such that a greater incidence of severe disease would be noted). We have data that may explain why glucocorticosteroid treatment fails to impact severe dengue presentation.

We investigated dexamethasone as a dengue therapeutic in primary monocyte-derived macrophages from dengue naïve donors. From these samples, we collected cytokine and viral titre measurements at days 1, 3, and 5 and note an interesting phenomenon that we believe complements the results obtained in patients (Figure 1). We observe a significant (Mann-Whitney U, $\alpha<0.05$) decrease in viral load on day 1 with dexamethasone treatment concomitant with decreased, but still elevated, levels of select inflammatory cytokines (RANTES, TNF- α, IFN-γ, IL-8, IL-10, IL-17A,

G-CSF, and MCP-1). By day 3, suppression of cytokines is still evident but viral titre has rebounded to the same level as untreated samples. Viral titre for dexamethasone treated samples does not exceed that for untreated samples at day 3 or day 5 presumably because the inflammatory response remains sufficiently intact to prevent enhanced viral load.

This finding has implications for the use of immunosuppressive therapies against dengue and other diseases that manifest through excessive immune activation (e.g. avian influenza, SARS-CoV, etc.). Although these drugs are capable of reducing inflammatory mediators in important targets of infection in tissues (macrophages), the systemic effects and related severe pathologies may not be impacted. Alternatively, the effectiveness of treatment may critically depend on time of drug administration. Immediate treatment following infection may be able to help direct the developing immune response to effective viral clearance while preventing severe symptoms in the subset of patients at risk of developing shock/haemorrhage; however, this is an unrealistic option in the clinical setting. We suggest that modest immunosuppression may be safe for use against these diseases as an adjunctive therapy in coordination with a direct acting antiviral capable of efficient reduction of pathogen load. Future experiments investigating such a strategy may unlock the therapeutic potential of otherwise non-viable options.

ACKNOWLEDGEMENTS

We would like to thank Prof. Raymond Dwek for helpful discussions and supervision.

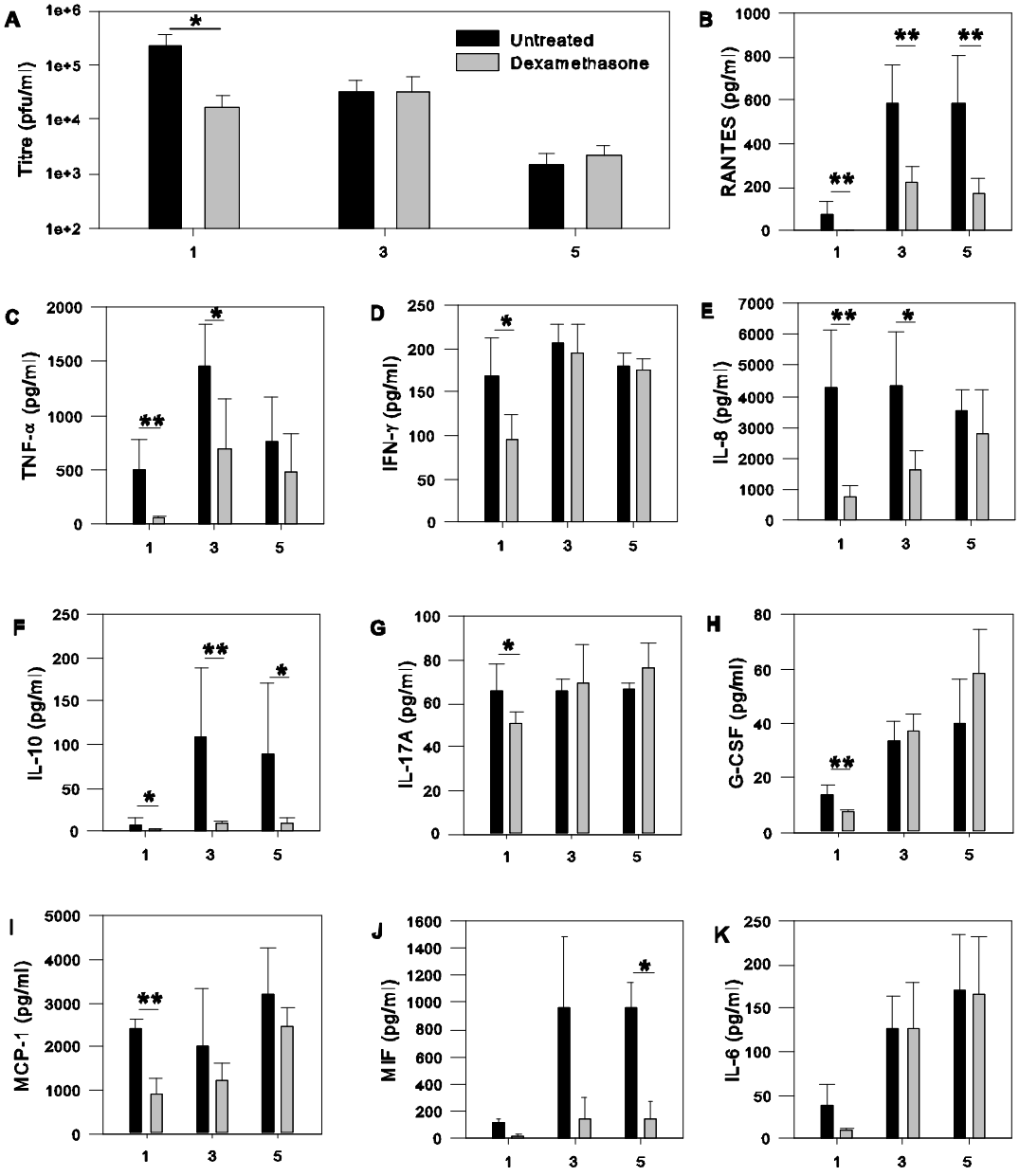

Figure 1. *A*, Dengue virus titre kinetics in primary monocyte-derived macrophages from five donors in the absence (black) and presence (grey) of dexamethasone as determined by LLC-MK_2 plaque assay. *B-K,* Equivalent kinetic assessment of cytokines/chemokines was conducted by custom BioPlex multiplex analysis on a Luminex 200. Error bars represent standard error with significance (* = α <0.05, ** = α <0.01) assessed by Mann-Whitney U non-parametric tests due to failure of Levene's test for homogeneity. All x-axis values are days post-infection.

REFERENCES

1. Tam DT, Ngoc TV, Tien NT, et al. Effects of short-course oral corticosteroid therapy in early dengue infection in vietnamese patients: a randomized, placebo-controlled trial. J Clin Infect Dis **2012**; 55(9):1216-24.
2. Tisoncik JR, Korth MJ, Simmons CP, Farrar J, Martin TR, Katze MG. Into the eye of the cytokine storm. Microbiol Mol Biol Rev **2012**; 76(1):16-32.
3. Rothman AL. Immunity to dengue virus: a tale of original antigenic sin and tropical cytokine storms. Nat Rev Immunol **2011**; 11(8):532-43.
4. Libraty DH, Endy TP, Houng HS, et al. Differing influences of virus burden and immune activation on disease severity in secondary dengue-3 virus infections. J Infect Dis **2002**; 185(9):1213-21.
5. Green S, Vaughn DW, Kalayanarooj S, et al. Early immune activation in acute dengue illness is related to development of plasma leakage and disease severity. J Infect Dis **1999**; 179(4):755-62.
6. Kularatne SA, Walathara C, Mahindawansa SI, et al. Efficacy of low dose dexamethasone in severe thrombocytopenia caused by dengue fever: a placebo controlled study. Postgrad Med J **2009;** 85(1008):525-9.
7. Srichaikul T, Punyagupta S, Sorakhunpipitkul L, Udomsubpayakul U. Adjunctive corticosteroid therapy in 149 grade II (non-shock) adult DHF patients: an analysis during January 2008-February 2010. J Med Assoc Thailand **2011**; 94(12):1419-23.
8. Tassniyom S, Vasanawathana S, Chirawatkul A, Rojanasuphot S. Failure of high-dose methylprednisolone in established dengue shock syndrome: a placebo-controlled, double-blind study. Pediatrics **1993**; 92(1):111-5.
9. Futrakul P, Poshyachinda M, Mitrakul C, et al. Hemodynamic response to high-dose methyl prednisolone and mannitol in severe dengue-shock patients unresponsive to fluid replacement. Southeast Asian J Trop Med Public Health **1987**; 18(3):373-9.
10. Barrett AD. Editorial commentary: short-course oral corticosteroid therapy is not effective in early dengue infection. J Clin Infect Dis **2012**; 55(9):1225-6.

Appendix III. Macrophage character

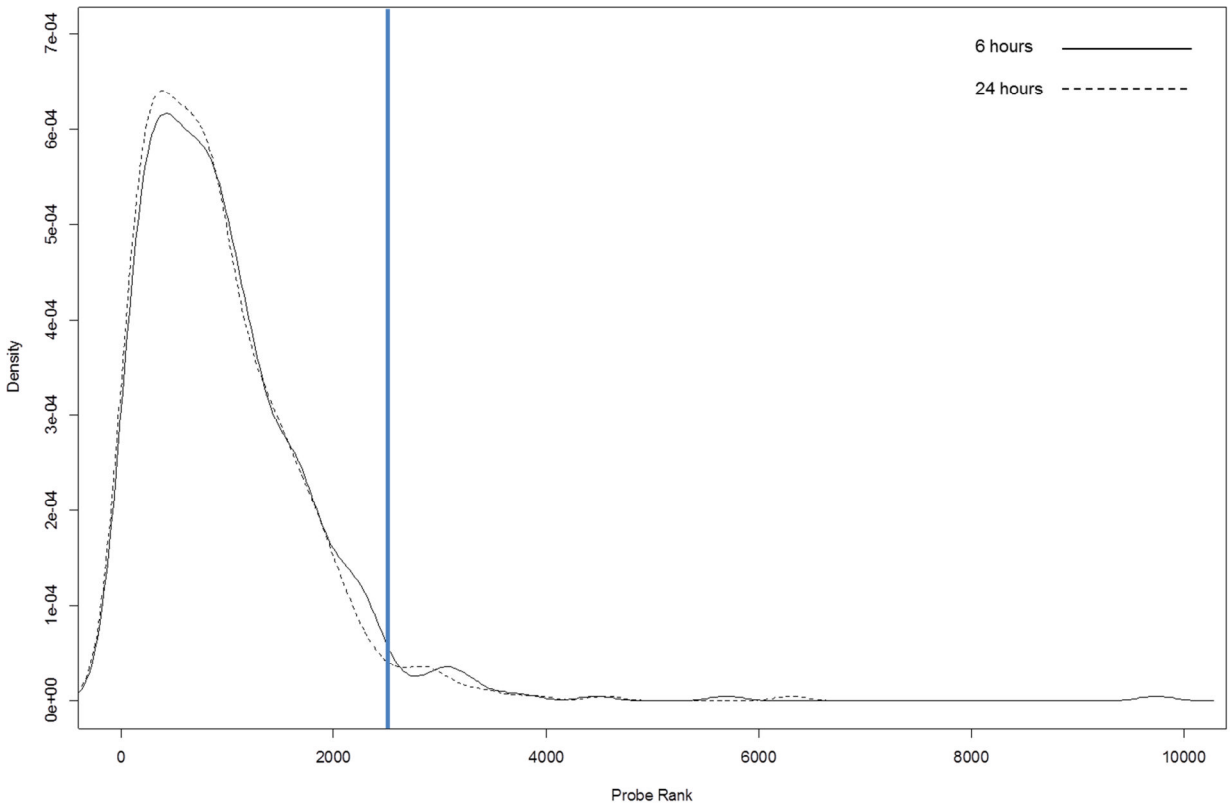

FIGURE AIII.1 Density plot of probe ranks of 490 genes characterising macrophage models. Absolute expression ranks of probes were generated for uninfected, untreated samples at both 6 hours (solid line) and 24 hours (dashed line) without removal of redundant probes for a given gene. The most abundant probe was set to rank 1, and a Gaussian kernel density function fit in R was used to describe the rank of genes previously determined to be highly expressed in diverse macrophage models for the most highly expressed probe for each gene. Given the inclusion of redundant probes, the 2500 most highly expressed probes (blue line) were considered to meet the criteria of "high expression" in macrophages. At 6 hours, all but 17 of the 490 genes were above this threshold and at 24 hours all but 15 of the genes were above this threshold. Probes below this line are still expressed, and most probes fall very close to this threshold as shown in *Table AII.1*.

TABLE AIII.1 Probe expression rank of non-highly expressed macrophage characterising genes

Gene Symbol	6hr Rank	24hr Rank
ABCA1	9736	6311
ACP2[a]	*2542*	***1652***[b]
ADAMDEC1	4472	2823
ANAPC5	3101	3030
CFLAR	2777	3335
CTSK	*2977*	***2499***
EPAS1	3042	2932
GSN	3583	3553
IL13RA1	3095	2940
ITGB5	2966	2304
MAP1LC3B	2628	2911
PGLS	3247	2858
SDHA	3227	2820
SQRDL	3792	3905
ST13	***2227***	*2820*
TNFRSF21	5698	4568
TPM3	3274	3281
UCP2	*2951*	***2285***
VPS4B	***2423***	*2677*

[a] Rows are *italicised* in the case that the gene was considered highly expressed at one time point

[b] Ranks indicating high expression at a given time are presented in **bold**

TABLE AIII.2 Probe expression ranks of macrophage characterising genes 6 hours post-infection

Gene Symbol	Rank	PROBE_ID
RPS29	6	ILMN_1694742
RPLP2	7	ILMN_1755733
UBC	8	ILMN_2331501
TPT1	9	ILMN_2094718
CSTB	12	ILMN_1761797
ITGB2	13	ILMN_1654396
EEF1A1	14	ILMN_1343291
ITGB2[a]	*15*	*ILMN_2175912*
B2M	19	ILMN_1725427
ACTG1	20	ILMN_2053178
OAZ1	25	ILMN_1773080
NPC2	29	ILMN_1716678
UBC	*34*	*ILMN_2038773*
ACTB	35	ILMN_2152131
PSAP	36	ILMN_1749109
TMSB10	37	ILMN_1812392
RPS27	41	ILMN_1660498
RPS29	*46*	*ILMN_1738243*
CD81	50	ILMN_1689953
PSAP	*52*	*ILMN_2355559*
ANXA2	*59*	*ILMN_2409167*
B2M	*60*	*ILMN_2148459*
RPLP1	64	ILMN_2247594
RPS27A	69	ILMN_2048326
VIM	70	ILMN_1782538
PFN1	71	ILMN_2151817
RPS19	72	ILMN_1784717
MYL6	73	ILMN_2326071
RPS16	74	ILMN_1651850
EEF1A1	*77*	*ILMN_1810810*
MYL6	*81*	*ILMN_1809013*
EEF1A1	*84*	*ILMN_2038774*

RPS12	90	ILMN_1782621	CYP1B1	218	ILMN_1693338
RPL38	102	ILMN_1765043	LGALS1	222	ILMN_1723978
GPNMB	105	ILMN_1801205	*RPS3A*	*226*	*ILMN_1673638*
UBA52	107	ILMN_1782977	S100A6	227	ILMN_1713636
ACTB	*108*	*ILMN_2038777*	*RPL18A*	*232*	*ILMN_2141452*
TYROBP	112	ILMN_1778977	*S100A4*	*233*	*ILMN_1684306*
RPL37A	115	ILMN_2051519	MDH1	238	ILMN_1656913
RPL38	*119*	*ILMN_2343775*	RPL19	242	ILMN_1701832
RPS27	*120*	*ILMN_2160819*	*H3F3A*	*243*	*ILMN_2106331*
LCP1	123	ILMN_1662932	CFL1	246	ILMN_1705617
RPL27A	124	ILMN_1713086	RPS15A	258	ILMN_1787949
RPS25	126	ILMN_1746516	ATP6V1F	259	ILMN_2099783
ATP5B	127	ILMN_1772132	*RPLP1*	*260*	*ILMN_2386530*
GNS	131	ILMN_1744517	CEBPB	263	ILMN_1693014
HEXB	137	ILMN_1806692	CTSH	265	ILMN_2390853
RPL6	138	ILMN_1690494	ATP6AP1	266	ILMN_1697694
RPS11	139	ILMN_1740587	UBB	270	ILMN_2191428
H3F3A	142	ILMN_1656082	GPX1	272	ILMN_1749662
H2AFY	145	ILMN_2373495	PRDX1	275	ILMN_2366388
RPL11	146	ILMN_1672446	HSPA8	276	ILMN_1686367
S100A4	147	ILMN_1688780	RPL27	281	ILMN_1656807
SQSTM1	151	ILMN_1662618	*PRDX1*	*282*	*ILMN_2366391*
ACTB	*152*	*ILMN_1777296*	LTA4H	284	ILMN_1690342
SLC25A5	153	ILMN_1774062	RPS6	285	ILMN_1656791
RPS17	154	ILMN_2207533	LAMP1	286	ILMN_1782292
PPT1	155	ILMN_1669273	RPL17	288	ILMN_1658283
RPL18	157	ILMN_2230624	RPL30	291	ILMN_1754303
DBI	160	ILMN_2305544	RPS28	292	ILMN_1651228
CYP27A1	162	ILMN_1704985	EIF4G2	297	ILMN_2380946
EIF4A1	164	ILMN_1722900	*GPNMB*	*301*	*ILMN_2407389*
RPS20	171	ILMN_1701596	RPS14	306	ILMN_1666635
TFRC	174	ILMN_1674243	LITAF	307	ILMN_1713934
RPL11	*175*	*ILMN_2114876*	*H3F3A*	*311*	*ILMN_1699015*
RPS10	176	ILMN_1686954	ARPC5	313	ILMN_1768394
RPL3	177	ILMN_2319996	CAP1	316	ILMN_1797604
RPL18A	180	ILMN_2141444	COX8A	317	ILMN_1809495
RPS29	*182*	*ILMN_2415722*	COX7C	318	ILMN_1798189
RPL18A	*184*	*ILMN_2141453*	*S100A10*	*324*	*ILMN_1796712*
VIM	*185*	*ILMN_2058251*	RPL24	325	ILMN_2160388
RPL39	188	ILMN_1737015	SERF2	330	ILMN_1789136
COX4I1	189	ILMN_1652207	*PFN1*	*335*	*ILMN_1712950*
ENO1	191	ILMN_1710756	*RPS15A*	*338*	*ILMN_2337241*
NACA	192	ILMN_2167617	APOC1	339	ILMN_1789007
S100A10	196	ILMN_2046730	*GPX4*	*340*	*ILMN_1734353*
AP2S1	199	ILMN_1809957	*RPS3A*	*343*	*ILMN_2139943*
GPX4	200	ILMN_2378952	ATP6V1B2	344	ILMN_1787705
RPS3A	204	ILMN_1657722	RPL10A	347	ILMN_2154566
ARHGDIB	209	ILMN_1678143	FCER1G	351	ILMN_2123743
LGALS3	212	ILMN_1803788	RPL35A	353	ILMN_1756360
GSTO1	213	ILMN_2227573	CYBA	355	ILMN_1744604
RPL9	215	ILMN_1750507	ATF4	356	ILMN_1672128

RPS13	360	ILMN_1777344	PABPC1	486	ILMN_1761155
IFI30	361	ILMN_1807277	PSMA6	491	ILMN_2151818
ATP5A1	364	ILMN_2341363	NEDD8	492	ILMN_2058070
ATP6AP2	370	ILMN_1677440	*UBB*	*493*	*ILMN_1762436*
ACP5	371	ILMN_2078599	PLA2G7	495	ILMN_1701195
CTSB	372	ILMN_2359742	RPS2	496	ILMN_2218277
NDUFA4	375	ILMN_1751258	UQCRH	497	ILMN_2232936
RPL31	376	ILMN_1754195	*ACTG1*	*499*	*ILMN_1704961*
COX5B	377	ILMN_1663512	GRN	501	ILMN_1724250
S100A9	384	ILMN_1750974	ATP6V0B	504	ILMN_1721391
CHCHD2	394	ILMN_2191681	RPS15	508	ILMN_2219134
SLC15A3	397	ILMN_2085862	*TOMM7*	*514*	*ILMN_2087060*
COX7A2	398	ILMN_1701293	RPS18	516	ILMN_1753534
ATP5H	399	ILMN_1794912	BTF3	517	ILMN_2319414
NDUFA1	402	ILMN_1784286	RPL35	519	ILMN_2142815
PGD	403	ILMN_1794165	GHITM	523	ILMN_1728467
PLIN2	407	ILMN_2138765	ARPC3	524	ILMN_1655561
PCBP1	408	ILMN_1673215	*ATP5H*	*525*	*ILMN_1666372*
RPL36AL	414	ILMN_2189936	*RPL9*	*536*	*ILMN_2408415*
PFDN5	415	ILMN_2356284	CNDP2	539	ILMN_1726769
SNX3	418	ILMN_1740180	YWHAZ	540	ILMN_1801928
PFDN5	*422*	*ILMN_1755536*	*GRN*	*542*	*ILMN_1811702*
RPS6	423	ILMN_1808939	CCNI	548	ILMN_1691942
FAU	424	ILMN_1664614	DDX5	549	ILMN_1805344
ATP5A1	*425*	*ILMN_1764494*	*RPS27A*	*554*	*ILMN_1755883*
RPL23	429	ILMN_1755115	GLA	558	ILMN_1766637
RPS27	*430*	*ILMN_1696839*	DNAJA1	561	ILMN_1672496
COX6C	431	ILMN_1654151	*RPL6*	*565*	*ILMN_1712155*
COX5A	435	ILMN_1704477	EMP3	566	ILMN_1765446
ANXA5	440	ILMN_1741003	RPS5	567	ILMN_1707810
RHOA	443	ILMN_1781290	SH3BGRL3	573	ILMN_1737163
TOMM7	444	ILMN_1674069	PSMB1	574	ILMN_1789176
GSTO1	*445*	*ILMN_1808196*	*RPL36AL*	*576*	*ILMN_2189933*
CD14	446	ILMN_2396444	APOE	584	ILMN_1740938
CST3	447	ILMN_1800354	ATP1B3	585	ILMN_1783304
RPL17	*449*	*ILMN_2383097*	RPS3	587	ILMN_1760714
NACA	*450*	*ILMN_2167616*	MMP9	593	ILMN_1796316
RPL3	*452*	*ILMN_2319994*	TKT	594	ILMN_1736597
MDH2	456	ILMN_2079004	SEC61B	596	ILMN_1801852
RPL12	460	ILMN_2116366	SDCBP	603	ILMN_2363586
FXYD5	463	ILMN_2309848	JTB	605	ILMN_2206716
LASP1	465	ILMN_1665909	RTN4	606	ILMN_1730611
FTH1	468	ILMN_1683146	H2AFZ	610	ILMN_1707858
NCOA4	469	ILMN_1773906	CTSD	613	ILMN_1674038
LPXN	471	ILMN_1742789	PTBP1	619	ILMN_2333319
NUCB1	472	ILMN_1722634	DAZAP2	622	ILMN_1718988
GSTP1	475	ILMN_1679809	*SDCBP*	*624*	*ILMN_2363591*
RPS14	*478*	*ILMN_2338785*	BCAP31	626	ILMN_1812403
TRAM1	479	ILMN_1737146	BRI3	629	ILMN_1781580
RNASET2	481	ILMN_1671565	CLIC1	631	ILMN_1756982
ANXA1	484	ILMN_2184184	ATP5F1	634	ILMN_1721989

YWHAB	636	ILMN_1694385	NDUFAB1	797	ILMN_2179018
HMGN1	638	ILMN_2151579	*RPS17*	*803*	*ILMN_2207539*
LIMS1	648	ILMN_1733176	FCGRT	804	ILMN_1705302
TIMP1	649	ILMN_1711566	NDUFB5	806	ILMN_1807397
RAB10	656	ILMN_1793433	UBE2E1	811	ILMN_1806778
UQCRFS1	665	ILMN_1701749	SH3BGRL	812	ILMN_1702835
RPL5	670	ILMN_2087080	RNF130	814	ILMN_1729294
NDUFB2	679	ILMN_2117330	*RPL12*	*816*	*ILMN_1653469*
ATP6V1G1	680	ILMN_1784523	PEA15	825	ILMN_1771376
FXYD5	*681*	*ILMN_1704286*	TMEM14C	827	ILMN_2175131
NDUFB8	683	ILMN_1661170	LY96	830	ILMN_1724533
PABPC1	*684*	*ILMN_2136133*	P4HB	833	ILMN_1719303
ATP5O	690	ILMN_1791332	CD48	835	ILMN_2061043
RPS4X	693	ILMN_1810577	NFKBIA	837	ILMN_1773154
DAD1	696	ILMN_1731619	NARS	842	ILMN_1732216
IFNGR2	699	ILMN_1764964	ALDH9A1	845	ILMN_1761804
IGF2R	702	ILMN_1807662	RHOQ	847	ILMN_1810559
EIF4G2	*706*	*ILMN_1761519*	ATOX1	851	ILMN_1670609
HSPD1	708	ILMN_2381397	ATP5J2	852	ILMN_2310621
ITGB1	712	ILMN_1723467	GLB1	854	ILMN_2397721
MTPN	714	ILMN_2180682	ZYX	859	ILMN_1701875
VAMP8	716	ILMN_2190084	COX7B	860	ILMN_2184049
TBCA	717	ILMN_1726239	PPP1CC	861	ILMN_1701855
KYNU	718	ILMN_1746517	*CTSB*	*862*	*ILMN_1696360*
M6PR	721	ILMN_2084353	CPVL	866	ILMN_2400759
AP2S1	*722*	*ILMN_1662426*	PRNP	868	ILMN_1737988
PLEK	724	ILMN_1795762	MGAT1	869	ILMN_1761912
ANP32B	726	ILMN_1684293	GLTSCR2	877	ILMN_1703565
SRP14	727	ILMN_2234758	GNB1	881	ILMN_1760320
VDAC3	729	ILMN_1729816	RPL36	885	ILMN_1685088
YWHAQ	730	ILMN_1674385	EEF1G	888	ILMN_2262288
DBI	*735*	*ILMN_1755926*	*ATP1B3*	*893*	*ILMN_1759628*
NINJ1	737	ILMN_1815086	SCARB2	894	ILMN_1814726
PCBP2	738	ILMN_2312296	*ATP5J2*	*895*	*ILMN_2307883*
ANXA2	*739*	*ILMN_1711899*	RPL26	897	ILMN_1731546
BASP1	742	ILMN_1651826	VKORC1	898	ILMN_1739946
RHEB	750	ILMN_1657949	MTCH1	901	ILMN_1703006
DPYSL2	754	ILMN_1672503	*LAMP2*	*902*	*ILMN_1673282*
SRP9	760	ILMN_2099594	*ATP6V1E1*	*903*	*ILMN_1798485*
CLCN7	765	ILMN_1694731	SPP1	909	ILMN_1651354
NDUFA3	766	ILMN_1784641	EFHD2	910	ILMN_1761463
BTF3	*770*	*ILMN_1659762*	IFNGR1	913	ILMN_1675939
EEF2	771	ILMN_1738383	PSME1	919	ILMN_1806017
PSMB3	773	ILMN_1748651	EMILIN2	920	ILMN_1697268
EIF4A2	776	ILMN_1685722	ACTR2	922	ILMN_2388605
S100A11	777	ILMN_1750101	PARK7	923	ILMN_1744713
ATP6V1E1	779	ILMN_2339779	NCF2	925	ILMN_1796642
PGK1	782	ILMN_1755749	HINT1	926	ILMN_1807710
MARCKS	785	ILMN_1807042	CD9	927	ILMN_1695423
PSMC1	786	ILMN_1736353	CEBPA	928	ILMN_1715715
MGST3	796	ILMN_1751956	DHX15	933	ILMN_2168449

RAC1	936	ILMN_2359789	HCLS1	1143	ILMN_1727402
ACTR3	947	ILMN_1657153	CAPG	1145	ILMN_1655821
TPI1	950	ILMN_1707627	ARHGEF2	1148	ILMN_1703477
UXT	951	ILMN_1671314	DAB2	1169	ILMN_1764228
SOD1	960	ILMN_1662438	NFE2L2	1170	ILMN_1790909
LAMP2	*962*	*ILMN_2279961*	KHDRBS1	1172	ILMN_2076640
FUCA1	969	ILMN_1752728	PPP1R11	1175	ILMN_1747598
GM2A	971	ILMN_2221046	ESD	1176	ILMN_1720285
HSD17B12	974	ILMN_2094106	PRDX3	1180	ILMN_2395974
KPNB1	975	ILMN_1703949	*PRKAR1A*	*1186*	*ILMN_2389590*
MAT2B	981	ILMN_1811367	*HMGN1*	*1187*	*ILMN_1652123*
VAT1	983	ILMN_1700690	AP1S2	1195	ILMN_2120273
SSR4	987	ILMN_1680403	PTTG1IP	1201	ILMN_2128750
ABR	988	ILMN_1672878	MAPRE1	1202	ILMN_1777721
PTBP1	*989*	*ILMN_1655154*	DDOST	1203	ILMN_1734231
MSN	990	ILMN_1659895	*PSMC1*	*1211*	*ILMN_1710406*
CSDA	993	ILMN_1782788	SET	1214	ILMN_1742238
TPT1	*996*	*ILMN_1789614*	SNRPB	1216	ILMN_1774661
TXNRD1	1003	ILMN_1717056	SLC16A3	1220	ILMN_2364022
STARD7	1019	ILMN_1740819	HEBP1	1221	ILMN_1802557
MORF4L1	1024	ILMN_1760676	SLC7A7	1225	ILMN_1810275
TM9SF2	1025	ILMN_1785765	LAPTM5	1232	ILMN_1772359
LAMP2	*1027*	*ILMN_2243687*	*TPI1*	*1233*	*ILMN_2181191*
SUMO3	1033	ILMN_1725642	*RTN4*	*1235*	*ILMN_2352036*
ATP6V1D	1041	ILMN_1797310	*H2AFY*	*1237*	*ILMN_1746171*
ACSL1	1043	ILMN_1684585	ATP5C1	1241	ILMN_1701269
GNPDA1	1044	ILMN_1784709	RPL13A	1252	ILMN_1713369
PSMC2	1048	ILMN_1768784	NDUFS3	1261	ILMN_1756355
GTF3A	1051	ILMN_1658464	MAT2A	1263	ILMN_1737298
RPLP1	*1056*	*ILMN_1689725*	UQCRC1	1273	ILMN_1671191
CCT8	1057	ILMN_1717868	TACC1	1275	ILMN_1770084
ATP6V0A1	1061	ILMN_1752579	GLB1	1277	ILMN_1735155
HK1	1063	ILMN_2382990	PABPC4	1282	ILMN_1757343
HSPA1A	1064	ILMN_1789074	PRDX6	1283	ILMN_1803180
RBX1	1065	ILMN_1666670	*PLIN2*	*1287*	*ILMN_1801077*
GSTK1	1073	ILMN_1725241	CSF1R	1292	ILMN_1686623
NONO	1074	ILMN_2052790	ZDHHC7	1301	ILMN_1730568
COX6A1	1078	ILMN_1783636	CALM1	1302	ILMN_1778242
TIMP2	*1079*	*ILMN_1721876*	RHOG	1304	ILMN_1739792
GUSB	1089	ILMN_1669878	LHFPL2	1311	ILMN_1747744
GDI2	1090	ILMN_1754178	RRAGD	1318	ILMN_1699772
PRKAR1A	1092	ILMN_1738632	GMFG	1319	ILMN_1711617
RPS4X	*1095*	*ILMN_2166831*	ATP1B1	1321	ILMN_2407824
COPA	1100	ILMN_1811615	*AP1S2*	*1322*	*ILMN_1766411*
QARS	1106	ILMN_1763080	*SPP1*	*1323*	*ILMN_2374449*
DNAJC8	1110	ILMN_1698258	ATP6V0D1	1326	ILMN_1795826
RPL4	1118	ILMN_1752285	CSNK2B	1331	ILMN_1800461
DARS	1125	ILMN_1813836	UBE2I	1335	ILMN_1810474
RPL15	1130	ILMN_1762747	HSD17B4	1336	ILMN_1673795
CTSZ	1132	ILMN_1666269	PSMB7	1348	ILMN_1814156
NAGK	1136	ILMN_1716547	GNAI2	1353	ILMN_1775762

CTSS	1357	ILMN_1743032	VAMP3	1675	ILMN_1714527
CTNNA1	1358	ILMN_1804854	MS4A7	1676	ILMN_2331082
NDUFV2	1363	ILMN_2086417	IDH3B	1686	ILMN_1721669
IRAK1	1400	ILMN_2379130	VPS35	1694	ILMN_1761721
TAX1BP1	1404	ILMN_1793118	*KYNU*	*1696*	*ILMN_1737514*
POLR2G	1407	ILMN_1748438	MAFB	1697	ILMN_1764709
TMEM14C	*1414*	*ILMN_1657857*	*ATP6V0B*	*1702*	*ILMN_2353642*
TAPBP	1434	ILMN_1742450	SH3GLB1	1704	ILMN_1766045
PDHB	1450	ILMN_1739274	LAP3	1705	ILMN_1683792
PSMA6	*1454*	*ILMN_1704094*	*H2AFY*	*1713*	*ILMN_1674034*
BLVRA	1456	ILMN_1691436	RAB32	1718	ILMN_2115434
BTG1	1457	ILMN_1775743	*LAMP2*	*1719*	*ILMN_1659753*
GLIPR1	1462	ILMN_1769245	*PGK1*	*1721*	*ILMN_2216852*
PRDX3	*1481*	*ILMN_2395969*	SNX2	1724	ILMN_1691575
CSK	1490	ILMN_1754121	*UQCRH*	*1735*	*ILMN_1792138*
HSPD1	*1514*	*ILMN_1766713*	*LAMP2*	*1755*	*ILMN_1752351*
A2M	1519	ILMN_1745607	PRDX4	1762	ILMN_2222234
GTF2A2	1527	ILMN_1753719	ACTN1	1768	ILMN_2232177
NPC1	1544	ILMN_1713505	CD36	1772	ILMN_1796094
CAPZA2	1545	ILMN_1768870	WAS	1783	ILMN_1760027
NPL	1547	ILMN_2149494	ADAR	1792	ILMN_1776777
ZMPSTE24	1548	ILMN_1656413	TTC3	1796	ILMN_1728605
ATP5F1	*1549*	*ILMN_1672191*	DCTN2	1817	ILMN_1662232
LYN	1555	ILMN_1781155	SLC29A3	1828	ILMN_1717326
SCPEP1	1562	ILMN_1767470	*RPL10A*	*1846*	*ILMN_1808041*
CD53	1565	ILMN_2413808	*ATP1B1*	*1861*	*ILMN_1730291*
AHCY	1569	ILMN_1657862	DHX15	1880	ILMN_1754839
DHRS7	1578	ILMN_1807455	GOLGA7	1892	ILMN_1778673
FEZ2	1584	ILMN_1739586	*ITGB1*	*1895*	*ILMN_2383934*
NPL	*1585*	*ILMN_1782070*	PLAUR	1896	ILMN_2374340
ANAPC13	1586	ILMN_1793894	MPP1	1911	ILMN_1733675
NCL	1593	ILMN_2121437	*EIF4A1*	*1912*	*ILMN_3251629*
SNRPB	*1617*	*ILMN_1799103*	UQCRC2	1913	ILMN_1718853
PAIP2	1623	ILMN_1784753	CIRBP	1923	ILMN_1674661
TXNRD1	*1624*	*ILMN_2324421*	AHCYL1	1924	ILMN_1770412
DUSP3	1625	ILMN_1797522	EIF4B	1932	ILMN_1655497
GLG1	1628	ILMN_1772261	ELF1	1952	ILMN_1664010
GNG10	1629	ILMN_1757074	SSR1	1959	ILMN_1750693
BANF1	1631	ILMN_2179837	PTDSS1	1991	ILMN_1688753
CORO1C	1632	ILMN_1745954	*MTPN*	*2004*	*ILMN_1791478*
CPVL	*1636*	*ILMN_1682928*	ID2	2016	ILMN_2086095
SRP14	*1643*	*ILMN_3251269*	TAF10	2022	ILMN_1721093
PSMB4	1644	ILMN_1737862	RAB8A	2040	ILMN_1760858
SSBP1	1649	ILMN_1809478	ECHS1	2049	ILMN_1718132
CLTA	1653	ILMN_2345837	TBXAS1	2050	ILMN_2282641
YWHAG	1654	ILMN_2228809	*CTNNA1*	*2051*	*ILMN_2230902*
MKRN1	1659	ILMN_1671583	SNX17	2055	ILMN_1732810
PCBP2	*1660*	*ILMN_1724825*	RAB11A	2109	ILMN_1712312
GNA13	1665	ILMN_1758906	RPL22	2113	ILMN_2079386
NTAN1	1666	ILMN_1815552	SYK	2117	ILMN_2059549
CAPNS1	1668	ILMN_1655418	*GNA13*	*2120*	*ILMN_2176037*

ARPC1B	2125	ILMN_2085760
APEX1	2128	ILMN_1661886
PILRA	2165	ILMN_2362858
CD53	*2181*	*ILMN_1662843*
PLAUR	*2186*	*ILMN_1691508*
PAPSS1	2205	ILMN_1781819
SF3B5	2210	ILMN_1689389
ZYX	*2213*	*ILMN_2371169*
RNF13	2218	ILMN_2339748
CTSH	*2220*	*ILMN_1752451*
ST13	2227	ILMN_1765204
YWHAG	*2241*	*ILMN_1750145*
HCK	2273	ILMN_1791771
LY86	2279	ILMN_1807825
PGAM1	2280	ILMN_2112417
HNMT	2284	ILMN_1790881
GLO1	2296	ILMN_1702177
CYBB	2302	ILMN_1682312
PSMB2	2304	ILMN_1764794
TAX1BP1	*2323*	*ILMN_2374770*
CD14	*2330*	*ILMN_1740015*
PPP1CA	2346	ILMN_1695827
HSD17B12	*2355*	*ILMN_1702168*
ALDH2	2370	ILMN_1793859
ERH	2380	ILMN_1781795
NEU1	2388	ILMN_1763144
SCAMP1	2393	ILMN_1728907
PRNP	*2419*	*ILMN_2360415*
VPS4B	2423	ILMN_1792587
RPS15A	*2429*	*ILMN_2255310*
STARD7	*2431*	*ILMN_2367782*
ATP1B1	*2508*	*ILMN_1658071*
DAB2	*2509*	*ILMN_2128428*
ACP2	**2542**	**ILMN_2104830**
CLTA	*2553*	*ILMN_1695420*
MAP1LC3B	**2628**	**ILMN_1703244**
ATP1B3	*2713*	*ILMN_1654322*
CD36	*2719*	*ILMN_1784863*
CFLAR	**2777**	**ILMN_1789830**
RPL17	*2906*	*ILMN_1655422*
APEX1	*2948*	*ILMN_2319344*
UCP2	**2951**	**ILMN_1685625**
ITGB5	**2966**	**ILMN_2311166**
FEZ2	*2967*	*ILMN_2403946*
CTSK	**2977**	**ILMN_1758895**
PLAUR	*2986*	*ILMN_2408543*
PTTG1IP	*2997*	*ILMN_1802251*
IDH3B	*3000*	*ILMN_2373632*
PAPSS1	*3036*	*ILMN_2224103*
HNMT	*3039*	*ILMN_1751789*
EPAS1	**3042**	**ILMN_1704753**
IL13RA1	**3095**	**ILMN_1768505**
ANAPC5	**3101**	**ILMN_1723177**
PILRA	*3119*	*ILMN_2241953*
CAPNS1	*3216*	*ILMN_2393254*
SDHA	**3227**	**ILMN_2051232**
PGLS	**3247**	**ILMN_1797005**
TPM3	**3274**	**ILMN_1697567**
ATF4	*3342*	*ILMN_2358457*
TIMP2	*3435*	*ILMN_1749078*
GSN	**3583**	**ILMN_1801043**
GNG10	*3636*	*ILMN_1652003*
SQRDL	**3792**	**ILMN_1667199**
ITGB5	*3832*	*ILMN_1668374*
ITGB1	*3851*	*ILMN_1714820*
ANXA2	*3885*	*ILMN_1755937*
RPL9	*3936*	*ILMN_1729033*
PGAM1	*3969*	*ILMN_1661366*
SDHA	*4076*	*ILMN_1744210*
PILRA	*4081*	*ILMN_1729915*
ID2	*4118*	*ILMN_1793990*
VKORC1	*4252*	*ILMN_1786139*
ADAMDEC1	**4472**	**ILMN_2103107**
MS4A7	*4496*	*ILMN_2331087*
EIF4G2	*4565*	*ILMN_2279635*
LIMS1	*5206*	*ILMN_1675387*
ESD	*5467*	*ILMN_1669818*
ADAR	*5611*	*ILMN_2320964*
TNFRSF21	**5698**	**ILMN_1699695**
NEDD8	*5757*	*ILMN_1785711*
SERF2	*6122*	*ILMN_3251501*
PPP1CA	*6697*	*ILMN_2377980*
UBE2E1	*6762*	*ILMN_2371685*
NCL	*6989*	*ILMN_1695422*
YWHAB	*7369*	*ILMN_2277099*
PCBP2	*7509*	*ILMN_3251155*
BANF1	*7713*	*ILMN_1749243*
MAT2B	*8012*	*ILMN_1680246*
SRP9	*8054*	*ILMN_1759883*
RPS29	*8113*	*ILMN_2298818*
EEF1A1	*8698*	*ILMN_3251737*
ADAMDEC1	*8721*	*ILMN_1716909*
RNF13	*9045*	*ILMN_1719867*
HNMT	*9128*	*ILMN_2284744*
NONO	*9396*	*ILMN_1740976*
UBA52	*9455*	*ILMN_2368576*
RPL6	*9689*	*ILMN_1717490*
HSPD1	*9713*	*ILMN_1784367*
ABCA1	**9736**	**ILMN_1766054**
FXYD5	*9966*	*ILMN_2235975*
TAPBP	*10232*	*ILMN_1782851*
SCAMP1	*10238*	*ILMN_1729058*

ITGB5	*10378*	*ILMN_1796755*	*PRKAR1A*	*14701*	*ILMN_2277077*
RPS15	*10397*	*ILMN_2219131*	*RPL37A*	*15066*	*ILMN_1808757*
YWHAZ	*10612*	*ILMN_1669286*	*TAPBP*	*15724*	*ILMN_1773031*
MAT2B	*10977*	*ILMN_1673960*	*RPL36*	*15920*	*ILMN_1771462*
PAIP2	*11422*	*ILMN_1782094*	*ABR*	*16631*	*ILMN_1655114*
ATF4	*11528*	*ILMN_1783394*	*GPX1*	*16846*	*ILMN_1787412*
LIMS1	*11559*	*ILMN_2381037*	*PCBP2*	*17131*	*ILMN_3249963*
BTF3	*11827*	*ILMN_2245676*	*HSPD1*	*17437*	*ILMN_1774410*
UXT	*12370*	*ILMN_1745499*	*SCAMP1*	*17476*	*ILMN_3251337*
HNMT	*12629*	*ILMN_1705984*	*UBE2I*	*18322*	*ILMN_1664542*
RHOQ	*12932*	*ILMN_3251455*	*PSME1*	*19148*	*ILMN_1726698*
HK1	*13053*	*ILMN_1761829*	*RAC1*	*20644*	*ILMN_1761938*
TPM3	*13166*	*ILMN_2353754*	*TPM3*	*21119*	*ILMN_1747696*
STARD7	*14217*	*ILMN_1687140*	*UBC*	*21233*	*ILMN_2252160*
GOLGA7	*14559*	*ILMN_2268921*			

[a] Probes for a gene symbol for which another probe for the same gene symbol was more highly expressed are presented in *grey italics*

TABLE AIII.3 Probe expression ranks of macrophage characterising genes 24 hours post-infection

SYMBOL	Rank	PROBE_ID
TPT1	5	ILMN_2094718
CSTB	6	ILMN_1761797
RPS29	7	ILMN_1694742
ITGB2	8	ILMN_2175912
RPLP2	10	ILMN_1755733
B2M	12	ILMN_1725427
ITGB2[a]	*14*	*ILMN_1654396*
UBC	15	ILMN_2331501
ANXA2	*19*	*ILMN_2409167*
EEF1A1	23	ILMN_1343291
TMSB10	26	ILMN_1812392
OAZ1	27	ILMN_1773080
RPS29	*28*	*ILMN_1738243*
ACTB	30	ILMN_2152131
ACTG1	33	ILMN_2053178
NPC2	35	ILMN_1716678
RPS27	36	ILMN_1660498
CD81	39	ILMN_1689953
VIM	45	ILMN_1782538
RPLP1	46	ILMN_2247594
PSAP	48	ILMN_1749109
EEF1A1	*51*	*ILMN_1810810*
GPNMB	58	ILMN_1801205
UBC	*59*	*ILMN_2038773*
B2M	*60*	*ILMN_2148459*
PSAP	*62*	*ILMN_2355559*
RPS27A	66	ILMN_2048326
EEF1A1	*68*	*ILMN_2038774*
MYL6	74	ILMN_2326071
PFN1	75	ILMN_2151817
RPL38	77	ILMN_1765043
RPS12	79	ILMN_1782621
ACTB	*83*	*ILMN_2038777*
MYL6	*84*	*ILMN_1809013*
RPS16	87	ILMN_1651850
UBA52	91	ILMN_1782977
CYP27A1	92	ILMN_1704985
RPS19	93	ILMN_1784717
RPL27A	100	ILMN_1713086
TYROBP	102	ILMN_1778977
ATP5B	104	ILMN_1772132
RPS17	110	ILMN_2207533
LCP1	111	ILMN_1662932
LTA4H	112	ILMN_1690342
HEXB	114	ILMN_1806692
RPL38	*115*	*ILMN_2343775*
LGALS1	117	ILMN_1723978
RPS25	118	ILMN_1746516
ACTB	*121*	*ILMN_1777296*
RPS11	122	ILMN_1740587
EIF4A1	125	ILMN_1722900
RPS27	*126*	*ILMN_2160819*
PPT1	127	ILMN_1669273
H2AFY	129	ILMN_2373495
DBI	132	ILMN_2305544
RPL6	133	ILMN_1690494
RPL37A	136	ILMN_2051519
TFRC	144	ILMN_1674243
RPL11	148	ILMN_1672446
SLC25A5	149	ILMN_1774062
PRDX1	150	ILMN_2366391
GNS	151	ILMN_1744517
NACA	154	ILMN_2167617
H3F3A	156	ILMN_1656082
SQSTM1	167	ILMN_1662618
CTSH	169	ILMN_2390853
AP2S1	171	ILMN_1809957
ENO1	175	ILMN_1710756
GPX4	177	ILMN_2378952
RPS20	178	ILMN_1701596
PRDX1	*179*	*ILMN_2366388*
RPS10	181	ILMN_1686954
VIM	*185*	*ILMN_2058251*
S100A4	187	ILMN_1688780
GSTO1	188	ILMN_2227573
ARHGDIB	191	ILMN_1678143
RPL18	193	ILMN_2230624
RPL11	*196*	*ILMN_2114876*
RPL18A	197	ILMN_2141444
RPS3A	199	ILMN_1657722
RPL3	200	ILMN_2319996
COX4I1	207	ILMN_1652207
S100A10	208	ILMN_2046730
RPL39	209	ILMN_1737015
LGALS3	210	ILMN_1803788
RPS29	*213*	*ILMN_2415722*
RPL9	221	ILMN_1750507
RPL18A	*223*	*ILMN_2141453*

RPL19	229	ILMN_1701832
RPS6	232	ILMN_1656791
ATP6AP1	233	ILMN_1697694
GPNMB	*234*	*ILMN_2407389*
S100A6	242	ILMN_1713636
MDH1	244	ILMN_1656913
H3F3A	*245*	*ILMN_2106331*
RPS15A	246	ILMN_1787949
LAMP1	248	ILMN_1782292
UBB	251	ILMN_2191428
RPLP1	*252*	*ILMN_2386530*
CEBPB	253	ILMN_1693014
LITAF	258	ILMN_1713934
RPS3A	*259*	*ILMN_1673638*
ATP6V1B2	260	ILMN_1787705
RPL17	264	ILMN_1658283
ATP6V1F	268	ILMN_2099783
ACP5	269	ILMN_2078599
COX5B	270	ILMN_1663512
RPL30	271	ILMN_1754303
S100A4	*273*	*ILMN_1684306*
GPX1	276	ILMN_1749662
RPL27	278	ILMN_1656807
RPS14	283	ILMN_1666635
APOC1	285	ILMN_1789007
CAP1	286	ILMN_1797604
CFL1	287	ILMN_1705617
SERF2	294	ILMN_1789136
FCER1G	295	ILMN_2123743
HSPA8	297	ILMN_1686367
FTH1	299	ILMN_1683146
RPS3A	300	ILMN_2139943
COX8A	301	ILMN_1809495
COX7C	305	ILMN_1798189
PLIN2	307	ILMN_2138765
CTSB	308	ILMN_2359742
H3F3A	*309*	*ILMN_1699015*
ATP5H	314	ILMN_1794912
SLC15A3	316	ILMN_2085862
MMP9	320	ILMN_1796316
CYBA	322	ILMN_1744604
ATP6AP2	323	ILMN_1677440
ARPC5	324	ILMN_1768394
RPS15A	*325*	*ILMN_2337241*
NDUFA4	326	ILMN_1751258
RPL35A	327	ILMN_1756360
ATP5A1	331	ILMN_2341363
GPX4	*337*	*ILMN_1734353*
FXYD5	338	ILMN_2309848
HSPA8	*340*	*ILMN_2413084*
EIF4G2	344	ILMN_2380946
RPL24	349	ILMN_2160388
PFN1	*350*	*ILMN_1712950*
RPS28	351	ILMN_1651228
ATF4	353	ILMN_1672128
RPL10A	354	ILMN_2154566
RPL31	355	ILMN_1754195
COX7A2	356	ILMN_1701293
PLA2G7	358	ILMN_1701195
S100A10	*359*	*ILMN_1796712*
ATP5A1	*362*	*ILMN_1764494*
PFDN5	367	ILMN_2356284
IFI30	370	ILMN_1807277
CHCHD2	373	ILMN_2191681
S100A9	377	ILMN_1750974
RPS13	378	ILMN_1777344
GSTO1	*380*	*ILMN_1808196*
COX5A	382	ILMN_1704477
SNX3	385	ILMN_1740180
ANXA5	386	ILMN_1741003
RHOA	388	ILMN_1781290
COX6C	391	ILMN_1654151
APOE	392	ILMN_1740938
RPL36AL	394	ILMN_2189936
RPL17	*397*	*ILMN_2383097*
RPL12	399	ILMN_2116366
NACA	*401*	*ILMN_2167616*
ATP5H	*402*	*ILMN_1666372*
GRN	403	ILMN_1724250
PFDN5	*404*	*ILMN_1755536*
NDUFA1	405	ILMN_1784286
TOMM7	408	ILMN_1674069
PGD	418	ILMN_1794165
UQCRH	420	ILMN_2232936
PSMA6	422	ILMN_2151818
NEDD8	423	ILMN_2058070
PCBP1	425	ILMN_1673215
FAU	427	ILMN_1664614
CST3	431	ILMN_1800354
NUCB1	432	ILMN_1722634
RPS6	*435*	*ILMN_1808939*
NCOA4	440	ILMN_1773906

TOMM7	*441*	*ILMN_2087060*
CTSD	442	ILMN_1674038
UBB	*447*	*ILMN_1762436*
MDH2	448	ILMN_2079004
ARPC3	450	ILMN_1655561
RNASET2	453	ILMN_1671565
RPS14	*456*	*ILMN_2338785*
RPL3	*459*	*ILMN_2319994*
LASP1	463	ILMN_1665909
RPL23	464	ILMN_1755115
TRAM1	468	ILMN_1737146
GHITM	470	ILMN_1728467
ACTG1	*472*	*ILMN_1704961*
CNDP2	475	ILMN_1726769
JTB	479	ILMN_2206716
PABPC1	483	ILMN_1761155
IGF2R	493	ILMN_1807662
YWHAB	494	ILMN_1694385
BTF3	498	ILMN_2319414
GSTP1	500	ILMN_1679809
ATP6V0B	503	ILMN_1721391
GRN	*504*	*ILMN_1811702*
RPS2	508	ILMN_2218277
RPS27	*510*	*ILMN_1696839*
SDCBP	513	ILMN_2363586
ANXA2	*514*	*ILMN_1711899*
ATP5F1	518	ILMN_1721989
RPL6	*520*	*ILMN_1712155*
RPL35	521	ILMN_2142815
CCNI	522	ILMN_1691942
BRI3	529	ILMN_1781580
LPXN	530	ILMN_1742789
TKT	542	ILMN_1736597
RPS18	545	ILMN_1753534
ATP1B3	547	ILMN_1783304
GLA	551	ILMN_1766637
RPS27A	*555*	*ILMN_1755883*
RPS3	557	ILMN_1760714
BCAP31	559	ILMN_1812403
RPS15	563	ILMN_2219134
ANXA1	564	ILMN_2184184
CYP1B1	567	ILMN_1693338
FXYD5	*570*	*ILMN_1704286*
RPL36AL	*571*	*ILMN_2189933*
NDUFB2	575	ILMN_2117330
HMGN1	576	ILMN_2151579
ATP5O	578	ILMN_1791332
SH3BGRL3	580	ILMN_1737163
RTN4	582	ILMN_1730611
IFNGR2	584	ILMN_1764964
CD14	586	ILMN_2396444
H2AFZ	588	ILMN_1707858
LY96	591	ILMN_1724533
YWHAZ	592	ILMN_1801928
RPS5	596	ILMN_1707810
SDCBP	597	ILMN_2363591
AP2S1	*598*	*ILMN_1662426*
ANP32B	602	ILMN_1684293
TBCA	606	ILMN_1726239
SEC61B	607	ILMN_1801852
IFNGR1	620	ILMN_1675939
DAD1	623	ILMN_1731619
S100A11	627	ILMN_1750101
RPL9	*634*	*ILMN_2408415*
TMEM14C	635	ILMN_2175131
BASP1	641	ILMN_1651826
PCBP2	643	ILMN_2312296
VAMP8	646	ILMN_2190084
NDUFB5	650	ILMN_1807397
PSMB1	651	ILMN_1789176
SRP14	652	ILMN_2234758
HSPD1	668	ILMN_2381397
ITGB1	669	ILMN_1723467
DDX5	671	ILMN_1805344
SH3BGRL	672	ILMN_1702835
DPYSL2	673	ILMN_1672503
RAB10	676	ILMN_1793433
ATOX1	679	ILMN_1670609
M6PR	680	ILMN_2084353
PLEK	683	ILMN_1795762
LIMS1	685	ILMN_1733176
SPP1	687	ILMN_1651354
EMP3	688	ILMN_1765446
MTPN	689	ILMN_2180682
RPS4X	690	ILMN_1810577
MGST3	692	ILMN_1751956
RPL12	*693*	*ILMN_1653469*
DNAJA1	697	ILMN_1672496
ATP6V1G1	698	ILMN_1784523
CD9	700	ILMN_1695423
PTBP1	702	ILMN_2333319
PABPC1	*704*	*ILMN_2136133*

CTSB	*705*	*ILMN_1696360*
EIF4A2	706	ILMN_1685722
NARS	708	ILMN_1732216
ALDH9A1	713	ILMN_1761804
VDAC3	715	ILMN_1729816
BTF3	*716*	*ILMN_1659762*
SRP9	718	ILMN_2099594
UQCRFS1	719	ILMN_1701749
NDUFB8	721	ILMN_1661170
CLIC1	722	ILMN_1756982
RPL5	723	ILMN_2087080
LAMP2	726	ILMN_1673282
NDUFA3	730	ILMN_1784641
EEF2	731	ILMN_1738383
CLCN7	733	ILMN_1694731
SOD1	739	ILMN_1662438
HINT1	744	ILMN_1807710
GLB1	756	ILMN_2397721
NDUFAB1	758	ILMN_2179018
PSMB3	759	ILMN_1748651
RHEB	763	ILMN_1657949
DBI	*766*	*ILMN_1755926*
ATP6V1E1	768	ILMN_2339779
DAZAP2	770	ILMN_1718988
VKORC1	773	ILMN_1739946
YWHAQ	774	ILMN_1674385
CTSZ	780	ILMN_1666269
TPT1	*781*	*ILMN_1789614*
P4HB	782	ILMN_1719303
NCF2	784	ILMN_1796642
RNF130	790	ILMN_1729294
KYNU	801	ILMN_1746517
ATP5J2	802	ILMN_2310621
TIMP1	808	ILMN_1711566
GTF3A	820	ILMN_1658464
PEA15	821	ILMN_1771376
PGK1	824	ILMN_1755749
ATP6V1E1	*826*	*ILMN_1798485*
ATP5J2	*827*	*ILMN_2307883*
RPL36	829	ILMN_1685088
UBE2E1	830	ILMN_1806778
PARK7	831	ILMN_1744713
GLTSCR2	836	ILMN_1703565
EEF1G	841	ILMN_2262288
RHOQ	844	ILMN_1810559
SCARB2	847	ILMN_1814726
MGAT1	848	ILMN_1761912
COX7B	851	ILMN_2184049
TPI1	853	ILMN_1707627
ATP1B3	*857*	*ILMN_1759628*
RPL26	858	ILMN_1731546
KPNB1	860	ILMN_1703949
ATP6V1D	861	ILMN_1797310
NAGK	863	ILMN_1716547
VAT1	864	ILMN_1700690
PSMC1	867	ILMN_1736353
GNB1	870	ILMN_1760320
EIF4G2	*876*	*ILMN_1761519*
GM2A	880	ILMN_2221046
RPS17	*885*	*ILMN_2207539*
ZYX	891	ILMN_1701875
EMILIN2	894	ILMN_1697268
PSME1	901	ILMN_1806017
ABR	902	ILMN_1672878
CD48	903	ILMN_2061043
ESD	904	ILMN_1720285
LAMP2	*910*	*ILMN_2243687*
CSDA	915	ILMN_1782788
SSR4	916	ILMN_1680403
CPVL	921	ILMN_2400759
GNPDA1	923	ILMN_1784709
PRKAR1A	925	ILMN_1738632
CEBPA	927	ILMN_1715715
NDUFS3	928	ILMN_1756355
MARCKS	929	ILMN_1807042
AP1S2	935	ILMN_2120273
TIMP2	948	ILMN_1721876
HSD17B12	950	ILMN_2094106
UXT	953	ILMN_1671314
QARS	954	ILMN_1763080
NINJ1	955	ILMN_1815086
SPP1	*961*	*ILMN_2374449*
FUCA1	962	ILMN_1752728
GUSB	963	ILMN_1669878
FCGRT	967	ILMN_1705302
NPL	969	ILMN_1782070
NONO	971	ILMN_2052790
ARHGEF2	975	ILMN_1703477
MSN	976	ILMN_1659895
EFHD2	980	ILMN_1761463
MTCH1	983	ILMN_1703006
HEBP1	985	ILMN_1802557

DAB2	986	ILMN_1764228
ATP6V0A1	987	ILMN_1752579
PTBP1	*989*	*ILMN_1655154*
SLC7A7	993	ILMN_1810275
RBX1	998	ILMN_1666670
PPP1R11	1001	ILMN_1747598
CCT8	1003	ILMN_1717868
MAT2B	1004	ILMN_1811367
DARS	1008	ILMN_1813836
GDI2	1011	ILMN_1754178
DNAJC8	1014	ILMN_1698258
HMGN1	*1019*	*ILMN_1652123*
HCLS1	1021	ILMN_1727402
PLIN2	*1022*	*ILMN_1801077*
RAC1	1026	ILMN_2359789
COX6A1	1027	ILMN_1783636
TM9SF2	1028	ILMN_1785765
NPL	*1031*	*ILMN_2149494*
LAMP2	*1032*	*ILMN_2279961*
SUMO3	1042	ILMN_1725642
PPP1CC	1044	ILMN_1701855
COPA	1045	ILMN_1811615
MORF4L1	1048	ILMN_1760676
PRDX3	1055	ILMN_2395974
DHX15	1056	ILMN_2168449
AP1S2	*1062*	*ILMN_1766411*
PRNP	1068	ILMN_1737988
GLB1	*1069*	*ILMN_1735155*
HSD17B4	1070	ILMN_1673795
NFKBIA	1071	ILMN_1773154
DDOST	1089	ILMN_1734231
DHRS7	1101	ILMN_1807455
PSMC2	1107	ILMN_1768784
PRKAR1A	*1112*	*ILMN_2389590*
TMEM14C	*1114*	*ILMN_1657857*
RPS4X	*1118*	*ILMN_2166831*
TPI1	*1119*	*ILMN_2181191*
A2M	1127	ILMN_1745607
ATP5C1	1128	ILMN_1701269
PRDX6	1131	ILMN_1803180
PTTG1IP	1138	ILMN_2128750
STARD7	1139	ILMN_1740819
CAPG	1140	ILMN_1655821
KHDRBS1	1141	ILMN_2076640
H2AFY	*1142*	*ILMN_1746171*
PABPC4	1145	ILMN_1757343
ACTR3	1151	ILMN_1657153
ATP6V0D1	1156	ILMN_1795826
GSTK1	1158	ILMN_1725241
NDUFV2	1177	ILMN_2086417
LAPTM5	1189	ILMN_1772359
MAPRE1	1197	ILMN_1777721
RPL15	1209	ILMN_1762747
POLR2G	1212	ILMN_1748438
PSMC1	*1214*	*ILMN_1710406*
UQCRC1	1217	ILMN_1671191
RPL4	1230	ILMN_1752285
SET	1247	ILMN_1742238
PDHB	1253	ILMN_1739274
HK1	1261	ILMN_2382990
UBE2I	1266	ILMN_1810474
PSMA6	1269	ILMN_1704094
GMFG	1271	ILMN_1711617
TAX1BP1	1278	ILMN_1793118
ACSL1	1286	ILMN_1684585
BLVRA	1287	ILMN_1691436
BTG1	1288	ILMN_1775743
PSMB7	1295	ILMN_1814156
SLC16A3	*1305*	*ILMN_2364022*
RPL13A	1307	ILMN_1713369
PRDX4	1312	ILMN_2222234
CTNNA1	1315	ILMN_1804854
RHOG	1320	ILMN_1739792
GNAI2	1323	ILMN_1775762
MAT2A	1329	ILMN_1737298
FEZ2	1330	ILMN_1739586
ACTN1	1335	ILMN_2232177
NFE2L2	1337	ILMN_1790909
SNRPB	1340	ILMN_1774661
CD36	1342	ILMN_1796094
CSNK2B	1353	ILMN_1800461
SLC29A3	1354	ILMN_1717326
RRAGD	1372	ILMN_1699772
LAMP2	*1374*	*ILMN_1659753*
CALM1	1377	ILMN_1778242
CORO1C	1379	ILMN_1745954
IRAK1	1385	ILMN_2379130
ZDHHC7	1393	ILMN_1730568
ATP5F1	*1408*	*ILMN_1672191*
TAPBP	1411	ILMN_1742450
PCBP2	*1416*	*ILMN_1724825*
SCPEP1	1419	ILMN_1767470

PRDX3	*1426*	*ILMN_2395969*
BANF1	1428	ILMN_2179837
TACC1	1430	ILMN_1770084
CAPNS1	1439	ILMN_1655418
VPS35	1444	ILMN_1761721
GTF2A2	1446	ILMN_1753719
ANAPC13	1449	ILMN_1793894
ATP1B1	1455	ILMN_2407824
RTN4	*1458*	*ILMN_2352036*
GLG1	1461	ILMN_1772261
HSPD1	*1462*	*ILMN_1766713*
CTSS	1465	ILMN_1743032
SSBP1	1469	ILMN_1809478
VAMP3	1482	ILMN_1714527
GLIPR1	1489	ILMN_1769245
ZMPSTE24	1491	ILMN_1656413
SRP14	*1492*	*ILMN_3251269*
CSF1R	1504	ILMN_1686623
AHCYL1	1508	ILMN_1770412
NPC1	1510	ILMN_1713505
CAPZA2	1518	ILMN_1768870
H2AFY	*1521*	*ILMN_1674034*
PSMB4	1531	ILMN_1737862
TTC3	1538	ILMN_1728605
SNX2	1542	ILMN_1691575
NTAN1	1548	ILMN_1815552
PAIP2	1553	ILMN_1784753
TXNRD1	1566	ILMN_1717056
RAB32	1599	ILMN_2115434
GNG10	1612	ILMN_1757074
MKRN1	1617	ILMN_1671583
NCL	1630	ILMN_2121437
CSK	1633	ILMN_1754121
SNRPB	*1638*	*ILMN_1799103*
ARPC1B	1646	ILMN_2085760
ACP2	1652	ILMN_2104830
CLTA	1666	ILMN_2345837
SYK	1668	ILMN_2059549
CYBB	1671	ILMN_1682312
DCTN2	1676	ILMN_1662232
SH3GLB1	1679	ILMN_1766045
CPVL	*1685*	*ILMN_1682928*
ADAR	1688	ILMN_1776777
DUSP3	1697	ILMN_1797522
PLAUR	1699	ILMN_1691508
RPLP1	*1702*	*ILMN_1689725*
IDH3B	1714	ILMN_1721669
WAS	1715	ILMN_1760027
CTSH	*1716*	*ILMN_1752451*
LAMP2	*1722*	*ILMN_1752351*
GOLGA7	1724	ILMN_1778673
LYN	1726	ILMN_1781155
ECHS1	1727	ILMN_1718132
ATP6V0B	*1732*	*ILMN_2353642*
PAPSS1	1733	ILMN_1781819
ID2	1747	ILMN_2086095
AHCY	1751	ILMN_1657862
EIF4A1	*1763*	*ILMN_3251629*
PLAUR	*1791*	*ILMN_2374340*
UQCRC2	1801	ILMN_1718853
MS4A7	1810	ILMN_2331082
MAFB	1821	ILMN_1764709
LAP3	1823	ILMN_1683792
ITGB1	*1834*	*ILMN_2383934*
EIF4B	1845	ILMN_1655497
HSPA1A	1848	ILMN_1789074
MPP1	1855	ILMN_1733675
SSR1	1858	ILMN_1750693
RPL22	1869	ILMN_2079386
MTPN	*1887*	*ILMN_1791478*
PILRA	1893	ILMN_2362858
SNX17	1896	ILMN_1732810
SCAMP1	1911	ILMN_1728907
YWHAG	1914	ILMN_2228809
PTDSS1	1934	ILMN_1688753
PGK1	*1940*	*ILMN_2216852*
CD53	1948	ILMN_2413808
GNA13	1951	ILMN_1758906
PSMB2	1953	ILMN_1764794
SF3B5	1955	ILMN_1689389
CTNNA1	*1962*	*ILMN_2230902*
PGAM1	1964	ILMN_2112417
HCK	1966	ILMN_1791771
TAF10	1968	ILMN_1721093
RPS15A	*1973*	*ILMN_2255310*
KYNU	*1996*	*ILMN_1737514*
APEX1	2017	ILMN_1661886
CD36	*2036*	*ILMN_1784863*
RAB8A	2045	ILMN_1760858
RPL10A	*2052*	*ILMN_1808041*
RNF13	2055	ILMN_2339748
LY86	2083	ILMN_1807825

ATP1B1	*2113*	*ILMN_1730291*
TBXAS1	2119	ILMN_2282641
PPP1CA	2138	ILMN_1695827
ELF1	2154	ILMN_1664010
LHFPL2	2163	ILMN_1747744
GLO1	2165	ILMN_1702177
DHX15	*2175*	*ILMN_1754839*
TXNRD1	*2181*	*ILMN_2324421*
ERH	2193	ILMN_1781795
CIRBP	2218	ILMN_1674661
NEU1	2242	ILMN_1763144
ZYX	*2248*	*ILMN_2371169*
UCP2	2285	ILMN_1685625
TAX1BP1	*2303*	*ILMN_2374770*
ITGB5	2304	ILMN_2311166
RAB11A	2331	ILMN_1712312
ATP1B1	*2347*	*ILMN_1658071*
HSD17B12	*2366*	*ILMN_1702168*
UQCRH	*2389*	*ILMN_1792138*
DAB2	*2405*	*ILMN_2128428*
ALDH2	2459	ILMN_1793859
HNMT	2480	ILMN_1790881
CTSK	2499	ILMN_1758895
FEZ2	*2509*	*ILMN_2403946*
ATP1B3	*2528*	*ILMN_1654322*
CLTA	*2548*	*ILMN_1695420*
ST13	**2581**	**ILMN_1765204**
STARD7	*2643*	*ILMN_2367782*
RPL17	*2674*	*ILMN_1655422*
VPS4B	**2677**	**ILMN_1792587**
CD53	*2714*	*ILMN_1662843*
PILRA	*2760*	*ILMN_2241953*
TIMP2	*2761*	*ILMN_1749078*
CD14	*2781*	*ILMN_1740015*
YWHAG	*2798*	*ILMN_1750145*
SDHA	**2820**	**ILMN_2051232**
ADAMDEC1	**2823**	**ILMN_2103107**
PGLS	**2858**	**ILMN_1797005**
PLAUR	*2867*	*ILMN_2408543*
CAPNS1	*2879*	*ILMN_2393254*
PTTG1IP	*2909*	*ILMN_1802251*
MAP1LC3B	**2911**	**ILMN_1703244**
ITGB5	*2919*	*ILMN_1668374*
EPAS1	**2932**	**ILMN_1704753**
IL13RA1	**2940**	**ILMN_1768505**
PRNP	*2953*	*ILMN_2360415*
ANAPC5	**3030**	**ILMN_1723177**
ANXA2	*3032*	*ILMN_1755937*
APEX1	*3041*	*ILMN_2319344*
PAPSS1	*3098*	*ILMN_2224103*
ITGB1	*3113*	*ILMN_1714820*
IDH3B	*3158*	*ILMN_2373632*
ID2	*3175*	*ILMN_1793990*
GNA13	*3204*	*ILMN_2176037*
PGAM1	*3259*	*ILMN_1661366*
TPM3	**3281**	**ILMN_1697567**
PILRA	*3302*	*ILMN_1729915*
CFLAR	**3335**	**ILMN_1789830**
ATF4	*3350*	*ILMN_2358457*
RPL9	*3357*	*ILMN_1729033*
HNMT	*3541*	*ILMN_1751789*
GSN	**3553**	**ILMN_1801043**
SDHA	*3786*	*ILMN_1744210*
SQRDL	**3905**	**ILMN_1667199**
VKORC1	*4349*	*ILMN_1786139*
MS4A7	*4383*	*ILMN_2331087*
ESD	*4559*	*ILMN_1669818*
TNFRSF21	**4568**	**ILMN_1699695**
GNG10	*4729*	*ILMN_1652003*
LIMS1	*4889*	*ILMN_1675387*
EIF4G2	*5142*	*ILMN_2279635*
NEDD8	*5464*	*ILMN_1785711*
ADAR	*5593*	*ILMN_2320964*
PPP1CA	*6190*	*ILMN_2377980*
ABCA1	**6311**	**ILMN_1766054**
SERF2	*6469*	*ILMN_3251501*
YWHAB	*6553*	*ILMN_2277099*
ADAMDEC1	*6618*	*ILMN_1716909*
UBE2E1	*6738*	*ILMN_2371685*
RPS29	*7042*	*ILMN_2298818*
NCL	*7555*	*ILMN_1695422*
SRP9	*7574*	*ILMN_1759883*
BANF1	*7598*	*ILMN_1749243*
MAT2B	*7742*	*ILMN_1680246*
PCBP2	*8168*	*ILMN_3251155*
NONO	*8885*	*ILMN_1740976*
FXYD5	*8991*	*ILMN_2235975*
ITGB5	*9008*	*ILMN_1796755*
RNF13	*9049*	*ILMN_1719867*
SCAMP1	*9155*	*ILMN_1729058*
TAPBP	*9196*	*ILMN_1782851*
HSPD1	*9256*	*ILMN_1784367*

RPL6	*9278*	*ILMN_1717490*
MAT2B	*9365*	*ILMN_1673960*
YWHAZ	*9582*	*ILMN_1669286*
EEF1A1	*9615*	*ILMN_3251737*
HNMT	*9795*	*ILMN_2284744*
RPS15	*10116*	*ILMN_2219131*
UBA52	*10309*	*ILMN_2368576*
TPM3	*11377*	*ILMN_2353754*
PAIP2	*11421*	*ILMN_1782094*
ATF4	*11667*	*ILMN_1783394*
PRKAR1A	*12384*	*ILMN_2277077*
LIMS1	*12968*	*ILMN_1751644*
HNMT	*13186*	*ILMN_1705984*
HK1	*13345*	*ILMN_1761829*
BTF3	*13614*	*ILMN_2245676*
UXT	*13902*	*ILMN_1745499*
TAPBP	*14332*	*ILMN_1773031*
RPL36	*14391*	*ILMN_1771462*
STARD7	*14473*	*ILMN_1687140*
LIMS1	*14632*	*ILMN_2381037*
RHOQ	*14843*	*ILMN_3251455*
GOLGA7	*15010*	*ILMN_2268921*
RPL37A	*15062*	*ILMN_1808757*
ABR	*16532*	*ILMN_1655114*
HSPD1	*16548*	*ILMN_1774410*
SCAMP1	*16551*	*ILMN_3251337*
UBE2I	*17094*	*ILMN_1662934*
PCBP2	*20275*	*ILMN_3249963*
RAC1	*20869*	*ILMN_1761938*
PSME1	*20889*	*ILMN_1726698*
TPM3	*21033*	*ILMN_1747696*
GPX1	*21190*	*ILMN_1787412*
UBC	*21538*	*ILMN_2252160*

[a] Probes for a gene symbol for which another probe for the same gene symbol was more highly expressed are presented in *grey italics*

Appendix IV. Transcriptomics data

The raw transcriptomics data from CGS can be found on the included CD as a file named ACS_raw_data.txt

Appendix V. Data processing

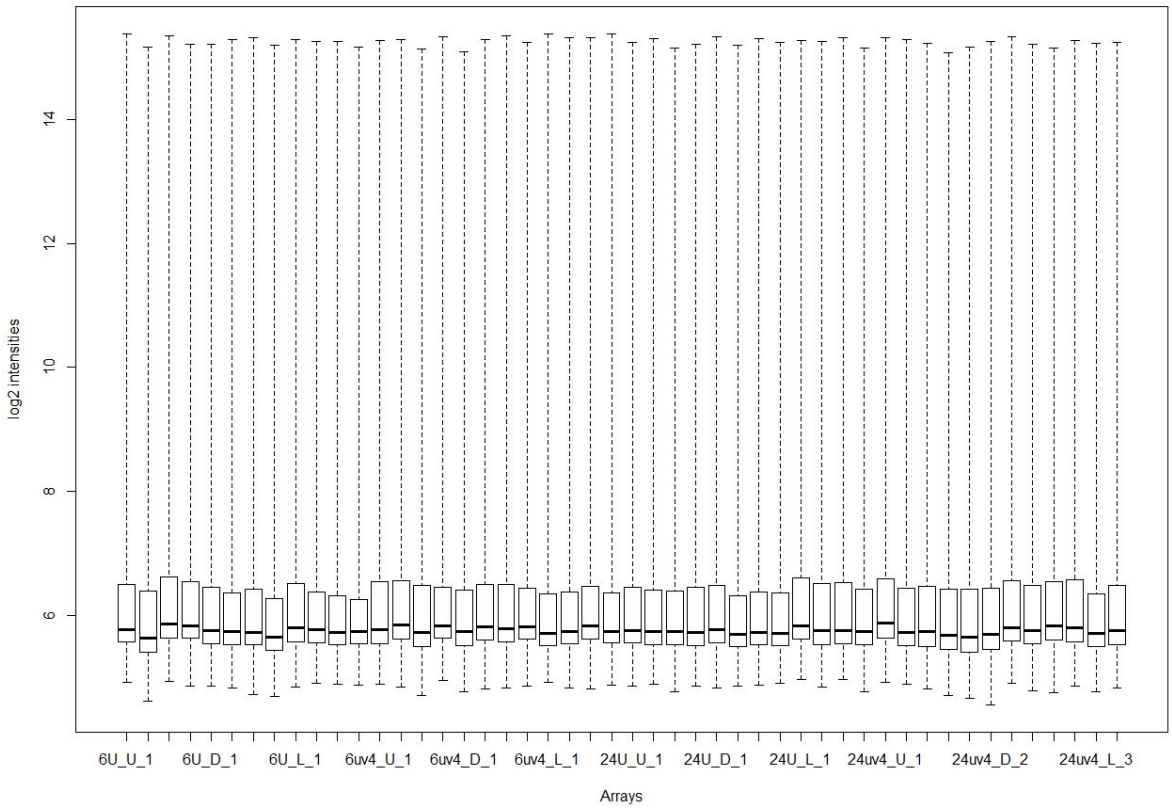

FIGURE AV.1 Raw $\log_2$ fluorescence intensities of all probes, including negative controls, by sample. Raw fluorescence intensities of all 47,216 experimental probes in addition to negative control probes were used to generate a boxplot by taking the base 2 logarithm of each value for each sample (individual donor, infection, treatment, time point sample). Donors are ordered sequentially (1 to 4) with the sample type for each set of four donors listed along the x-axis. The first number represents the time point (6 hours or 24 hours) followed by drug treatment (U is untreated, uv4 is treated with 25 μM MON-DNJ) then infection status (U is uninfected, D is DENV infected, and L is LPS treated).

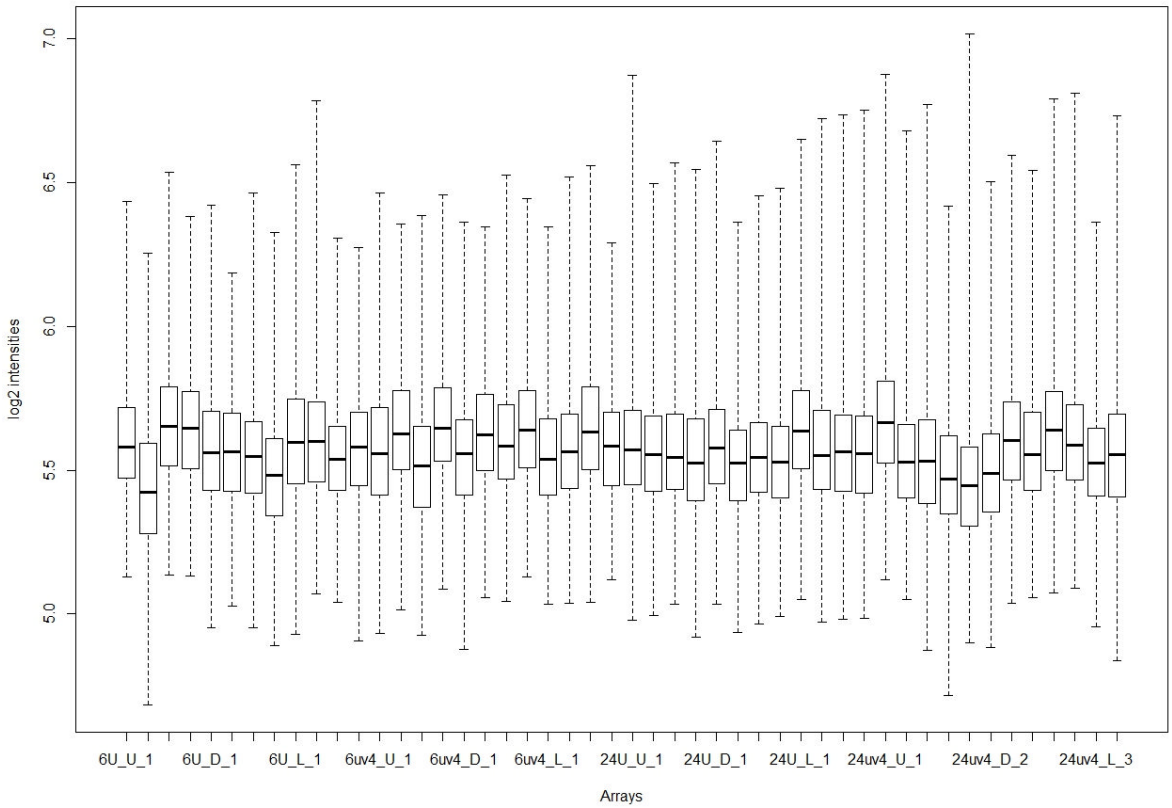

FIGURE AV.2 Raw $\log_2$ fluorescence intensities of negative control probes by sample. Raw fluorescence intensities of negative control probes were used to generate a boxplot by taking the base 2 logarithm of each value for each sample (individual donor, infection, treatment, time point sample). Donors are ordered sequentially (1 to 4) with the sample type for each set of four donors listed along the x-axis. The first number represents the time point (6 hours or 24 hours) followed by drug treatment (U is untreated, uv4 is treated with 25 μM MON-DNJ) then infection status (U is uninfected, D is DENV infected, and L is LPS treated).

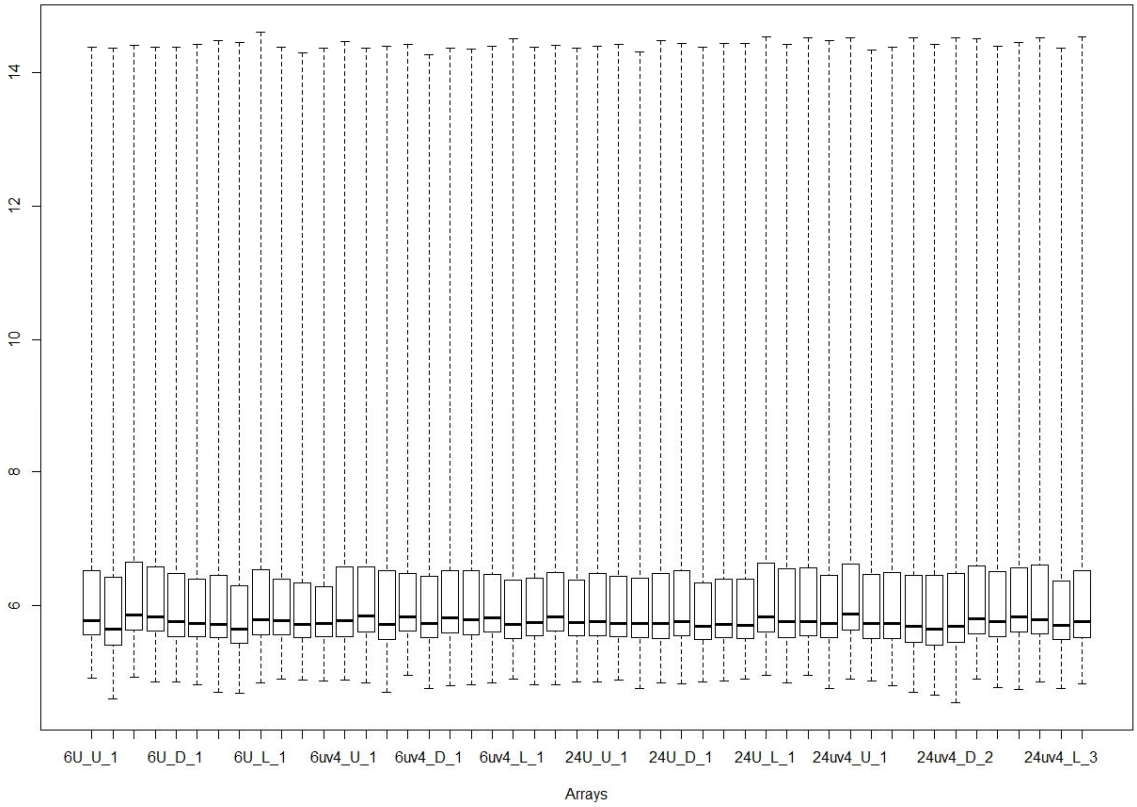

FIGURE AV.3 Raw $\log_2$ fluorescence intensities of experimental probes by sample. Raw fluorescence intensities of experimental probes were used to generate a boxplot by taking the base 2 logarithm of each value for each sample (individual donor, infection, treatment, time point sample). Donors are ordered sequentially (1 to 4) with the sample type for each set of four donors listed along the x-axis. The first number represents the time point (6 hours or 24 hours) followed by drug treatment (U is untreated, uv4 is treated with 25 μM MON-DNJ) then infection status (U is uninfected, D is DENV infected, and L is LPS treated).

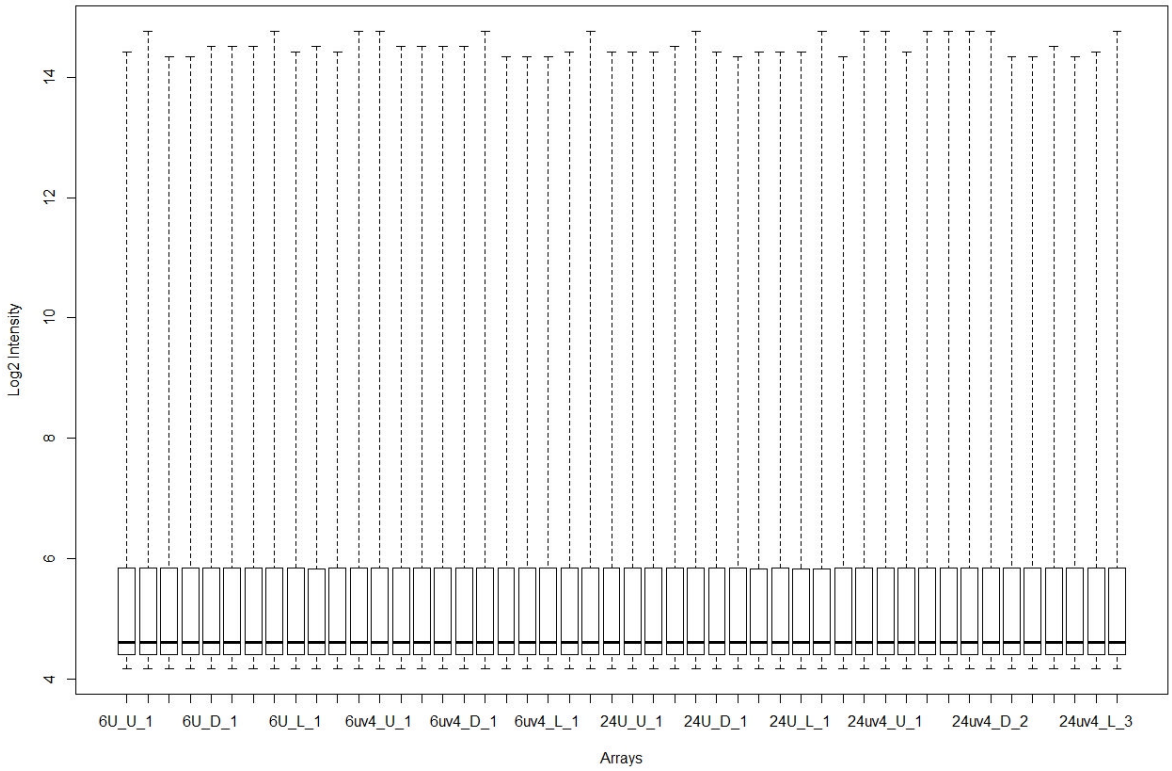

FIGURE AV.4 Neqc processed $\log_2$ fluorescence intensities of experimental probes by sample. Following processing by the neqc algorithm, intensities of experimental probes were used to generate a boxplot by taking the base 2 logarithm of each value for each sample (individual donor, infection, treatment, time point sample). Donors are ordered sequentially (1 to 4) with the sample type for each set of four donors listed along the x-axis. The first number represents the time point (6 hours or 24 hours) followed by drug treatment (U is untreated, uv4 is treated with 25 μM MON-DNJ) then infection status (U is uninfected, D is DENV infected, and L is LPS treated).

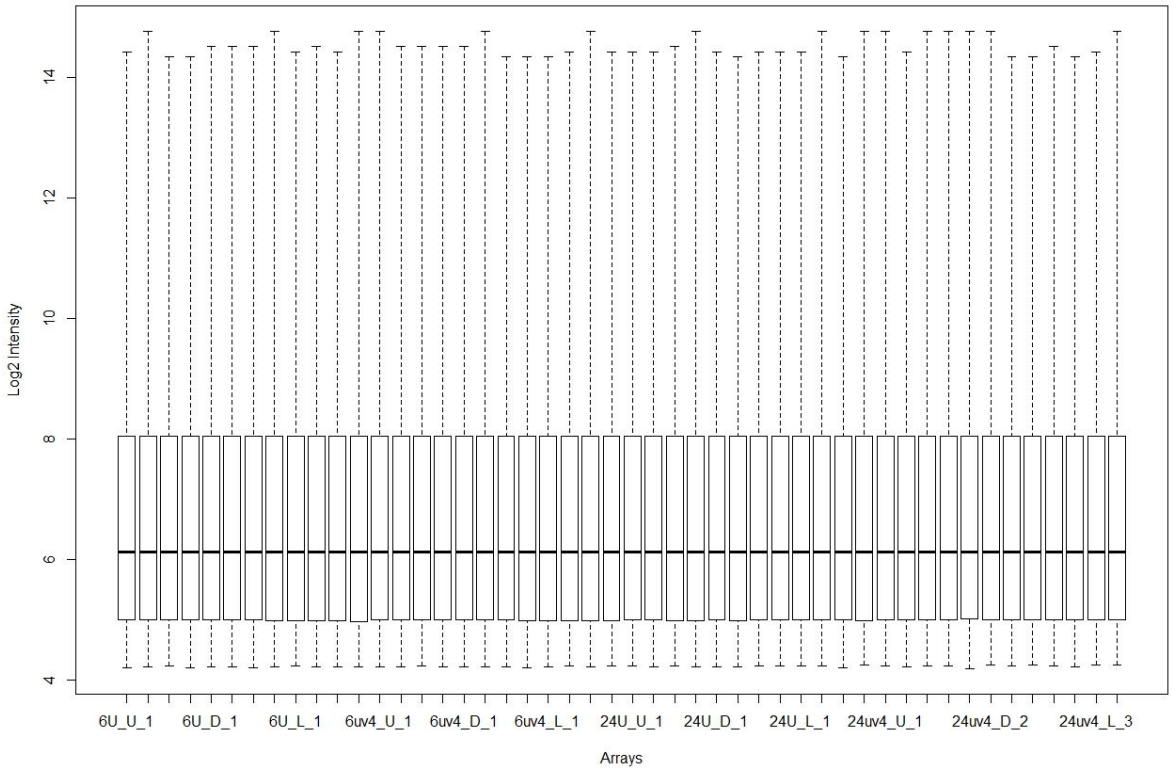

FIGURE AV.5 Neqc processed $\log_2$ fluorescence intensities of expressed experimental probes by sample. Following processing by the neqc algorithm, probes were queried for expression in any of the 48 samples submitted. If a probe demonstrated expression above background ($p_{detection} < 0.01$), the probe was included for analysis. By these means, the list of 47,216 probes was reduced to 21,705 expressed probes. Intensities of these processed, expressed probes were used to generate a boxplot by taking the base 2 logarithm of each value for each sample (individual donor, infection, treatment, time point sample). Donors are ordered sequentially (1 to 4) with the sample type for each set of four donors listed along the x-axis. The first number represents the time point (6 hours or 24 hours) followed by drug treatment (U is untreated, uv4 is treated with 25 μM MON-DNJ) then infection status (U is uninfected, D is DENV infected, and L is LPS treated).

Appendix VI. Expressed data

Transcriptomics data for probes processed as indicated in the *Materials and Methods* and executed in *Appendix V* can be found on the included CD as a file named ACS_processed_expressed.txt. All statistical analyses and subsequent upstream analyses were conducted using this data set.